

CHAPTER 7

Hardness of d-AHT crystals

S1. No.	Contents	Page
7.1	Application of Meyer's law & Kick's law to orthorhombic crystal :- d-AHT	94
7.1(a)	Meyer's law	94
7.1(b)	Kick's law	95
7.1(c)	Experimental	97
7.1(d)	Observations	98
7.1(e)	Results & Discussions	99
7.1(f)	Modification in Kick's law & Meyer's law	101
7.1(g)	Variation of standard hardness and exponent with orientation	104
7.1(h)	Curvilinear plots between diagonal length & applied load	107
7.1(i)	Conclusions	

References

7.1 Application of Meyer's Law and Kick's Law to orthorhombic crystal of d-AHT

From the hardness point of view, there are two ways of studying empirically the mechanical response of a material to the applied load:

- i) Variation of applied load (p in gm) with diagonal length (d in μm) of the indentation mark;
- ii) Variation of hardness (H in kg/sqmm) represented by hardness number, with applied load.

In this chapter, it is proposed to discuss quantitatively the variation of applied load with diagonal length of the indentation mark produced by a knoop indenter on prism, sphenoidal and cleavage faces of synthetic single crystals of ammonium hydrogen d-tartrate (d-AHT). For ball and pyramidal indenters, two empirical laws are suggested. They are as follows: (i) Meyer's law & ii) Kick's law.

7.1 (a) Meyer's Law:

On the basis of experimental observations, Meyer (1908) had given a relation between applied load and the diameter of the indentation mark produced by a ball indenter, viz. for a given diameter of a ball indenter, the variation of the applied load (p in gm) with the diameter of the indentation mark, (d in μm) is given by the following empirical relation:

$$P = ad^n \dots \quad (7.1)$$

where "a" and "n" are constants for a given material. The above expression symbolically represents Meyer's law (1). "n" varies from about 2.0 to 2.5 depending on the condition of the material. It has a higher value for a fully softened state and decreases with the degree of cold working given to the specimen. The value of "n" can be considered as the capacity for work hardening (2).

(b) Kick's Law:

Kick (1885) (3) has given a formula connecting applied load with diagonal length of the indentation mark produced by an indenter. It is given by :

$$P = ad^n \dots \quad (7.1)$$

where "a" is termed the "standard hardness" of the material for an indenter of fixed diameter and "n" is an exponent giving a measure of the variation in hardness as a function of "p" or "d". It has been shown that in case of Vicker's microhardness, "n" is equal to 2 (Kick's Law, 1885) for all indenters that give geometrically similar impressions. Hanemann and Schultz (1941) (4) from their observations concluded that in the low load region "n" generally has a value less than 2. Onitsch (1947) (5) found such low values of "n" (1 to 2) by observing variation of hardness with load while Grodzinski (1952) (6) found variation of "n" values from 1.3 to 4.9; the value of "n" was nearly found to be 1.8.

Since the applied load value (P) in the above formula is a product of two quantities, the change in the values of "n" for a constant "d" is accompanied by a change in the values of "a", the standard hardness of the material. Hence, these values thus obtained were expected to yield constant results but actual results obtained by different workers revealed disparities amounting to 30-50%. These disparities may be attributed to the following reasons:

- 1) Equation $P = ad^n$ is not valid;
- 2) Microstructures exercise considerable influence on measurements involving very small indentations;
- 3) The experimental errors due to mechanical polishing, preparation of specimen, vibrations, loading rate, indenter shape, measurement of impression, etc., affect the hardness determinations considerably.

In the present case, the microhardness refers to the applied loads ranging from the lowest possible load to maximum load of 200 gms. Further, in what follows the term "hardness" and "microhardness" of crystals are used to indicate the same meaning. d-AHT will be used to indicate ammonium hydrogen d-tartrate single crystals. In the tables the measured and calculated quantities are given upto three places after decimal, as the calculations were carried out by the use of mathematical tables/ calculators. However, the accuracy is upto the first figure after the decimal place. This value is normally considered during discussion. The present work is taken up with

the express purpose of critically re-examining the Meyer's Law and Kick's Law by systematically studying microhardness of synthetic single crystals of d-AHT. It is an extension of the work reported by earlier workers in this laboratory (7,8,9,10,11).

7.1 (c) Experimental:

Single crystals of d-AHT grown from gel by the method described in Chapter IV were used for the present study. The study was carried out on as-grown faces and cleavage faces of d-AHT. Freshly cleaved crystals and clean, smooth, as-grown faces of d-AHT having 2 mm thickness were fixed on glass plates with an adhesive. The levelling of the specimen was tested by using a table microscope. The hardness tester described in Chapter VI was used to produce indentations by using rhomb-based Knoop pyramidal indenter. The filar micrometer eyepiece was used to measure the surface dimensions of the indentation marks. In order to avoid the influence of one indentation mark on the other, the distance between two consecutive indentations was maintained at least four times the diagonal length of the indentation mark, the indentation time for all specimens was kept 15 seconds. The load was varied from 1.25 gms to 160 gms. Care was taken to see that errors introduced during the work of indentation and measurements were avoided or minimized. The indentation marks were produced for different orientations of the longer diagonal of the Knoop indenter with respect to directions [001] on a fresh cleavage plane (010) and m (110) surface and in

case of z(111) face along one of the edges parallel to [100]. These orientations were designated by angle "A" between the reference direction [001] and the longer diagonal of knoop indentation mark in case of cleavage (010) and m(110) and along one of the edges parallel to [100] in case of z(111) face.

The different faces for which measurements were made are:

I the sphenoidal faces : -

- 1) z(111)
- 2) z($\bar{1}\bar{1}\bar{1}$)

II the prism faces m(110) and

III the cleavage faces, (010)

The different angles in degrees for which measurements were made are :

0,10,20,30,40 ... 180 in steps of 10 degrees.

I (a) sphenoidal faces; z(111): 0 - 180°

I (b) sphenoidal faces; z($\bar{1}\bar{1}\bar{1}$): 0 - 180°

II Prism face; m(110); 0 - 180°

III Cleavage; (010); 0 - 180°

Due to non-availability of a hot stage and corresponding optical components of microscope to be used with it in hardness tester, the indentation work was carried out at room temperature (303° K) for studying the variations of hardness with load. For these experiments, crystals of approximately equal sizes were used.

7.1 (d) Observations:

The longer diagonals of the knoop indentation marks produced by various loads for different orientations of indenter were measured. It is assumed that there is negligible elastic recovery in the major diagonal direction compared to the minor diagonal direction when the indenter is removed (12). Several sets consisting of a large number of observations on as-grown faces and freshly cleaved faces of synthetic d-AHT single crystals indented by various loads at room temperature for different orientations of indenter were taken and a typical set of observations, recorded in table 7.1 a,b,c,d were studied graphically by plotting $\log d$ versus $\log P$ (Fig. 7.1(a)i-vi, (b)i-vi, (c)i-vi, (d)i-v) for different A's where P is the load in gms, "A" is the angle in degrees, "d" is the average value of the longer diagonal length of the indentation mark in microns.

7.1 (e) Results and Discussions:

i) Straight line plot of $\log P$ vs $\log d$:

Taking logarithms on both sides of the equation representing Meyer's law for ball indenter or Kick's law for pyramidal indenter yields:

$$\log P = \log a + n \log d \dots (7.2)$$

The values of constants "a" and "n" can thus be determined from a graph of $\log d$ versus $\log P$. Since the relation between $\log P$ and $\log d$ is linear, the graph is a straight line the slope of this line gives the value of "n" and the intercept on $\log P$ axis gives the value of $\log a$ and hence "a". For all indenters that

give geometrically similar shapes (impressions), Meyer's Law/Kick's law postulates a constant value of "n" viz. $n = 2$. This implies a constant hardness value for all loads according to the definition of knoop hardness number (KHN).

A careful study of the graphs ($\log d$ vs $\log P$) shows that there are two clearly recognizable straight lines for all faces including cleavage faces of d-AHT synthetic single crystals of different slopes meeting at a kink, which is obtained at a load of about 30 gms for all faces and all orientations.

The first part of the straight line corresponding to observations taken at low loads upto the kink at room temperature has slope (n_1) of higher value whereas for the second part of the straight line for higher load the slope (n_2) has values around or nearly equal to 2. Since "n" values are different in different regions of the graphs of $\log d$ versus $\log p$, being greater in the first region, the "a" values also vary in two regions being less in the first region of low loads and more in second region of high loads. For Knoop indentation on different faces of d-AHT; the values of "n" and "a" are recorded in Table (7.1) a,b,c,d.

It may be remarked that several workers have reported visible scattering in "n" values, e.g. Hanemann and Schultz (4), Onitsch (5), Grodzinski (6). However, none has reported the splitting of graphs into two straight lines and their characteristics. The study of the variation of load with diagonal length of Vickers indentation mark on faces of different types (c-,m-,d-, and o-

faces) of natural and synthetic barite crystals (13) has shown very clearly the existence of two distinctly recognizable straight lines of the graph of $\log d$ versus $\log p$. Later, Mehta (14), Shah (7), and Acharya (8) verified the splitting of the graph of $\log d$ versus $\log p$ on CaCO_3 , Zn, TGS, KBr, NaCl and KCl crystals. In the present investigation the author has verified for d-AHT, the splitting of the graph into two regions using Knoop pyramidal indenter. The splitting varies with the orientation of the indenter with respect to the crystal lattice. It is thus certain that the splitting of the graph into two straight lines in natural and is due to varied reactions of the crystal surfaces to different applied loads used for producing indentations.

7.1 (f) Modification in Kick's law and Meyer's law:

The analysis of hardness data based on Kick's law and Meyer's law postulates a constant value for n , viz. 2, for all indenters and for all geometrically similar impressions. Schultz and Hanemann (4) supported the above analysis by proposing that hardness number and macrohardness values are comparable. However, Kick's law represented by equation (7.1) has not received wide acceptance on account of the fact that " n " usually has a value less than 2. Hays and Kendall (16) attempted to overcome this difficulty by assuming that a resistance to deformation could be evaluated by considering it as a Newtonian resistance pressure of the specimen itself. They assumed that a part of the applied load is used in overcoming a resistance/pressure "W" which

depends on the nature of the material under test. It is further understood that "W" does not allow any plastic deformation. Hence according to them the effective load which produces indentation and therefore plastic deformation is $(P-W)$ for which the variation is proportional to the square of the diagonal length of the indentation mark, i.e. d . Thus modified Kick's law according to the above understanding is :

$$P - W = bd^n \quad \dots \dots \quad (7.3)$$

or

$$\log(P-W) = \log b + 2 \log d \quad \dots \dots \quad (7.4)$$

where "b" is a constant, likely to be the characteristic of the material and the exponent of "d" is 2. Since the factor "W" allows the limiting case to prevail where microhardness is independent of load, "n" should turn out to be 2. Elimination of P from equation 7.1 and 7.3 yields the value of "W" :

$$W = ad^n - bd^2 \quad \dots \dots \dots \quad (7.5)$$

or

$$d^n = b/ad^2 + W/a \quad \dots \dots \dots \quad (7.6)$$

The equations (7.2), (7.4) and (7.6) can be used to verify experimentally the validity of modified Kick's law (7.3) and assumption for the existence of resistance/pressure "W" by plotting graphs based on experimental observations. Thus by the plot of $\log d$ vs $\log P$ (Figs. 7.1,a,b,c,d) one can obtain the values of exponent "n" and standard hardness "a" as follows (cf.Figs. 7.1 a-d):

Slope = n
 Intercept = log a
 or a = Antilog (intercept) ... (7.7)
 Using the value of "n" from the above, a graph of d^n vs d^2 (Figs. 7.2 (a)i-vi, (b)i-vi ,(c)i-vi, (d)i-vi) can be plotted.
 The plot indicates it to be a straight line graph with the slope and intercept given by :

Slope = b/a
 Intercept = W/a (cf Figs. 7.2, a,b,c,d)
 Hence $b = a \times$ slope
 $W = a \times$ Intercept (7.8)

where the value of "a" obtained from (7.7) is substituted on the right hand side of (7.8). The values of b and W obtained above can be substituted in (7.4) for a plot of $\log(P-W)$ Vs $\log d$ (Figs 7.3, (a)i-iii, (b)i-vi , (c)i-vi, (d)i-vi). The slope n₃ of this graph should be 2 which in turn should establish the validity of modified Kick's law. This is indeed found to be the case for the present study of cleavage faces and as-grown faces of synthetic single crystals of d-AHT in the HLR. Modified Kick's law was also found valid for Calcite (18).

The graph of $\log d$ Vs $\log P$ (cf Figs. 7.1 a,b,c,d) consists of two recognizable straight lines with different slopes n_1 and n_2 and intercepts a_1 and a_2 for low load region (LLR) and high load region (HLR) respectively. Hence for d- AHT crystals, corresponding to two straight lines representing effects of LLR

and HLR, there should be two values of b and W viz. b_1 , W_1 , b_2 , W_2 . This was found to be so for calcite crystals also (18).

In the present case for all faces and for all orientations it was found that modified Kick's law was not applicable in the low load region.

The values for n_2 , n_3 , W_2 , b_2 and a_2 for the HLR of hardness of as-grown faces and cleavage faces of d-AHT single crystals are given in Table (7.2, a,b,c,d).

7.1 (g) Variation of standard hardness and exponent with orientation:

In order to determine the relative importance of various factors affecting the values of "a" and "n", the study was carried out for various orientations of indenter and crystal surfaces at room temperature. It is obvious from table 7.1 that the values of a_1 and n_1 for LLR show comparatively large differences for all orientations (A) of the indenter and for all faces of the crystal. Further their variations appear to have no clear relation with A whereas a_2 and n_2 values obtained from the second part of the graph are independent of A. In view of these observations it is not possible to develop with certainty empirical relations between these variables.

Application of modified Kick's law should eliminate the variation in the exponent of "d". The variations of standard hardness values a_1 and a_2 replaced by b_1 and b_2 with A will now be considered. Since modified Kick's law is not applicable in the

low load region, b_1 and w_1 values are not possible due to the non-linear plot of d^n Vs d^2 . The comparison of b_2 and a_2 values for different but constant A indicate that b_2 values are many times greater than a_2 values. " n_2 " and " n_3 " values are not significantly different from 2. This suggests that modified Kick's law is valid for HLR of hardness for as-grown and cleavage faces of d-AHT.

It is reported that "n" represents the capacity of workhardening of the crystal specimen and that a higher value (>2) of "n" indicates the fully softened state and a lower value the degree of cold-working of the specimen (2). Symbolically for d-AHT single crystals this can be represented in a tabular form:

Region	Meyer's/Kick's laws Exponent Intercept		Modified Kick's law Exponent Intercept
LLR	$n > 2$	a_1 low	not valid
HLR	$n > 2$	a_2 high	$n \approx 2$ b_2 high

It is clear from the above that the physical meaning of a fully softened state and degree of cold-working cannot be quantitatively deduced from the observations on applied load and dimension of the indentation mark. The indentation does produce plastic deformation and cold-working alongwith some elastic recovery. However, the above data is insufficient to explain the physics of static indentation hardness. It further implies that there are several factors such as surface energy, concentration of different types of impurities and imperfections and their interactions, effect of penetration of indenter in the surface

and propagation of stress waves along different directions in the crystal, anisotropy, etc. which operate in a way unpredictable from the present study and are responsible for experimentally observed deviations in the analysis.

A careful study of the values of n_3 and W_2 (Table 7.2, a,b,c,d) for different but constant values of A reveals surprising results. The modified n_3 values are more or less equal to 2 for different orientations of all the different as-grown and cleavage faces. Further, for all the values of "A"s the resistance pressure values " W_2 " are negative. This means that the resistance/pressure which is not assumed to produce plastic deformation helps applied load (HLR) in producing plastic deformation.

This interpretation defeats the very purpose of assuming resistance/pressure. Hence, this implied meaning cannot be accepted. This (negative value) can be understood in terms of reactions of the surface layers and bulk material of this crystal. The negative W_2 values in the HLR suggest that modified Kick's law is not applicable to HLR of hardness of d-AHT single crystals. Further modified values of n_3 namely 2 indicate that while considering the applicability of modified Kick's law, more weightage should be given to the negative values of " W_2 " and less to " n_3 " values.

The above discussion suggests that for $n = 2$ and finite resistance/pressure the Meyer's law/Kick's law is independent of the geometrical nature of the indenter. However, it should be

remarked that optical study of microstructures of indented surfaces by high resolution microscopy indicate that indentations for different applied loads and fixed orientations are similar but not identical.

The above analysis indicates that Kick's law and modified Kick's law are not fully applicable to all crystals (Barite, Calcite, sodium nitrate, Zn, TGS, KBr, KCl and d-AHT) studied in this laboratory. For most of the cases, the modified Kick's law is not valid in LLR due to the non-linear plot between d^n Vs d^2 . Further for some crystals "W" values are negative (e.g. d-AHT, Calcite, etc.). In the application of Kick's law, the variation in "n" and "a" are not fully explainable in LLR and HLR regions of plots of $\log d$ Vs $\log P$. It is therefore, necessary to study the experimental observations on load and indentation mark by considering the whole plot of $\log d$ Vs $\log P$ as a curve and applying the standard curve-fitting method. This assumes that the plot is continuous. Further this also supports the attributions made in section 7.1(b) while discussing the disparities reported by earlier workers.

7.1 (h) Curvilinear plots between diagonal length and applied load:

In the earlier analysis, the plot of $\log d$ Vs $\log P$ consisted of two straight lines with a kink in between them. Instead it is desirable to have a plot of "d" Vs P , so that the standard curve fitting method can be easily applied. Fig 7.4 shows one of

the typical plots of D Vs P. The curve passing through the points is plot of observed readings and the slightly curved straight line is the best fit for the observation. A careful analysis of the plot (19) indicates it to be a quadratic equation:

$$D = AP^2 + BP + C \dots\dots (7.9)$$

where A,B,C are constants obtained from the following equations: (19)

$$\sum_{k=1}^n x_k^4 A + \sum_{k=1}^n x_k^3 B + \sum_{k=1}^n x_k^2 C = \sum_{k=1}^n y_k x_k^2 \dots\dots (7.10)$$

$$\sum_{k=1}^n x_k^3 A + \sum_{k=1}^n x_k^2 B + \sum_{k=1}^n x_k C = \sum_{k=1}^n y_k x_k \dots\dots (7.11)$$

$$\sum_{k=1}^n x_k^2 A + \sum_{k=1}^n x_k B + N C = \sum_{k=1}^n y_k \dots\dots (7.12)$$

where k denoted the number of the observation and N, the total number of observations. The values of A,B & C for different faces and different orientations are recorded in Table .7.3 a,b,c,d.

In the actual work, load was applied to the indenter to produce indentation mark of longer diagonal length "d". The length was measured by a filar micrometer eyepiece. By introducing the values of A,B & C and putting the values of different loads in the equation (7.9), D values were calculated and a comparison of calculated D values with experimentally observed D values were made and the percentage deviation from the calculated D values were found. This is given in Table 7.4 for some orientations on all faces. Further this percentage variation is made for

equations i) $P = ad^n$ and ii) $D = AP^2 + BP + C$. It is clear from the table that the percentage variations for i) is more than the corresponding variations for ii). Hence the obvious conclusion is that experimental observations are graphically better represented by the curvilinear plot and the expression ii).

To verify the values of the constants A,B and C, the equation used was :

$$D_1 = AP_1^2 + BP_1 + C \dots \dots \dots (7.13)$$

$$D_2 = AP_2^2 + BP_2 + C \dots \dots \dots (7.14)$$

subtracting (7.13) - (7.14)

$$\begin{aligned} D_1 - D_2 &= A(P_1^2 - P_2^2) + B(P_1 - P_2) \\ &= A(P_1 + P_2)(P_1 - P_2) + B(P_1 - P_2) \end{aligned}$$

the equation on simplifying becomes,

$$(D_1 - D_2)/(P_1 - P_2) = A(P_1 + P_2) + B \dots \dots \dots (7.15)$$

which gives a straight line whose intercept is B and slope is A. These values were compared with the calculated values of A & B (Fig 7.5 (a)i,(b)i,ii,iii,(c)i,(d)i,ii,iii).

The equation (7.9) is based on the experimental observations. Hence it should be valid for other crystals also (8,11,18). A comparison of this equation with (7.2) and (7.4) indicates that kink at a certain load, is the point showing the splitting of the

two straight lines. The quadratic equation therefore suggests that the kink should be the point of inflexion. This point depends on applied load and the direction along which the indentation is carried out. It is also clear that dependence of kink point on direction is more than that on load. In the earlier studies it had been shown that this point was susceptible to the thermal treatment of the specimen. (11)

For Meyer's Law ($P=ad^n$), it was shown that taking,

$$\log P = \log a + n \log d,$$

there was a linear relation between $\log P$ and $\log d$, which in the present case was shown to be comprising of two straight lines. Solving the equation (eqn. 7.9) for A, B and C, it was found that C had a finite value when $P=0$, i.e. $C=d_0$, when $P=0$.

It is interesting to consider the consequences of having (i) a finite positive value (ii) zero value of C. If C is zero, the equation (7.9) becomes

$$D = AP^2 + BP$$

or

$$D/P = AP + B$$

Hence the plot of D/P Vs P should be a straight line. However, this is not the case. Hence, zero value of C is ruled out. The correlation between the splitting of the graphs of $\log P$ Vs $\log D$ and finite value of C, simply indicates that the C should be associated with the kink point which occurs for applied load of about 30 gm. It can thus be concluded that the finite positive

value of C should be held responsible for the splitting of the graph into two recognisable straight lines.

Alongwith the mathematical interpretation of finite value of C, it is also desirable to consider its physical meaning. Since hardness test is a convenient test of the plastic deformation behaviour of the material, it can be assumed that d_o represents plastic deformation for some unknown load. Hence $(D-d_o)$ should represent the actual deformation where D is the diagonal length for applied load, P.

Thus following Meyer's law/Kick's law,

$$P = ad^2$$

$$P_o = ad_o^2$$

$$P - P_o = a(d^2 - d_o^2) = a(d - d_o)(d + d_o)$$

$$P = a(d - d_o)(d + d_o) + P_o$$

Thus the above equation indicates that a plot of P Vs $(d - d_o)$ $(d + d_o)$ should be a straight line. However, this is not found to be the case. Hence, the obvious conclusion is that Meyer's law and Kick's Law are not valid when C has a finite positive value. Similarly, a plot of log P Vs log $(d + d_o)$ $(d - d_o)$ has not yielded meaningful result.

It was mentioned earlier (cf.chapter 6) that tensile stress operating in unidirectional compression or extension are entirely different from those used in static indentation. This can now be understood better by looking at the above analysis and a simple example of a solid under uniaxial stress. The behaviour

of a material subjected to stress, above the elastic range, may be divided into two parts: i) total plastic deformation and ii) fracture. Part i) can be further be subdivided into a) elastic deformation b) anelastic deformation and c) permanent plastic deformation. This behaviour of a material under unidirectional stress is shown in the stress-strain diagram (fig.7.8) The stress on the material is progressively increased, crossing the elastic range and from a certain point in the plastic region, it is suddenly removed. The material exhibits total strain OD consisting of elastic strain CD and plastic strain OC which includes permanent plastic strain and anelastic strain. In the case of static indentation test, on the removal of applied load, the anelastic strain does not exist whereas there is a plastic deformation which consists of a permanent set and elastic deformation. The observations and analysis indicate that d_0 is the minimum plastic deformation for some unknown applied load. $(D-d_0)$ represents the actual deformation for applied load, P. It consists of elastic deformation and plastic deformation. It is not possible to separate these deformations. Hence any plot involving applied load and $(D-d_0)$ should not yield a linear relation. This is indeed found to be the case as mentioned above.

This simply indicates that although d_0 represents plastic deformation and is associated with the Kink in the plot of $\log P$ Vs $\log d$ it is difficult to relate it to equations given by Meyer's law and Kick's law and hence modified Kick's law.

Conclusions:

The mathematical treatment of measurements of diagonal length (d) of indentation mark and applied load P, based on Meyer's law, Kick's Law and quadratic equation has shown very clearly that,

- a) the graphical analysis of variation of diagonal length of indentation mark with applied load clearly suggests that there are two regions of applied loads, namely low load region and high load region, where the behaviour of d-AHT appears to be different.
- b) Consideration of the values of intercepts and resistance/pressure shows clearly that application of modified Kick's law is highly limited.
- c) The indentation does produce plastic deformation (hence workhardening) and cold working along with some elastic recovery, however, the present analysis is insufficient to explain the physics of static indentation hardness.
- d) The values of intercepts slopes and resistance/pressure are indicative of the anisotropic character of the crystal. However, the present analysis is incapable of finding their individual effects on the anisotropic character.
- e) the kink observed in the straight line graphs of $\log P$ Vs $\log d$, is a point of inflexion in the curvilinear plot of $\log P$ vs $\log d$ or P vs d .
- f) The Kink is connected with d_0 , the plastic deformation for unknown load P_0 .

- g) For an applied load, P, the deformation (D_{do}) consists of elastic and plastic deformation which cannot be separated.
- h) The treatment based on empirical laws is insufficient to unfold the actual mechanism operating in a material under hardness test. However, the expression used for the best fit of the curve of P vs d (or $\log P$ vs $\log d$) appears to be more reliable than empirical laws.

REFERENCES

01. Meyer, L (1908)
Quoted in "The Science of Hardness Testing and its Research Applications", American Soc. for Metals, Ohio, 1973.
Quoted in "Microindentation Hardness Testing", Butterworths Scientific Publications, London, Ch.1, 1956.
02. Mott, B.W, "Microindentation Hardness Testing", Butterworth Scientific Publications, London, Ch.1., 1956.
03. Kick, F
Das Ge Setzder Proportionalen Widerstände and Science Ans Wandring (Leipzig Felix.ed) 1885.
04. Hanemann, H & Schultz, F; Metalkunde, Z 33, 122, 1941.
05. Onistsch, E.M
Microsekopie, 2, 131, 1947.
06. Grodzinski, P
Schwaiz, arch, angew wiss, 18, 282, 1952.
07. Shah, R.T
Ph.D Thesis, M S Uni. Baroda, 1976.
08. Acharya, C.T
Ph.D Thesis, M S Uni. Baroda, 1978.
09. Bhagia, L.J
Ph.D Thesis, M S Uni. Baroda, 1982.
10. Shah, A.J
Ph.D Thesis, M S Uni. Baroda, 1984.
11. Patel, M.B
Ph.D Thesis, M S Uni. Baroda, 1987.
12. Tabor, D
The Hardness of Metals, Oxford Uni Press, 100, 1951.
13. Saraf, C.L
Ph.D Thesis, M S Uni. Baroda, 1971.
14. Mehta, B.J
Ph.D Thesis, M S Uni. Baroda, 1972.

15. Bhagat, S.D
Dissertation, M S Uni. Baroda, 1982.
16. Hays, C & Kindall, E.G
Metallography, 6, 275, 1973.
17. Pratap, K.J & Haribabu, V
Bull. Mater Sci., 2, 43, 1980.
18. Joshi, D.R
Ph.D Thesis, M S Uni. Baroda, 1989.
19. Shah. C.C
Advances Topics in Engineering mathematics
IV edition 1966.

CHAPTER 7

Hardness of d-AHT crystals

Sl. No.	Contents	Page
7.2	Introduction	115
7.2(a)	Observations	121
7.2(b)	Results & Discussions	121
7.2(c)	Conclusions	126
	References	

Hardness Anisotropy of orthorhombic crystals:-

synthetic d-AHT single crystals

Sl. No.	Contents	Page
7.3	Introduction	127
7.3(a)	Observations	128
7.3(b)	Results & Discussions	129
7.3(c)	Conclusions	131
	References	
	List of Tables	
	Caption to Figures	

HARDNESS OF d-AHT

Introduction:

From the discussion of the previous chapter it is clear that application of modified Kick's law to the cleavage and as-grown faces of d-AHT is highly limited.

The present chapter considers this point alongwith a detailed study of variation of hardness expressed by hardness number with orientation of the knoop indenter with respect to the crystal lattice. The knoop hardness number, H, is defined by the equation (1):

$$H = 14230 P/d^2 \quad \dots \dots \dots \quad (7.16)$$

$$H = c P/d^2 \quad \dots \dots \dots \quad (7.17)$$

where applied load, "P" is in gms and the diagonal length "d" of the indentation mark is in microns and $c = 14230$, is a constant of the indenter geometry. This factor can be obtained in the following way from the general definition of Knoop hardness number :

$$H \text{ (kg/sq mm)} = \frac{\text{Applied load } P \text{ (kg)}}{\text{Projected area of the Knoop indentation mark } A \text{ (sq mm)}} \quad \dots \dots \dots \quad (7.17a)$$

The projected area A is given by :

$$A = 1/2 d^2 \cot 172.5/2 \tan 130/2$$

$$\begin{aligned} A &= 1/2 d^2 (0.0655) (2.1455) \\ &= d^2 (0.07028) \end{aligned}$$

where "d" is in mm and 172.5 and 130 are the angles made by the opposite edges of the indenter (cf. Chapter VI Fig. 6.1)

Thus :

$$\begin{aligned} H &= P/A \\ &= P / 0.07028 d^2 \\ &= 14.230 P/d^2 \text{ Kg/sqmm} \end{aligned}$$

In the above formula P is in Kg and d is in mm. In actual work P is in gms and d is in microns (μm). Hence following the usual conversion, one obtains,

$$H = 14230 P/d^2 \dots \dots \dots \quad (7.18)$$

where P is in gms and d is in microns.

The hardness number H is not an ordinary number, but a constant having dimensions of stress and has a deep but less understood physical meaning. The combination of (7.17) with Meyer's law / Kick's law ($P = ad^n$) yields:

$$H = c.a.d^{n-2} \dots \dots \dots \quad (7.19)$$

or in terms of applied load and hardness number it is given by :

$$H = c. a^{2/n} . p^{n-2/n} \dots \dots \dots \quad (7.20)$$

The above equation can be tested by comparing the values of left hand and right hand sides obtained from measurements. Thus H can be determined from (7.18) whereas on the right hand side the value of "a" can be substituted from the earlier studies of the above laws (Meyer's law). Since c and P or d are known, the right hand side value can be calculated. Comparison of values

obtained for the two sides of (7.19), (7.20) can indicate the degree of correlation of the experimental work with the theoretical work.

Instead of using Kick's law, it is also possible to use modified Kick's law by putting $n = 2$ and substituting $(P-W)$ instead of P in the above formulae. Thus :

$$\begin{aligned} H &= c \times (P-W)/d^2 \\ (P-W) &= bd^2 \\ H &= cb \dots \dots \dots \quad (7.21) \end{aligned}$$

Since c and b are constants, the above equation indicates that hardness is a constant quantity, independent of applied load and dimension of the indentation mark. It was shown earlier (Section 7.1) that modified Kick's law is independent of indenter (ball or pyramidal) geometry. Thus the above equation shows that the multiplication of geometrical constant (numerical figure) with "b" the standard hardness, gives the hardness number. The present work aims at analysing the hardness behaviour by examining the relations (7.19), (7.20) and (7.21) experimentally.

It also aims at studying variation of hardness with orientation.

It is mentioned above that the dimensions of hardness number and stress are the same. This similarity appears to have been obtained from the consideration of a solid subjected to uniaxial compression (or extension). For a uniaxially compressed solid, the Young's modulus of elasticity (E) is given by :

$$E = \sigma / \epsilon \quad \text{--- (7.22)}$$

where σ is the compressive stress defined as load per unit area.

$$\sigma = P/A \quad \text{--- (7.23)}$$

and the compressive strain ϵ is defined as the decrease in length per unit length. The area of cross-section, A , increases with compression. Hence for a constant volume of a geometrically well defined solid, length is inversely proportional to the area of cross-section. If A_0 represents the initial area of cross-section with a normal length l_0 and A , the final area with normal length l after small compression, one obtains:

$$l \cdot A = l_0 \cdot A_0 \quad \text{or}$$

$$l/l_0 = A_0/A \quad \text{--- (7.24)}$$

Therefore,

$$\begin{aligned} \epsilon &= (l-l_0)/l \\ &= (A_0-A)/A \quad \text{--- (7.25)} \end{aligned}$$

substitution of σ and ϵ from (7.23) and (7.25) in (7.22) gives :

$$E = P/(A_0 - A) \quad \text{--- (7.26)}$$

Hence, for a simple uniaxial compressive stress, when the area is a geometrical function of deformation, determined here by constant volume, the resistance to permanent deformation can be expressed simply in terms of load and corresponding area. In indentation process, the volume change is very very small; volume of solid can therefore be considered as constant. Hence the indentation hardness can be measured by using the above formula (7.26).

Indenters are made in various geometrical shapes such as spheres, pyramids, etc. The area over which the force due to load on the indenter acts, increases with the depth of penetration. The resistance to permanent deformation or hardness can be expressed in terms of force or load and area alone (and/or depth of penetration). These remarks are true for solids which are amorphous or highly homogeneous and isotropic.

The above analysis presents a highly simplified picture of the processes involved because there is a great difference between deforming a solid under a simple uniaxial compression and deforming a surface of a solid by pressing a small indenter into it. Around the indentation mark, the stress distribution is exceedingly complex and the stressed material is under the influence of multiaxial stresses. The sharp corners of a pyramidal indenter produces a sizeable amount of plastic deformation which may reach 30% or more at the tip of the indenter. This should be compared with the deformation of a crystalline material which is even less than one percent of its original dimension. Further the surface of contact is inclined by varying amounts to the directions of applied force. In view of these complications a simple expression corresponding to that for the modulus of elasticity cannot be derived for hardness. In the absence of any formula based on concrete theory an arbitrary expression is used which includes both known variables loads and area in the present case. Hence the hardness number, H , is defined as the ratio of the load to the area of impression:

$$H = P/A \text{ -----(7.27)}$$

For pyramidal indenters the load P varies as the square of the diagonal d . Thus for a given shape of pyramid :

$$P = ed^2 \text{ -----(7.28)}$$

where "e" is a constant which depends on the material and shape of the pyramid. The area of the impression, A , is also proportional to the square of the diagonal :

$$A = f d^2 \text{ -----(7.29)}$$

where "f" depends upon the shape of the pyramid. Combination of equations 7.27, 7.28 and 7.29 gives :

$$H = ed^2/fd^2 = e/f = \text{constant --- (7.28)}$$

Hence for a given shape of pyramidal indenter, hardness is independent of load and size of indentation. This statement represents Kick's law. In view of defining equation (7.17a) for hardness, hardness number can also be considered as hardness modulus.

Due to the complicated behaviour of indented anisotropic single crystals of various materials and arbitrary expression for hardness, it is clear that theoretical treatment of the problem is extremely difficult. Hence it is desirable to approach this problem via experimental observations, interpretations and with a probable development of empirical relations(s). Further the analysis can be used for developing model theory/theories of hardness. The present work is taken up from this phenomenological point of view and is an extension of the work carried out by earlier workers. (2-9)

7.2 (a)Observations:

The observations which were recorded for studying the Kick's law/Meyer's law ($P = ad^n$) are used in the present investigation. The Knoop hardness numbers are calculated using equation (7.16) for various orientations. (Table-7.5 a,b,c,d). The observations are graphically studied by plotting the graph of Hardness number H versus load P (Figs 7.6 (a)i-ii, (b)i-ii, (c)i, (d)i-ii). In what follows the hardness and Knoop hardness number will be used to indicate the same meaning.

7.2 (b)Results and Discussions:

Variation of Knoop Hardness number with applied load at constant temperature and indenter orientation:

It is clear from the graphical analysis of the variation of hardness number H with load P (Figs 7.6,a,b,c,d) that contrary to theoretical expectations, the hardness varies with load. For d-AHT single crystals, the hardness at first increases with load for all orientations, reaches a maximum value at a certain load, then gradually decreases with increasing load and attains almost a constant value for all higher applied loads. The complex behaviour of microhardness with load can be explained qualitatively on the basis of depth of penetration of the indenter. At small loads the indenter penetrates only surface layers, hence the effect is shown more sharply at these loads. However, as the depth of penetration increases, the effect of the surface layers become less dominant and after a certain depth of

penetration, the effect of the inner layers become more and more prominent than those of surface layers and ultimately there is practically no change in the value of hardness with load. This is apparent from the graphs of Knoop hardness number Vs load.

It is clear from the plots of H Vs P that the theoretical conclusion that hardness is independent of load appears to be true only at higher loads. The graph of H Vs P can be conveniently divided into three parts, AB, BC and CD, where the first part represents the linear relation between hardness and load, the second part the non-linear relation and the third part the linear one. In some cases BC part is absent. It should be noted that there is a fundamental difference between linear noted that there is a fundamental differences between linear portions AB and CD of the graph ABCD. This possibly reflects varied reactions of the surfaces to loads belonging to different regions.

The present approach for the study of hardness behaviour with a change in different parameters is an integrated one. Hence the graphical analysis of $\log d$ vs $\log P$ plots (cf. Chapter 7.1) should now be extended in the present work by studying the relations (7.19), (7.20) and (7.21) namely,

$$(7.19) \dots H = c.a.d(n-2)$$

$$(7.20) \dots H = c.a^{2/n} . p(n-2)/n$$

$$(7.21) \dots H = c. b..$$

For synthetic d-AHT single crystals, there exists two distinct regions of applied load, viz. LLR and HLR corresponding to plot of $\log d$ vs $\log P$ consisting of two straight lines with different slopes (n_1 & n_2) and intercepts (a_1 & a_2) or to two regions/parts on either side of the pointer of inflexion whereas the plot of H vs P (Fig. 7.6 a,b,c,d) shows three ranges of applied load, viz. low load region LLR, intermediate load region ILR and high load region HLR designated by AB, BC and CD respectively and that CD corresponds to that range of applied loads where hardness number calculated by using equation (7.14) is almost constant and independent of applied load. It is clear from the plots that for applied loads greater than 30 gms hardness is constant and independent of load. It is in this range hardness behaviour of these crystals is analysed and reported in the present work.

It was shown in the earlier chapter that the straight line plot of $\log d$ vs $\log P$ consists of two straight lines with different slopes and intercepts corresponding to LLR & HLR. The slope and intercept in this region (HLR) are n_2 and a_2 respectively. In the case of modified Kick's law b_2 corresponds to a_2 and $n_3 = 2$. This is equally true for curvilinear plots with a point of inflexion. It is therefore desirable to consider the following relations:

$$H = c a_2 d(n - 2) \dots \dots \dots (7.31)$$

$$H = c a_2 (2/n) . p(n - 2)/n \dots \dots \dots (7.32)$$

$$H = c b_2 \dots \dots \dots (7.33)$$

instead of (7.19), (7.20) & (7.21) and try to find the correlation amongst these relations. The observed graphical values of hardness can now be compared with the values of hardness at constant temperature and orientation, calculated from the formulae (7.32) & (7.33) and presented in a tabular form (Table 7.6). Table 7.7 indicates percentage deviation of hardness values from the observed values. It is clear from table 7.7 that the percentage deviation is very large indicating very little correlation between hardness values (Table 7.6). It can be concluded that hardness behaviour of synthetic d- AHT single crystals at constant temperature and orientation indicates very little correlation amongst Meyer's law/Kick's law, modified Kick's law and formula for hardness number. This was the case with calcite cleavages also, but not with sodium nitrate cleavages which gave a very good correlation amongst Meyer's law/Kick's law, modified Kick's law and formula for hardness number (9). This simply suggests that the basic symmetry elements physical and chemical properties of these different crystals might be intimately connected with the mechanical behaviour indicated by hardness at applied loads.

It is difficult to give the exact reason responsible for observing the three different regions in the hardness plot. There are several factors such as anisotropy, imperfections and their interactions, introduction of additional imperfections on indentations and their interactions among themselves and with the grown-in imperfections, range of hardness numbers etc., which should be acting in a way unpredictable from the present study.

Since the present approach for studying hardness is an integrated one, it is, therefore, natural to have the extension of the analysis of variation of load with diagonal length. Following the analysis, it is possible to represent hardness curve by a quadratic equation:

$$H = XP^2 + YP + Z \dots \dots (7.34)$$

where X, Y, Z are the constants of the equation. Following the method for the best fit curve, the values of these constants are obtained. These values are different for different faces. Thus, for cleavage face,

$$X = -0.002 \quad Y = 0.51 \quad Z = 10.28$$

For prism face,

$$X = -0.002 \quad Y = 0.44 \quad Z = 9.6$$

It is clear from the above values that X,Y,Z are not very much different for different faces.

For P=0, H=H_o, say. Putting these values in 7.34 one obtains,

$$H_o = Z$$

$$\text{Thus } H = XP^2 + YP + H_o \quad (7.35)$$

Using the above equation, a table is prepared showing the values of hardness number calculated on the basis of the above formula, H_{cal} and also the one which is obtained by using formula for Knoop hardness number, H_k (cf.eqn.7.18). The percentage deviation from the H_k values, namely $(H_k - H_{cal})/(H_k)$ are also shown in table 7.9. It is thus clear from the above table, that the percentage deviations are quite noticeable. Hence it can be

concluded that the above analysis, although mathematically exact, is incomplete, some unknown important parameter is also involved. This situation is similar to one experienced while analysing the quadratic equation (7.9), relating diagonal length of indentation mark and the applied load. It is thus clear that the present empirical analysis is unable to unfold the mechanism operating on an indented surface.

7.2 (c) Conclusions:

1. Hardness varies with load. It increases steeply initially with load for all orientations and for all the different faces, then the increase is gradual and attains almost a constant value for all higher applied loads. This behaviour reflects the varied reactions of the surfaces to the applied loads.
2. Irrespective of the indenter geometry, Meyer's law/Kick's law, modified Kick's law and hardness formula cannot be experimentally correlated with one another for synthetic d-AHT single crystals.

REFERENCES

01. Mott, B.L
"Microindentation Hardness Testing"
Butterworth Scientific Publication, London,
Ch.1, 1956.
02. Saraf, C.L
Ph.D Thesis, M S Uni. Baroda, 1971.
03. Mehta, B.J
Ph.D Thesis, M S Uni. Baroda, 1972.
04. Shah, R.T
Ph.D Thesis, M S Uni., Baroda, 1976.
05. Acharya, C.T
Ph.D Thesis, M S Uni., Baroda, 1978.
06. Bhagia, L.J
Ph.D Thesis, M S Uni., Baroda, 1982.
07. Shah, A.J
Ph.D Thesis, M S Uni., Baroda, 1984.
08. Patel, M.B
Ph.D Thesis, M S Uni., Baroda, 1987.
09. Joshi, D.R
Ph.D Thesis, M S Uni., Baroda, 1989.

HARDNESS ANISOTROPY OF ORTHORHOMBIC CRYSTALS

SYNTHETIC d-AHT SINGLE CRYSTALS.

7.3 Introduction:

In the earlier chapter the hardness of d-AHT was experimentally studied by considering their variation with applied load for different but constant orientations of the indenter with the crystal lattice. The present work aims at studying the microhardness anisotropy of d-AHT by employing Knoop indenter of low symmetry. An important feature of the Knoop hardness test is that the hardness value is dependent on the orientation of the major axis of the indenter in a given plane as well as on the orientation of the plane itself with reference to the principal axis of anisotropy (1). Further the depth of penetration of indenter is shallow. Hence brittle materials like glass or mineral could be indented without causing premature fracture. Besides, the indenter shape is relatively non-symmetric, the variation in hardness along different directions on a given surface can be determined. For such a study, single crystals can serve as ideal materials to establish the orientation dependence of hardness values. It is from this point of view that hardness anisotropy study of synthetic single crystals of d-AHT is carried out and reported here.

It is apparent from the hardness studies presented here that macroscopically there are three parameters affecting hardness viz. i) applied load; ii) orientation of the indenter diagonal (major) with reference to the crystal lattice; & iii) crystal

plane under indentation. The empirical formulae derived in the present work is valid for majority of crystals of different materials (2).

7.3 (a) Observations:

For studying the anisotropic behaviour of orthorhombic crystals of d-AHT, the observations recorded in Chapter 7.1 are used for considering in a quantitative manner the effect of the three major factors, viz. i) Applied Load (P); ii) Orientation of the major diagonal of indenter with reference to direction [001] on a fresh cleavage plane (010) and m(110) surface and in case of z(111) face along one of the edges parallel to [100] and iii) Crystal plane/face for indentation (F). For the purpose of quantitative study of the relations amongst P, A, H and F; variations between any two factors are considered by keeping remaining parameters constant. The applied load P should be considered as constant. However, it was shown (vide Chapter 7.2) that it represents a range of applied loads in HLR where hardness (H) is constant and independent of load. The range of applied loads was from 30 to 160 gms. In this range of applied loads, there is a slight change in values of hardness. In the discussion, mean value of hardness was considered. The hardness anisotropy for different orientations is studied at constant temperature, viz. room temperature. Thus the approach to hardness study is basically phenomenological. This approach is likely to be useful for the development of model theory of hardness of crystalline materials.

7.3 (b) Results and Discussions:

Table 7.8 presents values of Hardness number, H, in Kg/Sq.mm for different orientations of Knoop indenter (range 0-180°) and for cleavage, prism and sphenoidal faces. The plots of Hardness Vs Angle for prism and sphenoidal faces are shown in figs. 7.7(a) and 7.7(b). Following the curve fitting method, the equation showing the relation between hardness (H) and angle (A) is represented by a power series:

$$H = a_0 + a_1 A + a_2 A^2 + a_3 A^3 + a_4 A^4 + a_5 A^5 + \dots + a_n A^n \dots \quad (7.36)$$

where a_0 , a_1 , a_2 , ..., a_n are constants of the nth power equation. Following polynomial method for nth degree equation, the values of constants for different faces were computed and is given in Table 7.10. Since the coefficients are upto 10th degree of A, the above equation is rewritten as,

$$H = a_0 + a_1 A + a_2 A^2 + a_3 A^3 + a_4 A^4 + a_5 A^5 + a_6 A^6 + a_7 A^7 + a_8 A^8 + a_9 A^9 + a_{10} A^{10}$$

It is clear from the table 7.10 that the coefficients of As are decreasing with the increase in degree of A and becomes negligible but because of the power of A, they cannot be neglected. Further, the order of signs before the coefficients is important from the point of view of symmetry e.g. m-face and cleavage face has planes of symmetry. Hence the order of signs of coefficients of A, A^2 to ... A^{10} are alternately positive and negative, whereas this is not the case for z-face which does not possess any symmetry element. These coefficients are also

associated with anisotropy because hardness values are different along different directions on the same face i.e. planar anisotropy; even in space these values should be different. It is therefore, desirable to designate these coefficients as anisotropic coefficients.

When $A=0$, the hardness value has a finite value along a reference direction which is different for different faces. Thus for prism and cleavage face, the reference direction is [001] and for z-face it is [100]. Thus for these faces, a_0 values will be as follows:

For cleavage face c (010), $a_0 = 31.74 = H_{(001)} = H_0$
prism face m (110), $a_0 = 30.4 = H_{(001)} = H_0$
z-face z(111), $a_0 = 40.7 = H_{100} = H_0$

These values are in agreement with the observed ones mentioned in Table 7.8.

It is interesting to note that if the hardness values are taken upto 90° , the equation relating hardness and orientation is of the 2nd order in A instead of the tenth order (7.36). The 2nd degree equation is as follows:

$$H = a_0 + a_1 A + a_2 A^2$$

When this equation is applied to prism face m (110), the anisotropic coefficients are as under:

$$a_0 = 28.18$$

$$a_1 = 0.733$$

$$a_2 = -0.002$$

These values are obviously different because the observations are restricted upto 90° . This range of observations are taken in view of the observations on hardness and orientations reported by other workers for different crystals. The observations on hardness values for different orientations and for different crystals are presented in a tabular form in Table 7.11.

It is clear from the table on hardness anisotropic coefficients for the above mentioned crystals (Table 7.12) that for $A=0$, the values of a_0 for the above crystals agree with the observed values along the corresponding reference direction.

7.3 (d) Conclusions:

1. Hardness anisotropic coefficients are obtained from the graphical analysis of the observed data.
2. The analysis is extended to the observation reported in the literature for different crystals and the hardness anisotropic coefficients for these crystals are determined.

Angle >	0	10	20	30	40	50	60	70	80	90	100	110	120	130	140	150	160	170	180
Log(P) <																			
0.097	1.861	1.851	1.851	1.798	1.765	1.784	1.761	1.735	1.721	1.728	1.721	1.721	1.721	1.721	1.721	1.721	1.721	1.721	1.831
0.398	1.925	1.887	1.859	1.820	1.807	1.795	1.772	1.751	1.731	1.747	1.741	1.735	1.769	1.769	1.769	1.769	1.769	1.769	1.866
0.574	1.937	1.876	1.861	1.833	1.820	1.804	1.801	1.763	1.751	1.754	1.760	1.751	1.775	1.775	1.775	1.775	1.775	1.775	1.884
0.699	1.961	1.905	1.873	1.849	1.861	1.812	1.815	1.769	1.763	1.775	1.763	1.778	1.787	1.787	1.787	1.787	1.787	1.787	1.889
0.796	1.949	1.912	1.892	1.872	1.866	1.846	1.826	1.775	1.769	1.781	1.781	1.781	1.781	1.781	1.781	1.781	1.781	1.781	1.936
0.875	1.961	1.931	1.898	1.898	1.910	1.880	1.851	1.836	1.784	1.781	1.787	1.781	1.787	1.801	1.787	1.809	1.836	1.851	1.945
0.942	1.984	1.941	1.925	1.916	1.872	1.856	1.854	1.798	1.787	1.787	1.793	1.809	1.793	1.793	1.793	1.820	1.856	1.880	1.949
1.000	1.991	1.945	1.937	1.920	1.905	1.861	1.861	1.809	1.804	1.807	1.815	1.798	1.831	1.831	1.831	1.861	1.886	1.889	1.953
1.051	2.019	1.972	1.955	1.929	1.918	1.866	1.907	1.815	1.815	1.817	1.820	1.815	1.836	1.836	1.836	1.880	1.875	1.925	1.957
1.097	2.042	1.976	1.961	1.941	1.925	1.871	1.887	1.887	1.887	1.887	1.887	1.887	1.887	1.887	1.887	1.885	1.885	1.885	1.961
1.138	2.019	1.987	1.965	1.963	1.929	1.889	1.894	1.851	1.851	1.836	1.826	1.841	1.836	1.836	1.836	1.889	1.889	1.889	1.969
1.176	2.042	1.993	1.972	1.972	1.933	1.910	1.903	1.856	1.846	1.836	1.846	1.846	1.846	1.846	1.846	1.861	1.861	1.861	1.972
1.211	2.019	1.998	1.980	1.993	1.948	1.916	1.912	1.861	1.851	1.846	1.856	1.851	1.856	1.856	1.856	1.861	1.861	1.861	1.980
1.243	2.026	2.002	1.985	1.985	1.965	1.925	1.925	1.866	1.856	1.856	1.866	1.861	1.871	1.871	1.871	1.871	1.871	1.871	1.969
1.273	2.029	2.007	2.003	2.002	1.969	1.927	1.927	1.871	1.885	1.885	1.885	1.885	1.885	1.885	1.885	1.885	1.885	1.885	1.969
1.301	2.058	2.024	2.012	2.009	1.972	1.945	1.945	1.949	1.949	1.949	1.949	1.949	1.949	1.949	1.949	1.949	1.949	1.949	1.980
1.398	2.085	2.055	2.027	2.017	1.989	1.969	1.969	1.953	1.953	1.925	1.925	1.925	1.925	1.925	1.925	1.925	1.925	1.925	1.984
1.477	2.137	2.091	2.047	2.089	1.994	1.972	1.941	1.871	1.871	1.885	1.866	1.878	1.866	1.866	1.866	1.886	1.886	1.886	1.969
1.602	2.162	2.114	2.106	2.101	2.048	2.044	2.005	1.993	2.003	1.980	1.980	1.980	1.937	1.941	1.941	1.941	1.941	1.941	1.972
1.699	2.211	2.128	2.150	2.135	2.058	2.072	2.072	2.070	2.044	2.026	2.026	2.026	1.912	1.912	1.912	1.912	1.912	1.912	1.980
1.778	2.213	2.206	2.186	2.166	2.101	2.134	2.088	2.070	2.037	2.032	2.034	2.037	2.037	2.037	2.037	2.076	2.076	2.076	2.127
1.845	2.230	2.212	2.195	2.202	2.138	2.145	2.094	2.076	2.073	2.052	2.056	2.048	2.048	2.048	2.048	2.048	2.048	2.048	2.182
1.903	2.330	2.264	2.257	2.207	2.168	2.165	2.124	2.140	2.076	2.082	2.086	2.069	2.105	2.134	2.134	2.052	2.052	2.052	2.036
2.000	2.338	2.266	2.306	2.286	2.193	2.198	2.156	2.162	2.137	2.133	2.141	2.143	2.147	2.185	2.185	2.058	2.058	2.058	2.194
2.079	2.376	2.323	2.311	2.316	2.223	2.249	2.244	2.201	2.173	2.169	2.166	2.180	2.190	2.237	2.237	2.244	2.244	2.244	2.367
2.146	2.383	2.376	2.353	2.324	2.285	2.263	2.286	2.221	2.250	2.203	2.214	2.226	2.258	2.277	2.317	2.346	2.362	2.362	2.367
2.204	2.418	2.399	2.360	2.340	2.323	2.293	2.314	2.259	2.252	2.238	2.229	2.252	2.270	2.270	2.272	2.292	2.352	2.366	2.409
N1	6.904	6.083	5.746	4.373	5.258	5.896	5.606	6.044	6.091	7.119	6.639	6.138	7.388	5.465	5.831	5.252	6.525	6.400	7.879
N2	2.343	2.348	2.457	2.640	2.612	2.525	2.478	2.393	2.494	2.553	2.579	2.559	2.429	2.580	2.504	2.511	2.422	2.459	2.220
A1	1.6e-13	1.2e-11	6.8e-11	3.4e-08	9.1e-10	8.6e-11	3.1e-10	9.3e-11	8.8e-11	1.2e-12	7.7e-12	7.0e-11	2.7e-13	5.8e-10	1.0e-10	8.0e-10	2.8e-12	4.1e-12	4.1e-15
A2	3.4e-04	4.0e-04	2.5e-04	1.1e-04	1.7e-04	2.7e-04	3.7e-04	6.5e-04	4.4e-04	3.5e-04	3.2e-04	3.1e-04	5.6e-04	3.0e-04	2.4e-04	3.2e-04	2.3e-04	2.3e-04	6.3e-04

Room Temp. 30°C
Face m(110)

TABLE 7.1 (a)
Knoop indenter for prism face

Angle(°)	0	10	20	30	40	50	60	70	80	90	100	110	120	130	140	150	160	170	180
Log(P) <																			
0.097	1.894	1.851	1.866	1.880	1.826	1.836	1.793	1.738	1.744	1.731	1.856	1.809	1.804	1.826	1.836	1.841	1.851	1.851	1.898
0.398	1.903	1.836	1.894	1.898	1.836	1.896	1.809	1.804	1.751	1.757	1.744	1.866	1.831	1.815	1.846	1.856	1.856	1.856	1.916
0.574	1.912	1.871	1.903	1.907	1.846	1.851	1.815	1.763	1.763	1.751	1.871	1.851	1.851	1.841	1.856	1.866	1.866	1.866	1.933
0.699	1.925	1.880	1.912	1.912	1.856	1.861	1.831	1.826	1.775	1.769	1.763	1.875	1.871	1.831	1.861	1.880	1.880	1.889	1.949
0.796	1.941	1.894	1.916	1.916	1.861	1.866	1.841	1.831	1.787	1.775	1.880	1.875	1.836	1.836	1.866	1.866	1.889	1.889	1.957
0.875	1.961	1.898	1.920	1.925	1.866	1.875	1.846	1.836	1.798	1.787	1.889	1.880	1.841	1.841	1.861	1.871	1.898	1.907	1.957
0.942	1.965	1.925	1.925	1.937	1.880	1.885	1.851	1.846	1.804	1.793	1.798	1.798	1.889	1.889	1.846	1.875	1.912	1.925	1.965
1.000	1.969	1.929	1.929	1.949	1.889	1.889	1.866	1.861	1.809	1.798	1.804	1.803	1.894	1.894	1.851	1.880	1.925	1.945	1.972
1.051	1.972	1.933	1.933	1.953	1.898	1.898	1.880	1.875	1.815	1.815	1.815	1.815	1.907	1.907	1.861	1.885	1.933	1.949	1.976
1.097	1.976	1.953	1.937	1.965	1.912	1.907	1.894	1.889	1.831	1.836	1.826	1.826	1.912	1.920	1.871	1.898	1.941	1.953	1.980
1.138	1.984	1.984	1.961	1.953	1.969	1.916	1.912	1.903	1.851	1.851	1.836	1.836	1.916	1.933	1.880	1.912	1.949	1.955	1.972
1.176	1.987	1.987	1.969	1.969	1.984	1.920	1.920	1.912	1.866	1.866	1.866	1.866	1.920	1.949	1.889	1.933	1.929	1.957	1.976
1.211	2.012	1.994	1.976	2.002	1.929	1.929	1.929	1.920	1.875	1.875	1.861	1.861	1.925	1.953	1.907	1.945	1.941	1.965	2.012
1.243	2.015	1.984	2.015	1.984	2.009	1.933	1.937	1.945	1.903	1.903	1.893	1.893	1.933	1.933	1.880	1.912	1.949	1.961	1.984
1.273	2.019	2.019	1.991	2.012	1.945	1.945	1.945	1.945	1.903	1.903	1.893	1.893	1.933	1.933	1.880	1.912	1.949	1.961	1.984
1.301	2.052	2.039	2.002	2.022	1.961	1.953	1.961	1.961	1.937	1.937	1.937	1.937	1.941	1.941	1.941	1.945	1.945	1.965	1.984
1.398	2.058	2.052	2.019	2.032	1.980	2.002	1.969	1.969	1.949	1.949	1.949	1.949	1.941	1.941	1.941	1.945	1.957	1.972	2.036
1.477	2.096	2.067	2.061	2.073	2.009	2.026	1.998	1.998	1.953	1.953	1.953	1.953	1.989	1.989	1.933	1.961	1.945	1.976	2.055
1.602	2.150	2.129	2.099	2.124	2.052	2.032	2.032	2.029	1.991	1.991	1.991	1.991	1.941	1.941	1.969	1.965	1.991	1.984	2.076
1.699	2.202	2.177	2.129	2.162	2.082	2.082	2.082	2.039	2.019	2.045	2.045	2.045	2.071	2.071	1.984	2.005	2.002	2.008	2.094
1.778	2.232	2.219	2.204	2.204	2.119	2.116	2.055	2.076	2.042	2.042	1.985	1.985	1.929	1.929	1.998	1.998	2.022	2.022	2.113
1.845	2.242	2.268	2.217	2.221	2.152	2.154	2.108	2.113	2.105	2.105	2.079	2.079	2.127	2.127	2.147	2.147	2.147	2.147	2.246
1.903	2.264	2.292	2.234	2.228	2.162	2.190	2.129	2.165	2.119	2.082	2.110	2.110	2.165	2.165	2.167	2.179	2.177	2.202	2.275
2.000	2.311	2.338	2.266	2.283	2.208	2.217	2.181	2.174	2.181	2.119	2.132	2.197	2.197	2.199	2.199	2.206	2.215	2.223	2.283
2.041	2.318	2.343	2.285	2.290	2.215	2.228	2.190	2.186	2.190	2.129	2.140	2.221	2.221	2.223	2.223	2.232	2.244	2.294	2.333
2.079	2.356	2.374	2.297	2.311	2.238	2.266	2.260	2.204	2.160	2.167	2.228	2.242	2.242	2.242	2.248	2.266	2.310	2.318	2.351
2.146	2.392	2.396	2.328	2.346	2.272	2.285	2.285	2.246	2.228	2.208	2.202	2.256	2.256	2.279	2.279	2.281	2.304	2.353	2.386
2.204	2.435	2.417	2.379	2.362	2.292	2.292	2.292	2.250	2.219	2.264	2.283	2.308	2.308	2.310	2.313	2.340	2.371	2.383	2.420
N1	7.195	4.730	7.871	6.374	7.594	8.093	5.358	5.660	5.450	5.538	5.392	11.814	6.022	6.694	5.521	6.474	6.452	5.304	7.046
N2	2.280	2.227	2.439	2.613	2.642	2.463	2.446	2.649	2.534	2.730	2.692	2.552	2.528	2.459	2.672	2.448	2.225	2.412	2.497
A1	6.1e-14	6.1e-09	4.9e-15	3.1e-12	3.8e-14	4.1e-15	7.7e-10	2.2e-10	1.0e-09	7.4e-10	1.5e-09	3.0e-11	3.0e-11	2.9e-12	3.1e-10	4.6e-12	3.4e-12	4.8e-10	1.1e-13
A2	5.0e-04	6.5e-04	2.8e-04	1.1e-04	1.5e-04	3.4e-04	4.2e-04	1.7e-04	3.2e-04	4.2e-04	1.6e-04	2.5e-04	2.6e-04	3.7e-04	1.2e-04	3.4e-04	9.2e-04	3.1e-04	1.6e-04

TABLE 7.1 (b)

Room Temp. 30°C
Face C(010)

Angle->	0	10	20	30	40	50	60	70	80	90	100	110	120	130	140	150	160	170	180
-log(F) <																			
0.097	1.831	1.861	1.846	1.793	1.751	1.725	1.718	1.725	1.738	1.751	1.756	1.781	1.809	1.851	1.826	1.856	1.856	1.841	
0.398	1.851	1.866	1.851	1.809	1.757	1.733	1.725	1.738	1.751	1.763	1.861	1.793	1.815	1.861	1.836	1.861	1.861	1.851	
0.574	1.871	1.875	1.856	1.826	1.763	1.775	1.751	1.731	1.744	1.757	1.769	1.866	1.804	1.826	1.804	1.866	1.866	1.861	
0.699	1.889	1.875	1.861	1.836	1.775	1.781	1.763	1.738	1.757	1.763	1.781	1.871	1.815	1.889	1.851	1.875	1.875	1.866	
0.796	1.898	1.885	1.875	1.841	1.793	1.798	1.769	1.751	1.775	1.769	1.793	1.875	1.826	1.836	1.836	1.885	1.885	1.885	
0.875	1.907	1.894	1.889	1.851	1.809	1.820	1.775	1.763	1.793	1.781	1.804	1.880	1.831	1.846	1.836	1.898	1.898	1.895	
0.942	1.916	1.907	1.898	1.856	1.836	1.836	1.781	1.775	1.804	1.787	1.815	1.885	1.885	1.846	1.856	1.846	1.880	1.894	
1.000	1.925	1.925	1.907	1.861	1.851	1.851	1.793	1.787	1.815	1.798	1.831	1.889	1.889	1.866	1.866	1.866	1.870	1.870	
1.051	1.933	1.929	1.916	1.875	1.856	1.856	1.798	1.798	1.820	1.809	1.836	1.894	1.894	1.875	1.875	1.875	1.875	1.875	
1.097	1.941	1.933	1.920	1.889	1.866	1.866	1.804	1.809	1.831	1.820	1.856	1.903	1.866	1.894	1.898	1.898	1.894	1.894	
1.138	1.949	1.937	1.925	1.898	1.871	1.871	1.809	1.809	1.836	1.831	1.866	1.903	1.871	1.907	1.907	1.907	1.907	1.907	
1.176	1.957	1.941	1.933	1.907	1.875	1.875	1.820	1.820	1.846	1.846	1.866	1.912	1.871	1.912	1.929	1.929	1.929	1.916	
1.211	1.969	1.957	1.945	1.912	1.885	1.885	1.826	1.826	1.856	1.856	1.886	1.920	1.885	1.925	1.937	1.937	1.937	1.925	
1.243	1.994	1.991	1.972	1.925	1.925	1.925	1.871	1.871	1.899	1.899	1.920	1.956	1.920	1.949	1.953	1.953	1.953	1.929	
1.273	1.994	1.991	1.972	1.925	1.903	1.903	1.856	1.856	1.886	1.886	1.912	1.953	1.929	1.961	1.961	1.961	1.961	1.937	
1.301	2.005	2.012	1.984	1.933	1.920	1.903	1.856	1.856	1.886	1.886	1.912	1.953	1.937	1.965	1.965	1.965	1.965	1.953	
1.358	2.052	2.026	1.991	1.980	1.941	1.916	1.885	1.885	1.916	1.916	1.956	1.993	1.920	1.949	1.953	1.953	1.953	1.984	
1.477	2.067	2.045	2.029	1.998	1.965	1.941	1.916	1.898	1.898	1.898	1.912	1.956	1.993	1.920	1.929	1.929	1.929	1.984	
1.602	2.091	2.085	2.067	2.048	2.019	1.984	1.945	1.945	1.971	1.971	1.996	2.015	1.941	1.937	1.937	1.937	1.937	1.902	
1.699	2.140	2.127	2.102	2.073	2.045	2.029	2.015	1.965	1.998	2.015	1.986	2.015	1.975	1.920	1.925	1.925	1.925	1.953	
1.778	2.179	2.145	2.127	2.119	2.064	2.073	2.039	2.015	2.024	2.032	2.052	2.076	2.105	1.961	1.976	1.984	1.984	1.984	
1.845	2.193	2.160	2.157	2.147	2.099	2.094	2.073	2.058	2.073	2.082	2.102	2.142	2.129	2.137	2.137	2.137	2.137	2.160	
1.903	2.230	2.184	2.181	2.134	2.108	2.099	2.102	2.088	2.088	2.102	2.134	2.157	2.167	2.142	2.142	2.142	2.142	2.177	
2.000	2.270	2.202	2.223	2.184	2.174	2.152	2.137	2.113	2.113	2.132	2.155	2.174	2.202	2.195	2.234	2.234	2.234	2.272	
2.041	2.275	2.285	2.234	2.213	2.208	2.179	2.157	2.127	2.132	2.155	2.177	2.193	2.190	2.219	2.234	2.234	2.234	2.272	
2.079	2.317	2.294	2.272	2.236	2.230	2.217	2.167	2.167	2.169	2.169	2.217	2.204	2.223	2.244	2.262	2.262	2.262	2.306	
2.146	2.337	2.320	2.283	2.256	2.246	2.238	2.208	2.184	2.184	2.208	2.230	2.238	2.270	2.273	2.283	2.311	2.337	2.337	
2.204	2.346	2.338	2.294	2.288	2.254	2.264	2.223	2.223	2.244	2.244	2.273	2.301	2.292	2.306	2.341	2.345	2.351	2.351	
N1	5.854	6.316	6.510	6.592	5.343	5.825	7.475	5.654	5.830	6.630	5.726	10.544	6.594	4.769	9.340	4.858	6.221	5.876	
N2	2.526	2.502	2.699	2.550	2.467	2.402	2.372	2.426	2.534	2.471	2.476	2.672	2.470	2.505	2.592	2.343	2.359	2.581	
A1	4.6e-11	6.3e-12	3.2e-12	4.0e-12	1.3e-09	1.6e-10	3.4e-13	6.4e-10	2.4e-10	9.3e-12	2.9e-10	9.2e-20	5.3e-12	4.5e-12	1.1e-08	1.3e-17	4.7e-09	9.6e-12	
A2	1.8e-04	2.3e-04	1.0e-04	2.4e-04	4.2e-04	6.2e-04	8.3e-04	7.1e-04	4.1e-04	5.2e-04	4.3e-04	1.5e-04	3.7e-04	2.9e-04	1.7e-04	5.6e-04	4.7e-04	1.6e-04	

Room Temp. 30°C
Face Z(111)

TABLE 7.1 (c)
Knoop indenter for sphenoidal face

Angle->	0	10	20	30	40	50	60	70	80	90	100	110	120	130	140	150	160	170	180
Log(P) <	Log(P)																		
0.097	1.714	1.708	1.751	1.766	1.784	1.787	1.815	1.856	1.866	1.871	1.861	1.866	1.861	1.856	1.815	1.809	1.744	1.793	
0.398	1.731	1.725	1.781	1.778	1.831	1.823	1.831	1.861	1.889	1.889	1.889	1.889	1.889	1.889	1.866	1.866	1.757	1.798	
0.574	1.754	1.738	1.787	1.793	1.841	1.851	1.836	1.866	1.894	1.899	1.894	1.899	1.894	1.895	1.875	1.831	1.826	1.763	1.804
0.699	1.769	1.751	1.798	1.798	1.846	1.859	1.846	1.871	1.903	1.903	1.903	1.903	1.912	1.953	1.885	1.836	1.769	1.809	
0.796	1.784	1.775	1.804	1.815	1.856	1.866	1.851	1.880	1.907	1.903	1.907	1.903	1.980	1.894	1.898	1.846	1.787	1.815	
0.875	1.787	1.787	1.809	1.826	1.866	1.871	1.861	1.889	1.920	1.912	1.916	1.953	2.005	1.903	1.907	1.851	1.804	1.820	
0.942	1.801	1.793	1.820	1.841	1.871	1.894	1.866	1.903	1.925	1.916	1.925	1.972	2.029	1.912	1.920	1.861	1.856	1.826	
1.000	1.812	1.804	1.826	1.846	1.875	1.898	1.912	1.912	1.929	1.925	1.933	1.991	2.052	1.920	1.933	1.871	1.866	1.836	
1.051	1.815	1.815	1.836	1.851	1.880	1.903	1.933	1.920	1.945	1.929	1.941	2.032	2.076	1.929	1.937	1.881	1.861	1.841	
1.097	1.826	1.820	1.846	1.861	1.892	1.912	1.937	1.933	1.953	1.933	1.949	2.070	2.099	1.937	1.945	1.889	1.880	1.851	
1.138	1.831	1.831	1.856	1.866	1.893	1.931	1.941	1.941	1.961	1.941	1.957	2.105	2.121	1.945	1.953	1.903	1.885	1.856	
1.176	1.861	1.841	1.866	1.875	1.912	1.937	1.945	1.949	1.965	1.953	1.965	2.137	2.142	1.953	1.961	1.903	1.866	1.846	
1.211	1.866	1.846	1.873	1.880	1.916	1.953	1.949	1.959	1.972	1.961	1.976	2.147	2.152	1.991	1.969	1.929	1.885	1.865	
1.243	1.875	1.851	1.883	1.889	1.925	1.965	1.957	1.969	1.980	1.969	1.980	2.160	2.162	2.026	1.976	1.941	1.912	1.903	
1.273	1.880	1.866	1.886	1.898	1.933	1.972	1.976	1.976	1.991	1.984	1.991	2.172	2.172	2.058	1.984	1.989	1.933	1.886	
1.301	1.885	1.875	1.918	1.907	1.937	1.980	1.976	1.976	1.991	1.984	1.991	2.184	2.181	2.091	1.991	1.979	1.907	1.885	
1.398	1.894	1.903	1.925	1.941	1.949	1.994	1.991	2.012	2.009	2.010	2.005	2.208	2.188	2.116	2.019	1.984	1.953	1.949	
1.477	1.903	1.945	1.953	1.947	1.980	2.005	2.036	2.026	2.019	2.015	2.015	2.252	2.197	2.140	2.045	1.998	1.953	1.920	
1.602	1.945	1.972	1.976	1.989	2.048	2.012	2.047	2.045	2.045	2.045	2.048	2.275	2.213	2.186	2.096	2.005	2.015	2.026	
1.699	1.974	1.998	2.027	2.055	2.061	2.082	2.099	2.121	2.105	2.096	2.102	2.313	2.273	2.232	2.129	2.070	2.055	2.052	
2.000	2.113	2.133	2.137	2.143	2.185	2.187	2.205	2.179	2.206	2.206	2.208	2.348	2.327	2.273	2.160	2.110	2.099	2.076	
2.041	2.137	2.145	2.165	2.172	2.190	2.195	2.240	2.215	2.222	2.217	2.223	2.447	2.448	2.386	2.290	2.246	2.219	2.193	
2.079	2.160	2.156	2.174	2.186	2.206	2.245	2.246	2.248	2.272	2.250	2.458	2.457	2.799	2.313	2.266	2.234	2.219	2.215	
2.146	2.202	2.178	2.223	2.213	2.241	2.265	2.278	2.292	2.285	2.303	2.285	2.475	2.424	2.356	2.301	2.260	2.254	2.256	
2.204	2.210	2.232	2.248	2.241	2.321	2.322	2.315	2.339	2.311	2.327	2.503	2.493	2.448	2.396	2.333	2.285	2.286	2.294	

Room Temp. 30°C
Face Z(777)

TABLE 7.1 (d)

Knoop indenter for sphenoidal face

Angle	N2	N3	W	B	A2
0	2.343	2.772	-8.40254	0.00231	3.3591e-04
10	2.348	2.838	-8.34243	0.00277	4.0331e-04
20	2.457	2.348	-11.18001	0.00308	2.4835e-04
30	2.640	2.355	-16.01522	0.00348	1.0501e-04
40	2.612	2.375	-14.87219	0.00445	1.6951e-04
50	2.525	2.275	-13.02878	0.00442	2.6896e-04
60	2.478	2.897	-11.13580	0.00465	3.6707e-04
70	2.393	2.308	-9.65422	0.00509	6.4766e-04
80	2.494	2.951	-11.71940	0.00575	4.4163e-04
90	2.553	2.192	-13.58693	0.00613	3.4999e-04
100	2.579	2.139	-14.21116	0.00628	3.1543e-04
110	2.559	2.572	-13.79912	0.00578	3.1498e-04
120	2.429	2.147	-10.38594	0.00531	5.6338e-04
130	2.580	2.201	-14.27143	0.00495	2.3055e-04
140	2.504	2.232	-12.37873	0.00442	3.0077e-04
150	2.511	2.327	-12.25238	0.00381	2.4023e-04
160	2.422	2.163	-10.13444	0.00319	3.1604e-04
170	2.459	2.197	-11.07514	0.00291	2.3006e-04
180	2.220	2.281	-5.39730	0.00218	6.3115e-04

Table 7.2 (a)
(For High Load Region)

Room Temp. 30°C
d-AHT m (110)

Angle	N2	N3	W	B	A2
0	2.280	2.253	-7.15376	0.00241	5.0007e-04
10	2.227	2.183	-5.76343	0.00235	6.5386e-04
20	2.438	2.117	-11.45694	0.00318	2.8418e-04
30	2.613	2.146	-16.35463	0.00326	1.1062e-04
40	2.642	2.069	-17.18942	0.00455	1.4632e-04
50	2.463	2.246	-12.15192	0.00408	3.3719e-04
60	2.446	2.524	-11.40105	0.00452	4.1992e-04
70	2.649	2.361	-17.24219	0.00536	1.7491e-04
80	2.534	2.119	-14.09483	0.00537	3.2421e-04
90	2.730	2.238	-19.70381	0.00648	1.4752e-04
100	2.692	2.201	-18.43738	0.00596	1.6107e-04
110	2.552	2.052	-14.56596	0.00473	2.5060e-04
120	2.528	2.156	-13.75755	0.00441	2.6080e-04
130	2.459	2.140	-11.91762	0.00430	3.6752e-04
140	2.672	2.087	-17.88787	0.00435	1.1707e-04
150	2.448	2.092	-11.57066	0.00383	3.3924e-04
160	2.225	2.202	-5.55978	0.00316	9.1924e-04
170	2.412	2.238	-10.61417	0.00303	3.0960e-04
180	2.497	2.078	-12.99466	0.00260	1.5967e-04

Table 7.2 (b))
(For High Load Region)

Room Temp. 30°C
d-AHT C (010)

Angle	N2	N3	W	B	A2
0	2.526	2.159	-13.93359	0.00332	1.8396e-04
10	2.502	2.297	-13.12973	0.00360	2.3360e-04
20	2.699	2.157	-18.80193	0.00432	1.0034e-04
30	2.550	2.115	-14.70438	0.00454	2.4016e-04
40	2.467	2.144	-12.25568	0.00495	4.1765e-04
50	2.402	2.159	-10.36370	0.00515	6.2128e-04
60	2.372	2.034	-9.64897	0.00574	8.2678e-04
70	2.426	2.244	-11.07029	0.00636	7.0516e-04
80	2.534	2.232	-14.02321	0.00644	4.0834e-04
90	2.471	2.036	-12.36170	0.00597	5.1626e-04
100	2.476	2.187	-12.53499	0.00528	4.3201e-04
110	2.672	2.073	-17.88597	0.00527	1.5117e-04
120	2.470	2.192	-12.35516	0.00449	3.6518e-04
130	2.505	2.014	-13.36080	0.00439	2.9354e-04
140	2.592	2.115	-15.85614	0.00418	1.7198e-04
150	2.343	2.042	-8.79227	0.00363	5.6353e-04
160	2.359	2.108	-9.26181	0.00334	4.6856e-04
170	2.581	2.036	-15.40124	0.00370	1.5603e-04
180	2.470	2.131	-12.31499	0.00336	2.5578e-04

Table 7.2 (c)
(For High Load Region)

Room Temp. 30°C
d-AHT Z (111)

Angle	N2	N3	W	B	A2
0	2.589	2.282	-15.45296	0.00669	3.2069e-04
10	2.599	2.069	-15.90561	0.00641	2.8842e-04
20	2.617	2.227	-16.41067	0.00574	2.2753e-04
30	2.678	2.254	-18.28559	0.00577	1.6570e-04
40	2.822	2.272	-22.22561	0.00562	7.3689e-05
50	2.576	2.552	-15.04397	0.00448	2.0505e-04
60	2.543	2.277	-14.41434	0.00402	2.1345e-04
70	2.686	2.410	-18.33018	0.00433	1.0798e-04
80	2.622	2.249	-16.30312	0.00421	1.4722e-04
90	2.613	2.324	-16.18884	0.00419	1.5368e-04
100	2.656	2.196	-17.31542	0.00430	1.2574e-04
110	2.760	2.042	-20.69219	0.00169	1.9629e-05
120	2.636	2.488	-16.94509	0.00171	4.1532e-05
130	2.364	2.089	-9.55115	0.00202	2.5101e-04
140	2.227	2.074	-5.66309	0.00294	8.4006e-04
150	2.326	2.162	-8.28605	0.00379	6.5133e-04
160	2.439	2.087	-11.48076	0.00450	4.3151e-04
170	2.473	2.049	-12.31865	0.00480	3.8972e-04
180	2.483	2.106	-12.55843	0.00481	3.7021e-04

Table 7.2 (d)
(For High Load Region)

Room Temp. 30°C
d-AHT Z (111)

TABLE 7.3 (a)

Constants A,B,C derived from

 the quadratic equation

Room Temp : 30°C ; d-AHT :- m (110)

Angle	A in 10^{-3}	B	C
0	-1.1604	1.0971	89.1440
10	-0.5702	1.7985	83.9216
20	-1.2523	1.0285	77.2929
30	-1.7709	1.0496	75.3128
40	1.0081	0.5351	75.3447
50	-0.9095	0.8242	67.0688
60	1.7289	0.4593	70.2465
70	-0.5942	0.7307	59.9416
80	0.6904	0.5410	60.3053
90	0.2484	0.5517	60.4566
100	0.3072	0.5272	61.4309
110	0.1123	0.5926	60.7581
120	0.4402	0.5676	63.3301
130	-0.1035	0.6660	67.4987
140	-0.2402	0.7224	69.1932
150	0.6737	0.6730	76.0811
160	-0.1802	0.8813	75.9200
170	-1.7057	1.1304	76.0204
180	-2.8075	1.4269	77.5908

TABLE 7.3 (b)

Constants A,B,C derived from

 the quadratic equation

Room Temp : 30°C ; d-AHT :- c (010)

Angle	A in 10^{-3}	B	C
0	-2.4147	1.5537	77.7907
10	-4.6847	1.9638	66.4063
20	-2.7492	1.4291	72.5800
30	-3.6318	1.5437	74.3236
40	-2.6835	1.2303	65.8468
50	-2.2890	1.2213	66.3484
60	-0.9431	0.9934	65.2419
70	-2.3291	1.1086	62.4334
80	-3.2206	1.2840	53.3674
90	-2.3434	1.0433	55.8830
100	-2.2324	1.0836	55.4372
110	-1.5433	1.0201	69.0070
120	-1.2448	1.0302	69.3390
130	-2.0654	1.2024	61.8619
140	-2.5472	1.2533	66.1945
150	-1.5927	1.1799	67.5230
160	-1.0783	1.2219	70.4560
170	-2.6438	1.4721	71.4328
180	-2.9744	1.5921	79.5498

TABLE 7.3 (c)

Constants A,B,C derived from

the quadratic equation

Room Temp : 30°C ; d-AHT :- z (111)

Angle	A in 10^3	B	C
0	-3.7420	1.5575	69.3289
10	-2.0661	1.2506	71.5900
20	-3.1794	1.3222	67.9298
30	-3.1417	1.3018	61.7225
40	-2.9195	1.2527	56.3890
50	-1.6673	1.0481	58.3756
60	-2.0851	1.0787	51.6042
70	-1.7826	0.9852	51.7500
80	-1.7142	0.9606	54.7600
90	-2.0906	1.0545	53.4263
100	-2.6858	1.1828	55.7782
110	-0.9756	0.8868	69.5011
120	-2.2396	1.1937	60.3371
130	-2.9105	1.2970	61.7000
140	-3.7076	1.4488	60.6846
150	-1.4438	1.1657	69.6240
160	-2.9770	1.4579	65.9775
170	-2.5353	1.3137	71.0310
180	-2.8954	1.4353	68.3514

TABLE 7.3 (d)

Constants A,B,C derived from

 the quadratic equation

Room Temp : 30°C ; d-AHT :- z $\bar{1}\bar{1}\bar{1}$

Angle	A in 10^3	B	C
0	-1.5388	0.9222	55.5154
10	-2.2582	1.0520	53.1553
20	-2.2231	1.0794	57.6602
30	-2.8634	1.1583	58.2332
40	-2.2324	1.0711	64.9972
50	-1.1626	1.0129	69.3240
60	-2.9883	1.3337	66.5243
70	-1.7681	1.0958	72.2270
80	-0.5599	0.9286	76.9780
90	-1.3179	1.0430	74.1580
100	-0.8953	0.9863	76.3370
110	-1.0702	3.1157	77.8179
120	-0.8826	2.7826	85.0484
130	-0.7494	2.5109	63.5396
140	-1.1128	1.2618	72.2600
150	-1.7916	1.2286	63.6662
160	-2.5676	1.2369	61.1353
170	-2.3810	1.2027	57.8682
180	-1.4879	1.0639	60.3195

TABLE 7.4 (a)

Percentage deviation of the observed diagonal length

from the diagonal length calculated from the equations

(a) $P = ad^n$ (b) $D = AP^2 + BP + C$ for d-AHT

Room Temp : 30° C ; Angle = 0° ; d-AHT :- c (010)

P	P = ad^n			D = AP^2 + BP + C		
	D obs	D calc	% deviation	D calc	% deviation	
1.25	78.34	85.58	8.46	79.73	1.74	
2.50	79.97	94.48	15.36	81.66	2.07	
3.75	81.60	100.19	18.55	83.58	2.37	
5.00	84.05	104.32	19.43	85.49	1.68	
6.25	87.31	107.69	18.92	87.41	0.11	
7.50	91.39	110.54	17.32	89.31	-2.33	
8.75	92.21	113.00	18.40	91.20	-1.11	
10.00	93.01	115.18	19.25	93.08	0.08	
11.25	93.84	117.13	19.88	94.96	1.18	
12.50	94.66	118.91	20.39	96.83	2.24	
13.75	96.29	120.54	20.12	98.69	2.43	
15.00	97.10	122.05	20.44	100.55	3.43	
16.25	102.82	123.45	16.71	102.40	-0.41	
17.50	103.63	124.76	16.94	104.24	0.59	
18.75	104.45	126.00	17.10	106.07	1.53	
20.00	112.61	127.17	11.45	107.89	-4.37	
25.00	114.24	142.07	19.59	115.12	0.76	
30.00	124.85	153.79	18.82	122.22	-2.15	
40.00	141.17	174.28	19.00	135.07	-3.75	
50.00	159.12	192.04	17.14	149.44	-6.48	
60.00	170.54	207.88	17.96	162.32	-5.06	
70.00	174.62	222.29	21.44	174.71	0.05	
80.00	183.60	235.58	22.06	186.63	1.62	
100.00	204.82	259.58	21.10	209.01	2.00	
110.00	208.08	270.57	23.10	219.47	5.19	
120.00	226.85	280.99	19.27	229.46	1.14	
140.00	246.43	300.48	17.99	247.97	0.62	
160.00	272.54	318.44	14.41	264.56	-3.02	

TABLE 7.4 (b)

Percentage deviation of the observed diagonal length

from the diagonal length calculated from the equations

(a) $P = ad^n$ (b) $D = AP^2 + BP + C$ for d-AHT

Room Temp : 30° C ; Angle = 0° ; d-AHT :- z (111)

P	P = ad^n			D = AP^2 + BP + C		
	D obs.	D calc	% deviation	D calc	% deviation	
1.25	67.73	56.91	-19.01	71.26	4.95	
2.50	70.99	69.00	-2.88	73.19	3.01	
3.75	74.26	77.22	3.83	75.12	1.14	
5.00	77.52	83.65	7.33	77.02	-0.65	
6.25	79.15	89.00	11.07	78.92	-0.29	
7.50	80.78	93.82	13.72	80.79	0.01	
8.75	82.42	97.71	15.65	82.67	0.30	
10.00	84.05	101.41	17.12	84.53	0.57	
11.25	85.68	104.78	16.23	86.38	0.61	
12.50	87.31	107.89	19.07	88.21	1.02	
13.75	88.94	110.79	19.72	90.03	1.21	
15.00	90.58	113.50	20.19	91.85	1.38	
16.25	93.01	116.05	19.85	93.65	0.68	
17.50	98.74	118.46	16.65	95.43	-3.47	
18.75	98.74	120.75	18.23	97.21	-1.57	
20.00	101.18	122.94	17.70	98.98	-2.22	
25.00	112.61	130.80	18.91	105.93	-6.31	
30.00	116.69	137.60	15.20	112.69	-3.55	
40.00	123.22	151.97	18.92	125.64	1.93	
50.00	137.90	169.01	18.41	137.85	-0.04	
60.00	150.96	184.34	18.11	149.31	-1.11	
70.00	155.86	198.38	21.43	160.02	2.60	
80.00	169.73	211.40	19.71	169.98	0.15	
100.00	186.05	235.10	20.86	187.66	0.86	
110.00	188.49	246.02	23.38	195.38	3.53	
120.00	207.26	256.43	19.17	202.34	-2.43	
140.00	217.06	275.96	21.34	214.04	-1.41	
160.00	221.95	294.07	24.52	222.73	0.35	

TABLE 7.4 (c)

Percentage deviation of the observed diagonal length

from the diagonal length calculated from the equations

(a) $P = ad^n$ (b) $D = AP^2 + BP + C$ for d-AHT

Room Temp : 30°C ; Angle = 0° ; d-AHT :- z (111)

P	D obs	P = ad ⁿ		D = AP ² + BP + C	
		D calc	% deviation	D calc	% deviation
1.25	51.82	45.87	-12.97	56.66	8.54
2.50	53.86	51.78	-4.02	57.81	6.83
3.75	56.71	55.59	-2.01	58.95	3.80
5.00	58.75	58.46	-0.50	60.08	2.21
6.25	60.79	60.79	0.00	61.21	0.69
7.50	61.20	62.76	2.49	62.34	1.83
8.75	63.24	64.48	1.92	63.46	0.35
10.00	64.87	66.00	1.71	64.58	-0.45
11.25	65.28	67.37	3.10	65.69	0.62
12.50	66.91	68.63	2.51	66.80	-0.16
13.75	71.81	69.78	-2.91	67.90	-5.76
15.00	72.62	70.85	-2.50	69.00	-5.25
16.25	73.44	71.85	-2.21	70.09	-4.78
17.50	75.07	72.79	-3.13	71.18	-5.47
18.75	75.89	73.67	-3.01	72.26	-5.02
20.00	76.70	74.51	-2.94	73.34	-4.58
25.00	78.34	77.48	-1.11	77.61	-0.94
30.00	79.97	79.99	0.03	81.79	2.23
40.00	88.13	87.68	-0.51	89.94	2.01
50.00	94.25	96.65	2.48	97.77	3.80
60.00	106.89	104.66	-2.13	105.31	-1.50
70.00	111.79	111.95	0.14	112.53	0.66
80.00	117.91	118.67	0.64	119.44	1.28
100.00	129.74	130.82	0.83	132.35	1.97
110.00	137.09	136.38	-0.52	138.34	0.90
120.00	144.43	141.66	-1.96	144.02	-0.28
140.00	159.12	151.53	-5.01	154.46	-3.02
160.00	162.06	160.62	-0.90	163.67	0.98

TABLE 7.4 (d)

Percentage deviation of the observed diagonal length

from the diagonal length calculated from the equations

(a) $P = ad^n$ (b) $D = AP^2 + BP + C$ for d-AHT

Room Temp : 30°C ; Angle = 20° ; d-AHT :- σ (010)

P	P = ad ⁿ			D = AP ² + BP + C		
	D obs	D calc	% deviation	D calc	% deviation	
1.25	73.44	57.24	-28.30	74.36	1.24	
2.50	78.34	69.24	-13.14	76.14	-2.89	
3.75	79.97	77.40	-3.32	77.90	-2.66	
5.00	81.60	83.77	2.59	79.66	-2.44	
6.25	82.42	89.06	7.46	81.40	-1.25	
7.50	83.23	93.64	11.12	83.14	-0.11	
8.75	84.05	97.69	13.96	84.57	0.61	
10.00	84.86	101.34	16.26	86.59	2.00	
11.25	85.68	104.67	18.14	88.31	2.98	
12.50	86.49	107.75	19.73	90.01	3.91	
13.75	89.76	110.60	18.84	91.71	2.13	
15.00	93.02	113.28	17.88	93.39	0.40	
16.25	94.66	115.80	18.26	95.08	0.44	
17.50	96.29	118.18	18.52	96.75	0.48	
18.75	97.92	120.44	18.70	98.41	0.50	
20.00	100.37	122.60	18.13	100.06	-0.31	
25.00	104.45	126.10	17.17	106.59	2.01	
30.00	115.08	136.45	15.68	112.98	-1.84	
40.00	125.68	154.55	18.69	125.35	-0.25	
50.00	134.64	170.22	20.90	137.16	1.84	
60.00	159.94	184.20	13.17	148.43	-7.75	
70.00	164.83	196.92	16.30	159.14	-3.58	
80.00	171.36	208.63	17.86	169.31	-1.21	
100.00	184.42	229.79	19.74	187.99	1.90	
110.00	192.58	239.47	19.58	196.52	2.00	
120.00	198.29	248.67	20.26	204.48	3.03	
140.00	212.98	265.83	19.88	218.77	2.65	
160.00	239.09	281.65	15.11	230.86	-3.56	

TABLE 7.4 (e)

Percentage deviation of the observed diagonal length

from the diagonal length calculated from the equations

(a) $P = ad^n$ (b) $D = AP^2 + BP + C$ for d-AHT

Room Temp : 30° C ; Angle = 20° ; d-AHT :- z (111)

P	P = ad^n			D = AP^2 + BP + C		
	D obs	D calc	% deviation	D calc	% deviation	
1.25	70.18	55.04	-27.51	69.58	-0.87	
2.50	70.99	66.62	-6.56	71.22	0.32	
3.75	71.80	74.50	3.62	72.84	1.43	
5.00	72.62	80.64	9.95	74.46	2.47	
6.25	75.07	85.75	12.45	76.06	1.30	
7.50	77.52	90.17	14.03	77.87	0.19	
8.75	79.15	94.08	15.87	79.25	0.13	
10.00	80.78	97.61	17.24	80.83	0.06	
11.25	82.42	100.83	18.26	82.40	-0.02	
12.50	83.23	103.80	19.82	83.98	0.87	
13.75	84.05	106.56	21.12	85.51	1.71	
15.00	85.68	109.14	21.50	87.05	1.57	
16.25	88.13	111.58	21.02	88.57	0.50	
17.50	93.84	113.88	17.60	90.09	-4.16	
18.75	93.84	116.06	19.15	91.60	-2.45	
20.00	96.29	118.15	18.50	93.10	-3.43	
25.00	97.92	117.98	17.00	98.99	1.08	
30.00	106.89	126.66	15.81	104.73	-2.06	
40.00	116.69	141.66	17.63	115.73	-0.83	
50.00	126.48	154.51	18.14	126.09	-0.31	
60.00	133.82	165.87	19.32	135.82	1.47	
70.00	143.62	176.12	18.45	144.90	0.88	
80.00	151.78	185.52	18.19	153.35	1.02	
100.00	167.28	202.34	17.33	168.35	0.64	
110.00	171.36	209.99	18.40	174.89	2.02	
120.00	186.86	217.22	13.98	180.81	-3.35	
140.00	191.76	230.65	16.86	190.72	-0.55	
160.00	196.66	242.95	19.05	198.08	0.72	

TABLE 7.4 (f)

Percentage deviation of the observed diagonal length

from the diagonal length calculated from the equations

(a) $P = ad^n$ (b) $D = AP^2 + BP + C$ for d-AHT

Room Temp : 30°C ; Angle = 20° ; d-AHT :- z $\langle \bar{1}\bar{1}\bar{1} \rangle$

P	P = ad^n			D = AP^2 + BP + C		
	D obs	D calc	% deviation	D calc	% deviation	
1.25	56.30	55.44	-1.55	59.01	4.59	
2.50	60.38	60.15	-0.38	60.34	-0.07	
3.75	61.20	63.09	3.00	61.68	0.78	
5.00	62.83	65.27	3.74	63.00	0.27	
6.25	63.65	67.00	5.00	64.32	1.04	
7.50	64.46	68.45	5.83	65.63	1.78	
8.75	66.09	69.71	5.19	66.93	1.26	
10.00	66.91	70.81	5.51	68.23	1.93	
11.25	68.54	71.80	4.54	69.52	1.41	
12.50	70.18	72.69	3.45	70.81	0.89	
13.75	71.81	73.51	2.31	72.08	0.37	
15.00	73.44	74.27	1.12	73.35	-0.12	
16.25	74.86	74.97	0.41	74.61	-0.07	
17.50	76.29	75.63	-0.87	75.87	-0.55	
18.75	79.97	76.25	-4.88	77.11	-3.71	
20.00	82.82	76.83	-7.80	78.36	-5.69	
25.00	84.05	82.70	-1.63	83.26	-0.95	
30.00	89.76	88.96	-0.90	88.04	-1.95	
40.00	94.66	99.81	5.16	97.28	2.69	
50.00	106.49	109.13	2.42	106.07	-0.40	
60.00	118.73	117.39	-1.14	114.42	-3.77	
70.00	124.85	124.85	0.00	122.32	-2.07	
80.00	133.82	131.70	-1.61	129.78	-3.11	
100.00	137.09	144.00	4.80	143.37	4.38	
110.00	146.06	149.59	2.36	149.49	2.29	
120.00	149.33	154.89	3.59	155.17	3.76	
140.00	167.28	164.74	-1.54	165.20	-1.26	
160.00	177.07	173.78	-1.89	173.45	-2.09	

Angle°		Hardness in kg/mm²																		
P(gas)	<	0	10	20	30	40	50	60	70	80	90	100	110	120	130	140	150	160	170	180
1.250	3.373	3.529	4.506	5.255	4.813	5.338	6.041	6.421	6.041	6.227	6.421	5.225	5.452	5.299	4.122	3.878	3.741	3.373		
2.500	5.036	5.983	6.821	8.143	8.670	9.129	10.165	11.222	12.265	11.386	11.726	12.082	10.306	9.498	8.561	7.755	7.395	6.576	6.244	
3.750	7.133	8.606	10.118	11.494	12.215	13.172	13.343	15.898	16.833	16.592	16.124	16.833	15.039	13.172	12.367	10.836	10.588	9.618	9.117	
5.000	8.518	11.013	12.763	14.281	13.490	16.907	16.696	20.612	21.197	20.052	19.780	21.197	18.996	17.121	14.965	13.798	13.192	12.355	11.810	
6.250	11.242	13.357	14.645	14.645	16.490	18.060	19.864	25.064	25.766	24.372	23.746	24.392	22.528	20.870	18.060	16.490	14.890	15.116	11.938	
7.500	12.778	14.678	17.035	16.190	18.532	21.176	22.716	28.878	29.270	28.495	26.686	28.495	25.682	22.716	21.176	18.937	17.035	17.574	13.742	
8.750	13.430	16.353	17.626	18.731	20.503	24.147	24.424	31.539	33.244	32.375	29.963	32.375	28.501	24.147	21.621	18.331	18.151	15.739		
10.000	14.841	18.322	19.020	20.541	22.027	26.980	26.980	34.243	35.127	34.680	33.392	36.045	31.022	26.980	26.384	20.144	20.541	19.384	17.662	
11.250	14.674	18.179	19.690	22.229	23.337	29.682	24.531	37.566	38.523	37.101	36.644	37.566	34.074	27.798	26.405	22.229	22.646	21.398	19.513	
12.500	14.658	19.853	21.296	23.333	25.180	32.259	29.914	36.543	38.777	40.716	37.860	38.777	36.119	30.233	28.687	23.775	24.001	22.903	21.296	
13.750	17.935	20.751	23.013	23.218	27.168	32.560	31.985	38.823	41.646	43.702	40.671	41.646	37.946	32.560	29.982	25.666	25.908	23.426	22.611	
15.000	17.589	22.077	24.239	24.239	29.076	32.379	33.378	41.395	43.343	45.432	43.343	43.343	40.470	33.040	31.116	27.231	27.231	25.105	24.239	
16.250	21.196	23.332	25.369	23.917	29.445	34.044	34.728	43.843	45.882	46.955	44.845	45.882	42.974	34.044	32.734	27.934	27.934	26.722	25.369	
17.500	22.130	24.720	26.633	25.127	29.289	35.252	35.947	46.172	48.294	48.294	46.172	47.215	45.163	35.947	34.578	27.794	29.289	28.279	26.860	
18.750	23.350	25.852	26.272	26.496	30.833	37.406	34.999	48.389	45.349	49.470	46.832	49.470	47.342	37.770	36.345	29.272	28.060	25.852	27.827	
20.000	21.807	25.487	26.922	27.355	32.319	36.644	35.975	42.742	47.360	50.499	48.373	49.418	48.373	38.040	37.332	30.697	27.798	24.551	24.163	
25.000	24.065	27.653	31.372	32.866	37.414	41.111	44.155	50.361	57.973	53.427	53.427	51.353	53.427	45.805	43.363	37.729	32.106	28.466	22.823	
30.000	22.716	28.118	34.410	28.306	43.790	48.479	52.036	57.602	64.113	61.623	61.623	62.724	59.276	50.657	43.075	43.075	36.798	23.837		
40.000	26.980	33.602	34.902	35.812	45.545	46.559	55.596	58.872	56.047	62.447	71.295	52.175	57.433	48.326	44.888	40.940	36.518	34.243	24.577	
50.000	26.983	39.488	35.703	38.258	54.518	51.175	51.531	58.199	66.775	63.228	74.927	62.266	56.932	54.518	42.002	36.974	33.349	29.138	28.780	
60.000	32.056	35.040	36.279	39.797	53.718	45.977	56.989	61.837	71.947	73.592	73.037	71.947	65.421	60.155	52.021	45.977	39.140	38.289	31.581	
70.000	34.578	37.587	40.581	39.342	52.689	51.160	64.749	70.181	71.152	78.553	76.873	79.704	64.325	59.548	57.713	49.988	39.748	37.776	26.080	
80.000	24.906	33.771	34.847	43.831	52.476	53.359	64.349	59.861	80.206	78.053	76.495	83.025	70.253	61.303	52.186	52.334	42.318	35.005	26.710	
100.000	29.978	41.842	34.747	38.209	58.581	57.077	69.386	67.450	75.719	77.090	74.385	73.515	72.238	69.789	56.202	47.327	43.955	34.194	28.780	
120.000	30.284	38.527	40.706	39.907	61.024	54.211	55.479	67.790	76.998	78.280	79.593	74.528	71.039	58.710	55.479	51.110	37.647	34.919	31.463	
140.000	34.148	35.332	39.135	44.775	53.719	59.364	53.492	71.894	62.956	78.281	74.426	70.505	60.708	55.587	46.375	40.440	37.623	31.745		
160.000	33.184	36.280	43.304	47.607	51.369	59.117	53.589	69.069	71.295	76.080	79.416	71.295	65.777	64.920	59.364	45.051	42.245	42.998	34.570	

Table 7.5 (a)
Hardness H in Kg/mm²

Room Temp. 30°C
d-AHT

Angle P(gas)	Hardness in kg/sq.in.																		
	0	10	20	30	40	50	60	70	80	90	100	110	120	130	140	150	160	170	180
1.250	2.899	3.529	3.298	3.089	3.973	3.786	4.625	4.625	5.951	5.777	6.133	3.450	4.280	4.391	3.973	3.786	3.697	3.529	2.839
2.500	5.563	7.572	5.797	5.678	7.572	7.224	8.561	8.782	11.222	10.904	11.554	6.596	7.755	8.348	7.572	7.224	7.059	6.899	5.237
3.750	8.014	9.678	8.345	8.177	10.836	10.588	12.522	12.522	15.898	15.898	16.833	9.678	10.588	12.215	11.092	10.349	9.894	10.118	7.269
5.000	10.072	12.355	10.685	10.685	13.798	13.490	15.511	15.892	20.052	20.612	21.197	12.625	12.904	15.511	14.117	13.490	12.355	12.904	9.161
6.250	11.666	14.493	13.094	13.094	16.863	16.490	18.487	19.389	23.746	25.064	25.064	15.443	15.781	18.930	17.248	16.490	14.800	14.800	11.242
7.500	12.778	17.055	15.406	15.108	19.788	18.937	21.671	22.716	27.034	28.495	28.495	17.760	18.532	21.184	20.235	19.355	17.035	16.354	13.009
8.750	14.645	17.626	17.626	16.643	21.621	21.163	24.706	25.283	30.736	32.375	31.539	19.874	20.720	25.283	23.086	22.093	18.700	17.626	14.645
10.000	16.444	19.759	19.759	17.988	23.680	23.680	26.980	26.384	34.243	36.045	35.127	22.252	23.189	28.235	25.807	24.709	20.144	18.522	16.160
11.250	18.179	21.807	21.807	19.870	25.553	25.553	27.798	28.405	37.566	37.566	37.566	24.531	24.531	30.353	27.210	26.640	21.807	20.236	17.867
12.500	19.853	22.077	23.775	20.921	26.714	27.256	28.986	29.600	38.777	37.860	39.729	26.714	25.676	32.259	28.392	23.333	22.077	19.515	
13.750	21.104	23.426	24.285	22.611	28.806	29.385	30.597	30.597	38.823	38.823	41.646	28.806	26.653	33.975	28.806	29.385	24.733	23.426	21.104
15.000	22.637	24.666	24.666	23.022	30.812	30.812	32.056	32.056	39.576	39.576	43.343	30.812	35.520	35.520	29.076	29.638	26.018	24.666	22.261
16.250	21.874	23.720	25.808	22.954	32.108	32.108	33.379	41.030	41.937	43.843	32.734	28.701	35.433	29.774	30.333	27.197	24.941	21.874	
17.500	23.188	23.188	26.860	23.936	33.922	33.285	32.064	34.578	42.326	44.186	42.326	34.578	30.354	35.252	28.814	30.354	28.279	24.720	21.143
18.750	24.457	27.827	25.290	34.354	34.354	33.116	36.345	44.400	46.330	42.588	36.345	31.944	34.354	29.779	30.833	29.272	24.457	20.739	
20.000	22.444	23.804	28.252	25.695	34.074	35.324	34.074	38.040	45.427	47.360	42.742	37.332	32.889	33.473	29.682	30.697	30.183	24.163	20.052
25.000	27.259	28.055	32.610	30.663	39.029	35.315	41.111	44.969	53.427	52.375	44.969	42.592	38.371	39.029	34.747	35.315	35.315	28.466	23.125
30.000	27.388	31.353	32.248	30.494	41.032	37.537	43.075	50.210	59.276	46.045	47.646	46.835	43.075	43.790	38.527	38.527	32.711	25.360	
40.000	28.562	31.399	36.045	32.174	44.888	49.461	49.813	50.384	51.369	59.364	59.364	52.175	50.582	52.175	44.888	42.998	44.888	39.559	29.234
50.000	28.101	31.562	39.249	33.725	48.783	48.783	59.509	65.219	57.772	63.228	57.772	54.518	53.747	53.747	48.131	46.864	46.250	39.729	30.887
60.000	29.355	31.116	33.378	33.378	49.468	50.088	66.366	61.837	60.155	70.357	65.421	55.499	55.499	54.067	50.088	48.859	46.533	39.140	31.738
70.000	32.666	29.032	36.662	35.947	49.411	53.640	60.491	59.174	61.471	72.144	69.229	54.948	55.621	53.640	50.567	49.984	46.172	38.159	32.064
80.000	33.771	29.682	38.768	39.900	53.960	47.360	62.798	53.359	65.957	78.053	68.486	53.359	52.768	49.954	50.499	44.942	36.986	32.040	
100.000	33.922	29.978	41.842	38.698	54.512	52.375	61.773	61.773	82.447	77.555	57.373	56.783	55.067	52.897	50.853	39.705	38.698	33.387	
110.000	36.152	32.247	42.208	41.155	58.187	54.863	65.119	66.512	65.119	86.347	82.308	58.770	56.488	55.938	53.818	50.856	40.475	39.164	33.729
120.000	33.183	30.494	43.430	40.706	57.060	50.210	51.570	67.443	66.757	81.858	79.152	59.650	55.999	55.999	54.461	50.210	41.032	39.439	33.911
140.000	32.805	32.163	43.921	40.440	57.053	53.719	53.719	64.128	69.825	76.317	78.683	61.259	55.111	56.070	54.641	49.041	41.347	39.277	33.691
160.000	33.392	33.392	42.998	39.830	59.364	55.596	59.364	71.295	71.295	82.976	67.543	61.917	55.150	54.710	53.845	47.607	41.225	39.027	32.979

Table 7.5 (b)
Hardness H in Kg/mm²

Room Temp. 30°C
d-AHT C (010)

Angle (°)	Hardness in kg/mm²																		
	0	10	20	30	40	50	60	70	80	90	100	110	120	130	140	150	160	170	180
1.250	3.378	3.373	3.612	4.625	5.611	5.452	6.323	6.522	6.323	5.951	5.611	3.450	4.878	4.280	4.878	3.529	3.973	3.450	3.677
2.500	7.059	6.596	7.059	8.561	10.904	10.599	11.902	12.646	11.902	10.599	6.745	9.250	8.348	9.250	6.745	7.572	6.745	7.059	
3.750	9.678	10.359	11.919	15.998	15.039	16.833	18.398	17.332	16.355	15.459	9.894	13.172	11.919	13.172	9.468	11.092	9.894	10.118	
5.000	11.840	12.625	13.490	15.144	20.052	19.513	21.197	23.804	21.807	21.197	19.513	12.904	16.696	15.511	16.696	11.840	14.117	12.625	13.192
6.250	14.196	15.116	15.781	18.487	23.125	22.528	25.766	28.055	25.064	25.766	23.125	15.781	19.864	14.493	19.864	16.863	15.116	15.781	
7.500	16.354	17.392	17.760	21.176	25.682	24.430	30.077	31.796	27.750	29.270	26.345	18.532	23.266	21.671	22.716	17.035	19.355	17.035	18.140
8.750	18.331	19.079	19.874	24.147	26.502	34.148	35.090	30.736	33.244	29.218	21.163	25.982	24.147	25.283	19.471	21.621	19.079	20.290	
10.000	20.144	20.144	21.805	26.980	28.235	28.235	37.000	37.993	33.392	36.045	31.022	23.680	28.235	26.384	26.980	21.805	23.680	20.541	21.805
11.250	21.807	22.229	23.569	28.405	31.046	31.046	40.550	40.550	36.644	38.523	34.074	26.088	31.046	28.405	29.033	24.042	24.531	22.229	23.569
12.500	23.353	24.230	25.676	29.600	32.980	32.980	43.908	42.804	38.777	40.716	36.119	28.392	33.725	30.233	30.233	26.187	25.180	23.775	25.180
13.750	24.733	26.453	27.698	31.231	35.485	35.485	47.084	41.646	42.655	37.946	30.597	36.278	31.885	31.231	27.698	25.666	25.193	27.168	
15.000	26.018	27.999	29.076	32.707	37.874	37.874	48.859	47.675	43.343	44.369	39.576	32.056	38.711	33.378	32.056	29.638	25.555	26.493	28.530
16.250	26.722	28.186	29.774	34.728	39.303	39.303	51.648	49.217	44.845	46.955	41.030	33.379	39.303	34.728	32.734	30.908	27.197	27.685	28.701
17.500	25.544	25.972	28.279	35.252	38.941	39.748	50.567	48.294	45.163	48.294	40.581	33.922	35.947	34.578	31.478	30.908	27.794	26.840	26.860
18.750	27.369	27.827	30.299	37.770	41.723	42.588	54.179	51.744	48.389	51.744	43.479	36.345	38.515	37.048	33.727	33.116	29.779	28.778	28.778
20.000	27.798	26.922	30.697	38.768	41.082	44.504	55.194	52.768	50.499	52.768	44.504	37.332	38.040	38.040	34.074	34.074	31.224	29.193	28.252
25.000	28.055	31.614	37.102	39.029	46.666	52.375	60.466	63.123	61.773	55.630	51.353	42.592	39.705	41.111	32.610	36.492	34.747	30.663	28.055
30.000	31.353	34.663	37.360	43.075	50.210	55.999	62.850	68.140	64.113	58.152	52.036	44.523	39.131	43.075	35.706	37.937	33.666	32.248	31.796
40.000	37.491	38.505	41.803	45.545	52.175	61.373	61.393	73.289	68.147	62.447	53.845	53.000	49.813	44.888	40.658	44.244	38.505	37.491	36.045
50.000	37.413	39.729	44.477	50.823	57.772	62.246	66.250	83.683	71.792	66.250	60.408	59.509	50.823	48.783	45.056	46.250	42.804	40.716	37.860
60.000	37.466	43.851	47.675	49.468	63.592	60.987	71.411	79.500	76.617	73.592	67.351	60.155	52.690	50.720	45.432	47.099	44.369	43.343	40.929
70.000	41.007	47.750	48.294	50.567	63.078	64.749	71.152	76.325	71.152	68.297	62.267	56.305	51.764	48.848	46.956	41.879	44.670	44.186	
80.000	41.114	39.517	48.891	49.418	51.052	61.303	69.361	72.090	71.162	75.986	59.861	61.303	55.194	52.768	47.360	42.742	45.427	44.962	
100.000	44.055	42.208	53.306	58.770	59.963	68.687	75.891	87.404	85.310	76.761	69.436	64.439	65.119	57.046	53.306	48.570	43.676	47.699	44.828
110.000	44.190	39.750	46.903	57.602	59.276	62.850	79.152	82.790	80.039	78.280	62.850	66.757	61.024	55.479	51.110	49.479	42.035	47.646	41.697
120.000	42.285	45.653	54.177	61.259	64.128	66.570	76.317	85.560	84.652	76.317	69.155	66.570	56.558	54.177	47.490	43.586	47.490	42.285	
140.000	46.218	47.965	58.872	60.366	70.648	67.543	74.665	80.577	79.035	73.972	64.638	56.966	59.364	55.596	47.254	45.880	46.539	45.215	

Table 7.5 (c)
Hardness H in kg/mm²

Room Temp. 30°C
d-AHT Z (111)

P (kg/mm²) <	Angle->																		
	0	10	20	30	40	50	60	70	80	90	100	110	120	130	140	150	160	170	180
Hardness in kg/mm²/square.																			
1.250	6.625	6.839	5.611	5.225	4.813	4.749	4.174	3.450	3.298	3.226	3.373	3.298	3.373	3.450	4.174	4.280	5.777	4.625	
2.500	12.265	12.646	9.757	9.890	7.755	8.044	7.755	6.745	5.920	6.177	5.920	6.177	5.797	6.596	8.143	8.143	10.904	9.011	
3.750	16.592	17.853	14.247	13.875	11.072	10.588	11.358	9.894	8.696	8.880	8.696	8.880	7.554	9.468	11.633	11.919	15.898	15.172	
5.000	20.612	22.444	18.022	14.448	13.643	14.448	12.904	11.126	11.595	11.126	10.685	10.685	12.093	11.840	15.144	15.144	20.612	17.121	
6.250	24.065	25.064	21.954	20.870	17.248	16.490	17.647	15.443	13.628	13.908	13.628	12.115	9.757	14.493	14.196	18.060	23.746	20.870	
7.500	28.495	28.495	25.682	23.837	19.788	19.355	20.255	17.760	15.406	16.028	15.712	13.246	10.424	16.689	16.354	21.176	26.345	24.430	
8.750	31.134	32.375	28.501	25.882	22.581	20.280	23.086	19.471	17.626	18.331	17.626	14.140	10.897	18.700	17.973	23.608	24.147	27.810	
10.000	33.814	35.127	31.783	28.895	25.249	22.713	21.371	19.759	20.144	19.384	14.841	11.222	20.541	19.384	25.807	26.384	28.895	30.288	
11.250	37.566	37.566	34.074	31.764	27.798	25.034	21.807	23.109	20.612	22.229	21.000	13.798	11.279	22.229	21.398	27.798	29.053	30.353	
12.500	39.729	40.716	36.119	33.725	29.291	26.714	23.775	24.230	22.077	24.230	22.484	12.883	11.264	23.775	22.903	29.600	30.887	31.562	
13.750	42.655	42.655	37.946	36.278	30.597	26.909	25.666	23.426	25.666	23.850	12.075	11.197	25.193	24.285	30.597	33.256	32.560	37.946	
15.000	40.470	44.369	39.576	37.874	32.056	28.530	27.493	26.981	25.105	26.493	25.105	11.358	11.072	26.493	25.555	31.425	35.520	39.576	
16.250	42.874	46.955	41.480	40.152	34.044	28.701	29.230	27.934	26.259	27.685	25.808	11.739	11.470	24.117	26.722	32.108	36.909	35.433	39.303
17.500	44.186	49.411	42.780	41.440	35.252	29.289	30.354	28.777	27.321	28.777	27.321	11.938	11.804	22.130	27.794	32.666	38.159	37.399	38.941
18.750	46.330	49.470	41.723	42.588	36.345	30.299	30.833	29.779	28.778	29.779	28.778	12.097	12.097	20.444	28.778	33.116	38.515	38.515	39.576
20.000	48.373	50.499	44.488	43.610	38.040	31.224	31.764	27.798	29.682	30.697	29.682	12.223	12.355	18.746	29.682	32.889	38.768	39.517	37.352
25.000	57.973	55.630	50.361	46.666	44.969	36.492	37.102	33.653	34.194	33.922	34.747	13.628	14.957	20.870	32.610	38.371	44.155	44.969	42.572
30.000	66.757	54.967	52.986	50.461	46.835	41.697	36.245	37.937	39.131	39.750	14.678	17.212	22.448	34.663	43.075	48.479	48.479	46.045	
40.000	73.289	64.638	63.528	59.862	45.545	53.845	45.880	46.218	38.505	45.545	16.020	21.371	24.186	36.518	50.582	55.596	53.000	50.582	
50.000	80.100	71.792	62.744	55.305	53.747	48.783	45.056	40.716	43.908	45.647	44.477	16.826	20.199	24.463	39.249	51.531	55.305	56.932	56.110
60.000	74.719	73.592	60.569	64.042	59.339	55.136	46.533	45.432	50.088	50.088	17.205	18.988	24.239	40.929	51.364	54.067	59.339	60.155	
70.000	79.704	74.715	65.906	57.002	67.383	57.356	44.186	49.128	47.750	53.640	48.294	17.307	17.666	23.745	41.879	49.984	52.378	59.925	63.078
80.000	81.880	74.983	63.566	61.672	64.349	51.052	45.899	53.658	52.768	51.615	52.768	17.121	16.387	22.940	41.900	48.373	50.499	59.861	64.349
100.000	84.534	76.997	75.719	73.515	60.789	60.145	55.348	62.443	55.067	54.512	55.067	19.157	18.88	25.411	41.474	49.875	55.067	61.773	64.518
110.000	85.291	80.394	73.369	70.970	65.119	65.770	51.815	58.187	56.212	57.612	55.938	19.982	19.866	26.472	41.155	50.386	57.046	62.462	64.437
120.000	81.858	83.263	76.578	72.559	66.081	55.222	49.768	54.967	54.461	48.903	53.963	20.698	20.816	27.210	40.384	50.210	58.152	62.232	63.477
140.000	78.683	87.894	71.194	74.798	65.638	58.838	55.349	51.943	53.719	49.440	53.719	21.737	22.335	28.326	38.714	49.845	60.165	61.817	61.259
160.000	86.693	78.280	72.615	75.191	51.770	53.293	47.786	54.448	50.388	22.481	23.556	28.895	36.757	49.061	61.393	60.876	58.872		

Table 7.5 (d)
Hardness H in Kg/mm²

Room Temp. 30°C
d-AHT z (111)

TABLE 7.6

Knoop Hardness values obtained from plot of

H vs P (mean hardness H) from equations

(7.31) & (7.30) respectively for d-AHT

Room Temp : 30°C ;

Face	Angle	H̄	H = cb₂		$\frac{2/n_1(n_2-2)}{n_2}P$
			H	P	
m (110)	0	30.34	34.56		30.62
z (111)	0	81.27	96.05		83.10
c (010)	0	31.91	22.31		21.17
z (111)	0	40.63	24.86		25.81
m (110)	10	38.61	32.07		29.79
z (111)	10	76.65	101.76		77.82
c (010)	10	31.11	19.92		19.59
z (111)	10	45.49	28.40		28.89
m (110)	20	37.80	49.56		39.96
z (111)	20	68.38	85.79		68.64
c (010)	20	39.53	25.30		25.77
z (111)	20	49.78	39.49		34.86
m (110)	30	40.84	50.50		42.84
z (111)	30	66.49	100.36		71.45
c (010)	30	37.91	31.00		29.63
z (111)	30	54.66	39.46		37.50
m (110)	40	53.74	61.93		55.06
z (111)	40	61.98	81.60		63.68
c (010)	40	53.27	54.34		36.44
m (110)	50	52.65	70.38		54.93
z (111)	50	55.61	80.54		42.84
c (010)	50	51.57	40.23		13.06
z (111)	50	65.49	44.82		43.17
m (110)	60	58.35	54.16		134.80
z (111)	60	49.16	52.14		48.54
c (010)	60	59.07	32.99		111.07
z (111)	60	72.40	54.33		49.99
m (110)	70	65.02	75.56		67.69
z (111)	70	51.59	55.92		51.94
c (010)	70	63.21	42.90		41.74
z (111)	70	80.56	54.64		56.27
m (110)	80	70.34	72.93		115.60
z (111)	80	50.79	56.07		46.15
c (010)	80	63.21	43.26		43.47
z (111)	80	78.23	59.25		52.30
m (110)	90	73.96	83.33		76.09
z (111)	90	50.44	57.67		50.12
c (010)	90	75.31	47.12		44.19
z (111)	90	73.74	52.48		49.57
m (110)	100	76.02	83.81		74.77
z (111)	100	51.02	54.63		50.66
z (111)	100	65.49	53.00		45.79

TABLE 7.7

Percentage deviation of calculated H by using

equations (7.31) & (7.30) from the observed

graphical value (mean Hardness, \bar{H})

Room Temp : 30°C ;

Face	Angle	% deviation (a)	% deviation (b)
m (110)	0	-13.91	-0.92
z (111)	0	-18.19	-2.25
c (010)	0	30.08	33.66
z (111)	0	38.82	36.48
m (110)	10	12.40	18.63
z (111)	10	-32.76	-1.53
c (010)	10	35.97	37.03
z (111)	10	37.57	36.49
m (110)	20	-31.11	-5.71
z (111)	20	-25.46	-0.38
c (010)	20	36.00	34.81
z (111)	20	20.67	29.97
m (110)	30	-23.65	-4.90
z (111)	30	-50.94	-7.46
c (010)	30	18.23	21.84
z (111)	30	27.81	31.39
m (110)	40	-15.24	-2.46
z (111)	40	-31.66	-2.74
c (010)	40	-2.01	31.59
m (110)	50	-33.88	-4.33
z (111)	50	-44.83	22.96
c (010)	50	21.99	74.68
z (111)	50	31.56	34.08
m (110)	60	7.18	-181.02
z (111)	60	-6.06	1.26
c (010)	60	44.15	-88.03
z (111)	60	24.96	30.95
m (110)	70	-16.21	-4.11
z (111)	70	-8.39	-0.68
c (010)	70	32.13	33.97
z (111)	70	32.17	30.15
m (110)	80	-3.68	-64.34
z (111)	80	-10.40	9.14
c (010)	80	31.56	31.23
z (111)	80	24.26	33.15
m (110)	90	-12.57	-2.88
z (111)	90	-14.33	0.63
c (010)	90	37.43	41.32
z (111)	90	28.83	32.78
m (110)	100	-10.25	1.64
z (111)	100	-7.08	0.71
z (111)	100	19.07	30.08

(a) = % deviation from \bar{H} of $H = cb_2 \frac{2}{n_2} P^{(n_2-2)/n_2}$

(b) = % deviation from \bar{H} of $H = c * e_2 \frac{2}{n_2} P^{(n_2-2)/n_2}$

TABLE 7.8

Hardness H in Kg/sqmm

Angle	Faces		
	cleavage	Prism	sphenoidal
	c (010)	m (110)	z (111)
0	31.917	30.344	80.475
10	31.106	36.608	76.655
20	39.533	37.800	68.379
30	37.912	40.844	66.491
40	53.268	53.738	61.978
50	51.569	53.111	55.612
60	59.072	58.351	49.160
70	63.214	65.017	51.598
80	63.215	70.344	50.798
90	75.309	73.956	50.441
100	70.550	76.023	51.024
110	56.967	71.431	18.853
120	54.834	65.991	19.990
130	54.418	59.043	22.699
140	46.272	54.217	39.895
150	48.777	45.948	50.121
160	43.259	39.887	55.967
170	38.918	36.488	59.822
180	32.367	29.405	60.683
			40.424

TABLE 7.9

Prism face m(110)			Cleavage face c(010)		
H _K	H	% deviation	H _K	H	% deviation
	calc	deviation		calc	deviation
3.370	10.147	-201.09	2.89	10.914	-277.66
5.036	10.688	-112.22	5.56	11.542	-107.60
7.133	11.222	-57.32	8.01	12.164	-51.86
8.518	11.750	-37.94	10.07	12.780	-26.91
11.242	12.272	-9.16	11.67	13.389	-14.73
12.778	12.788	-0.07	12.78	13.993	-9.49
13.430	13.297	0.99	14.65	14.589	0.41
14.840	13.800	7.01	16.44	15.180	7.66
14.670	14.297	2.54	18.18	15.764	13.29
14.660	14.788	-0.87	19.85	16.343	17.67
17.940	15.272	14.87	21.10	16.914	19.84
17.590	15.750	10.46	22.64	17.480	22.79
21.190	16.222	23.45	21.87	18.039	17.52
22.130	16.688	24.59	23.19	18.593	19.83
23.350	17.147	26.57	24.46	19.139	21.75
21.810	17.600	19.30	22.44	19.680	12.30
24.060	19.350	19.58	27.26	21.780	20.10
22.720	21.000	7.57	27.39	23.780	13.18
26.980	24.000	11.05	28.56	27.480	3.78
26.980	26.600	1.41	28.10	30.780	-9.54
32.060	28.800	10.17	29.38	33.680	-14.71
34.580	30.600	11.51	32.67	36.180	-10.74
24.910	32.000	-28.46	33.77	38.280	-13.36
29.980	33.600	-12.07	33.92	41.280	-21.70
30.280	33.600	-10.96	33.18	42.680	-28.63
34.150	32.000	6.30	32.61	42.480	-29.47
33.180	28.800	13.20	30.65	40.680	-32.72

For prism face m(110) $H_{\text{calc}} = -0.002*P^2 + 0.44*P + 9.6$

For cleavage face c(010) $H_{\text{calc}} = -0.002*P^2 + 0.51*P + 10.28$

TABLE 7.10

Anisotropic co-efficients for different
 faces of d-AHT single crystals

Values of anisotropic coefficients	prism	cleavage	<i>z</i> - face
	<i>m</i> (110)	<i>c</i> (010)	<i>z</i> (111)
<i>a</i> ₀	+ 30.40	+ 31.74	+ 40.68
<i>a</i> ₁	+ 3.90	+ 1.05	+ 0.09
<i>a</i> ₂	- 0.50	- 2.33	+ 0.06
<i>a</i> ₃	+ 0.03	+ 1.90 × 10 ⁻³	+ 4.00 × 10 ⁻³
<i>a</i> ₄	- 1.00 × 10 ⁻³	- 7.00 × 10 ⁻⁴	- 9.52 × 10 ⁻⁵
<i>a</i> ₅	+ 2.35 × 10 ⁻⁵	+ 1.60 × 10 ⁻⁶	- 9.12 × 10 ⁻⁷
<i>a</i> ₆	- 2.70 × 10 ⁻⁷	- 2.04 × 10 ⁻⁷	- 3.27 × 10 ⁻⁹
<i>a</i> ₇	+ 2.04 × 10 ⁻⁹	+ 1.59 × 10 ⁻⁹	+ 1.41 × 10 ⁻¹⁰
<i>a</i> ₈	- 9.29 × 10 ⁻¹²	- 7.45 × 10 ⁻¹²	- 1.17 × 10 ⁻¹²
<i>a</i> ₉	+ 2.35 × 10 ⁻¹⁴	+ 1.92 × 10 ⁻¹⁴	+ 4.32 × 10 ⁻¹⁵
<i>a</i> ₁₀	- 2.55 × 10 ⁻¹⁷	- 2.29 × 10 ⁻¹⁷	- 6.00 × 10 ⁻¹⁸

TABLE 7.11

Hardness number H_K of different crystals for different orientations

Aluminium				Calcium Fluoride				Tungsten				Tantalum carbide				Calcite				Sodium nitrate			
Plane	(100)	Plane	(001)	Plane	(110)	Plane	(001)	Plane	(100)	Plane	(100)	Plane	(100)	Plane	(100)	Plane	(100)	Plane	(100)	Plane	(100)	Plane	(100)
Ref direction	[100]	Ref direction	[100]	Ref direction	[100]	Ref direction	[100]	Ref direction	[100]	Ref direction	[100]	Ref direction	[100]	Ref direction	[100]	Ref direction	[100]	Ref direction	[100]	Ref direction	[100]	Ref direction	[100]
Orient- ation in deg A	Knoop	Orient- ation in deg A	Knoop	Orient- ation in deg A	Knoop	Orient- ation in deg A	Knoop	Orient- ation in deg A	Knoop	Orient- ation in deg A	Knoop	Orient- ation in deg A	Knoop	Orient- ation in deg A	Knoop	Orient- ation in deg A	Knoop	Orient- ation in deg A	Knoop	Orient- ation in deg A	Knoop		
0.00	23.30	0.00	176.25	0.00	401.00	0.00	1645.81	7.00	29.24	13.00	16.49	1.00	1593.73	14.00	42.64	26.00	21.59	1.00	1572.90	21.00	50.26	39.00	26.04
10.00	22.60	10.00	173.75	8.00	406.00	10.00	1593.73	14.00	42.64	13.00	16.49	1.00	1510.42	28.00	57.74	52.00	30.13	1.00	1531.25	56.00	83.95	83.00	69.28
18.33	21.30	19.44	167.50	18.00	405.00	20.00	1572.90	21.00	50.26	13.00	16.49	1.00	1489.58	35.00	59.59	65.00	35.02	1.00	1531.25	83.00	92.01	92.00	89.00
27.47	19.30	29.16	161.25	27.00	410.00	30.00	1510.42	28.00	57.74	13.00	16.49	1.00	1488.76	42.00	65.19	78.00	41.67	1.00	1531.25	83.00	92.01	92.00	89.00
37.47	18.00	38.88	157.50	38.00	403.00	40.00	1489.58	35.00	59.59	13.00	16.49	1.00	1541.66	49.00	69.28	78.00	41.67	1.00	1531.25	83.00	92.01	92.00	89.00
45.00	17.00	48.86	157.50	48.00	400.00	45.00	1488.76	42.00	65.19	13.00	16.49	1.00	1531.25	56.00	83.95	83.00	69.28	1.00	1531.25	83.00	92.01	92.00	89.00
54.98	18.00	58.32	160.00	56.00	407.00	50.00	1541.66	49.00	69.28	13.00	16.49	1.00	1531.25	56.00	83.95	83.00	69.28	1.00	1531.25	83.00	92.01	92.00	89.00
63.32	19.30	68.04	162.50	62.00	423.00	60.00	1531.25	56.00	83.95	13.00	16.49	1.00	1531.25	56.00	83.95	83.00	69.28	1.00	1531.25	83.00	92.01	92.00	89.00
71.66	21.30	77.76	170.00	70.00	444.00	70.00	1583.32	63.00	92.01	13.00	16.49	1.00	1583.32	63.00	92.01	92.00	89.00	1.00	1583.32	83.00	92.01	92.00	89.00
80.00	22.60	87.48	180.00	81.00	470.00	80.00	1624.98	70.00	96.46	13.00	16.49	1.00	1624.98	70.00	96.46	96.46	89.00	1.00	1624.98	83.00	92.01	92.00	89.00
90.00	23.30	97.20	182.50	90.00	480.00	90.00	1639.39	78.00	101.79	13.00	16.49	1.00	1639.39	78.00	101.79	101.79	92.01	1.00	1639.39	83.00	92.01	92.00	89.00

TABLE 7.12

Hardness anisotropic coefficients for different crystals

Hardness	Aluminum	Calcium	Tungsten	Tantalum	Carbide	Calcite	Sodium nitrate
Anisotropic coefficients	Aluminium Flouride						
a ₀	24.45	178.84	409.69	1645	29.24	16.49	
a ₁	- 0.26	- 0.89	- 0.95	- 6.25	1.03	0.28	
a ₂	0.0029	0.0098	0.019	0.07	- 0.0004	0.001	

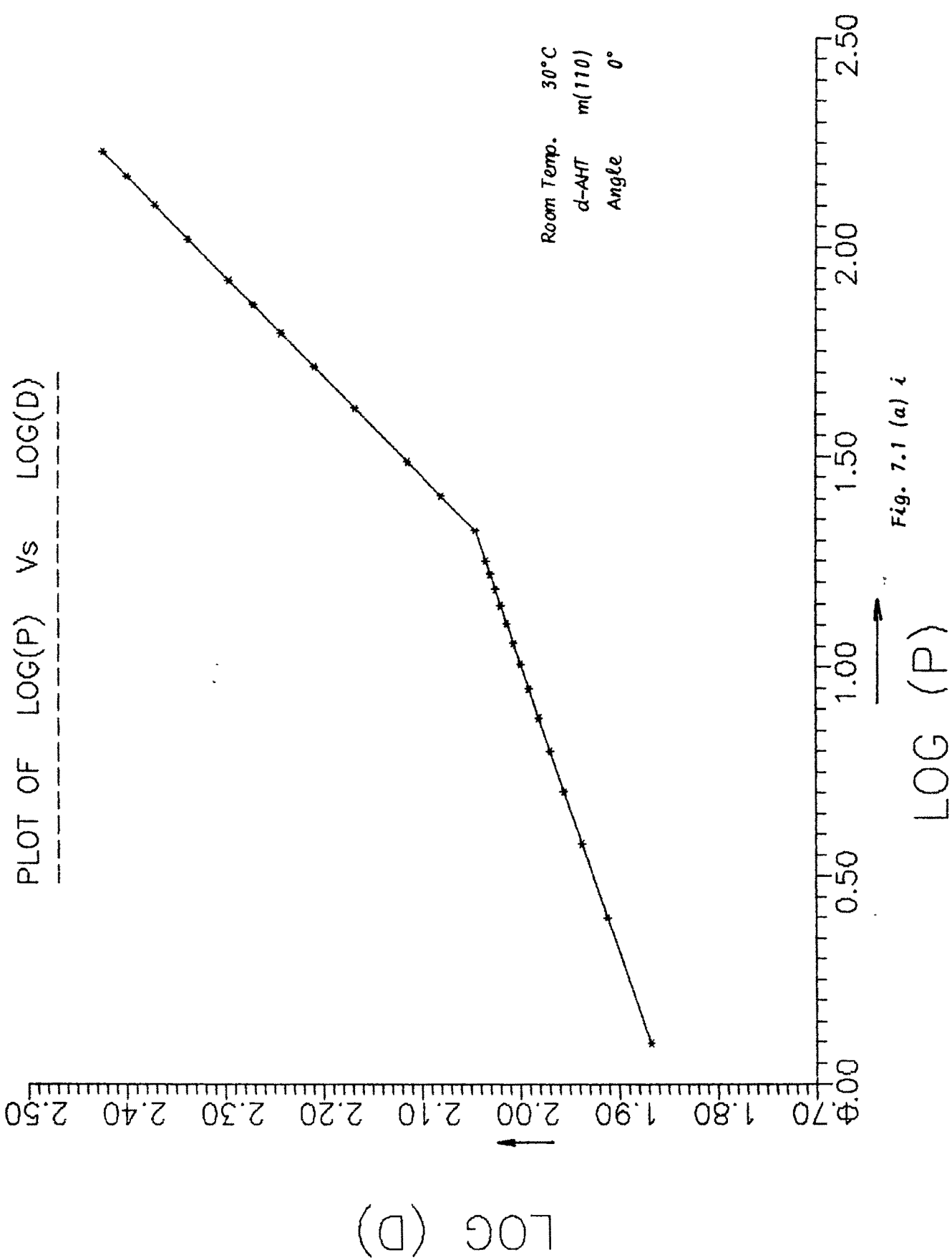
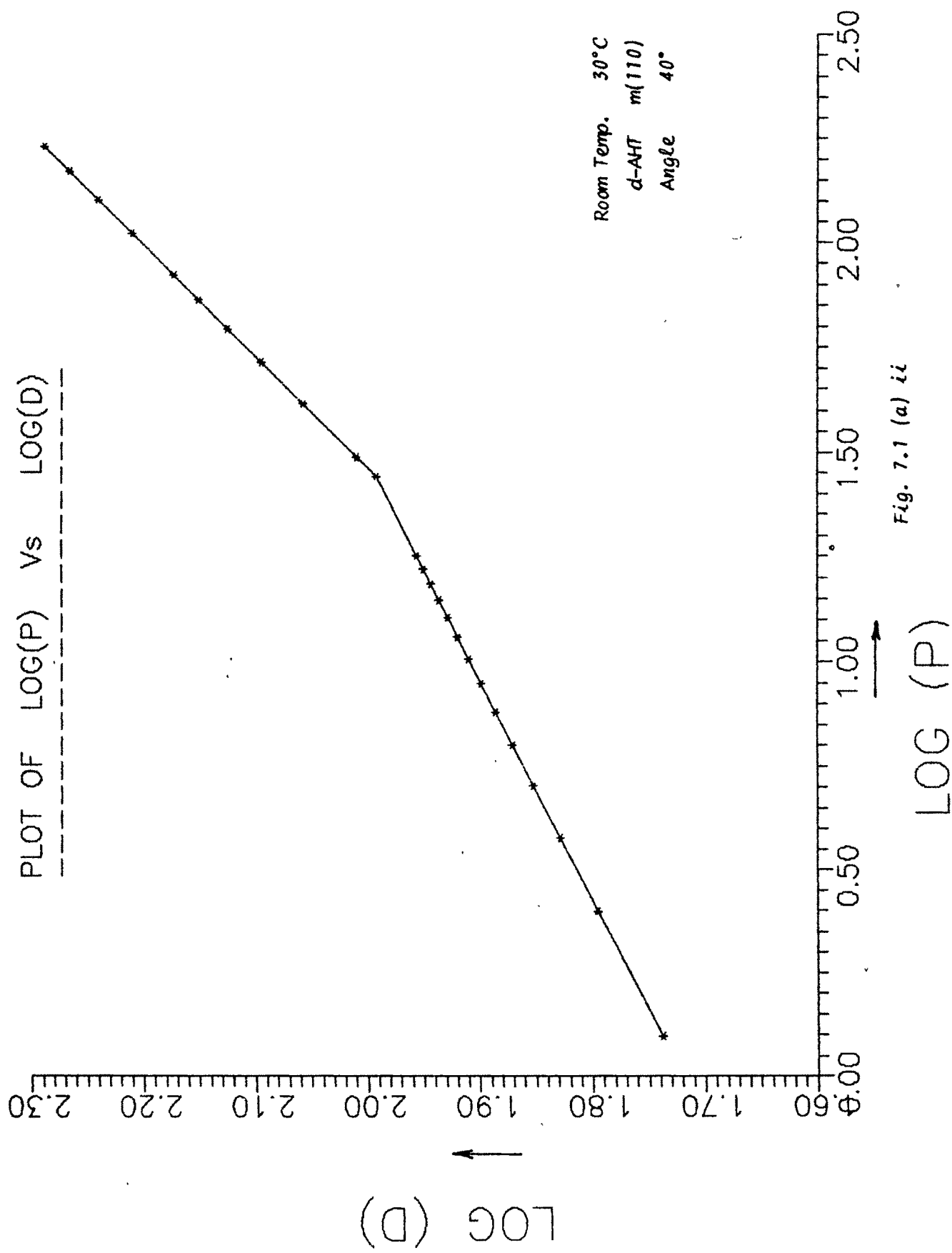


Fig. 7.1 (a) i



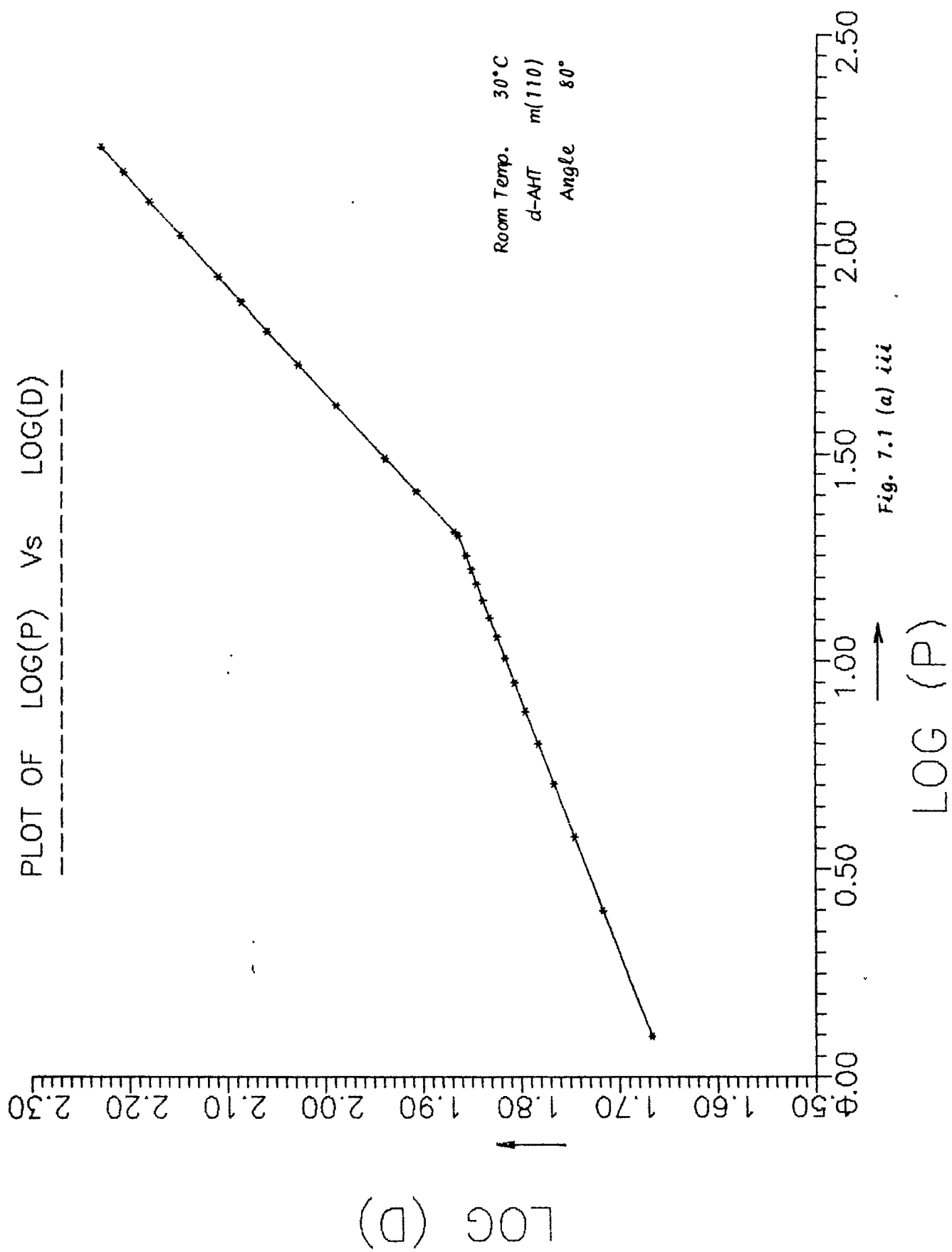
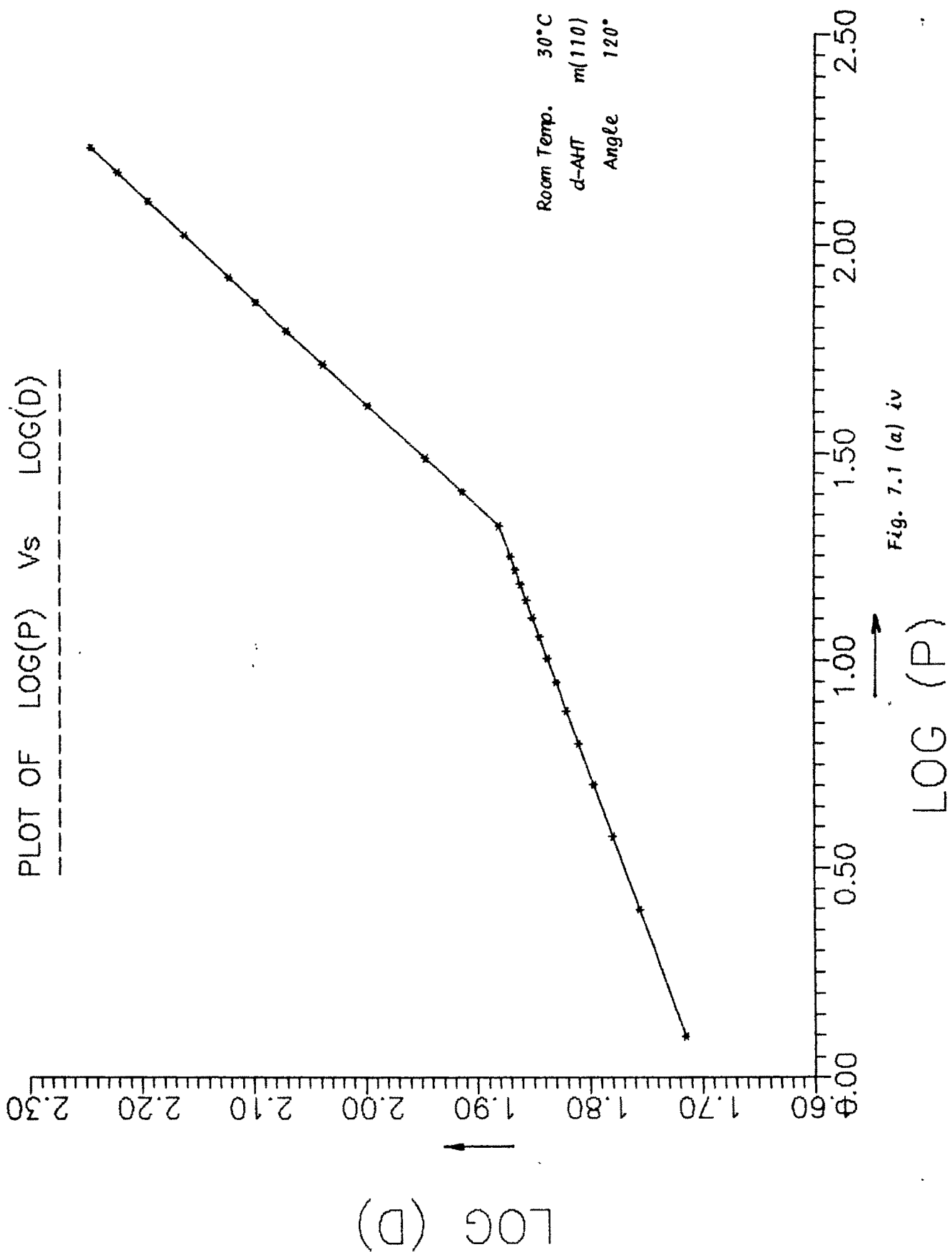
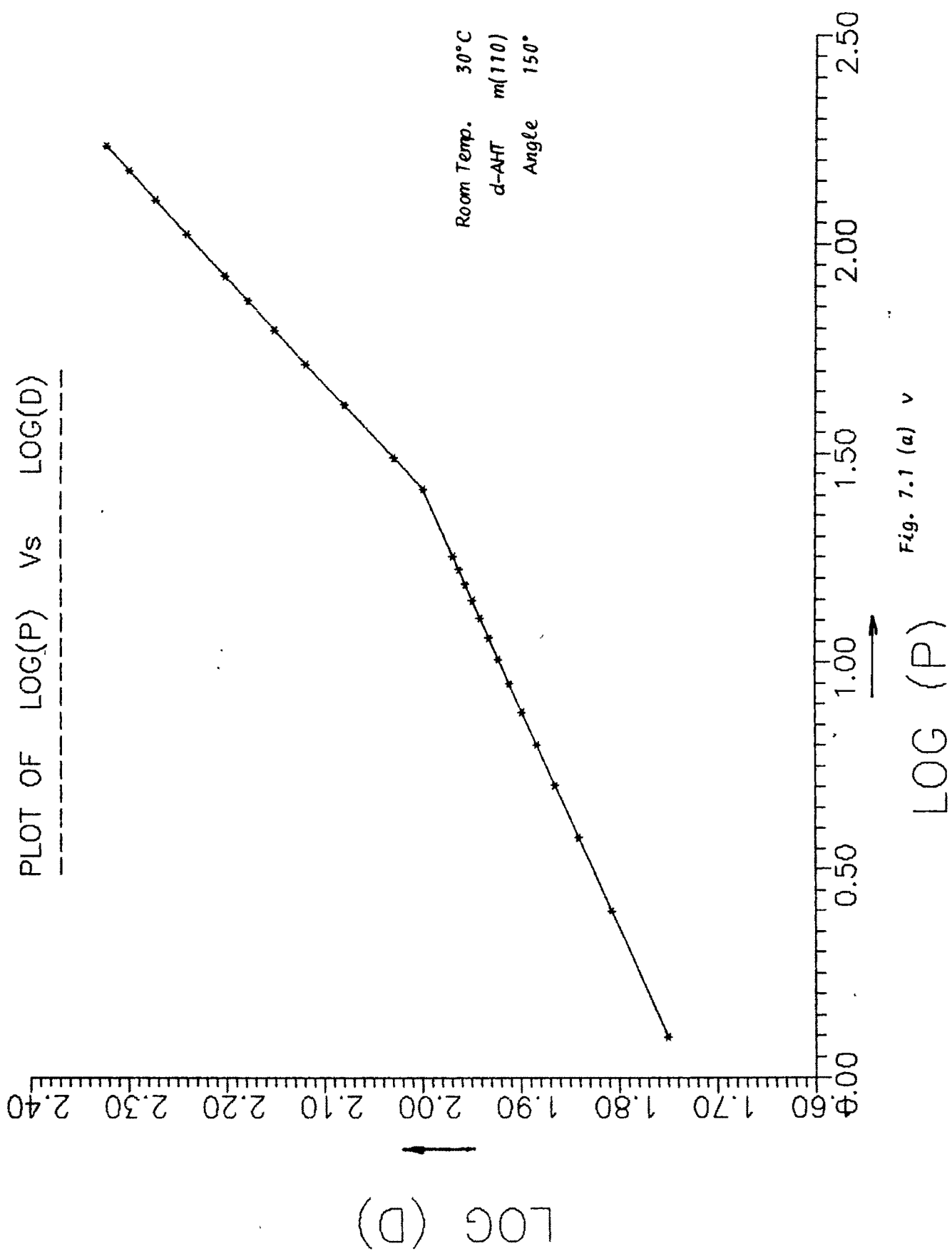


Fig. 7.1 (a) iii

PLOT OF LOG(P) VS LOG(D)





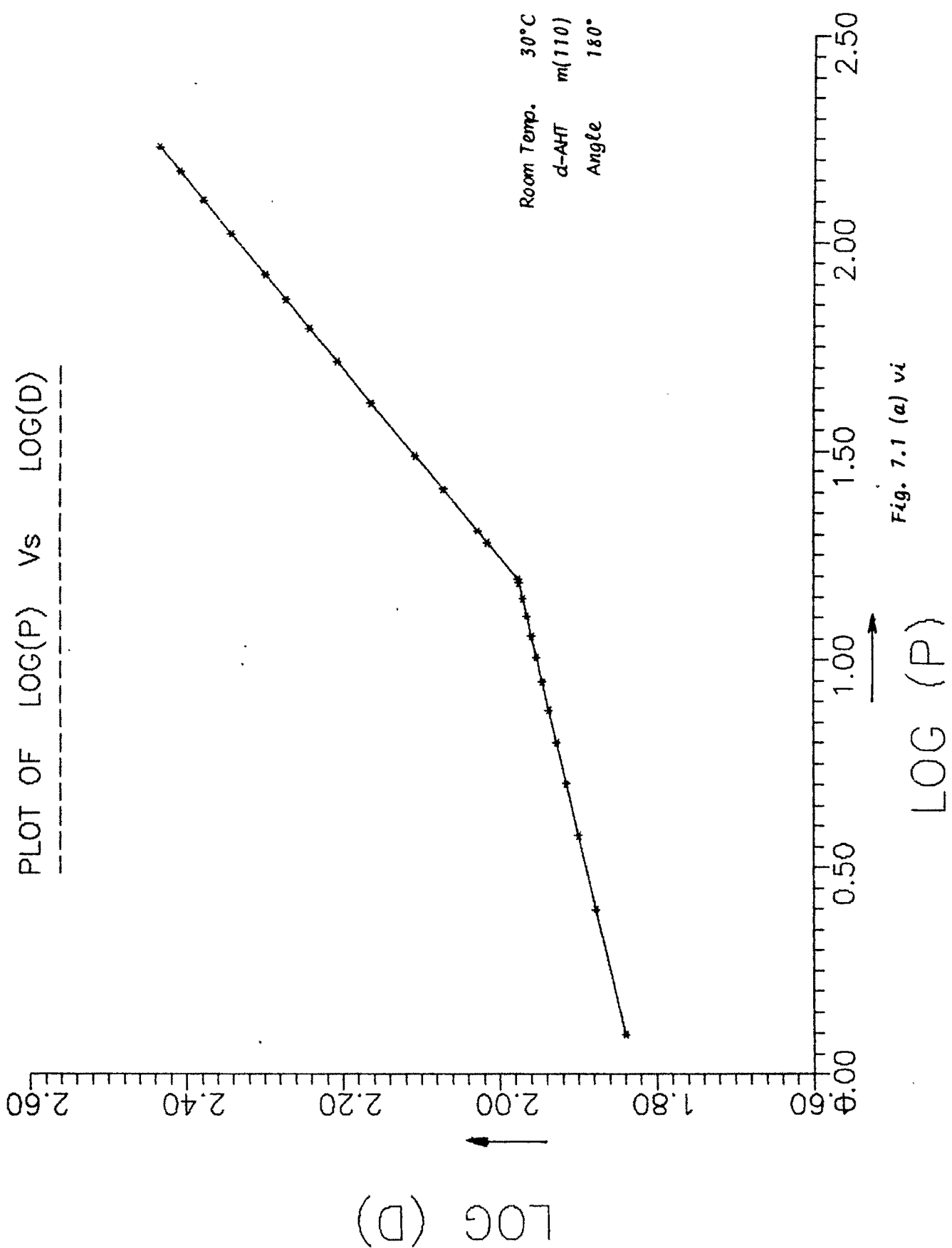


Fig. 7.1 (a) vi

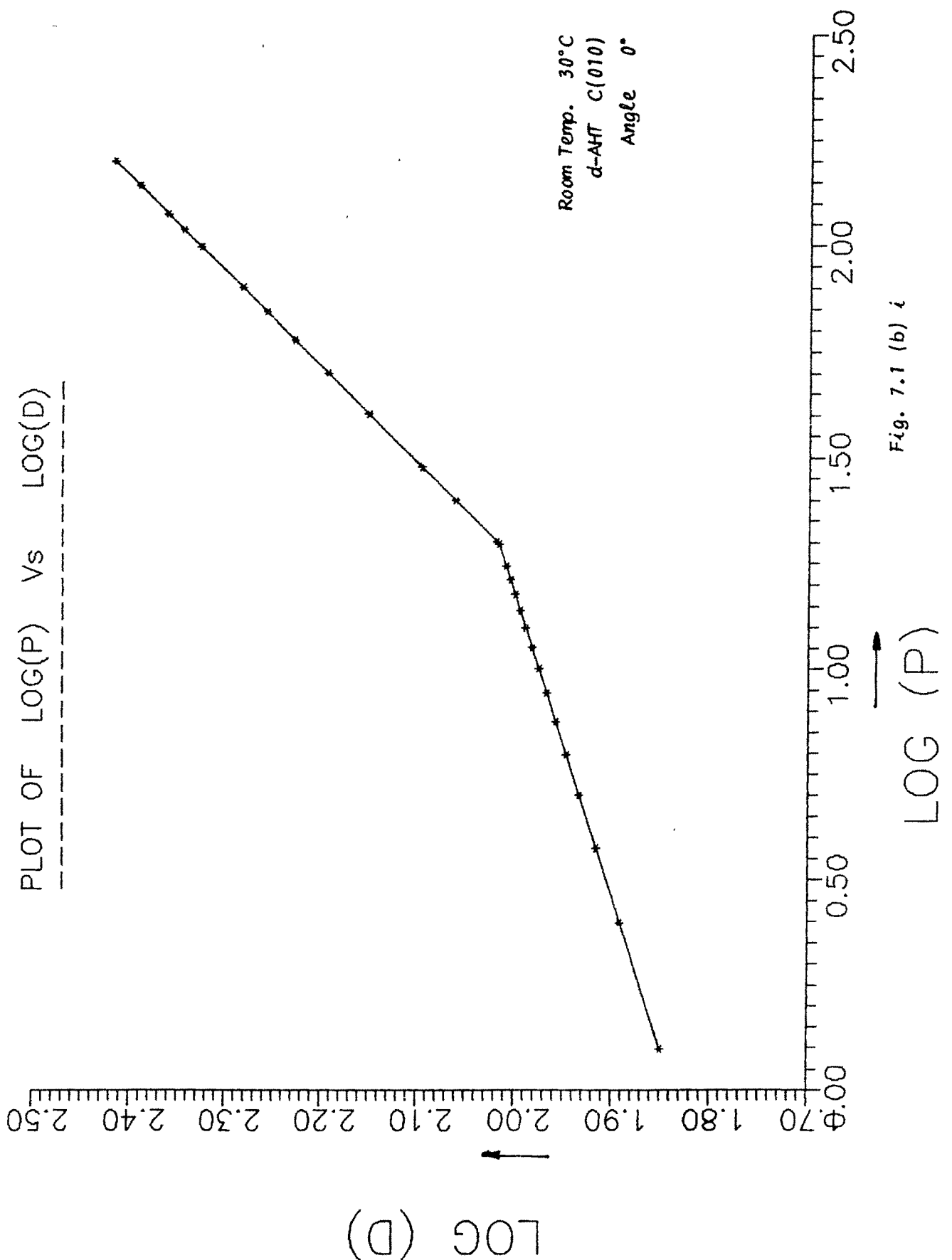


Fig. 7.1 (b) i

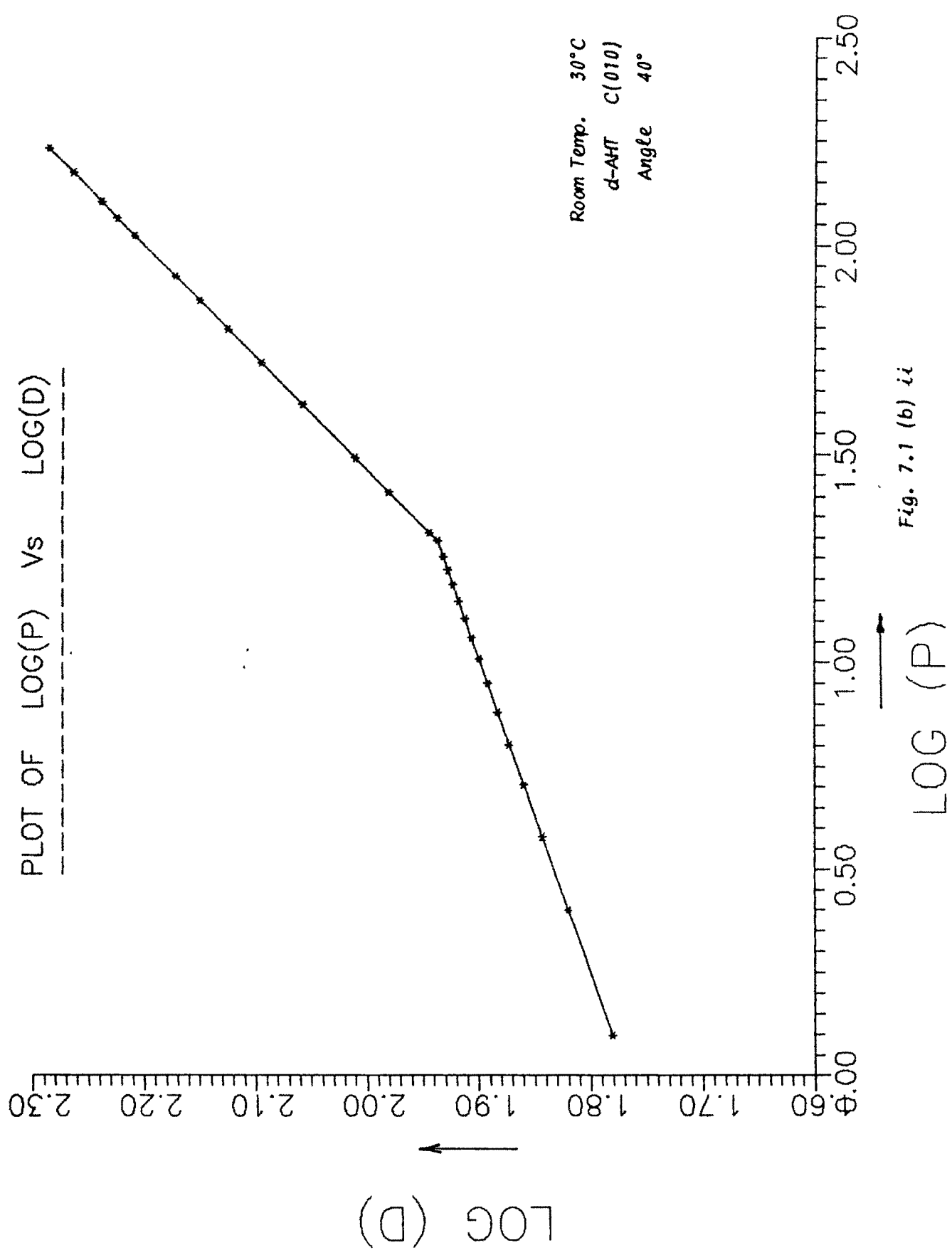


Fig. 7.1 (b) ii

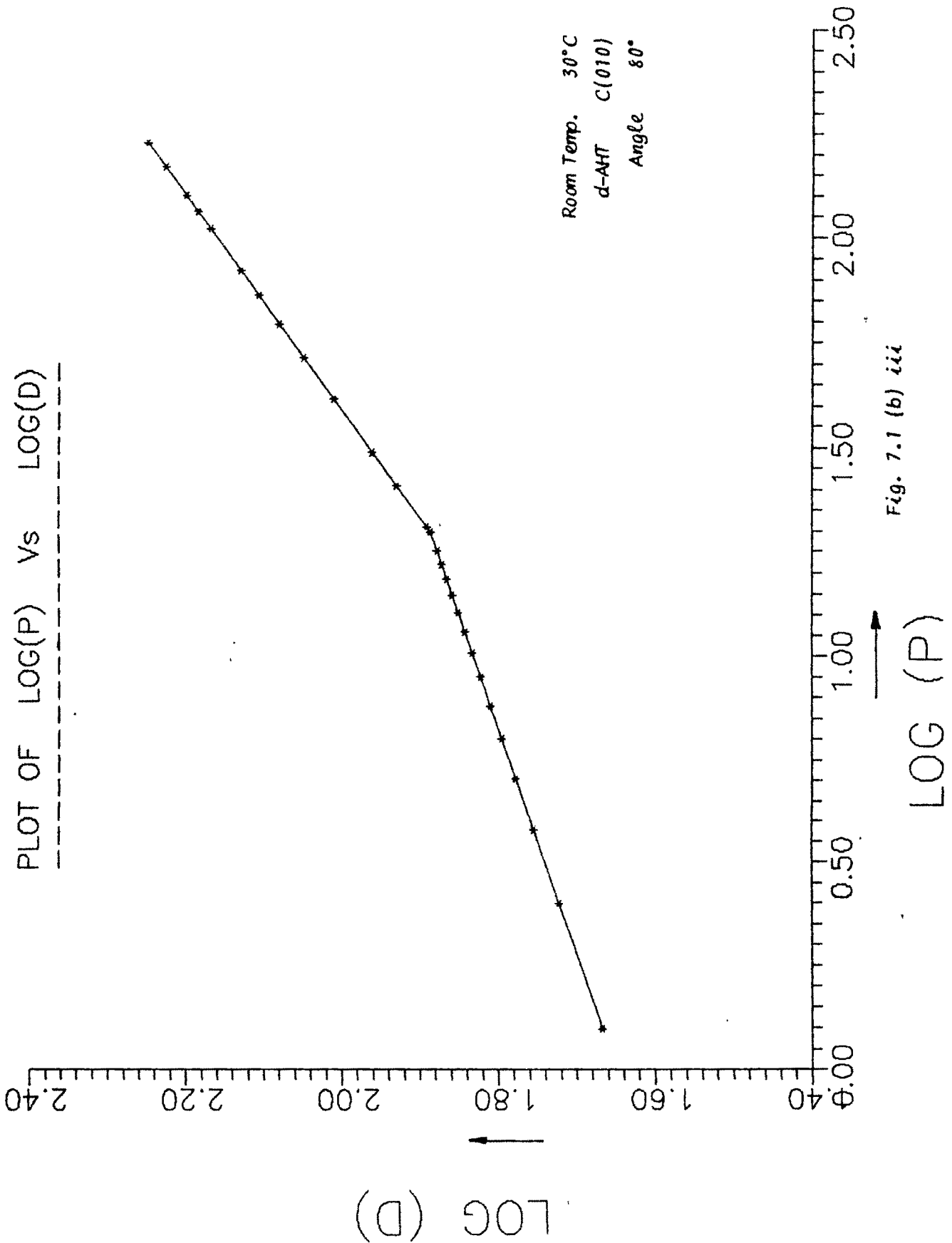
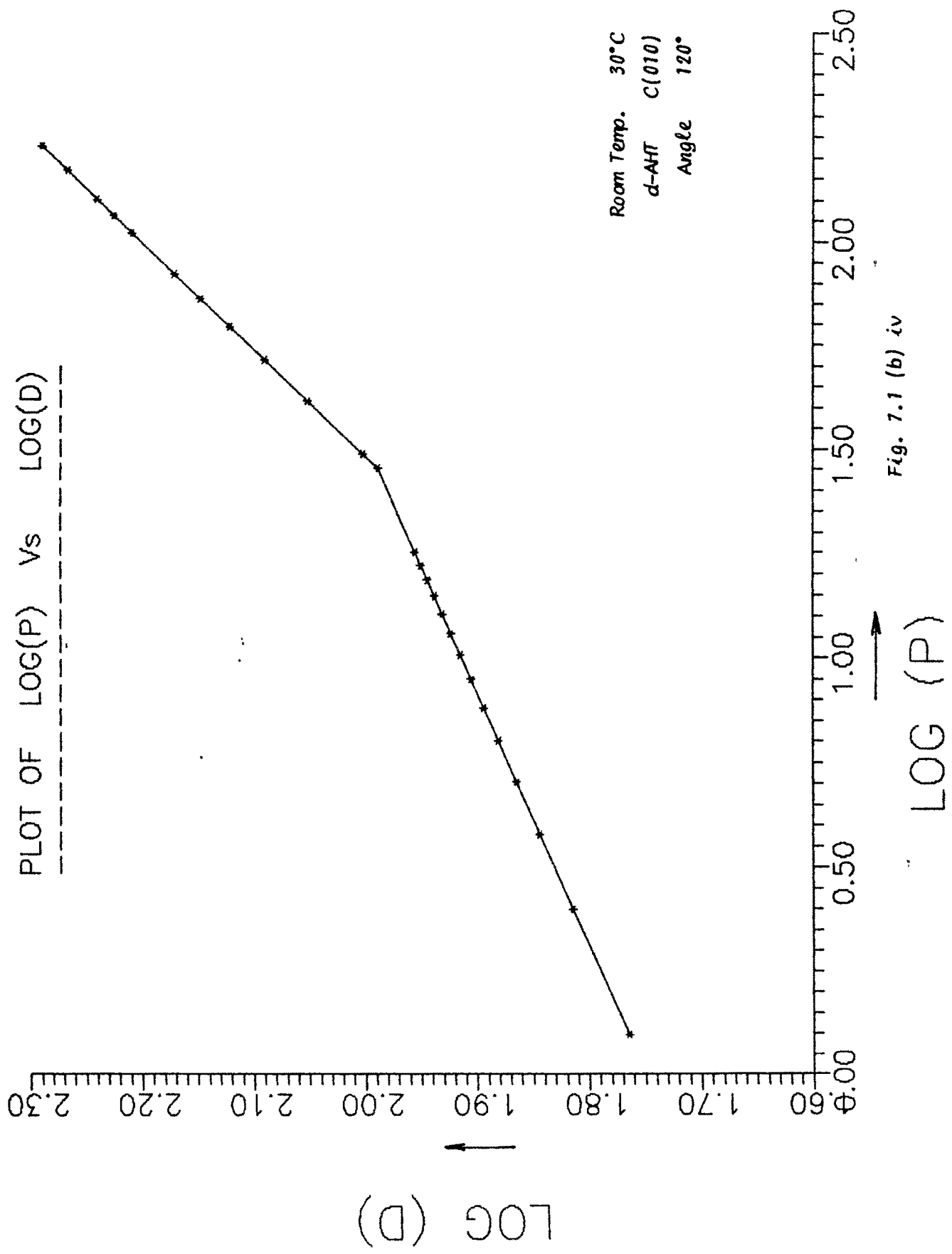
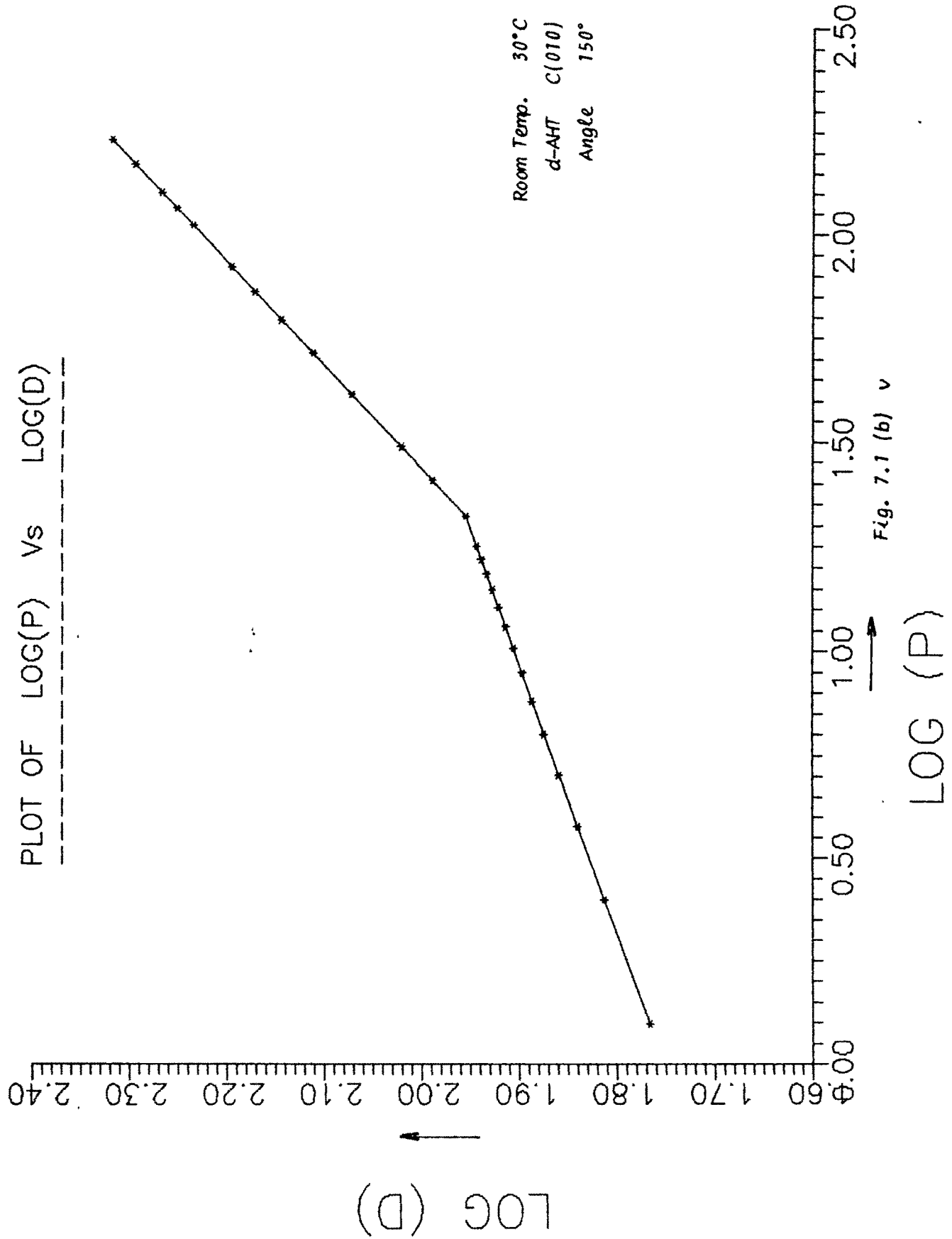


Fig. 7.1 (b) iii





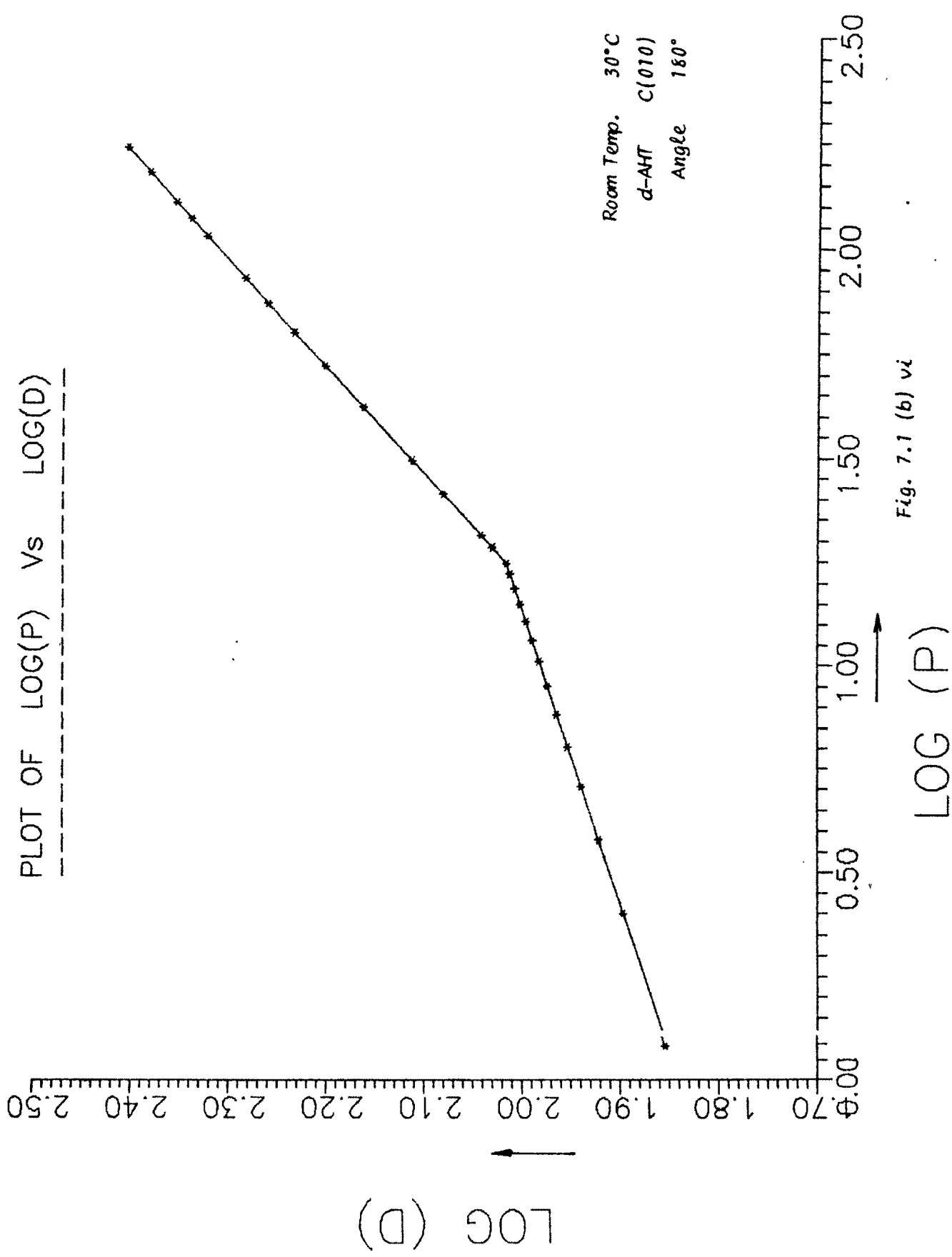


Fig. 7.1 (b) vi

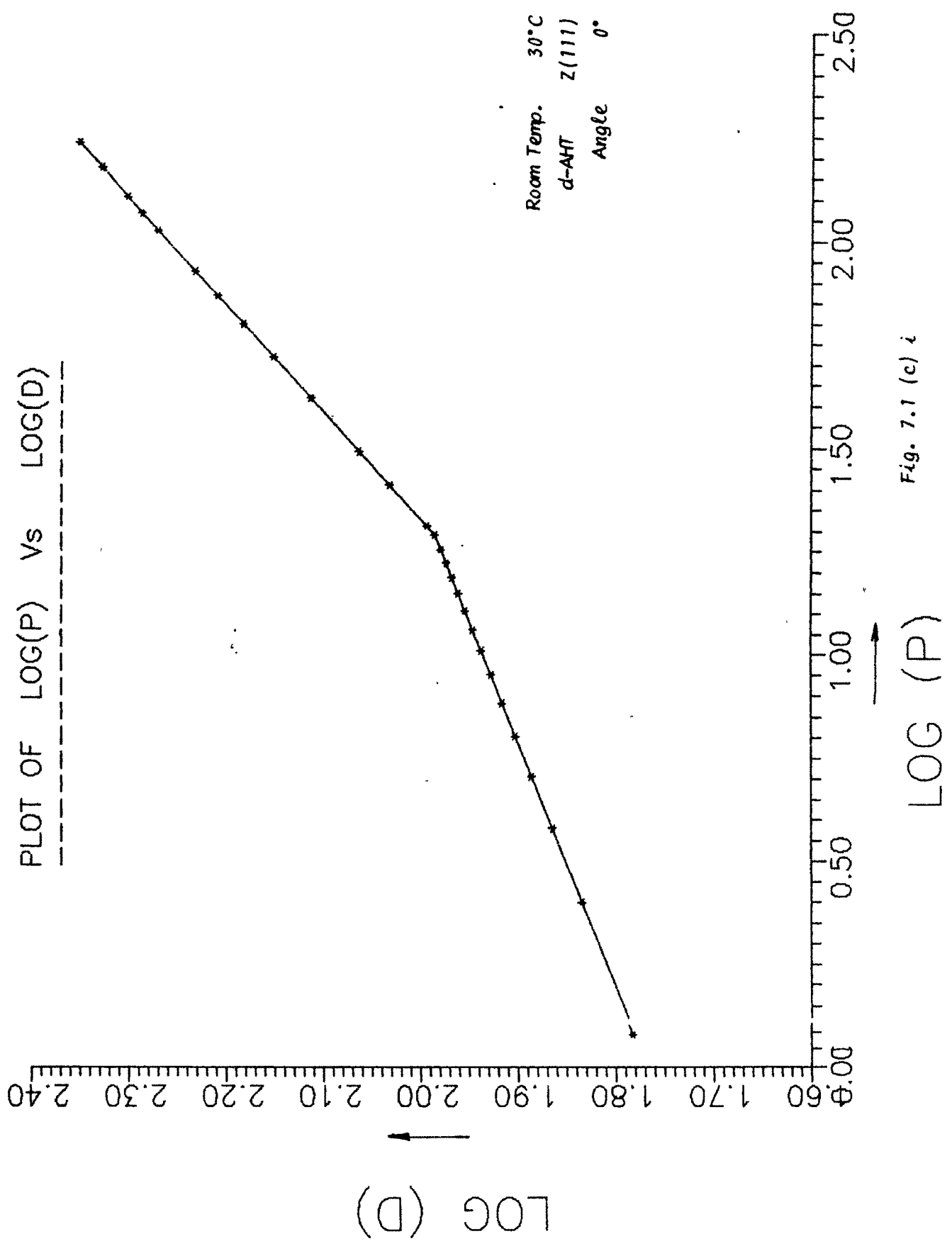


Fig. 7.1 (c) i

PLOT OF LOG(P) Vs LOG(D)

2.40
2.20
2.00
1.80
1.60
0.40
0.00



LOG (D)

Room Temp. 30°C
d-AHT Z(111)
Angle 40°

Fig. 7.1 (c) ii

LOG (P)

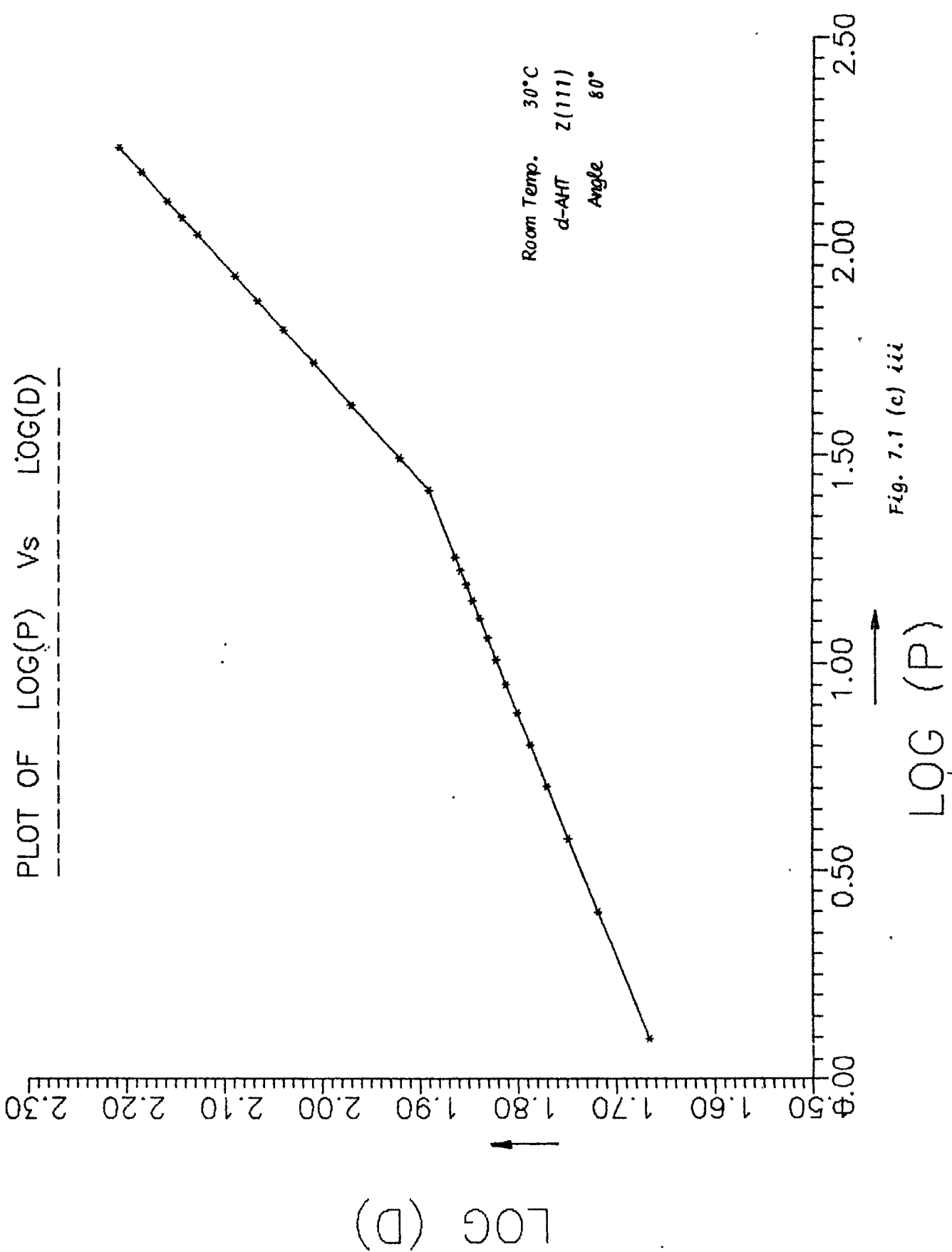
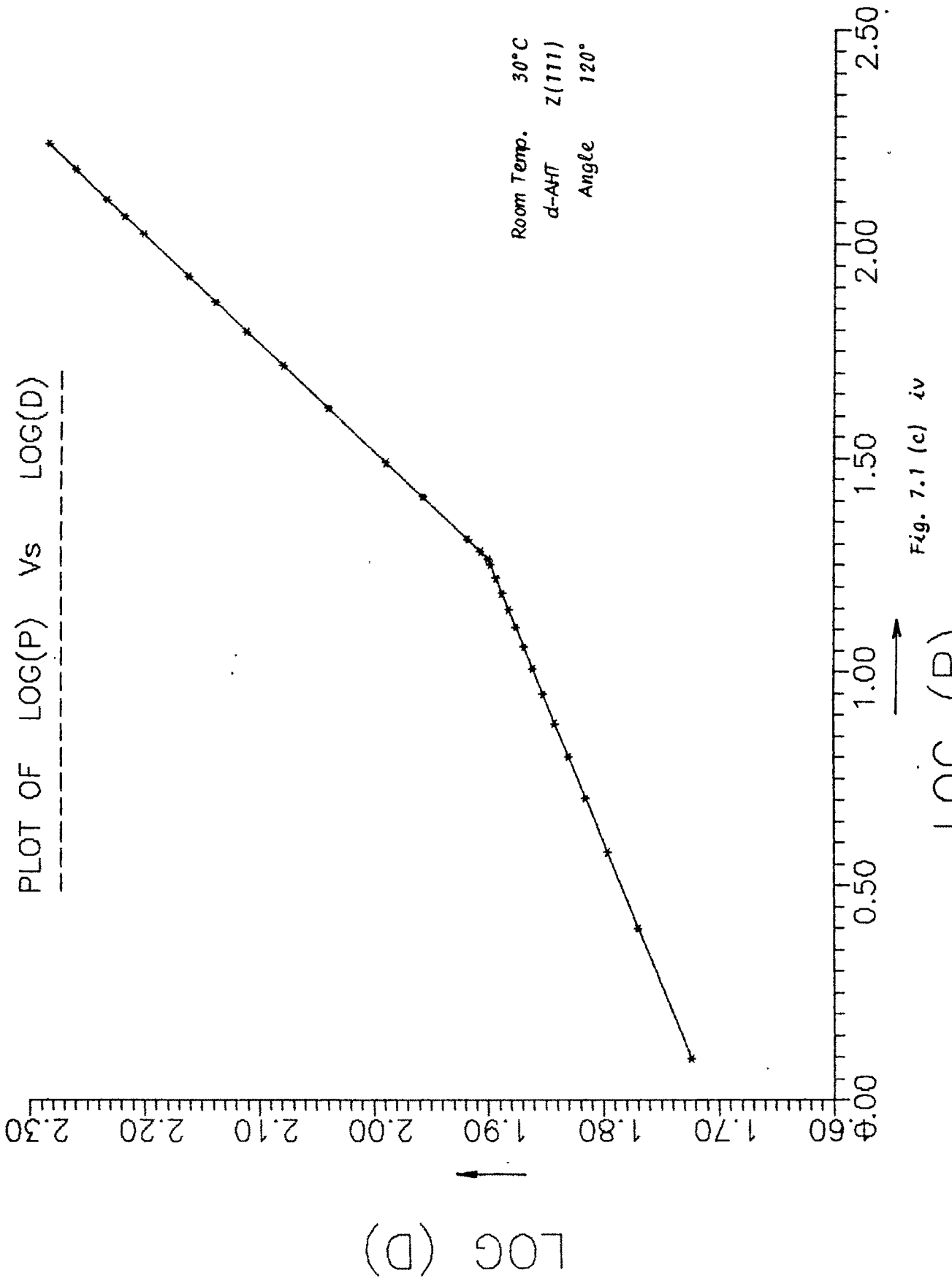


Fig. 7.1 (c) iii



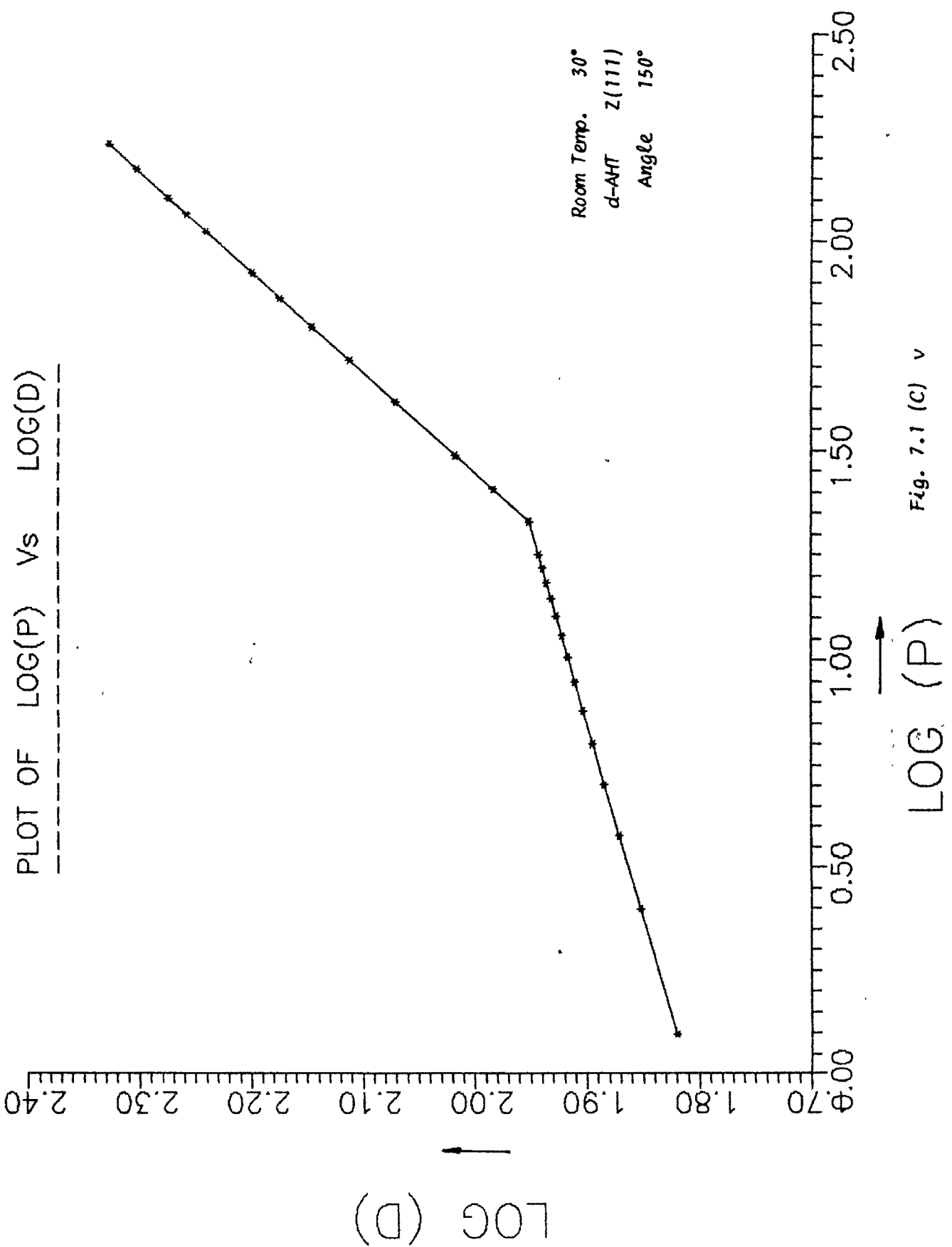


Fig. 7.1 (c) v

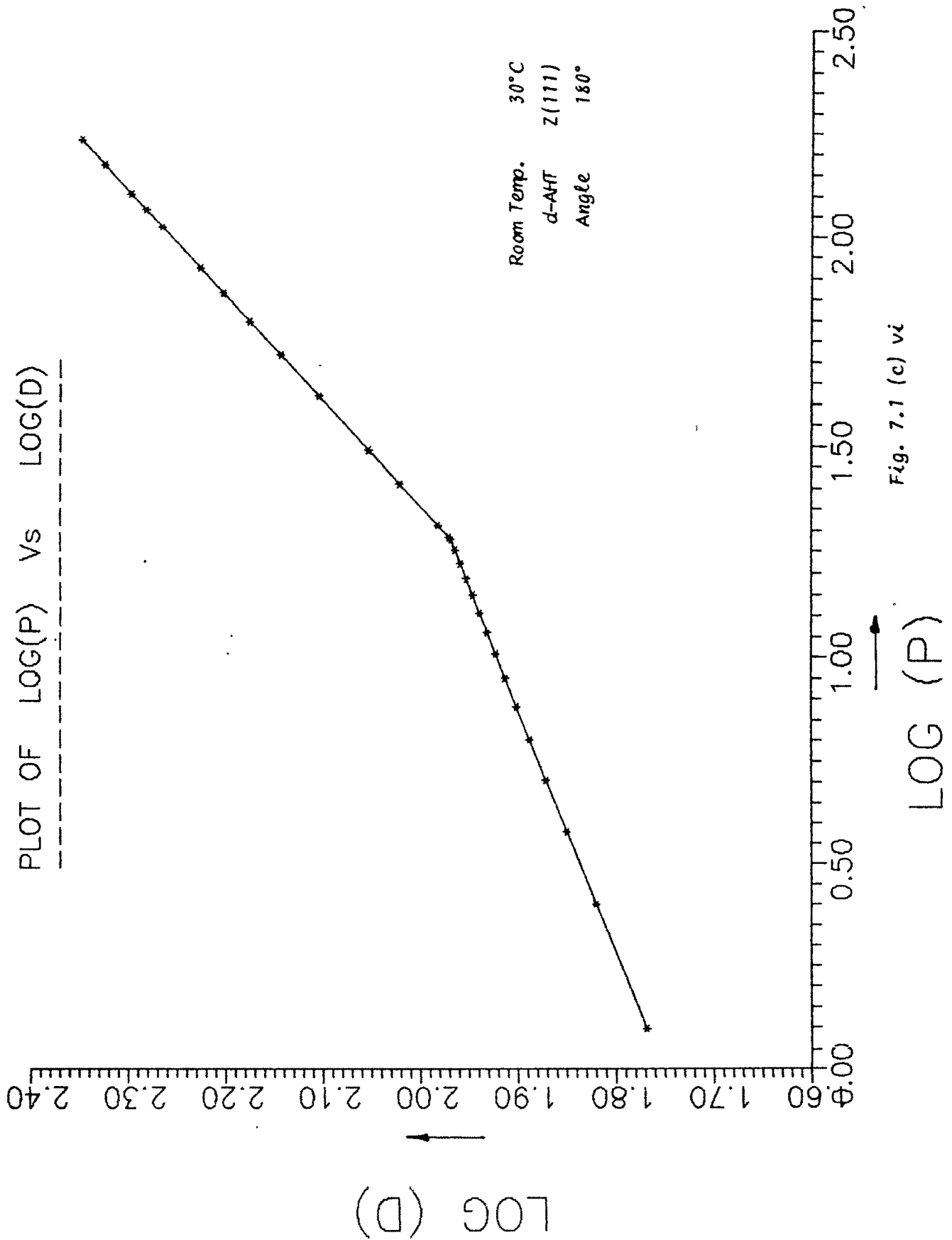


Fig. 7.1 (c) vi

PLOT OF LOG(P) Vs LOG(D)

0.50 1.60 1.70 1.80 1.90 2.00 2.10 2.20 2.30



LOG (D)

Room Temp. $30^{\circ}C$
d-AHT Z(777)
Angle 0°

2.50

2.00

1.50

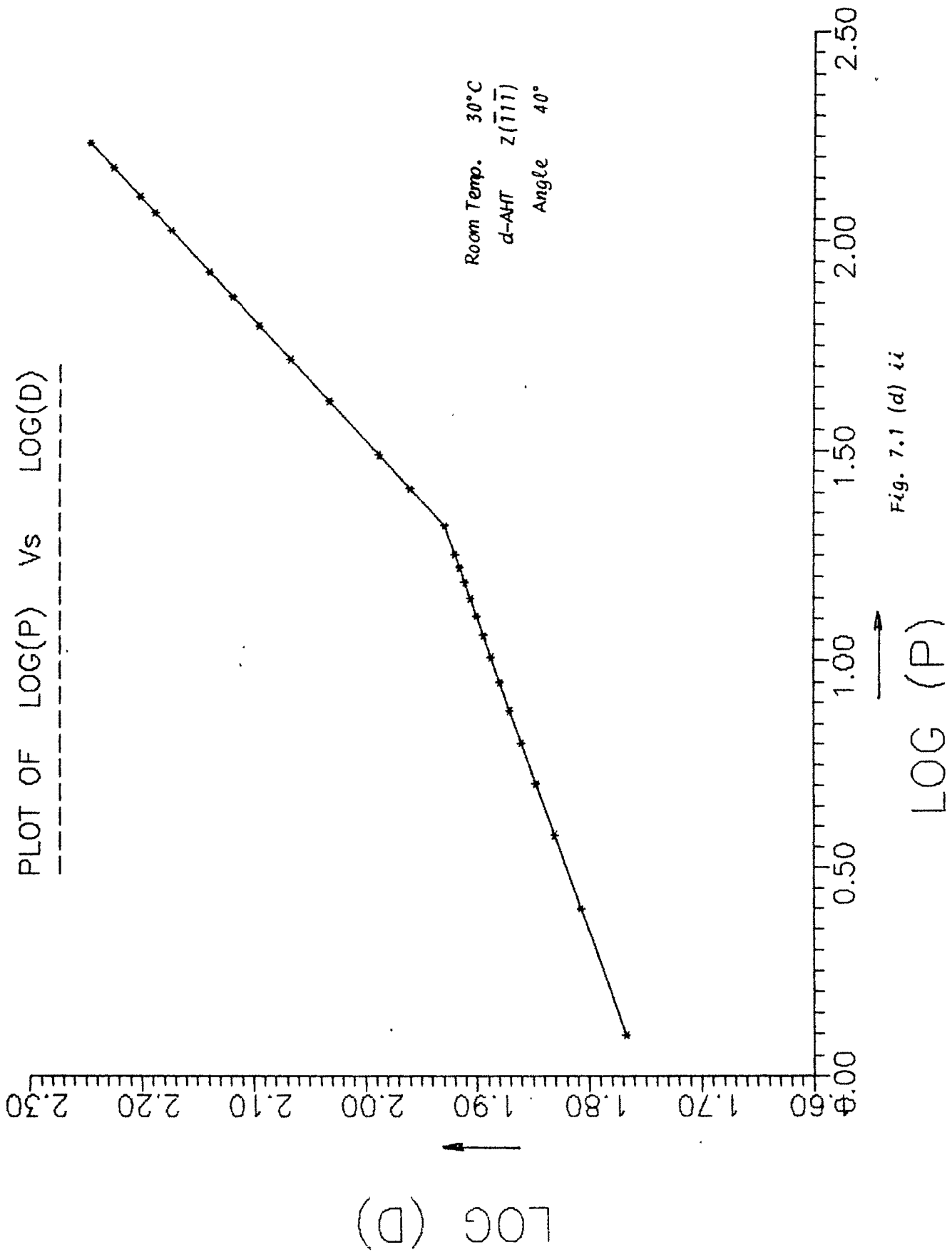
1.00

0.50

0.00

Fig. 7.1 (d) i

LOG (P)



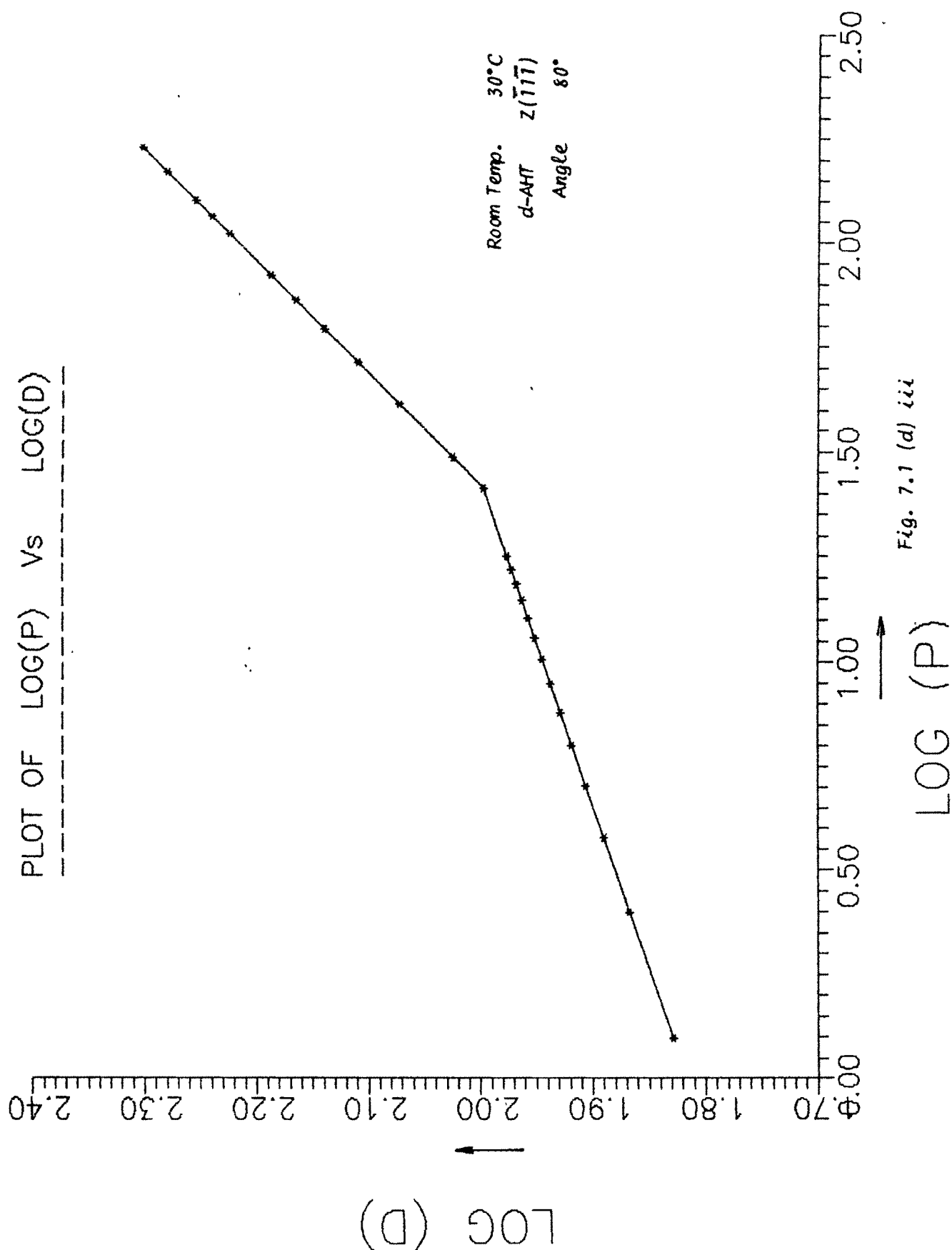


Fig. 7.1 (d) iii

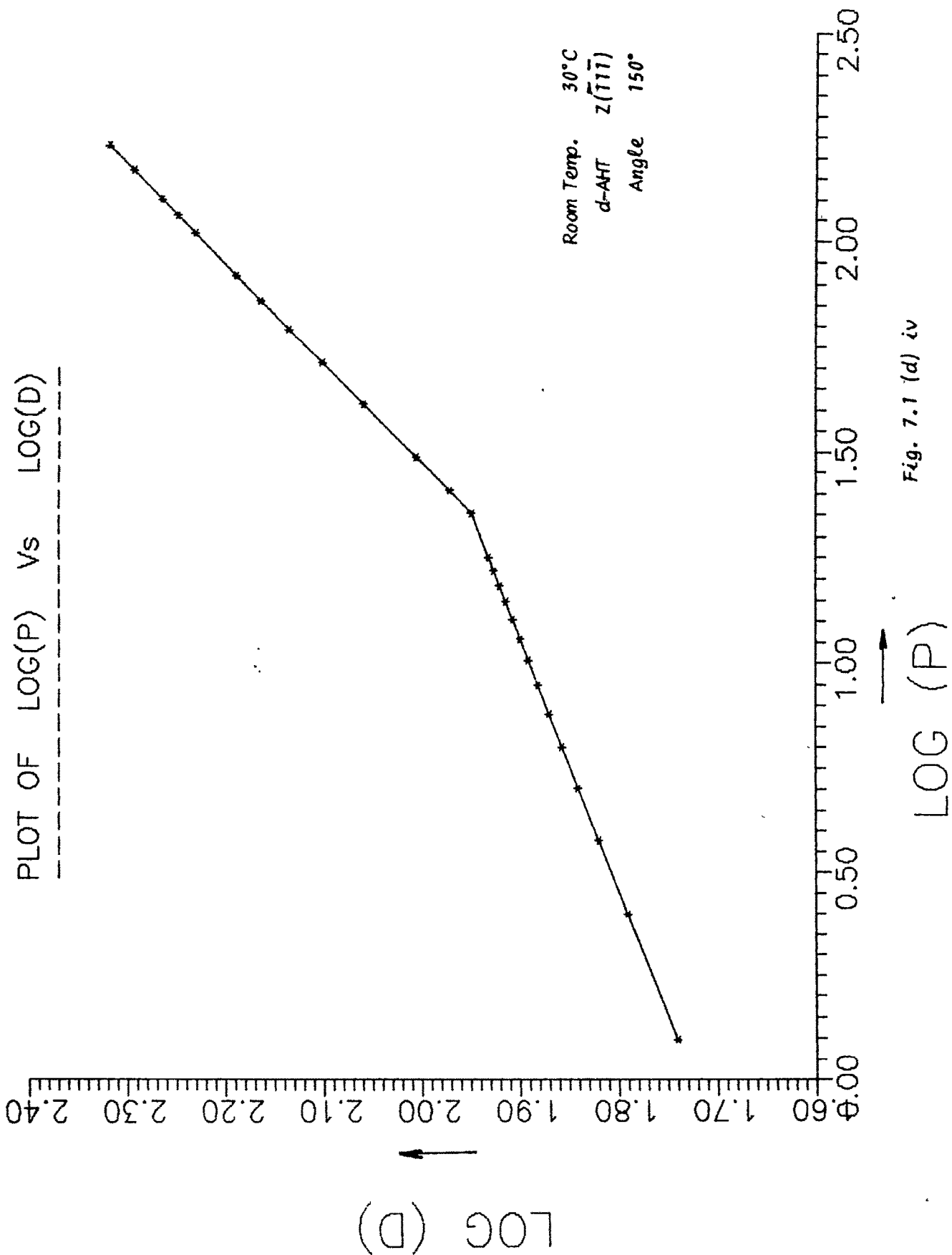
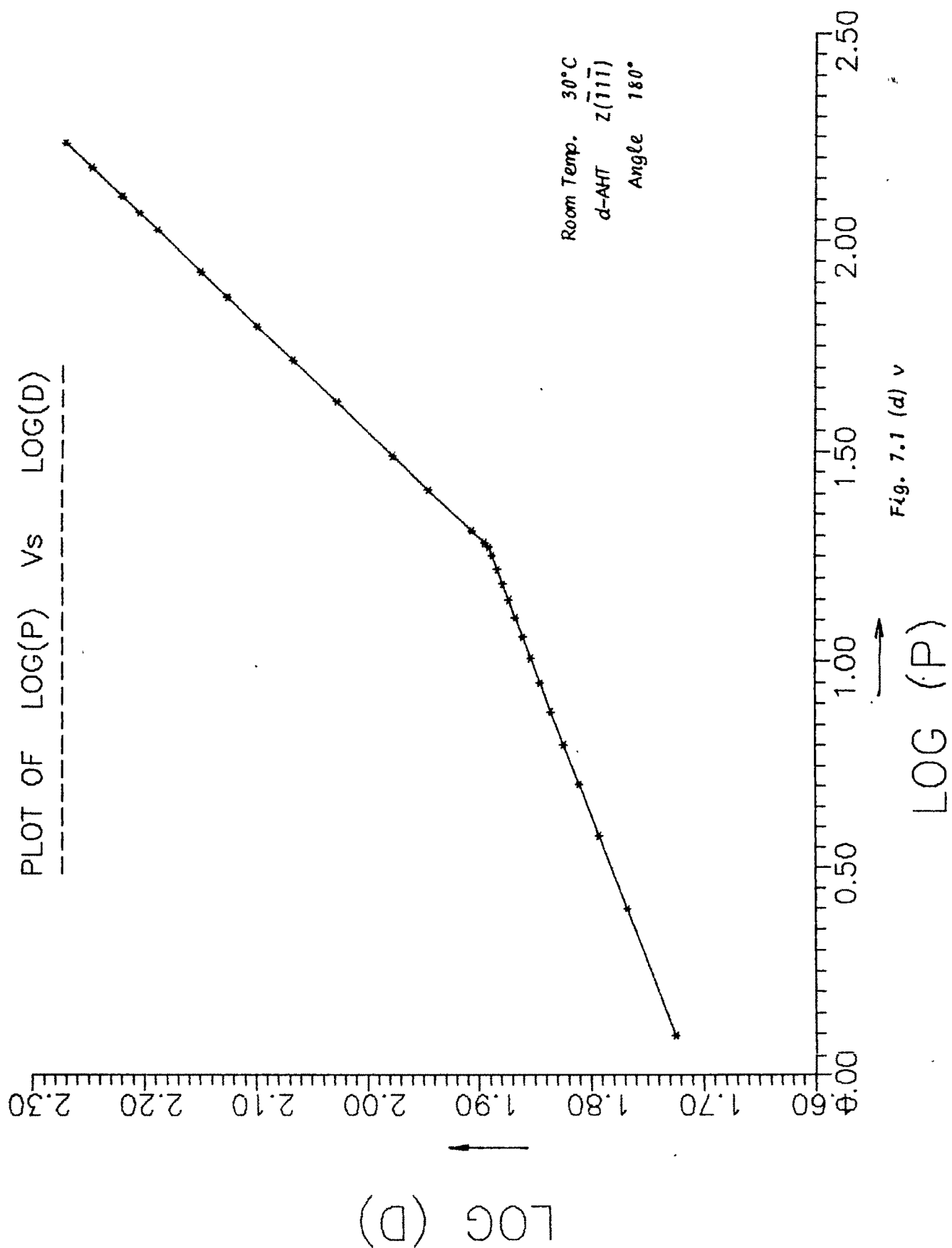
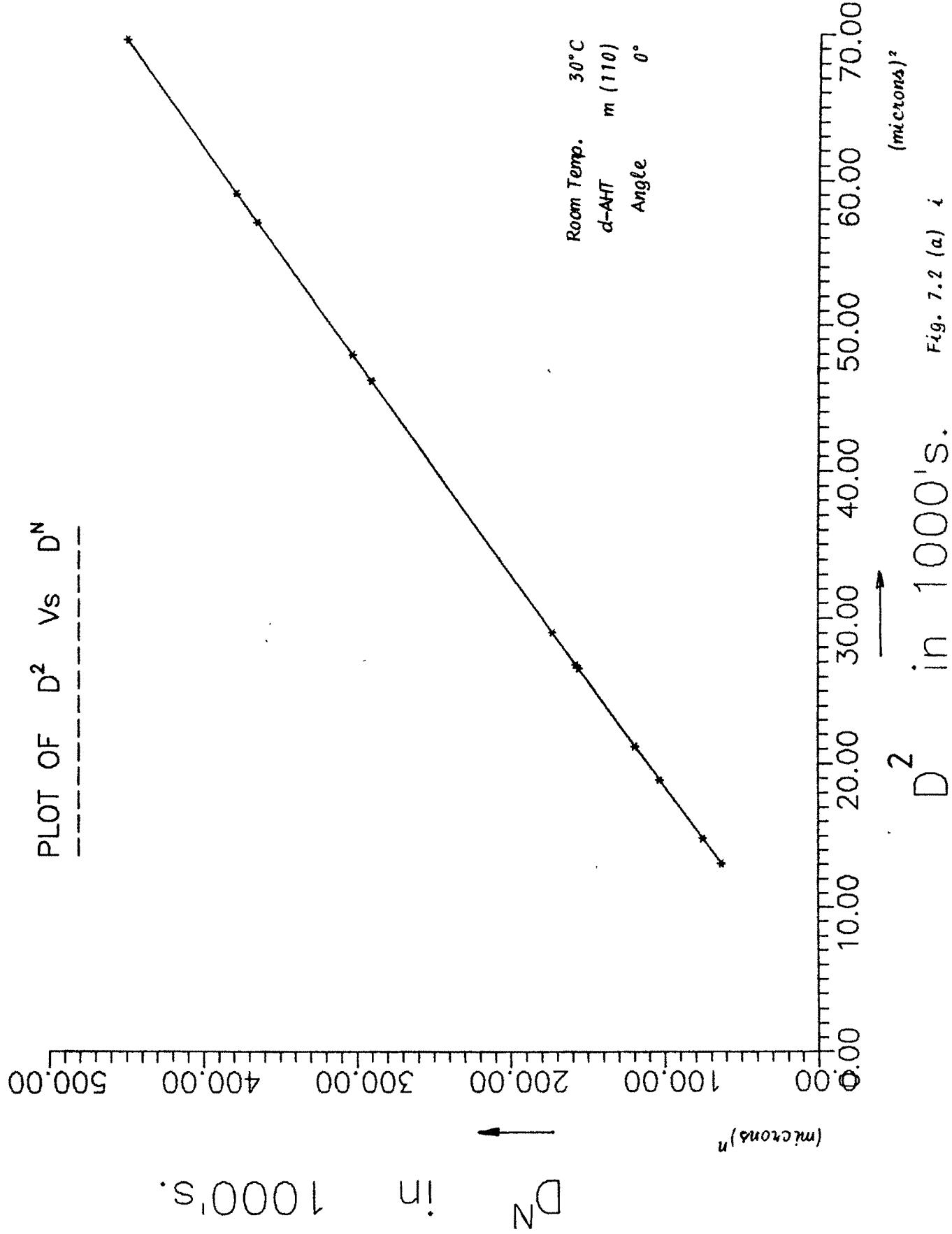


Fig. 7.1 (d) iv





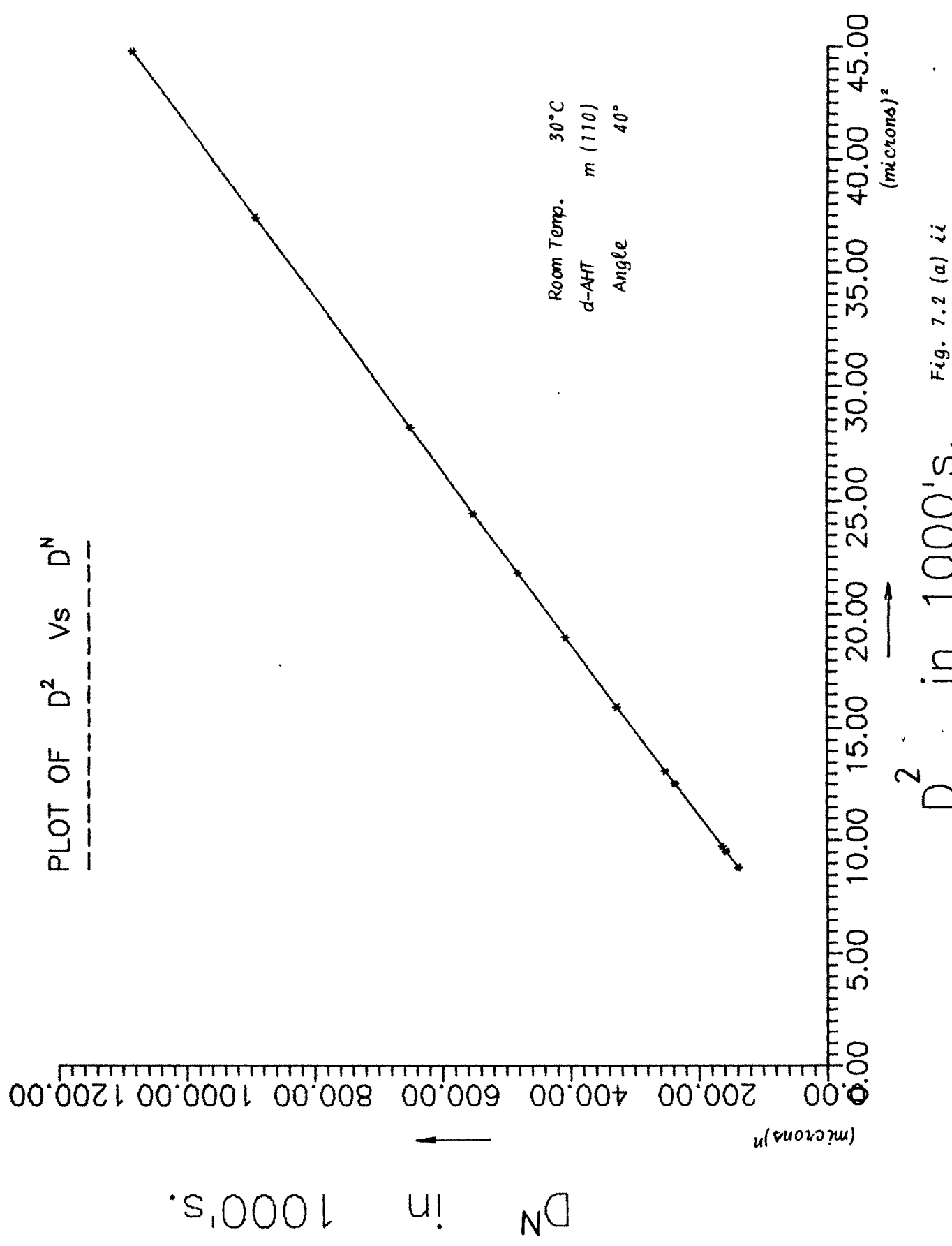


Fig. 7.2 (a) in

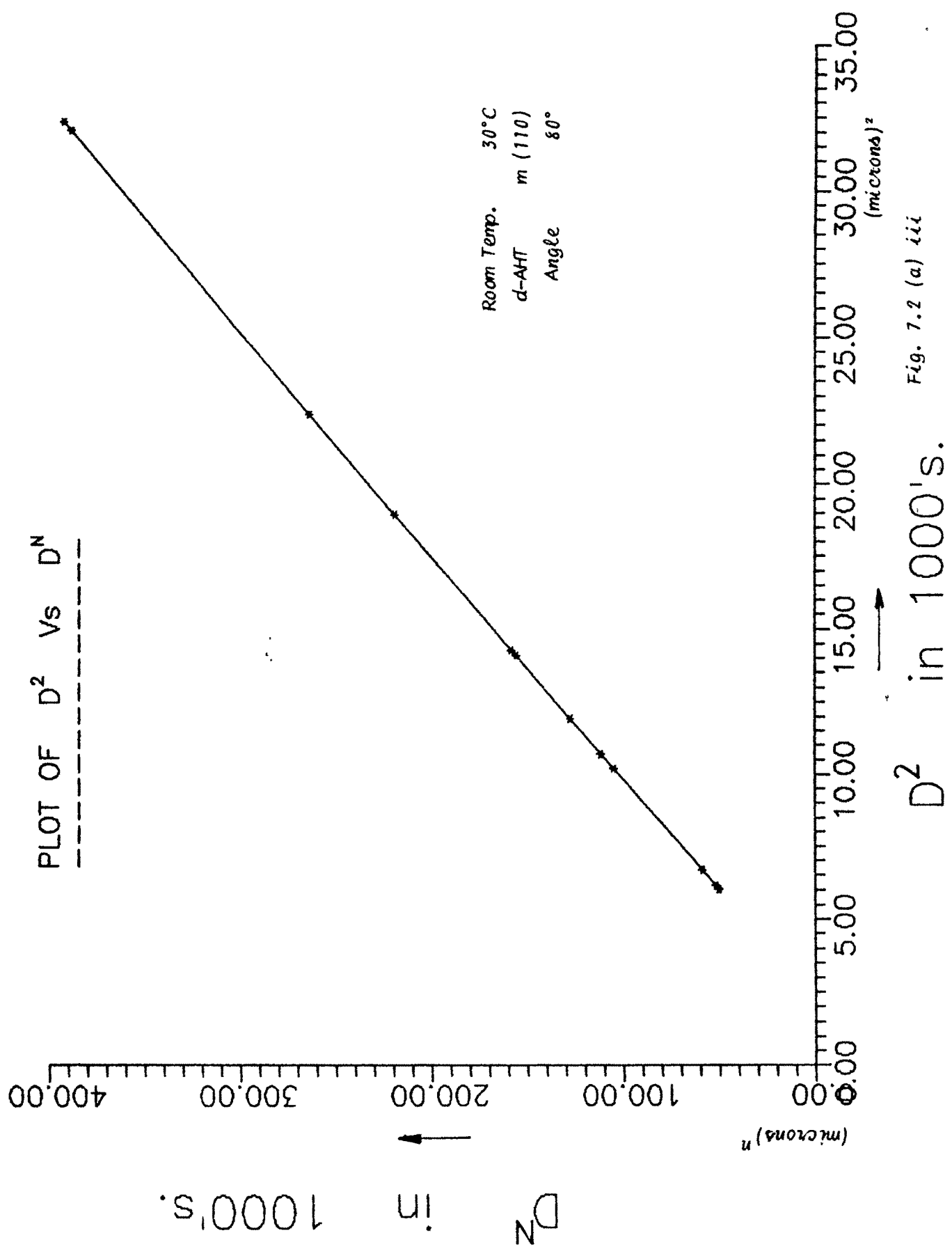


Fig. 7.2 (a) *i.i*

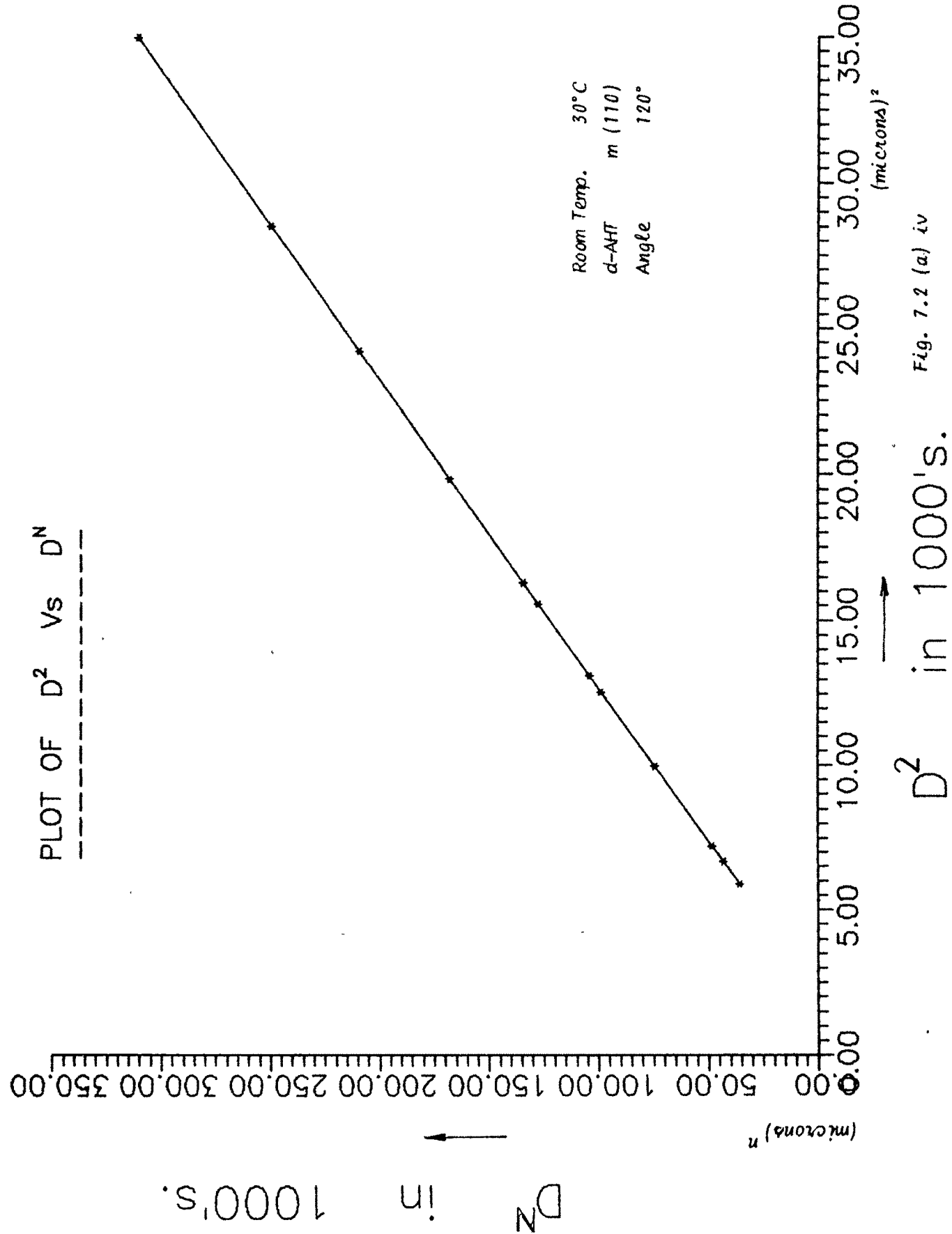
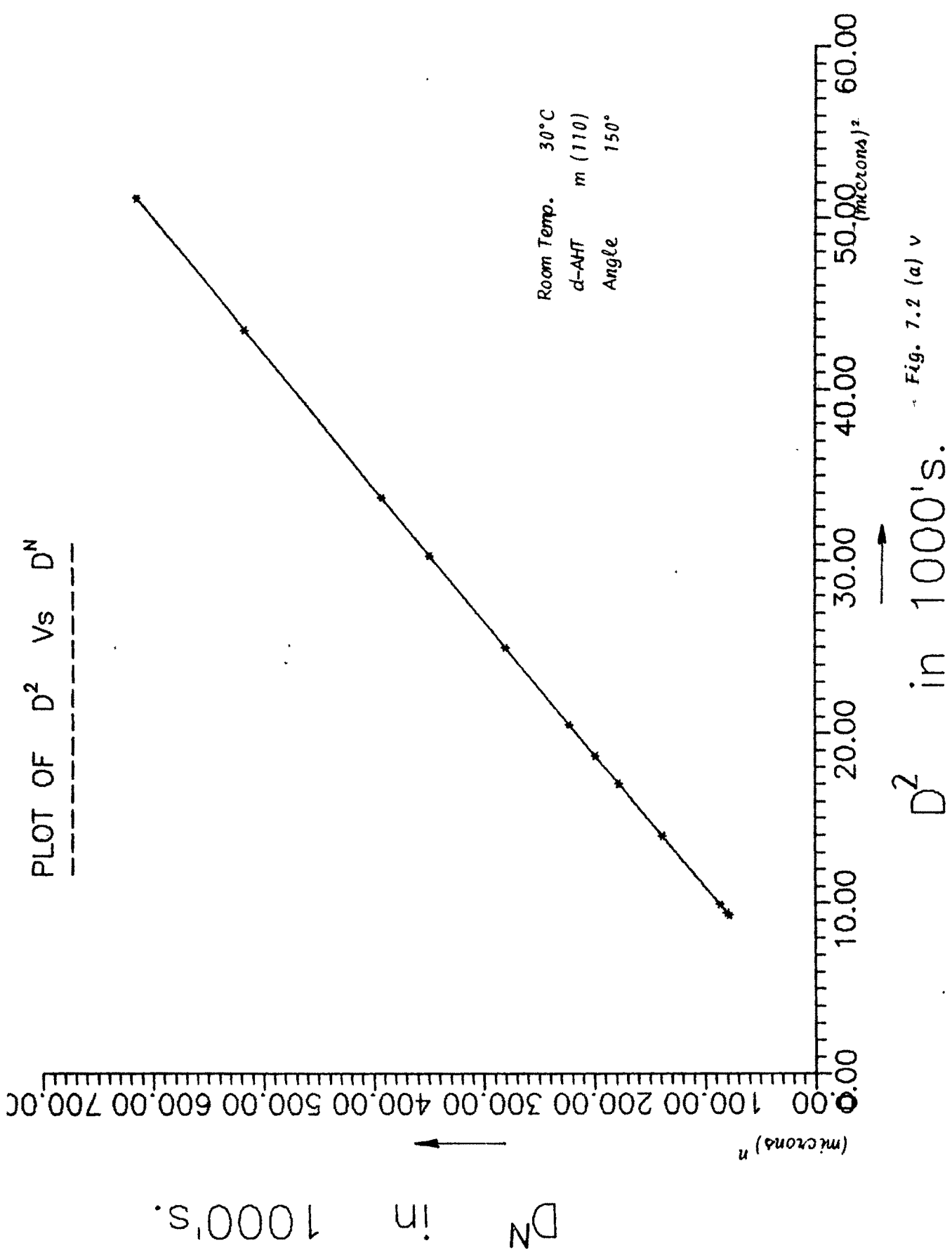


Fig. 7.2 (a) iv



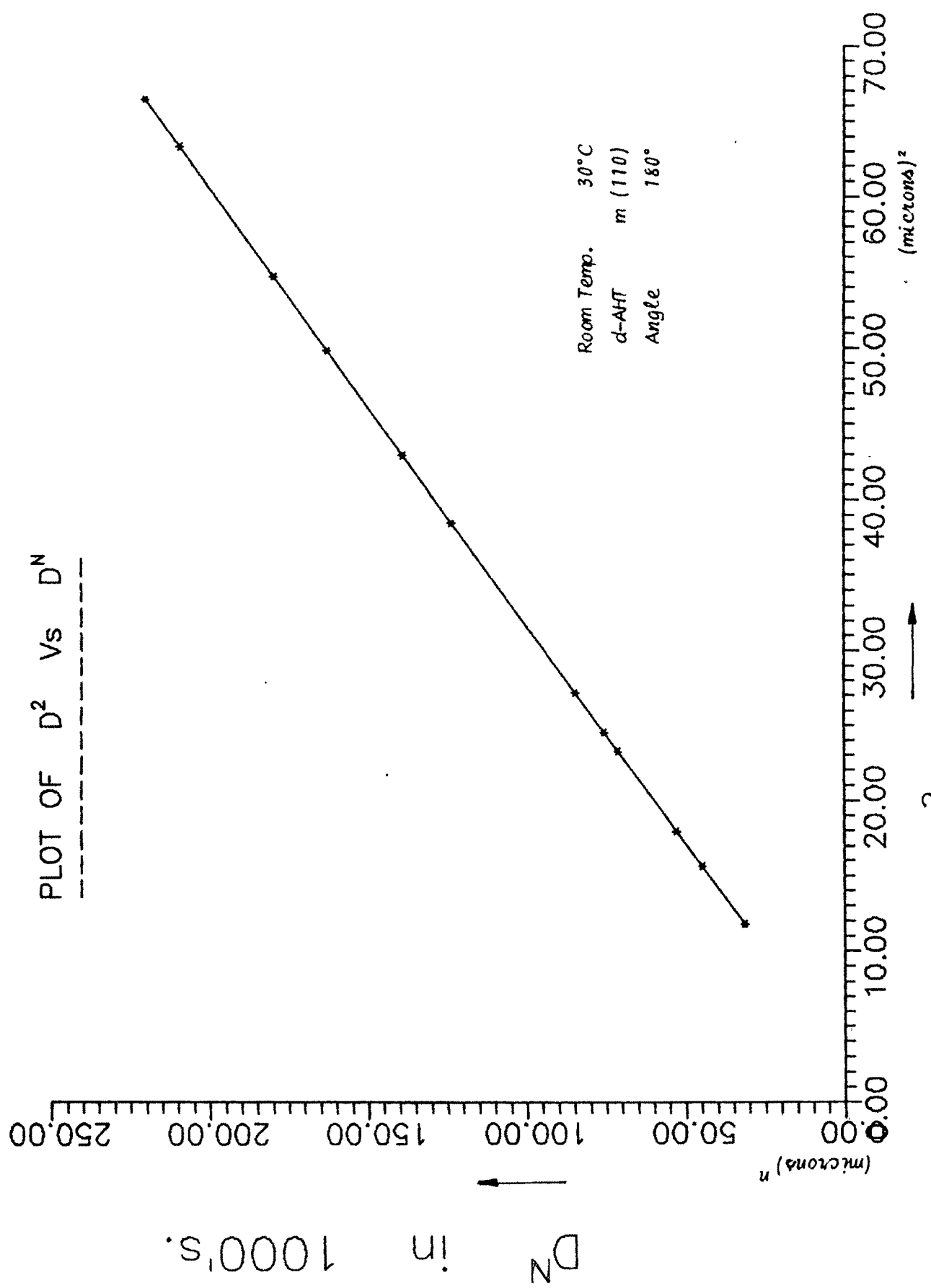
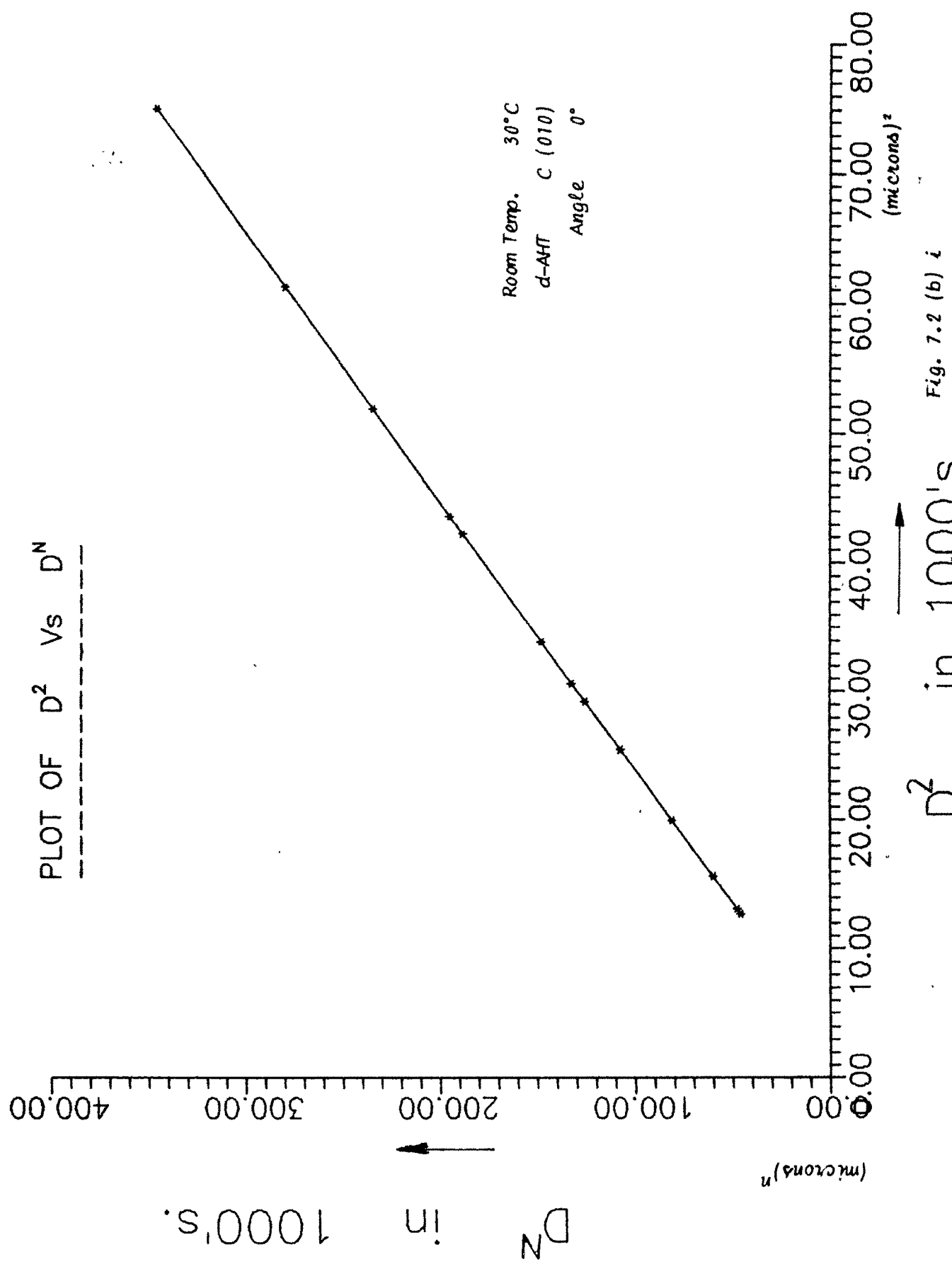


Fig. 7.2 (a) vi



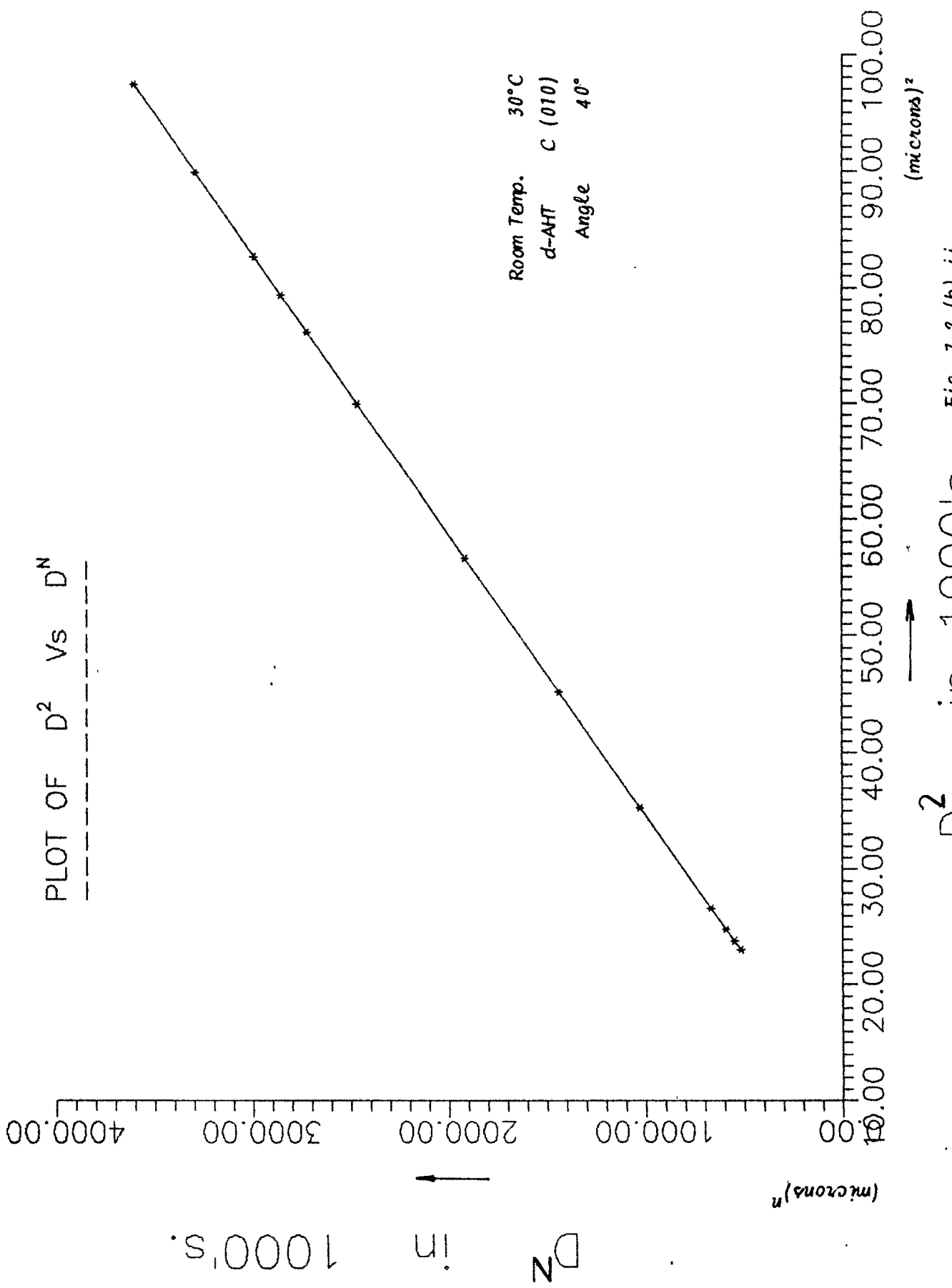


Fig. 7.2 (b) in

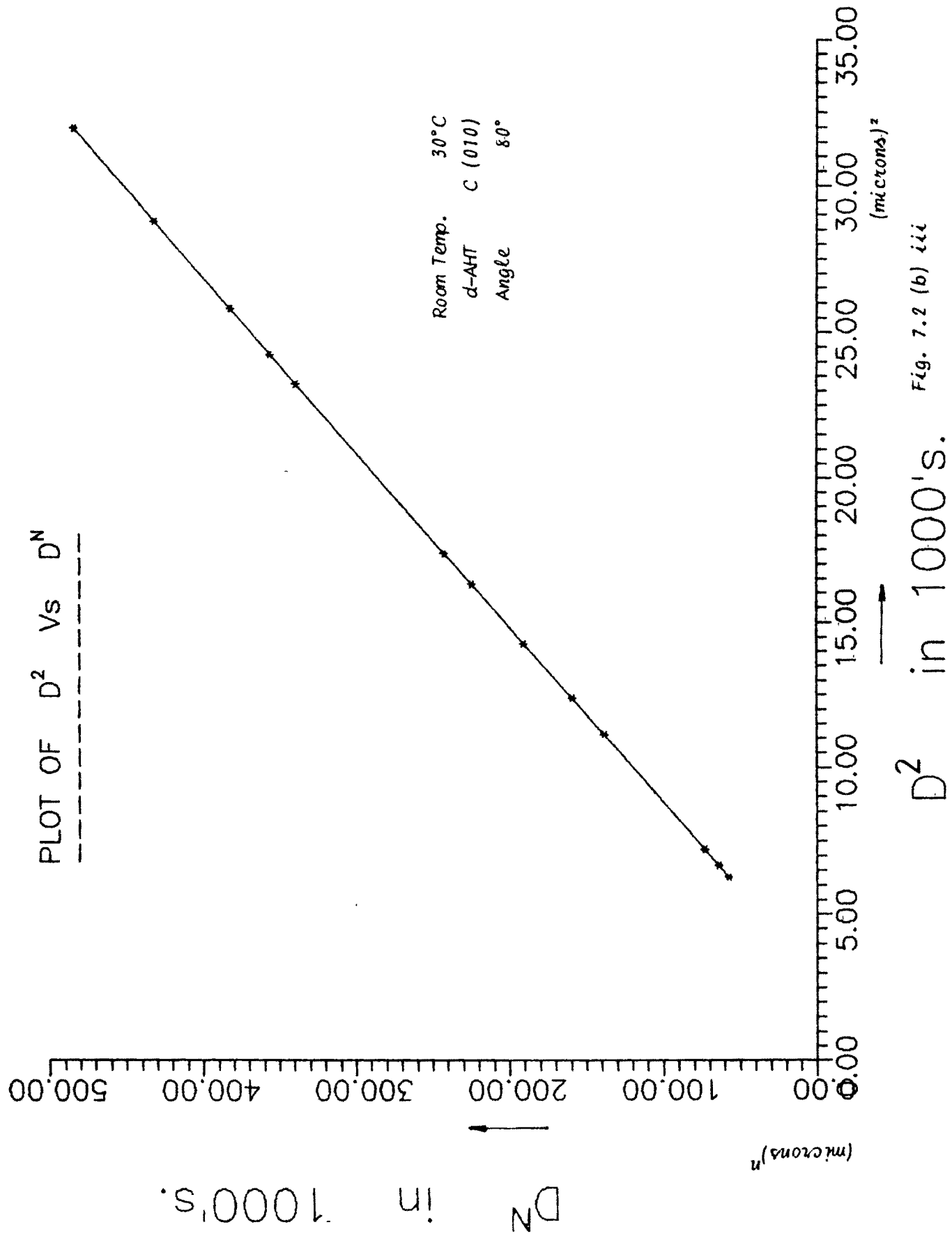


Fig. 7.2 (b) iii

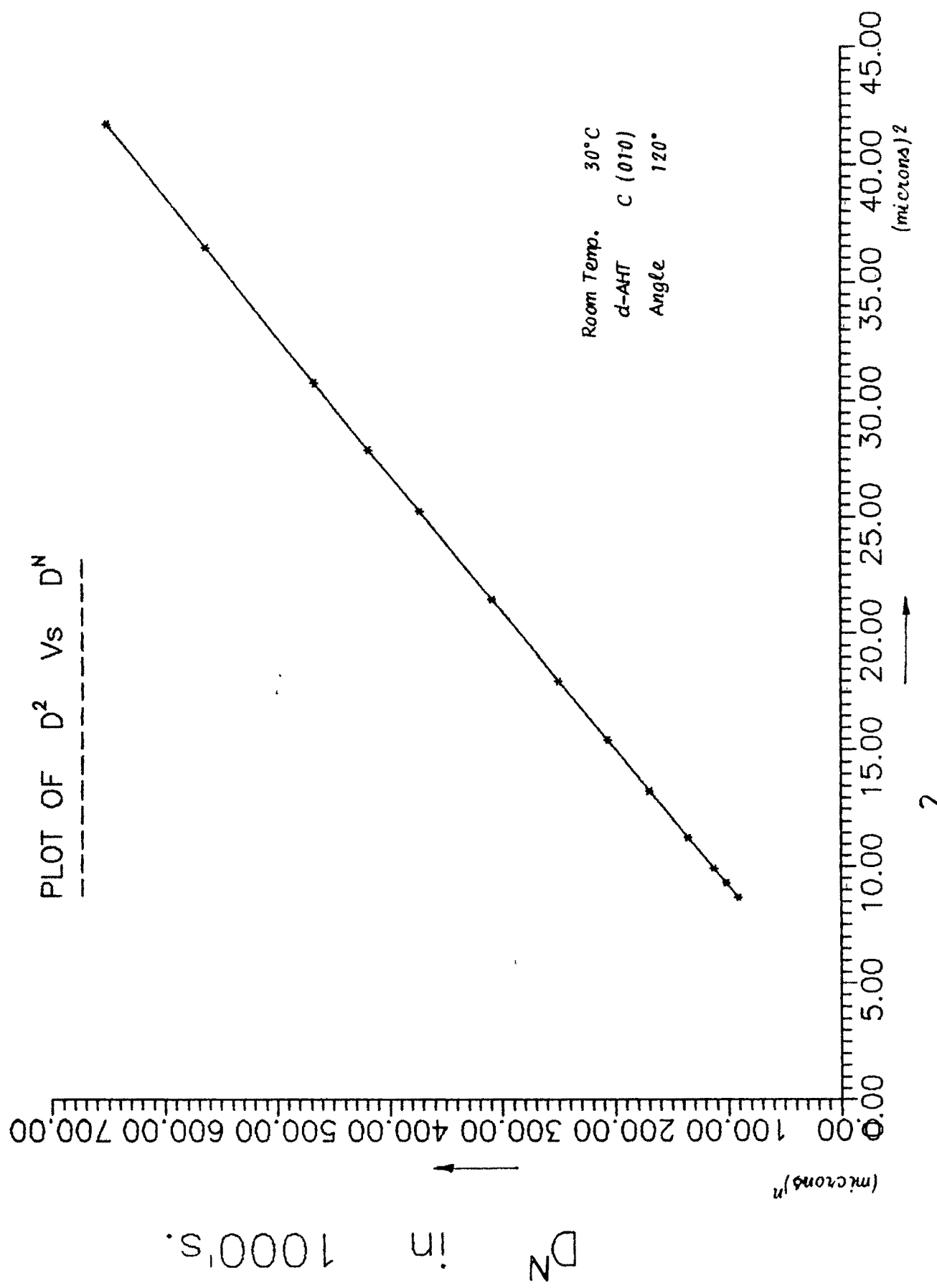
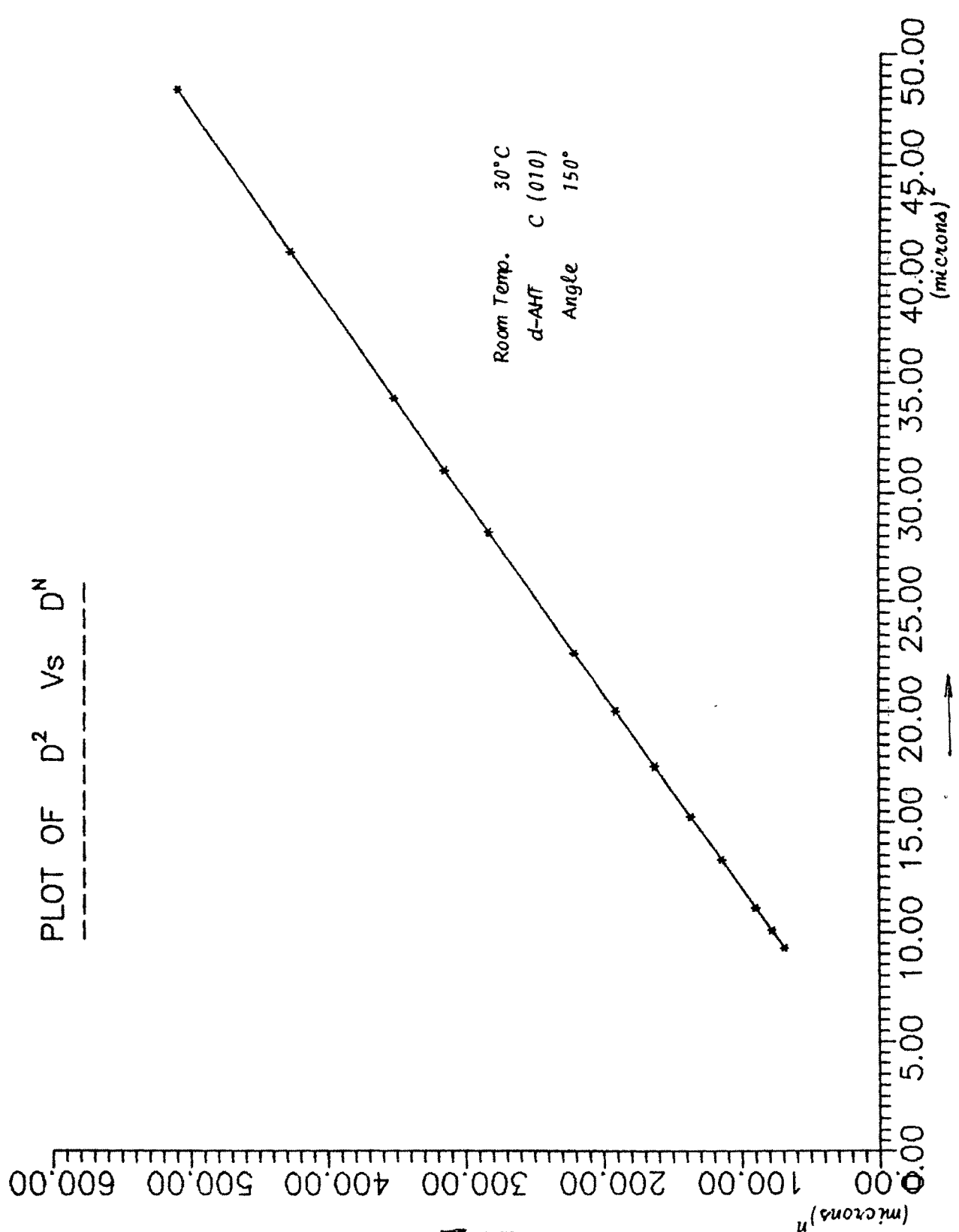
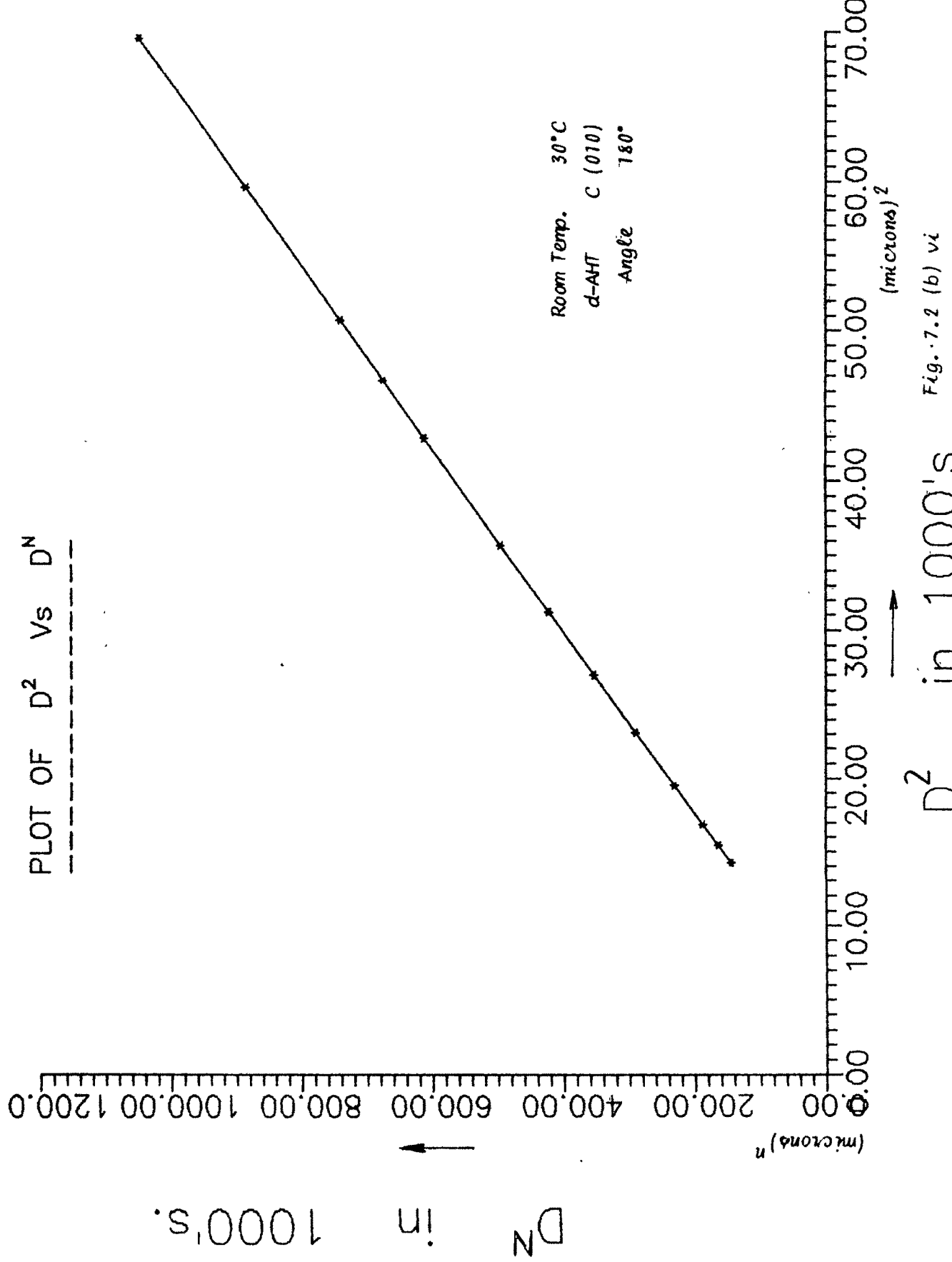
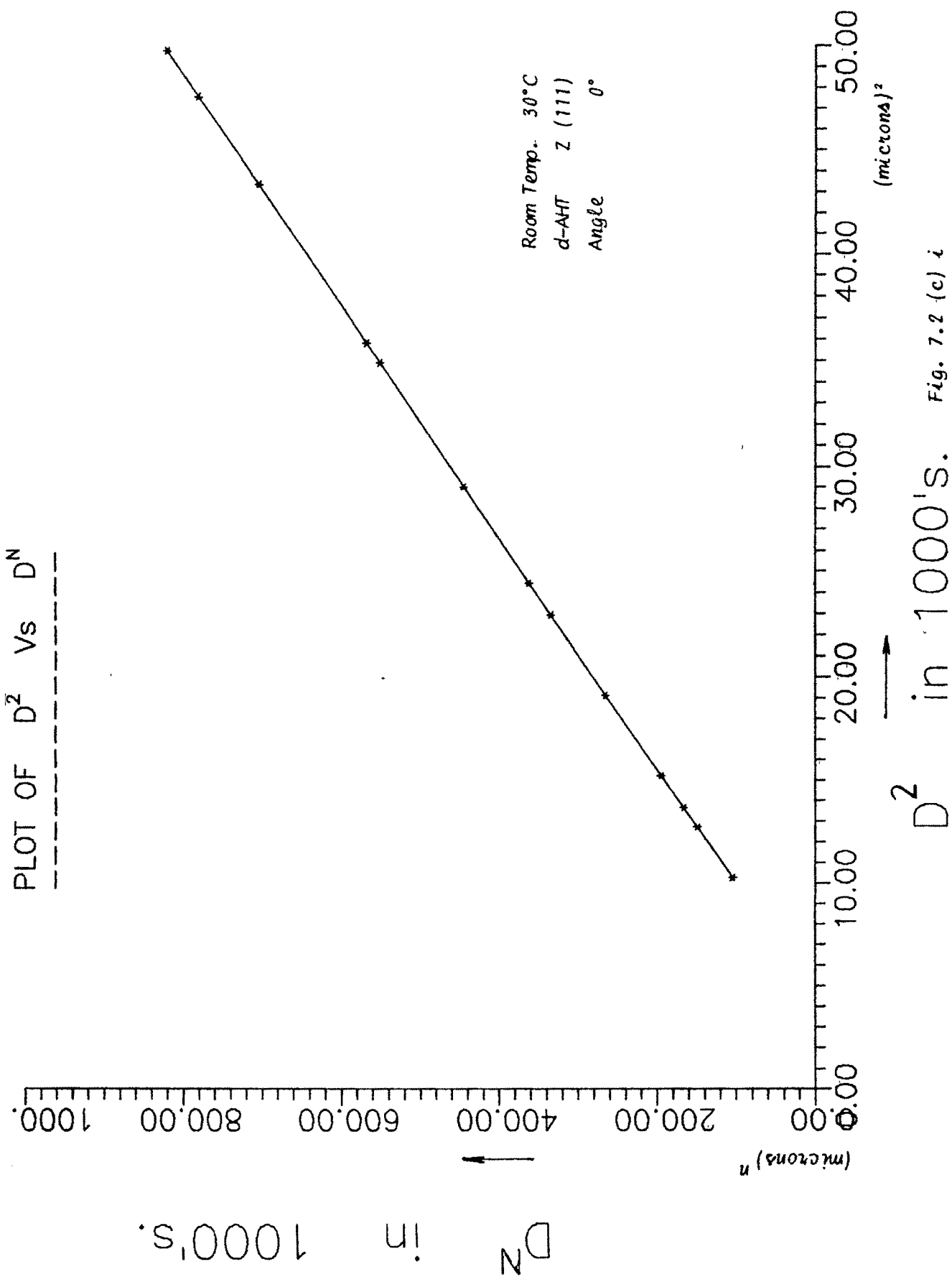


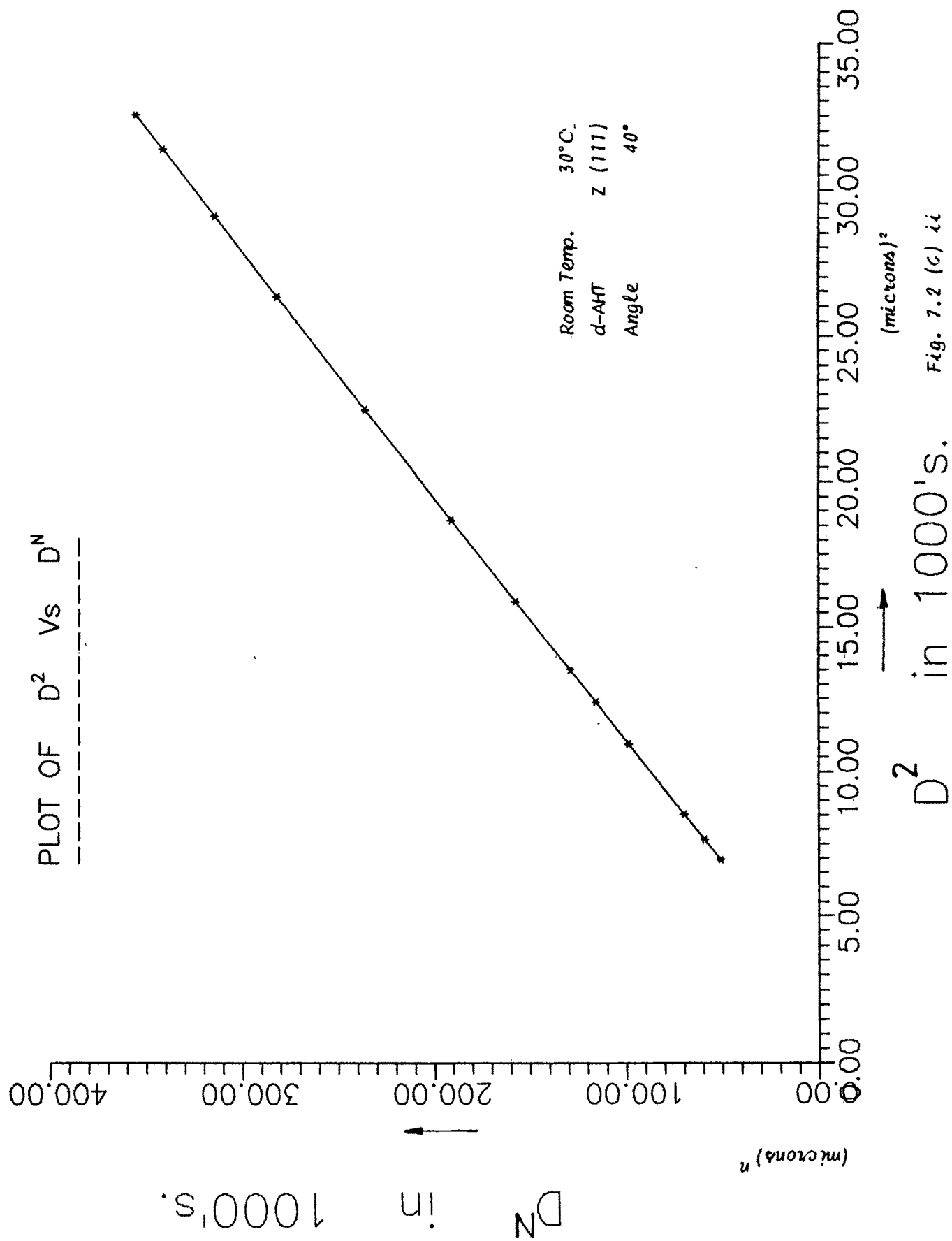
Fig. 7.2 (b) iv



D^2 in 1000's.
 Fig. 7.2 (b) v







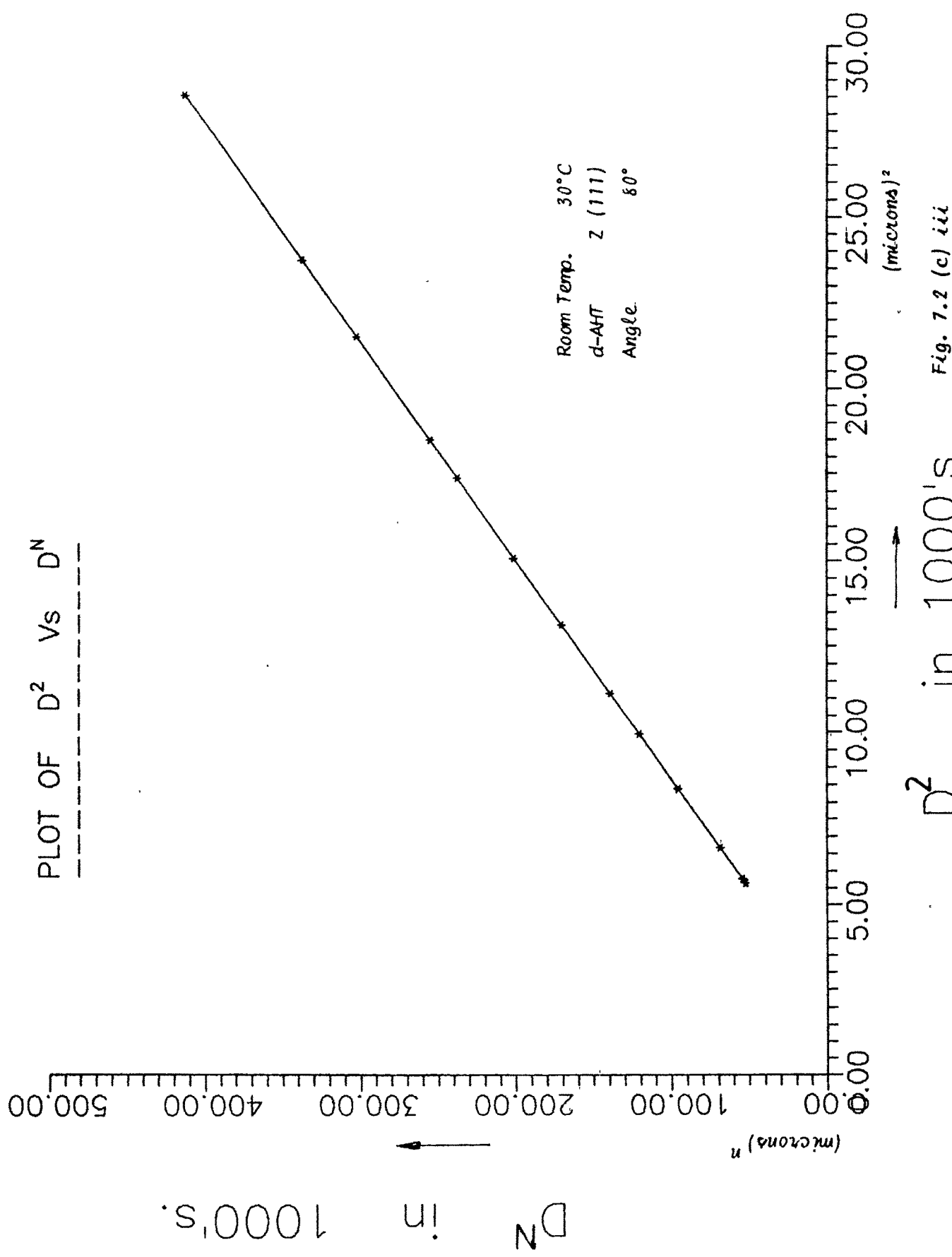


Fig. 7.2 (c) iii

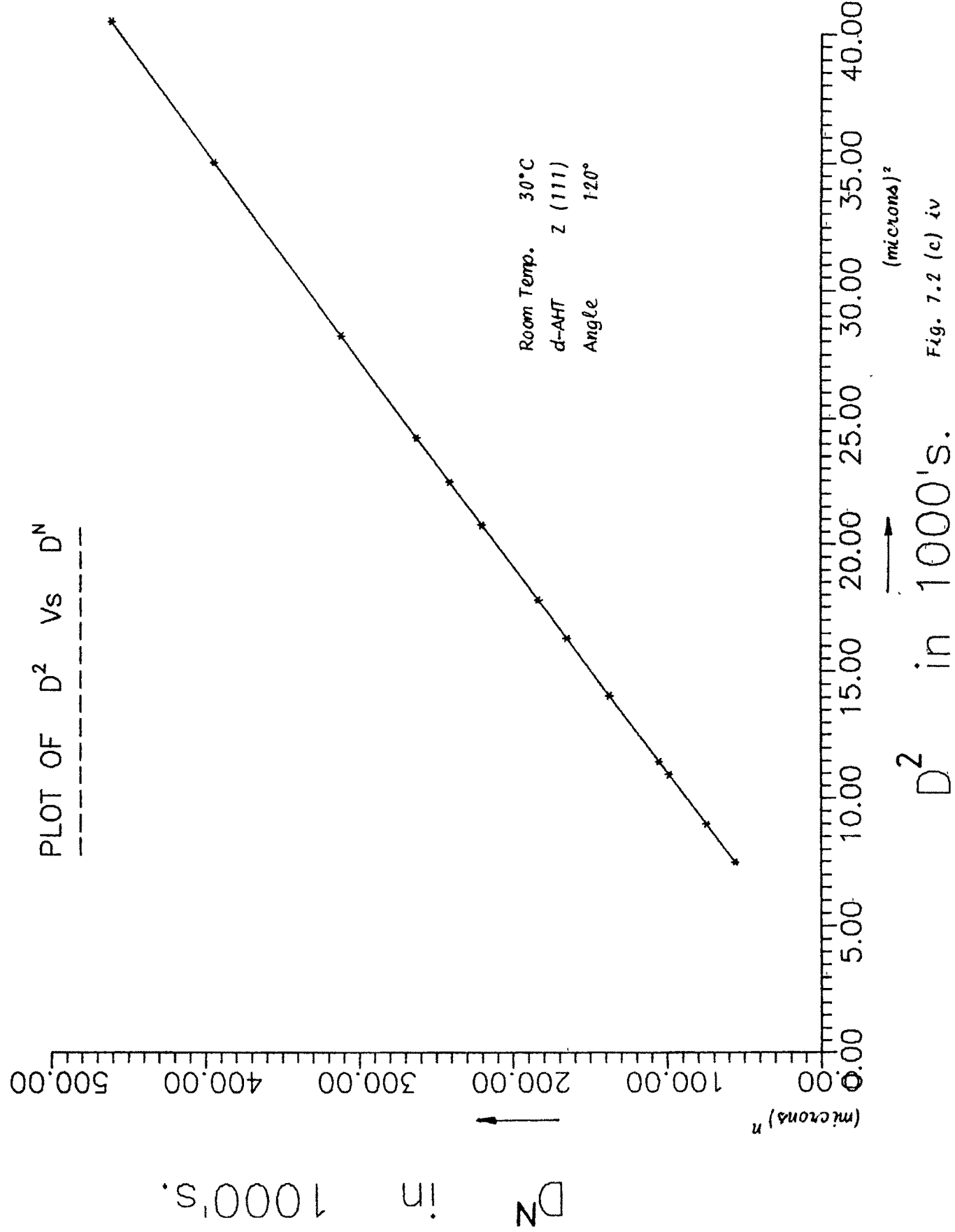


Fig. 7.2 (c) iv

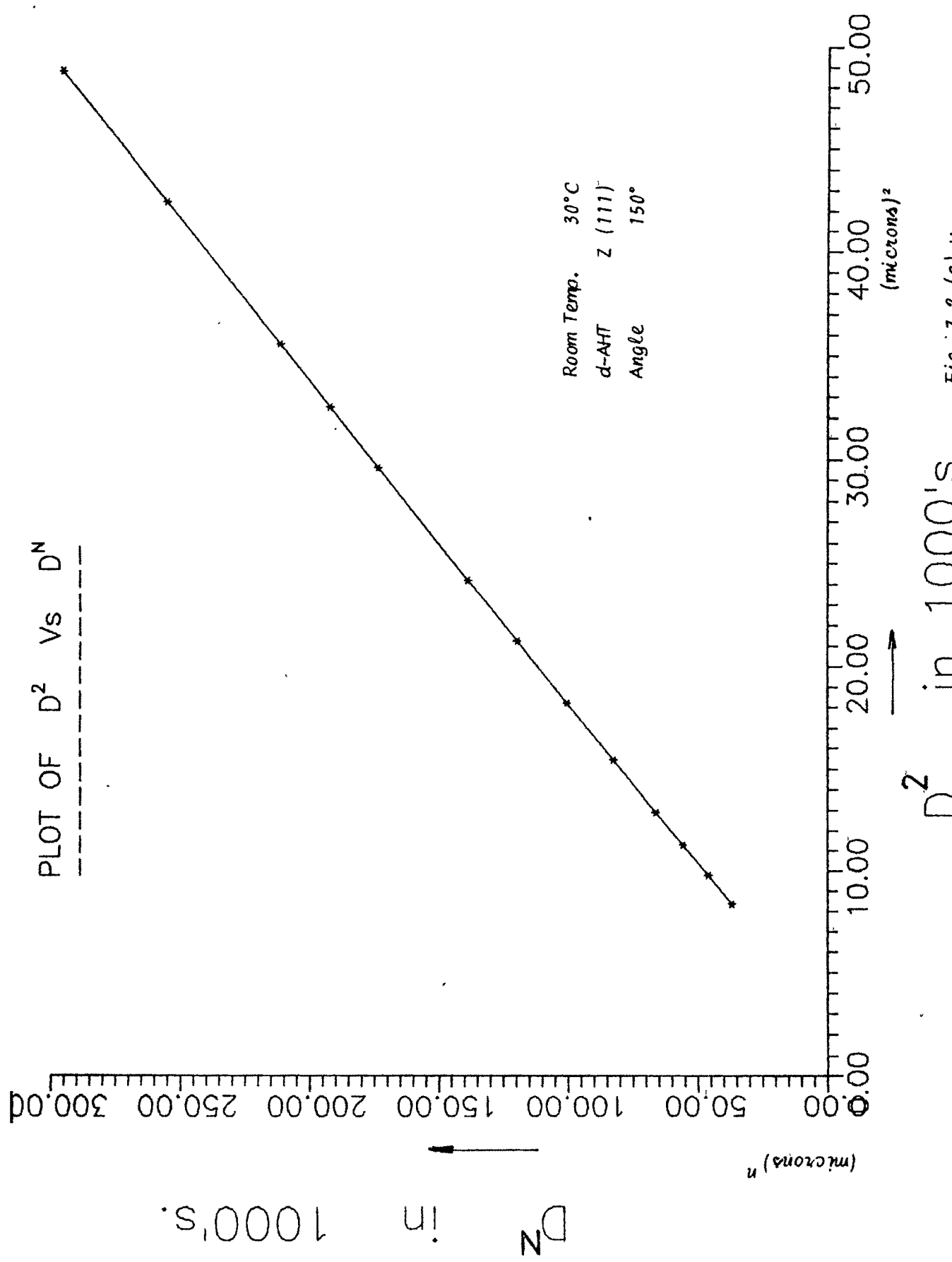
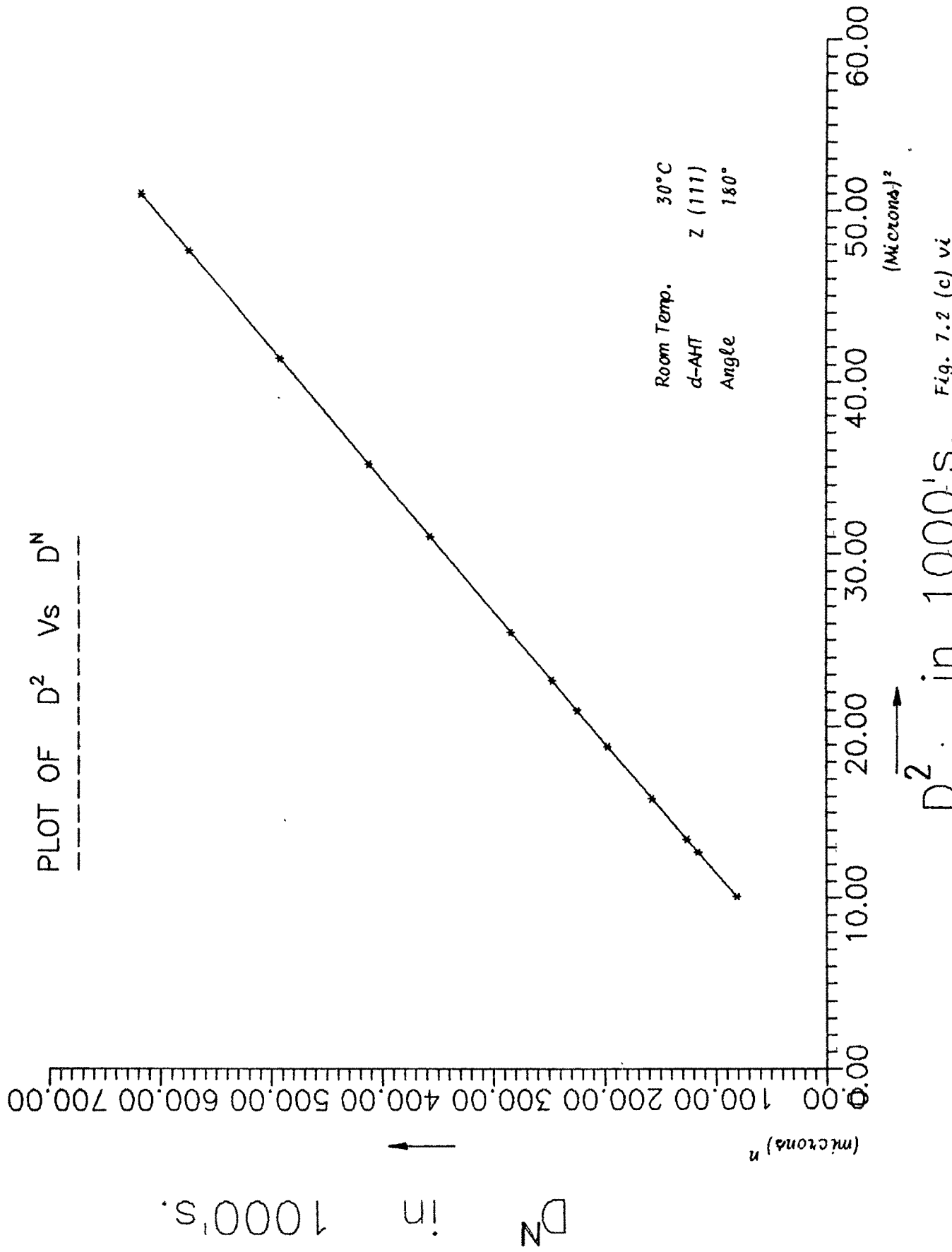
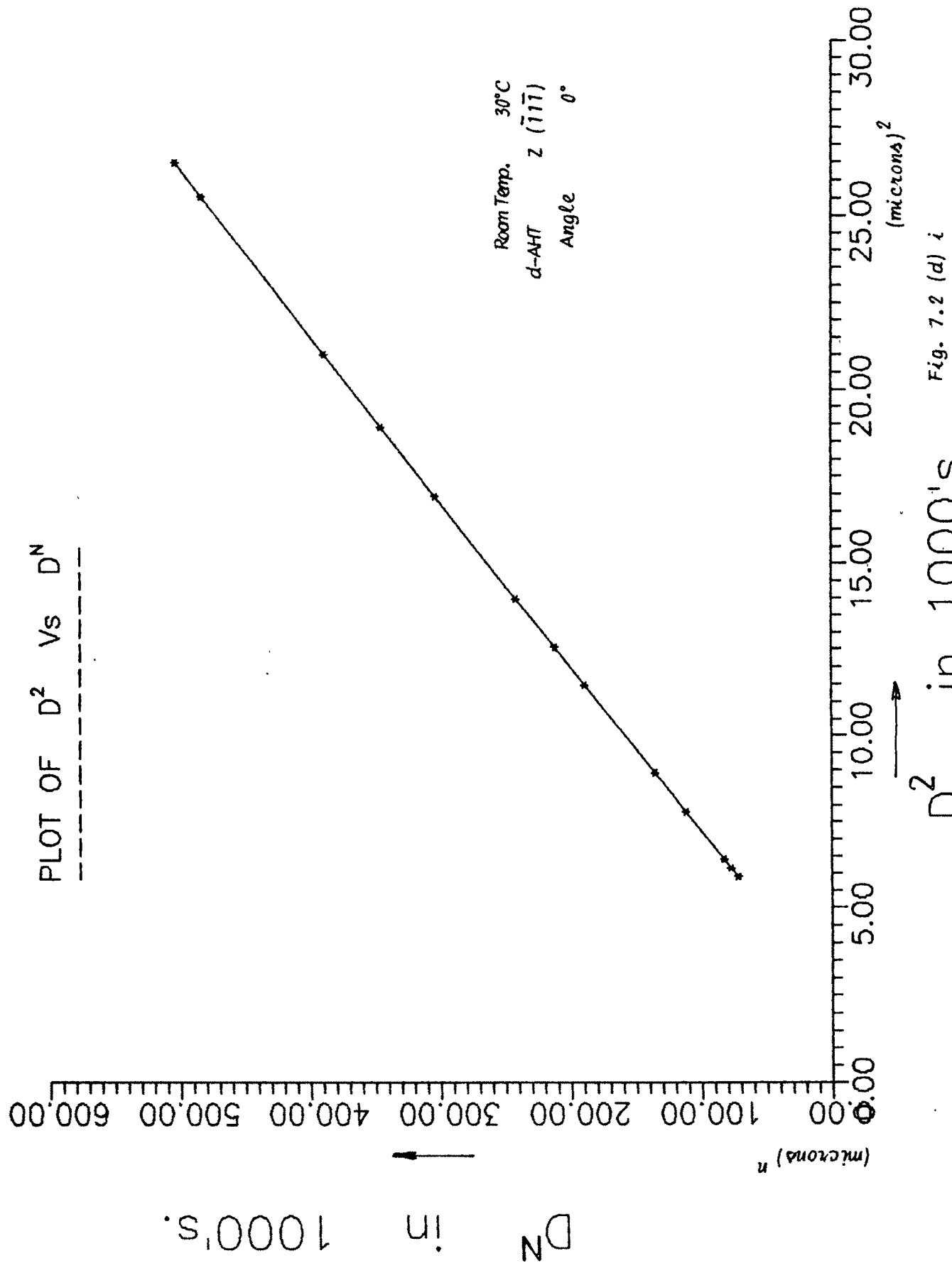
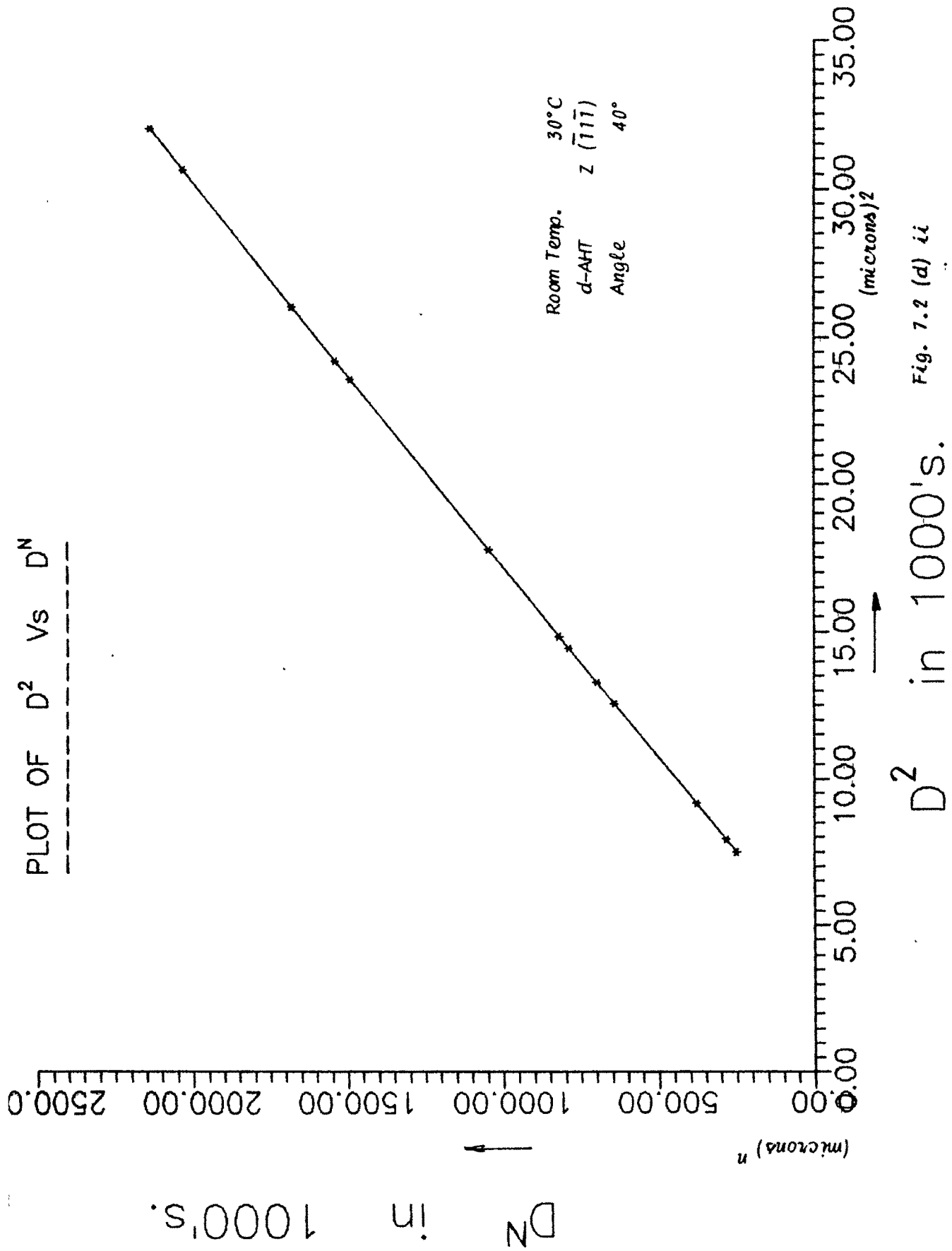


Fig. 7.2 (c)







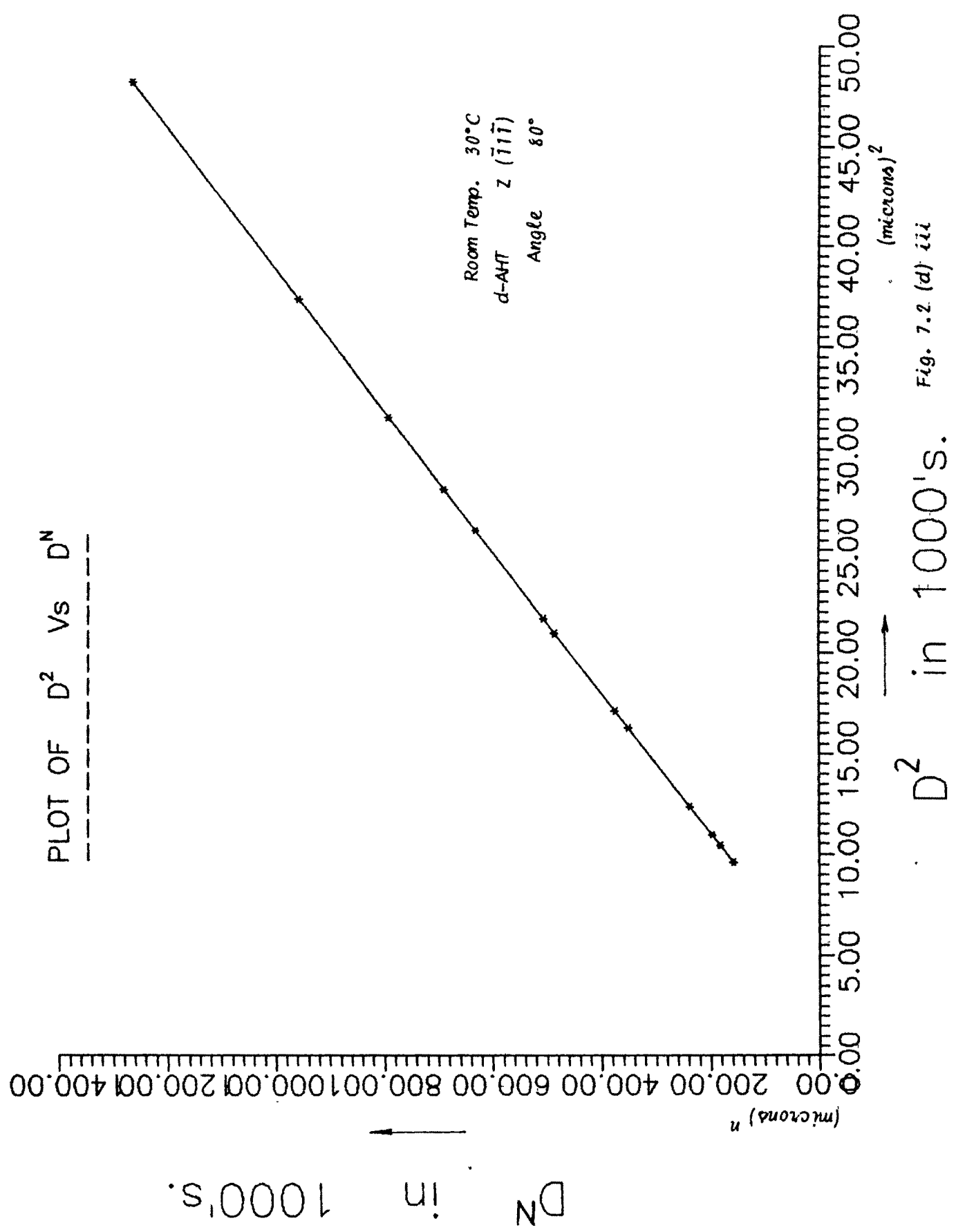


Fig. 7.2 (d) ii

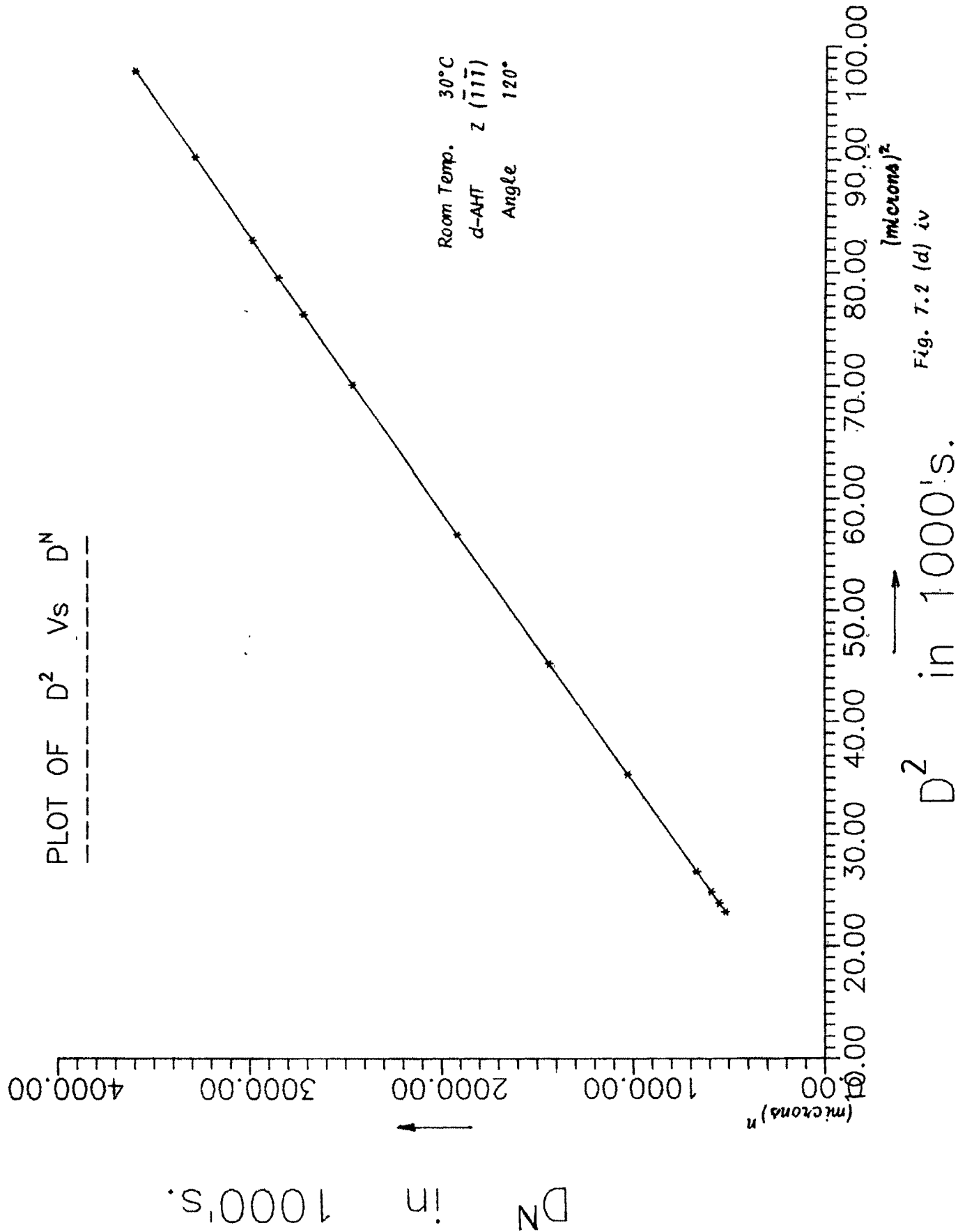
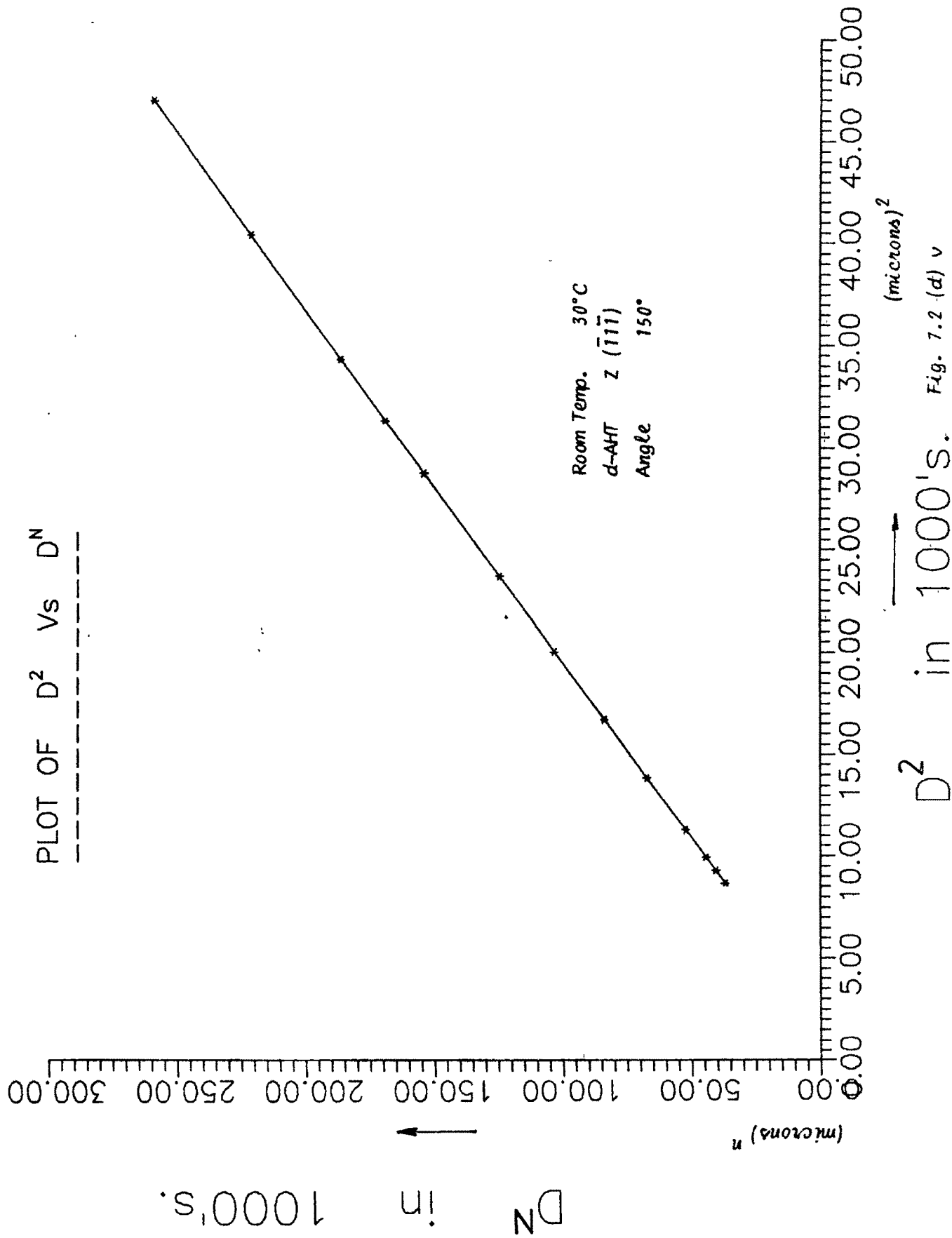
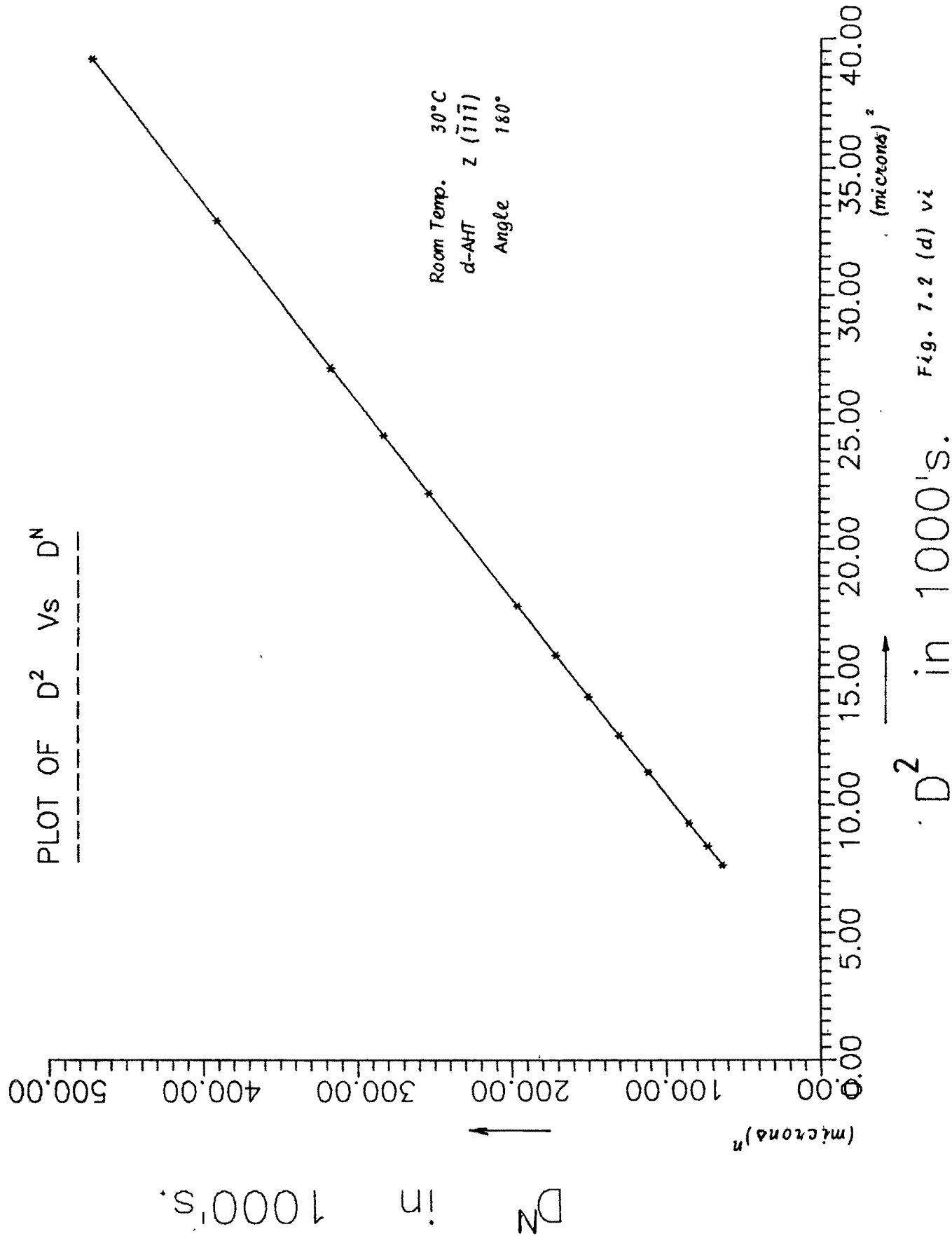


Fig. 7.2 (d) iv





Plot of Log(D) Vs Log(P - W)

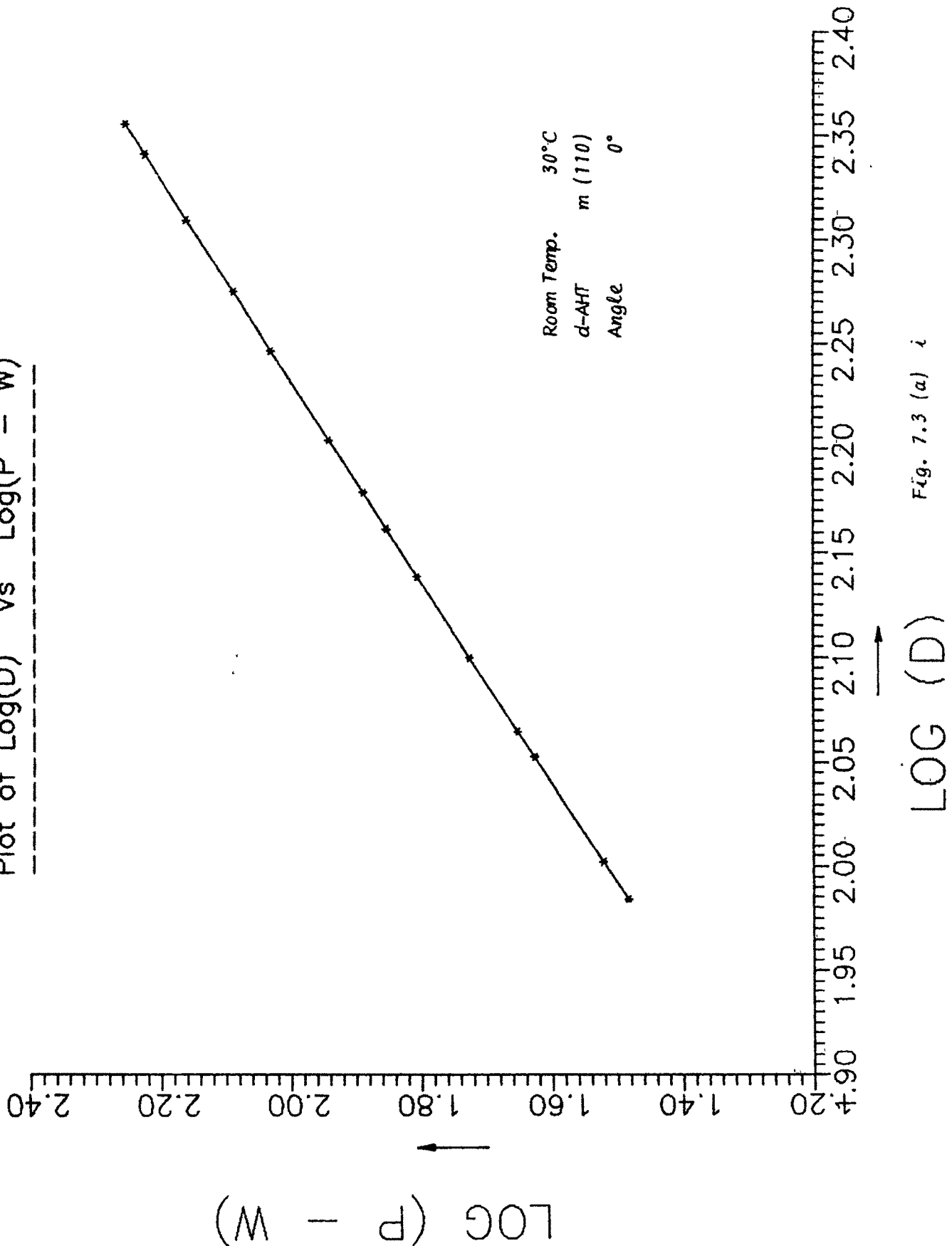
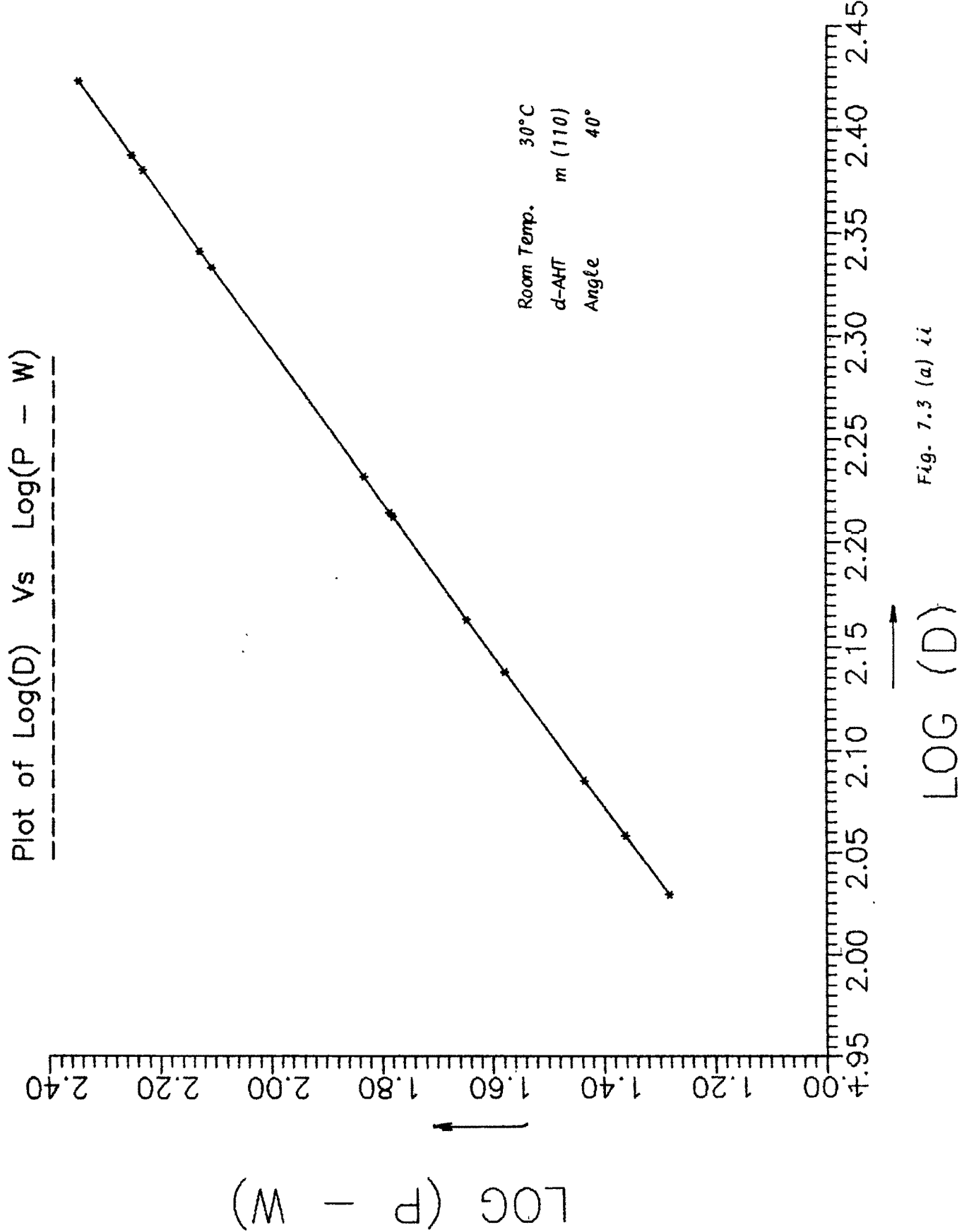
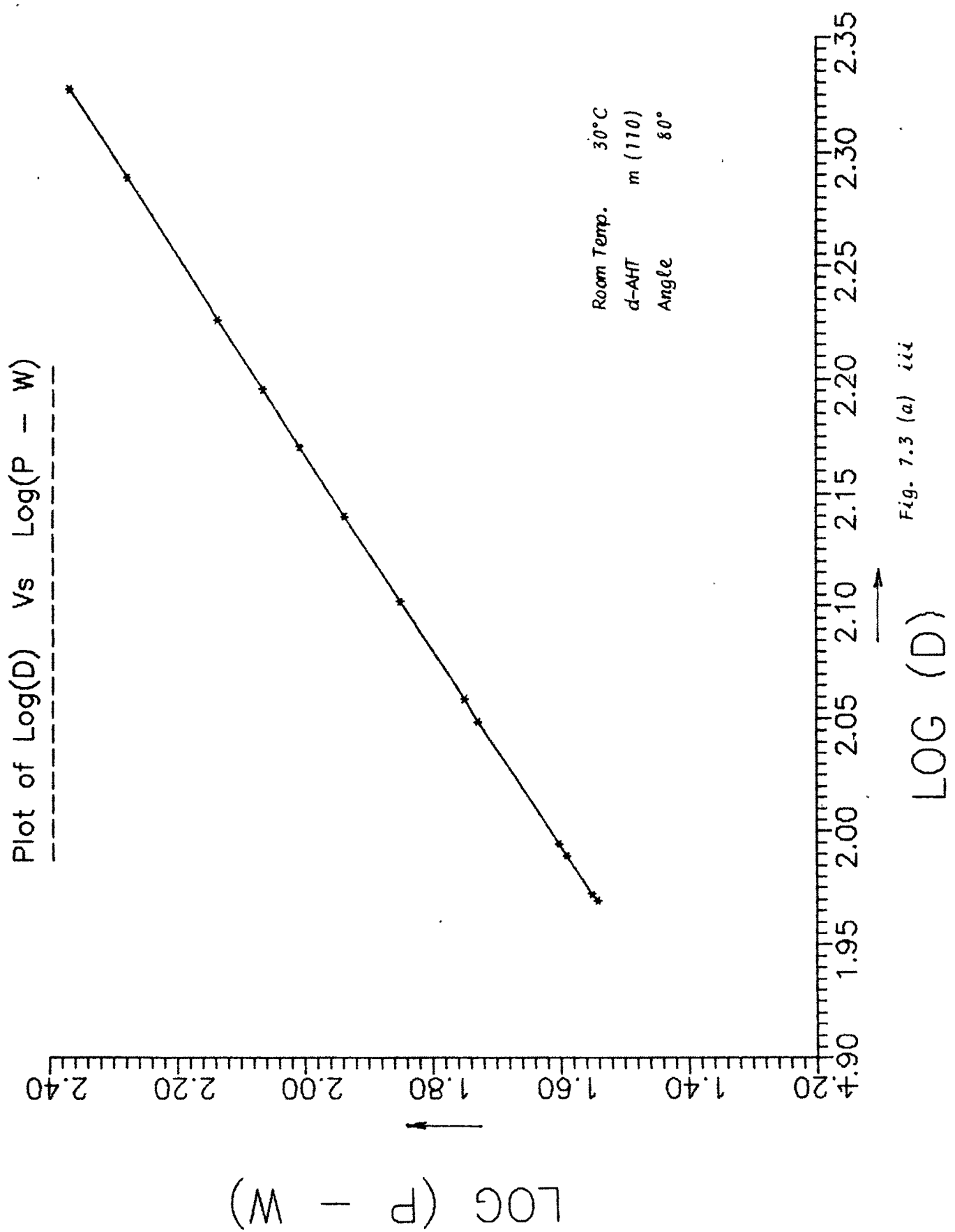


Fig. 7.3 (a) i





Plot of Log(D) Vs Log(P - W)

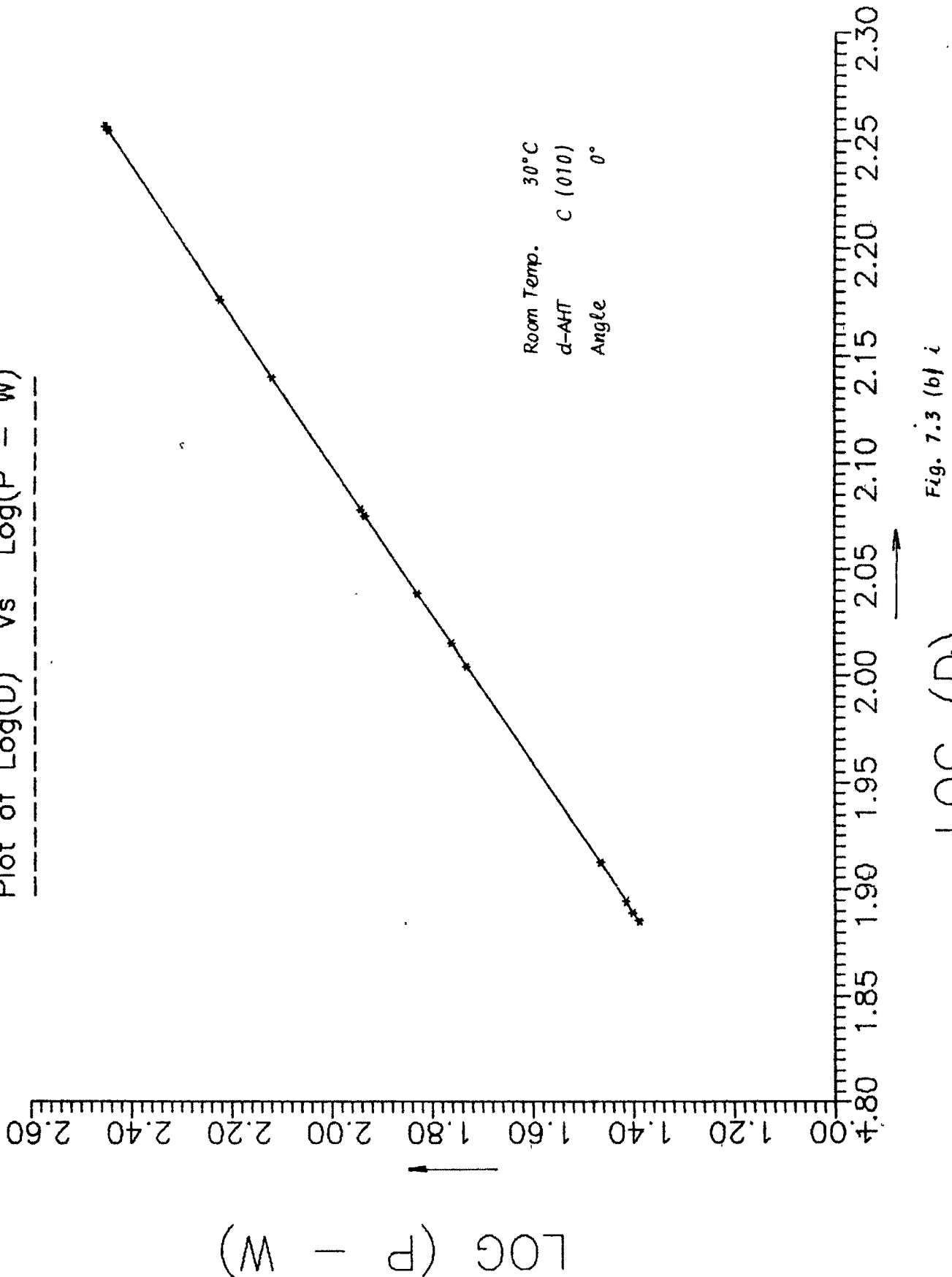


Fig. 7.3 (b) i

$$\text{LOG } (P - W)$$

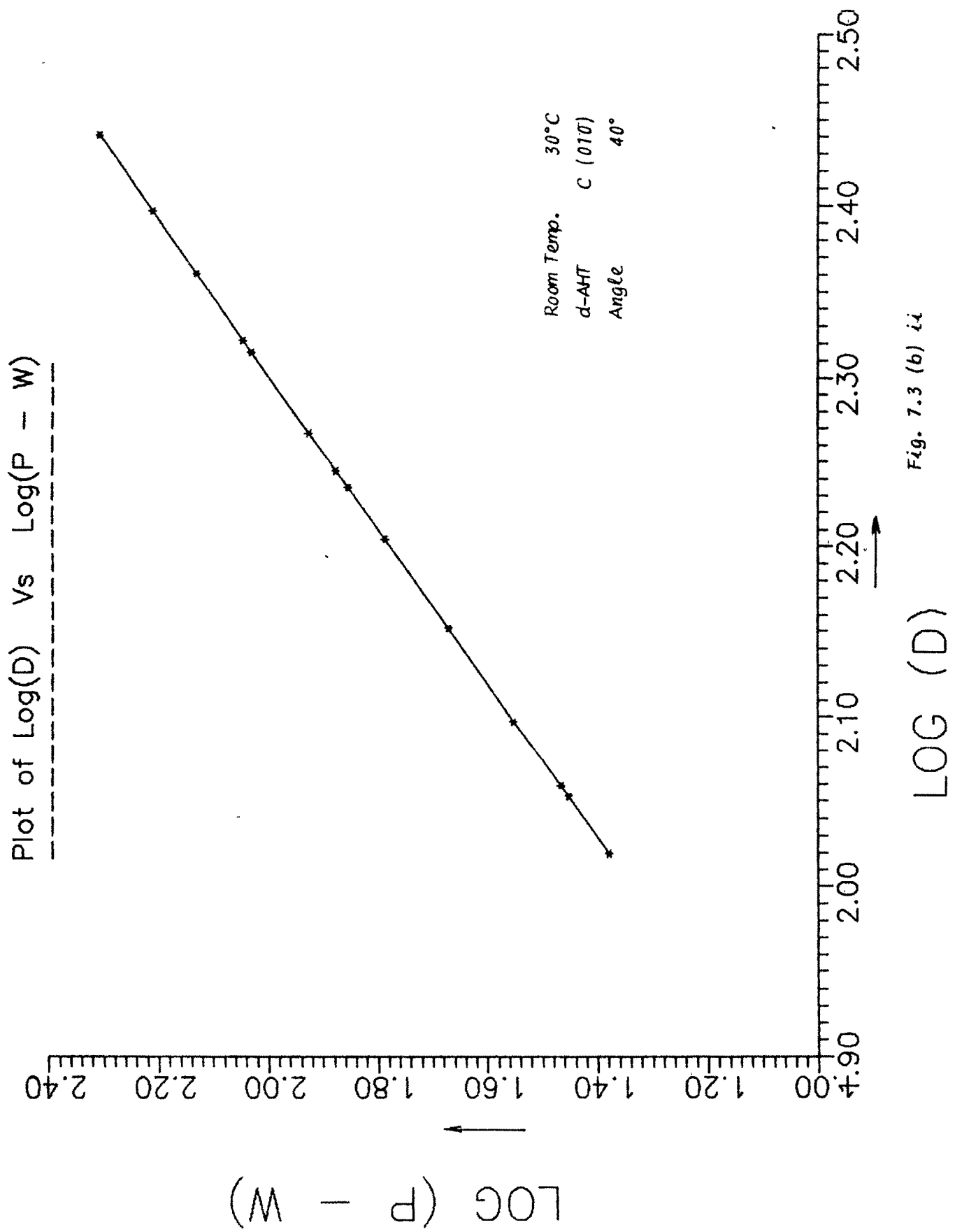
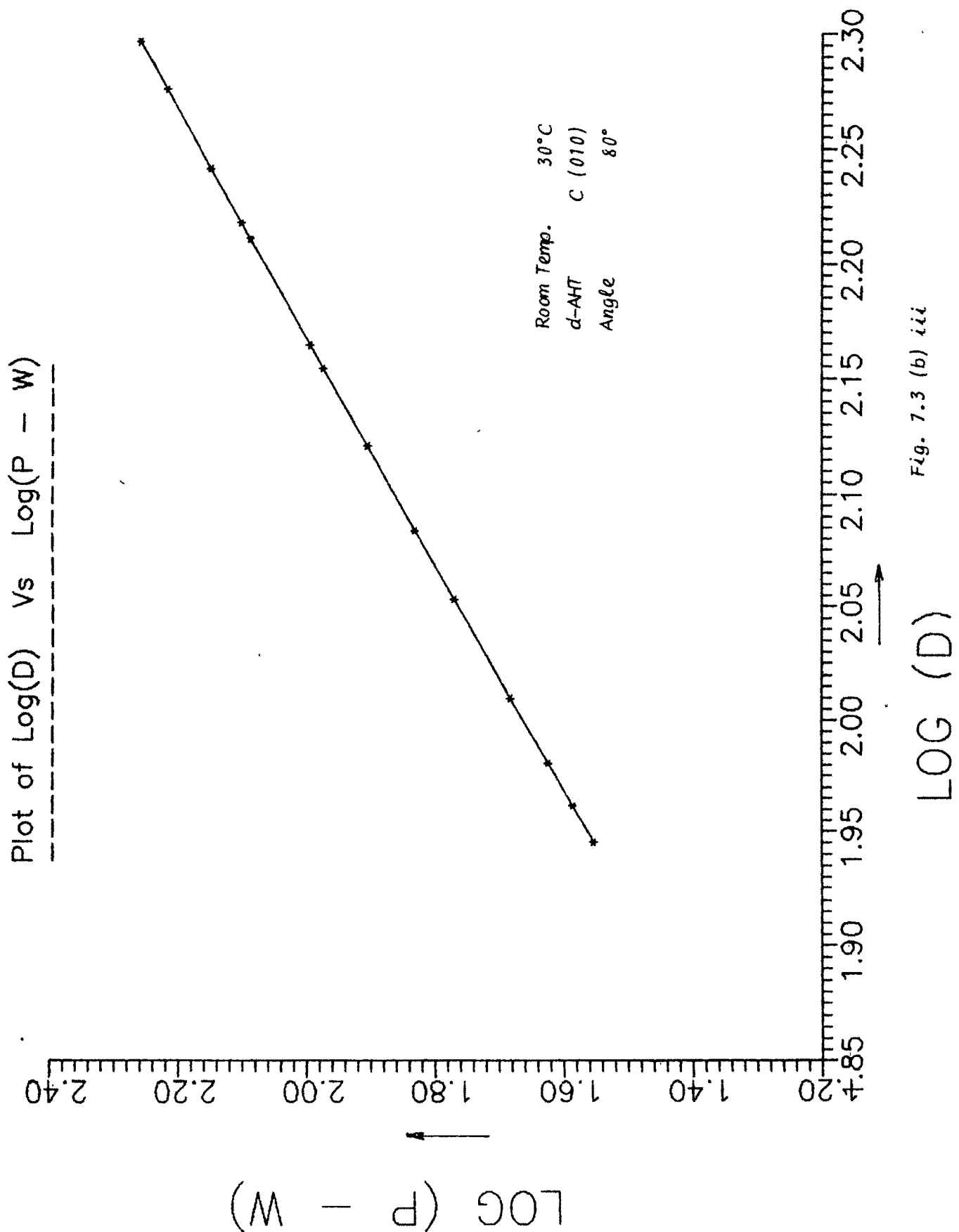


Fig. 7.3 (b) i-i



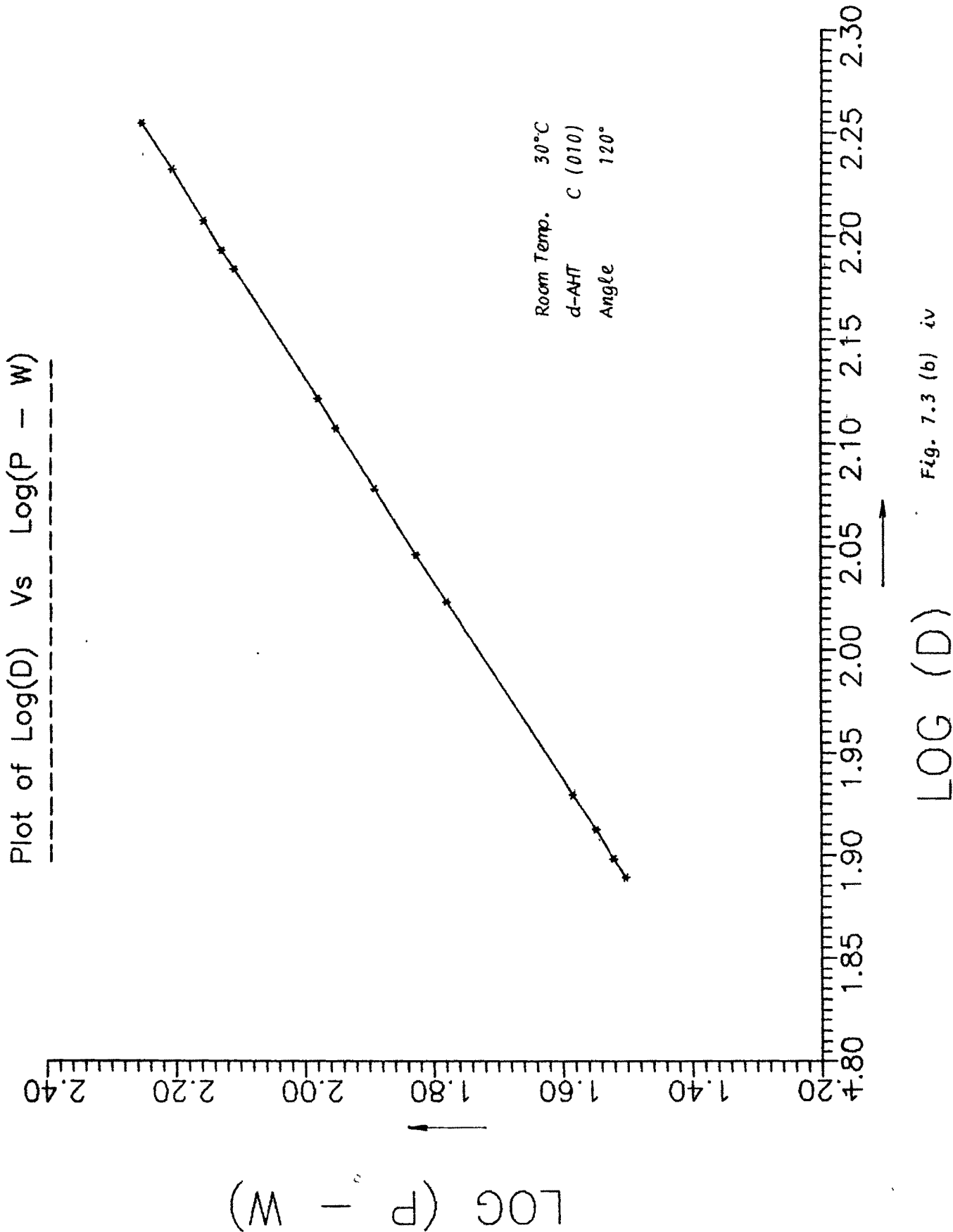
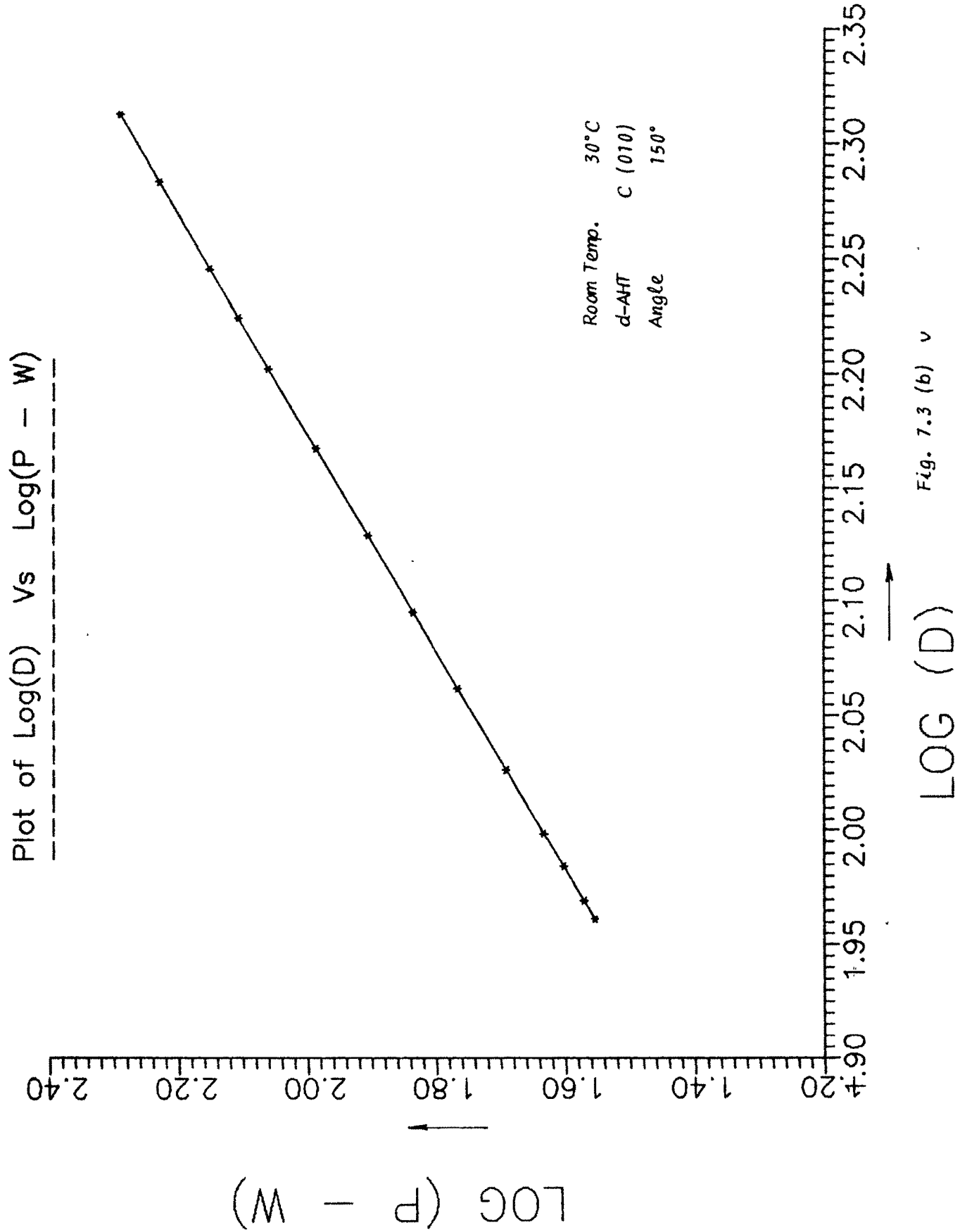
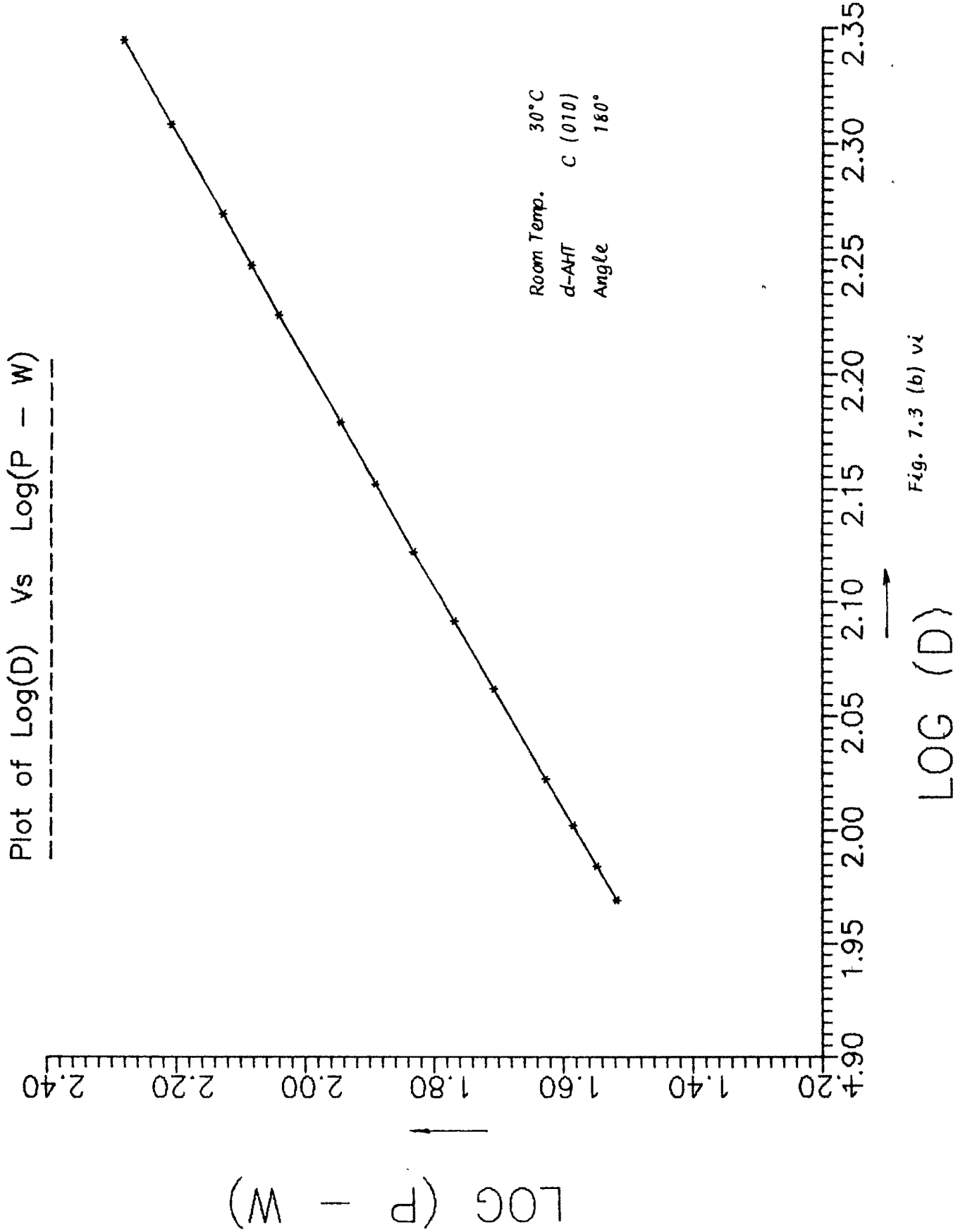
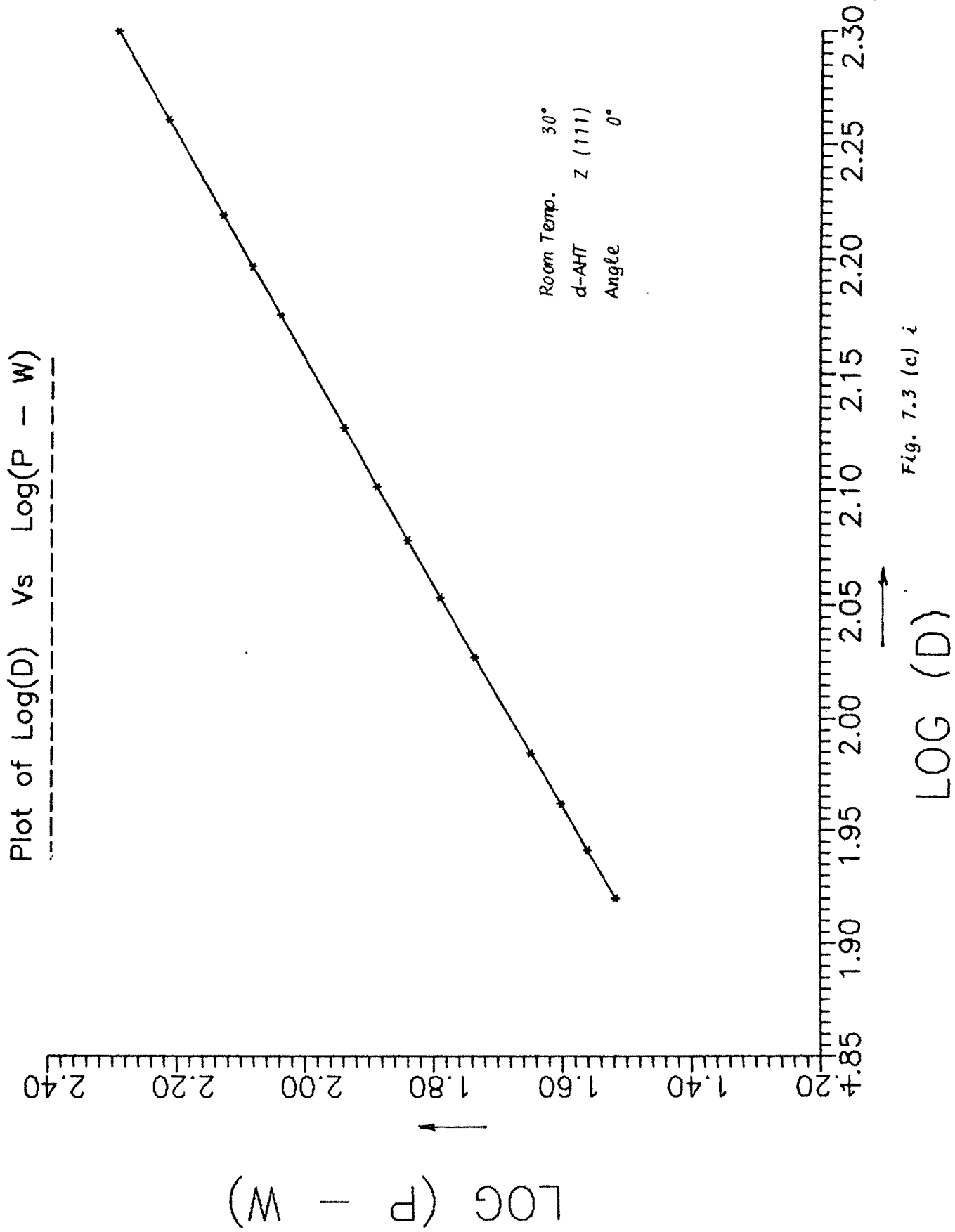


Fig. 7.3 (b) iv





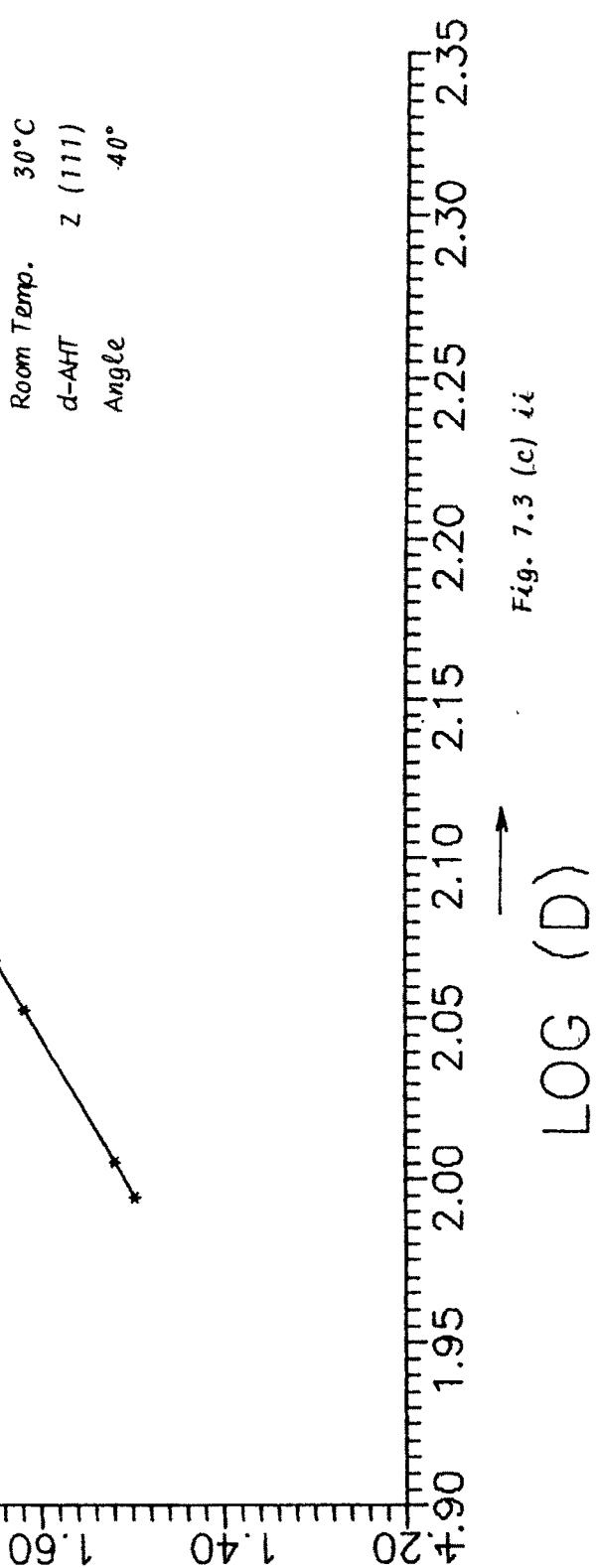
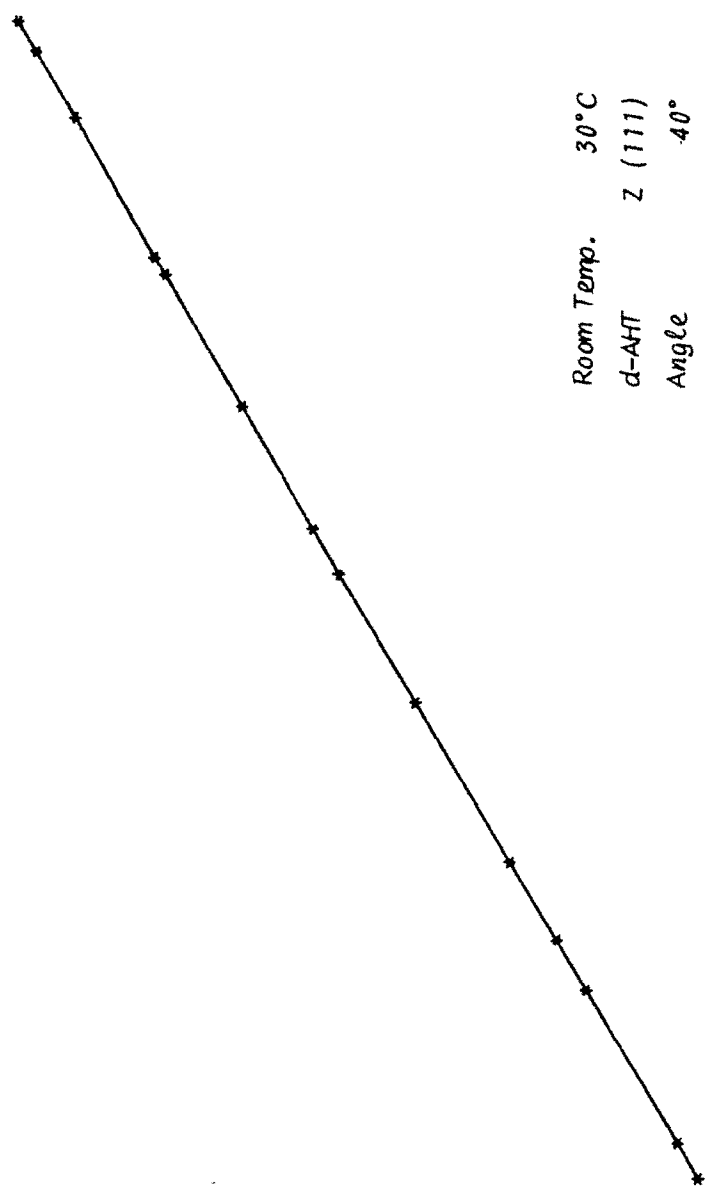


Plot of Log(D) Vs Log(P - W)

2.40
2.20
2.00
1.80
1.60
1.40
1.20

↓

LOG (P - W)



Plot of Log(D) vs Log(P - W)

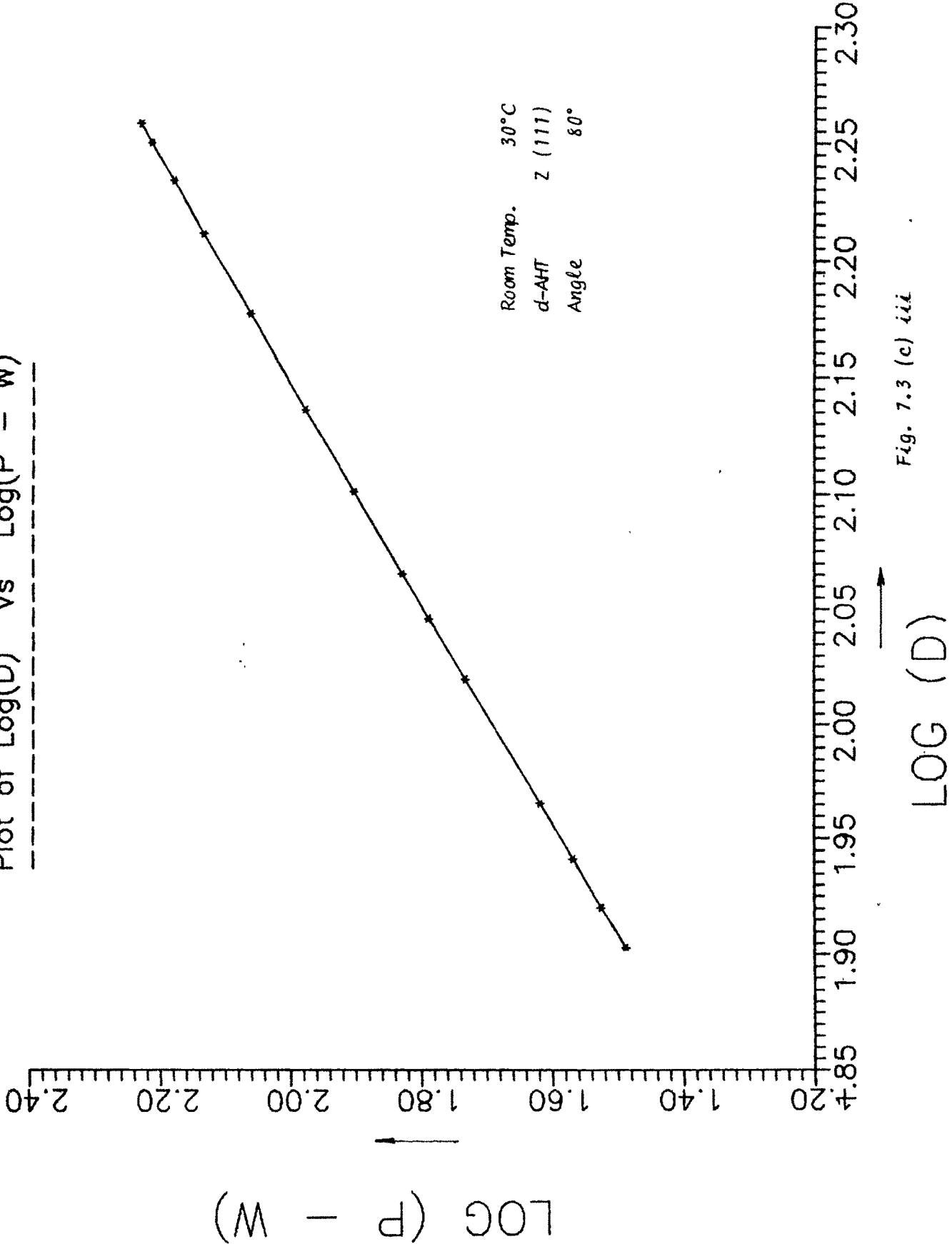
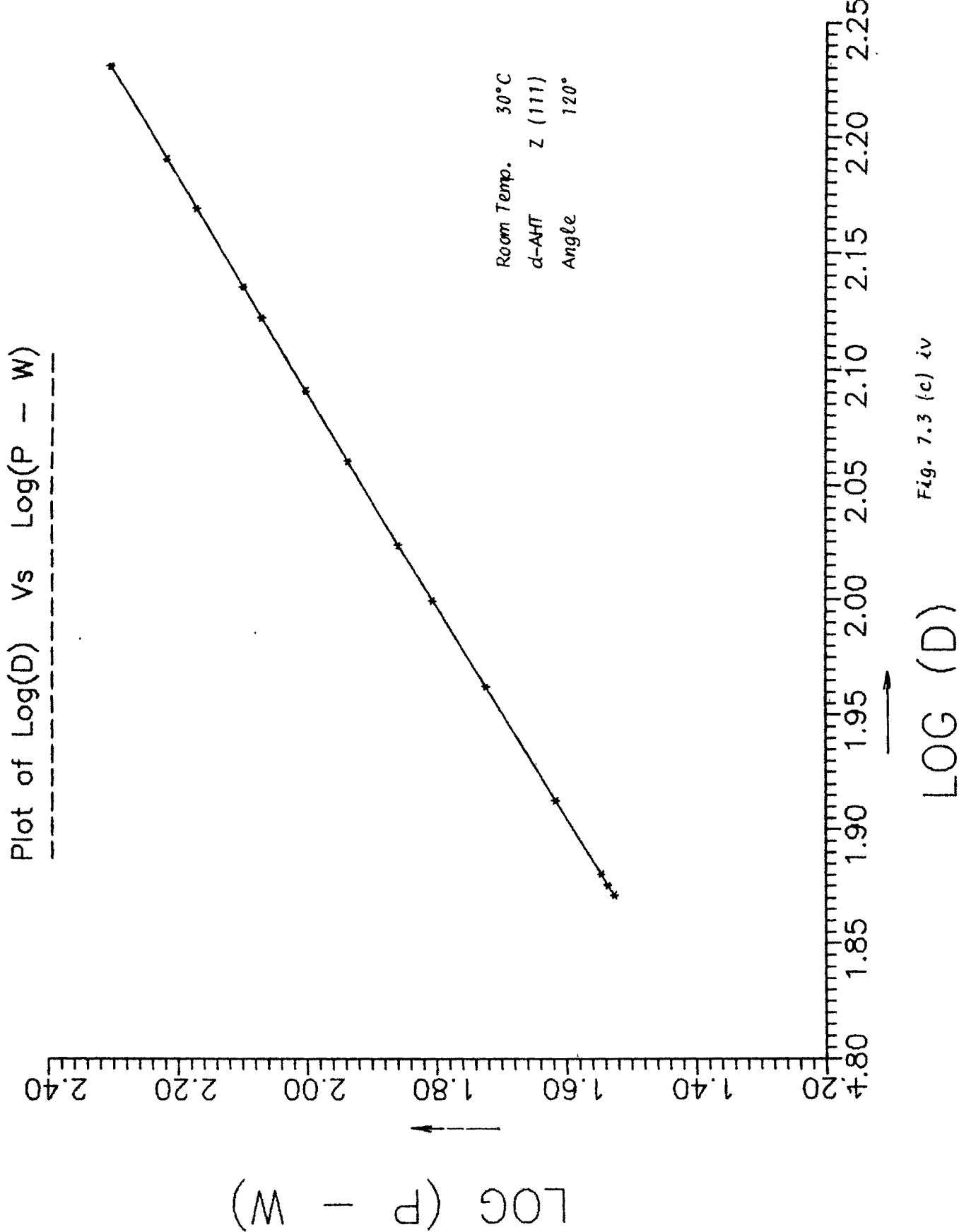


Fig. 7.3 (c) iii



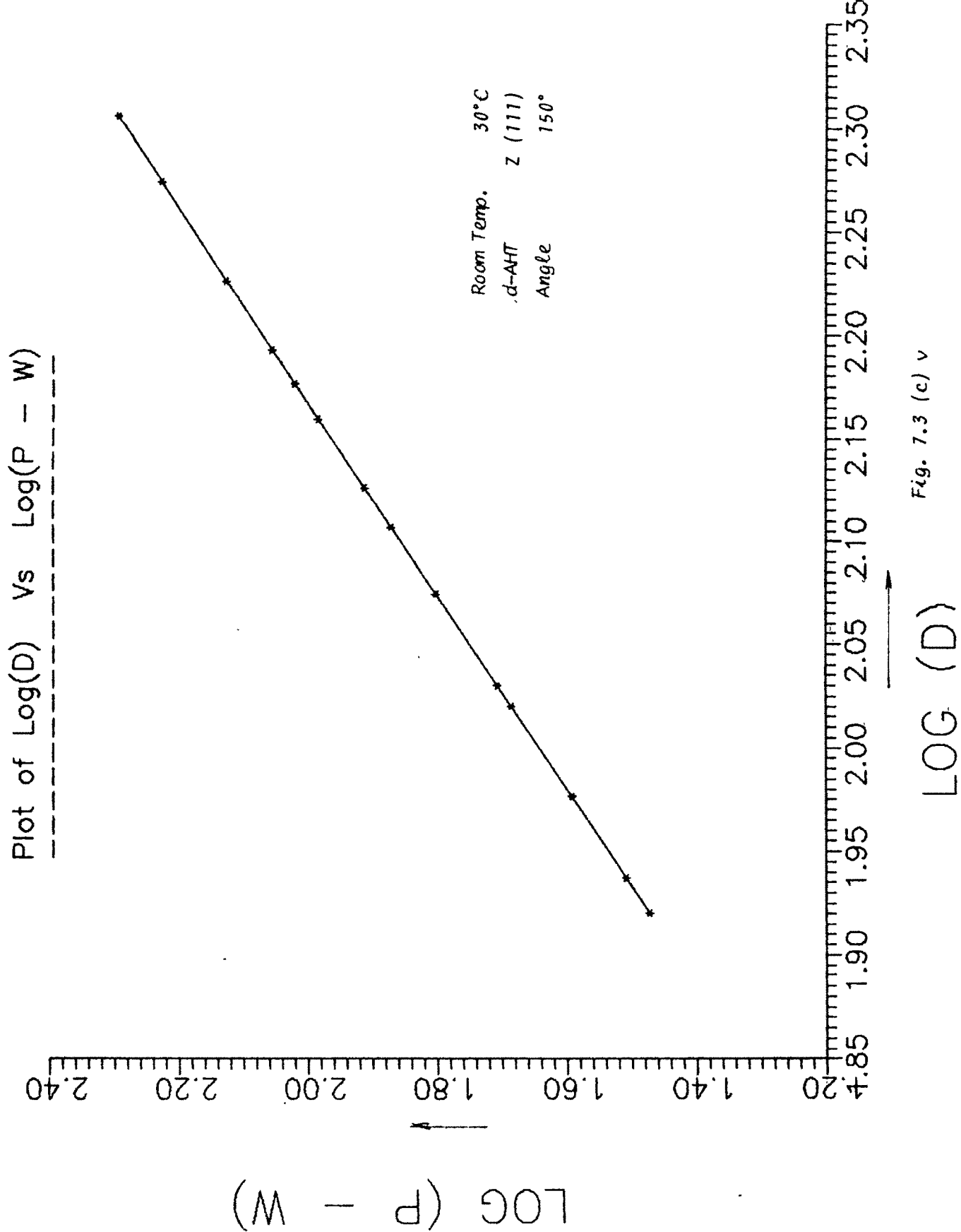


Fig. 7.3 (c) v

Plot of Log(D) Vs Log(P - W)

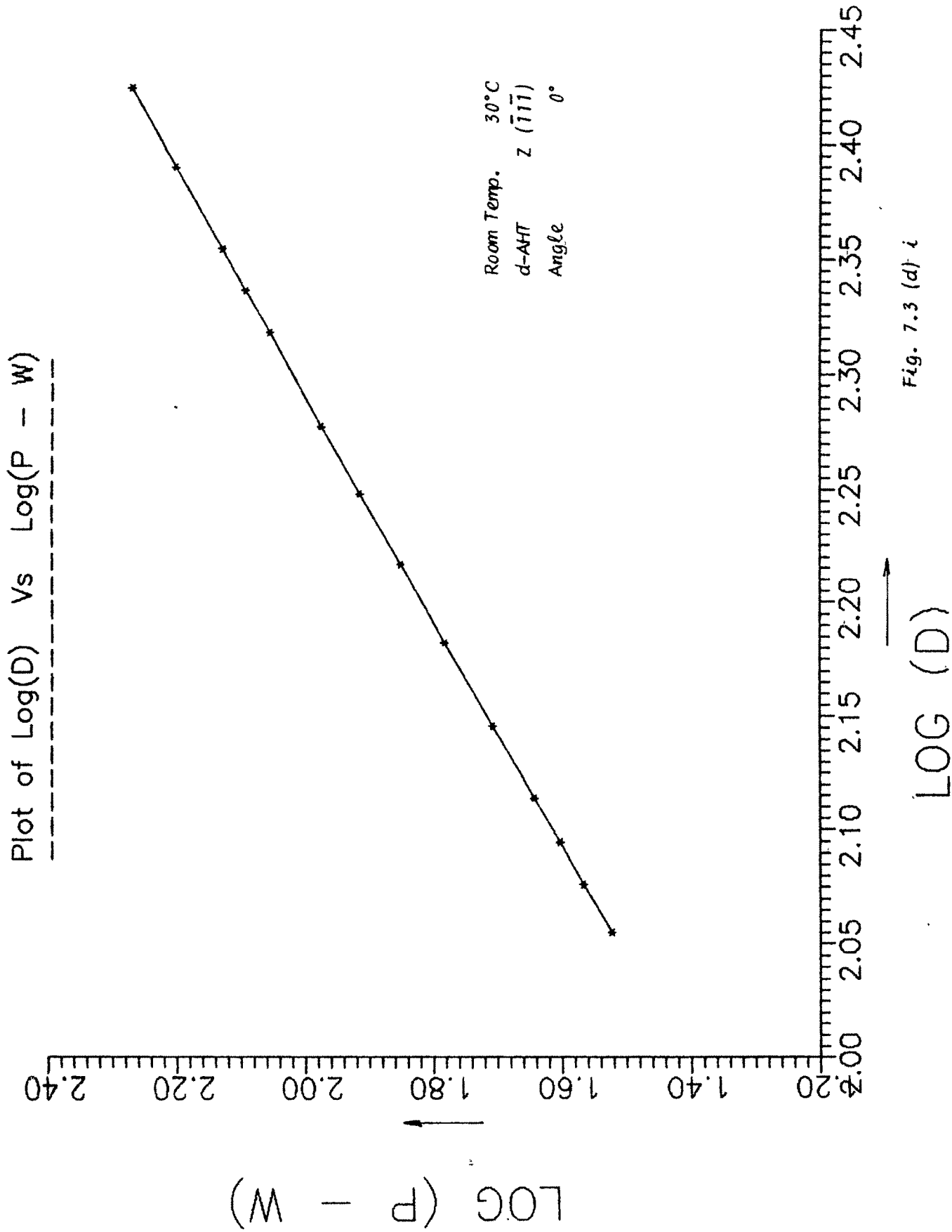
LOG (P - W)

.20 .195 .190 .180 .170 .160 .150 .140 .130 .120

LOG (D)

Room Temp. 30°C
d-AHT z (111)
Angle 180°

Fig. 7.3 (c) vi.



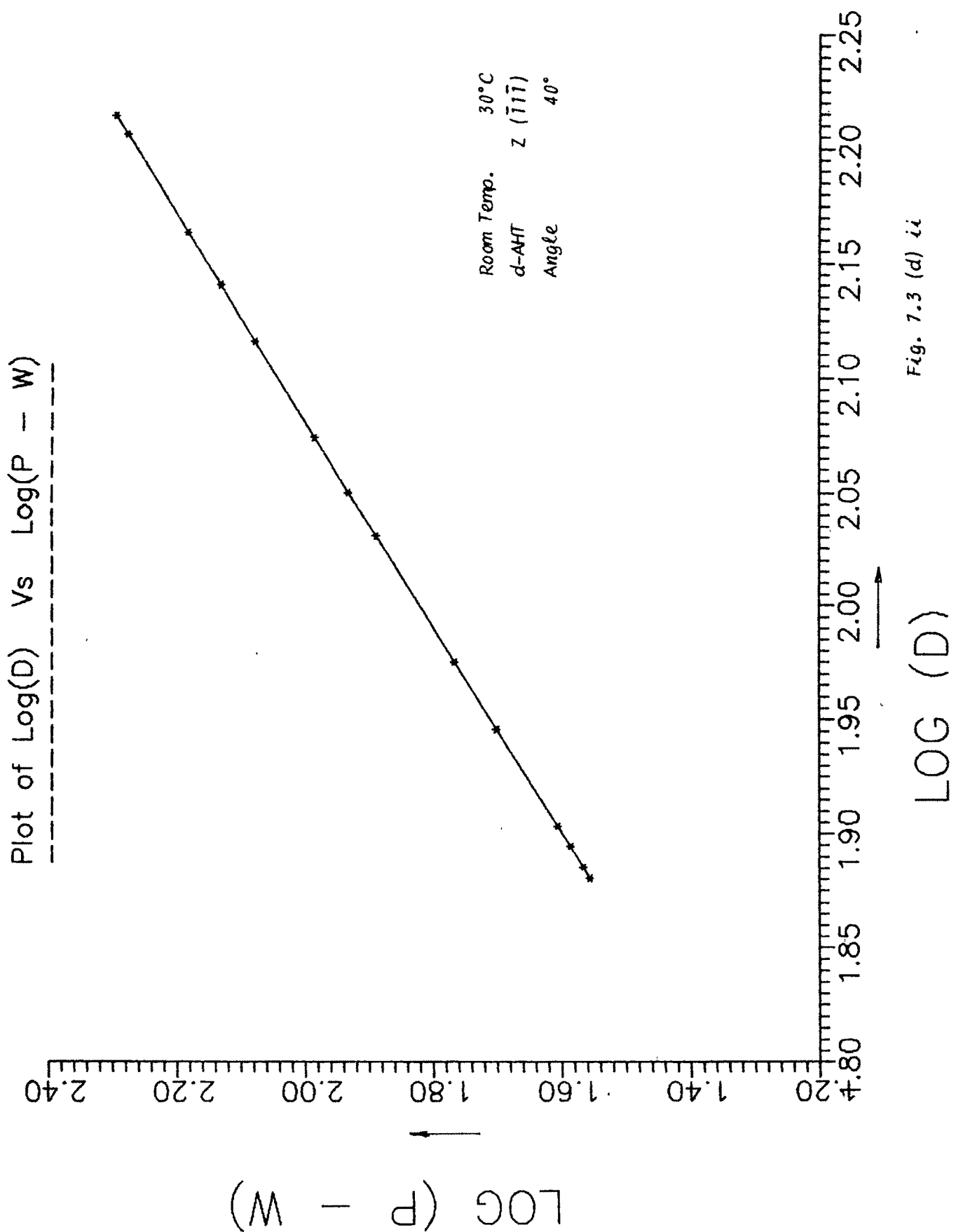
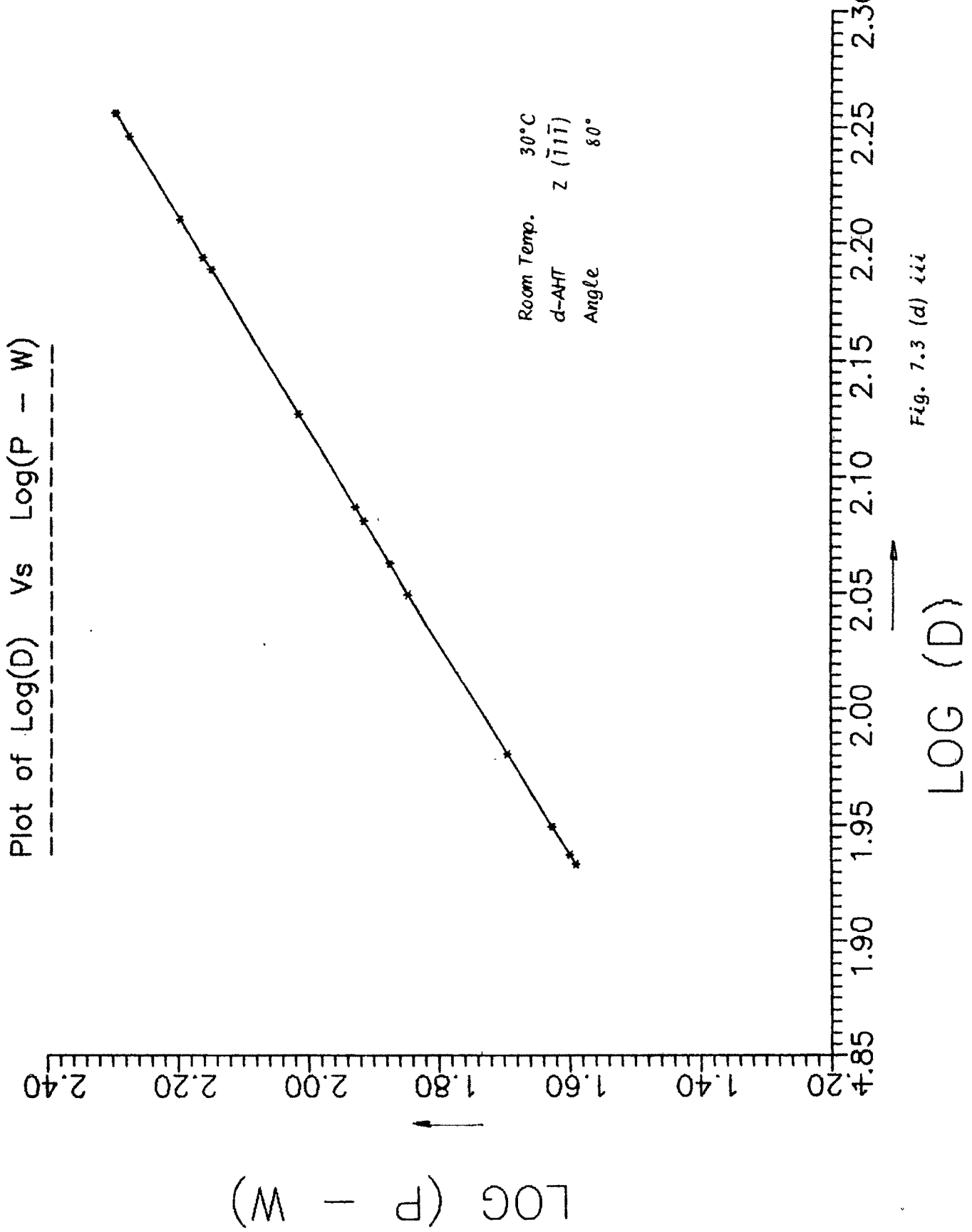
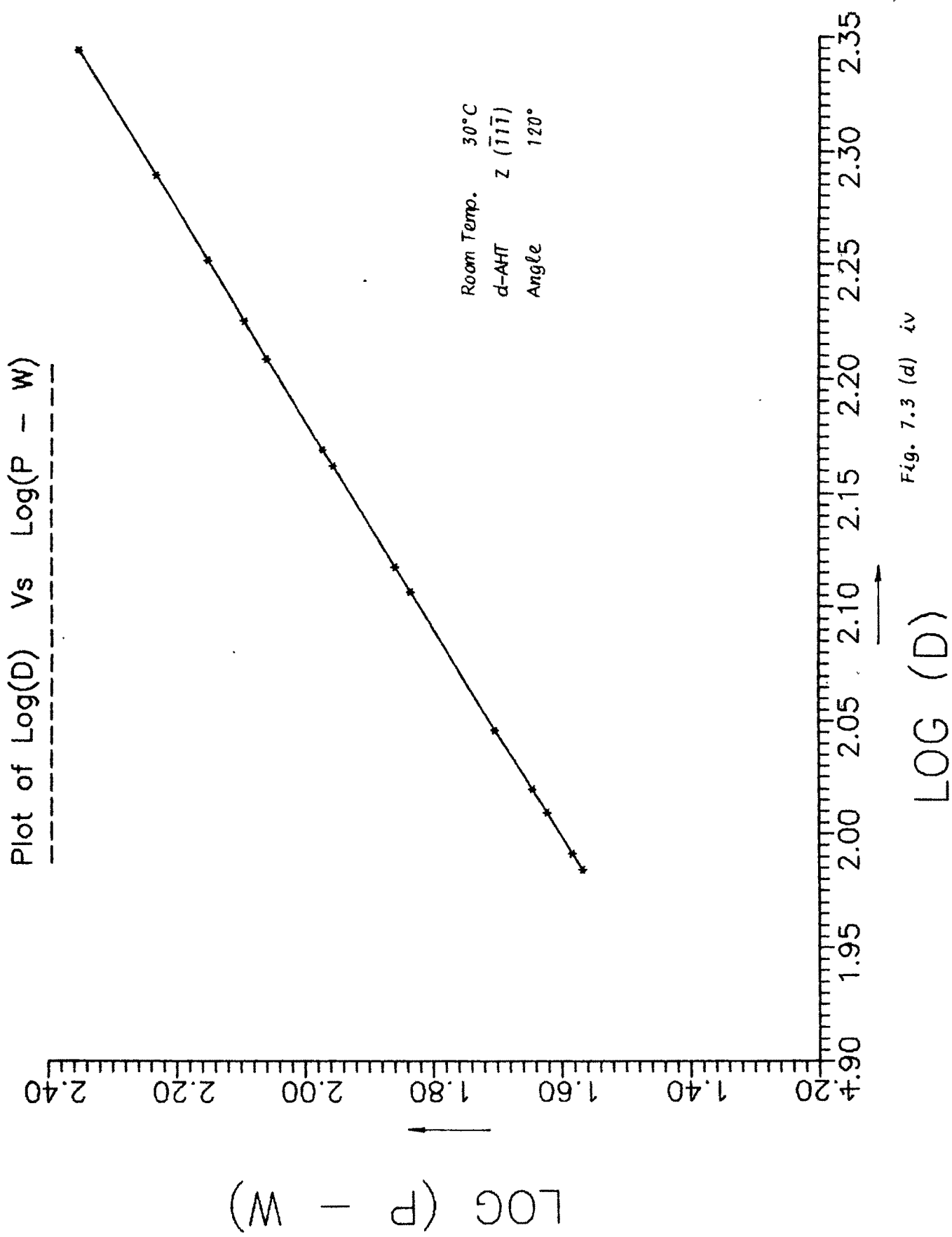
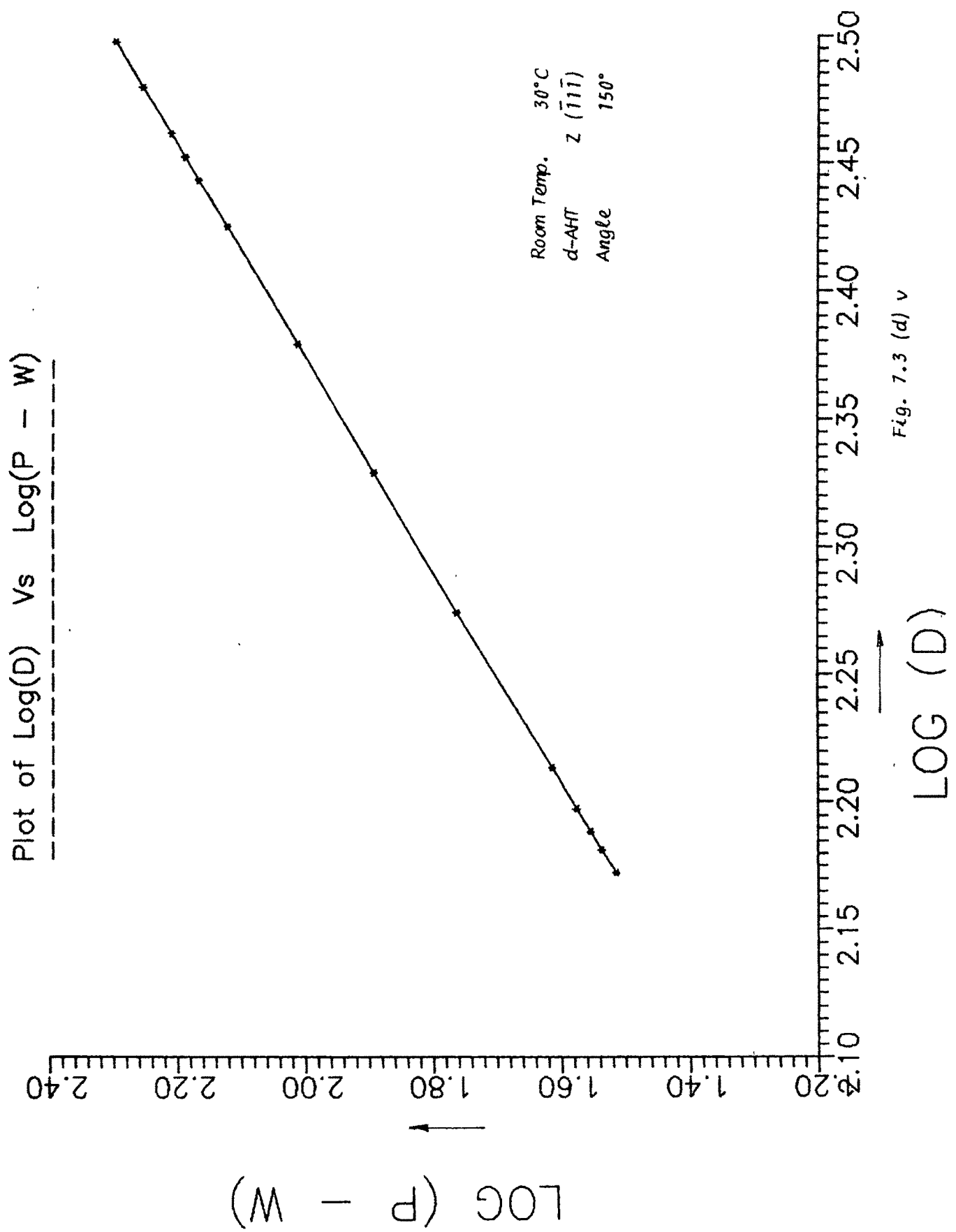


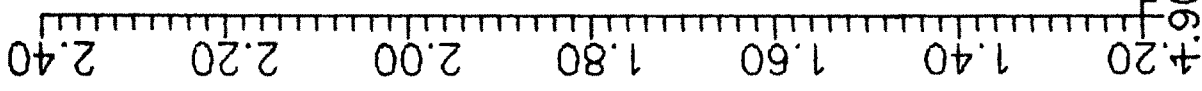
Fig. 1.3 (d) ii







Plot of Log(D) vs Log(P - W)



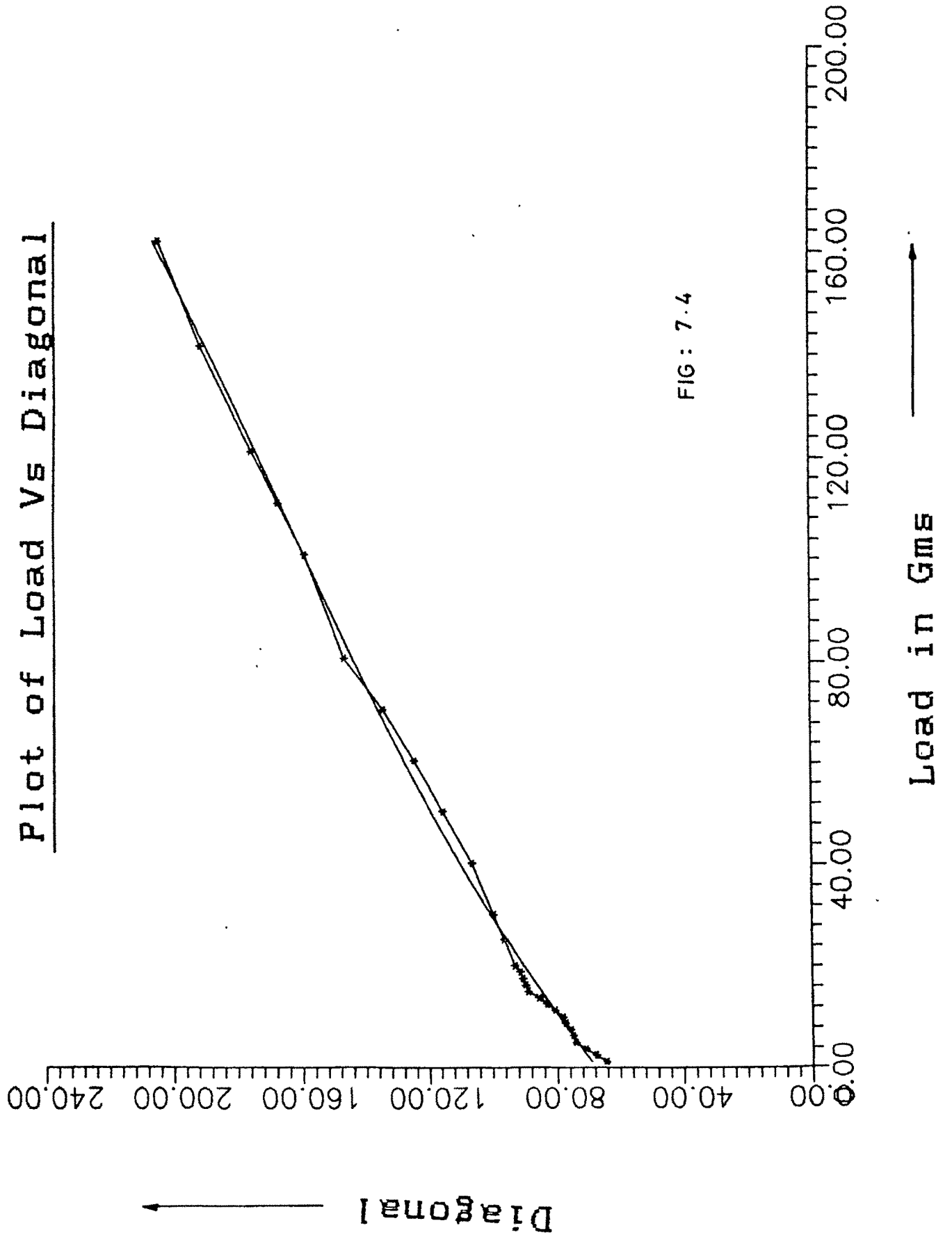
LOG (P - W)

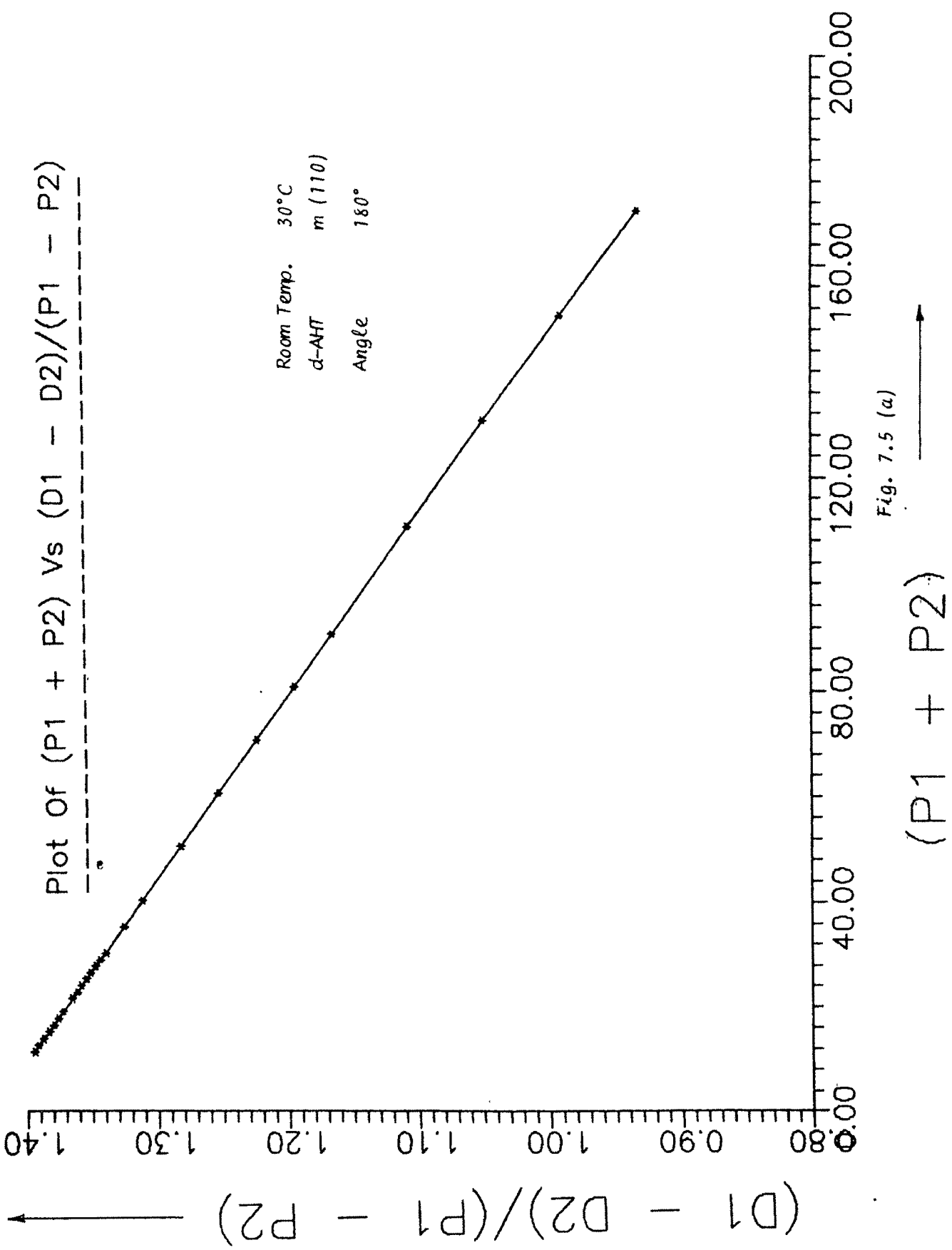
Room Temp. 30°C
d-AHT Z ($\bar{1}\bar{1}\bar{1}$)
Angle 180°

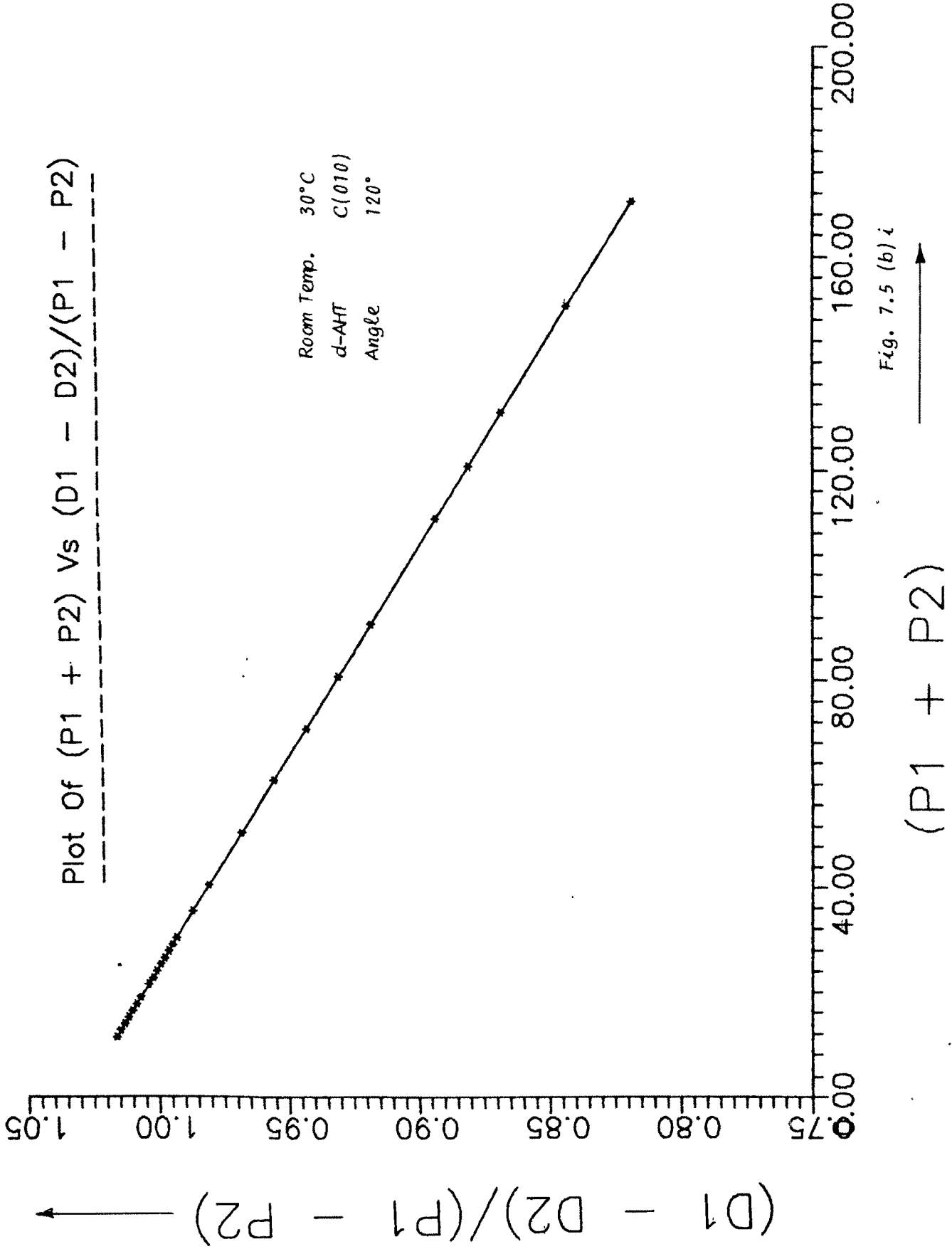
Fig. 7.3 (d) vi

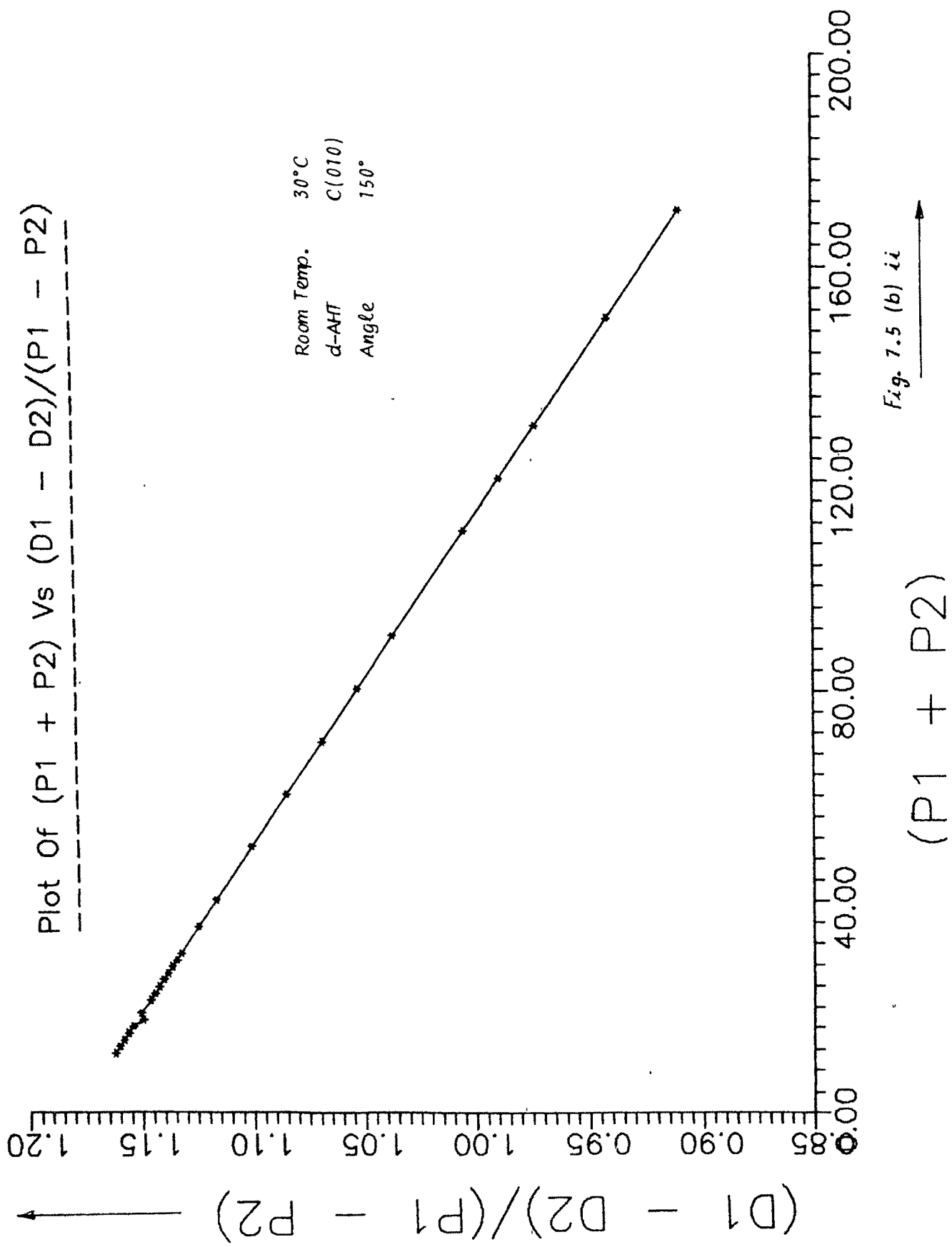
LOG (D)

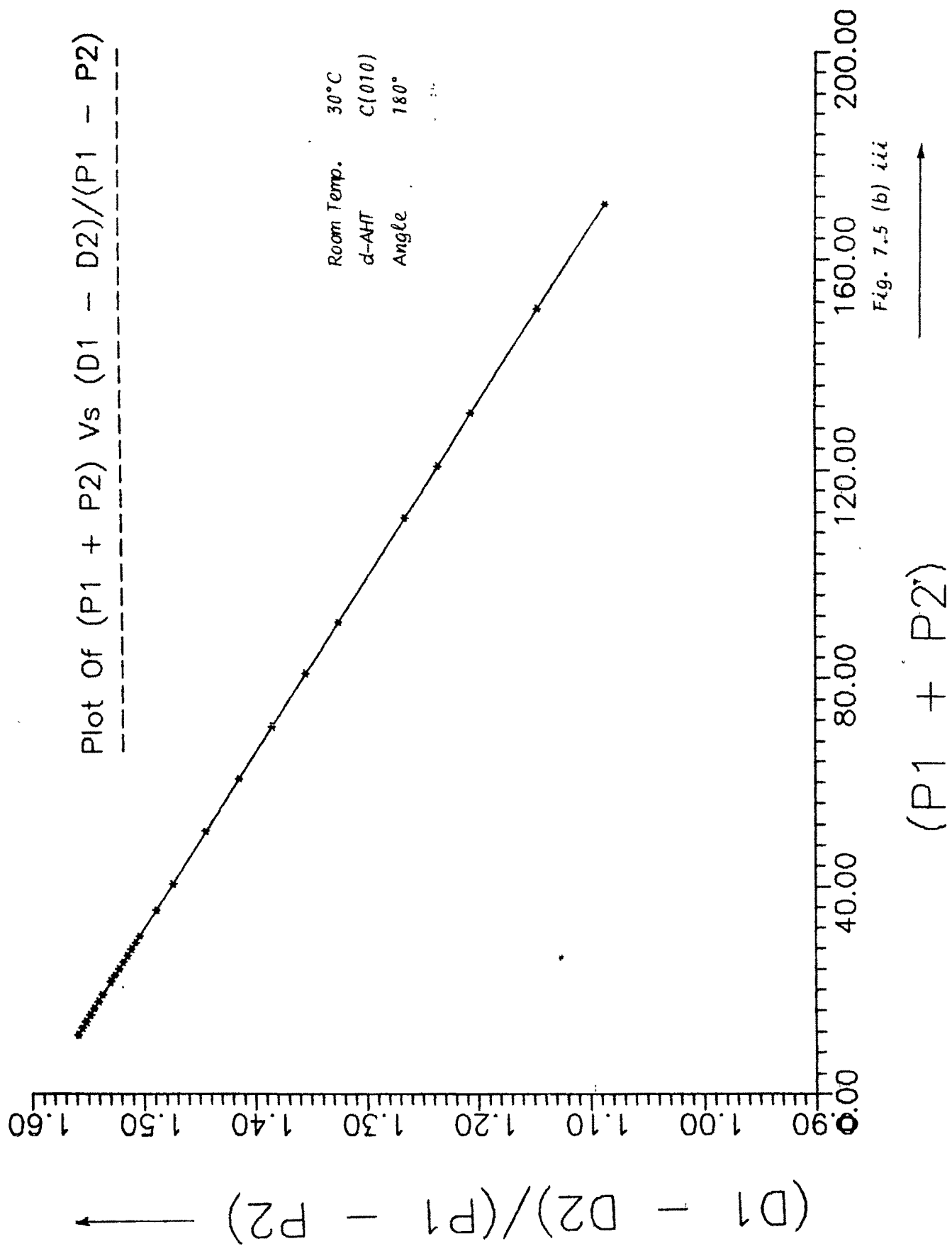
Plot of Load Vs Diagonal

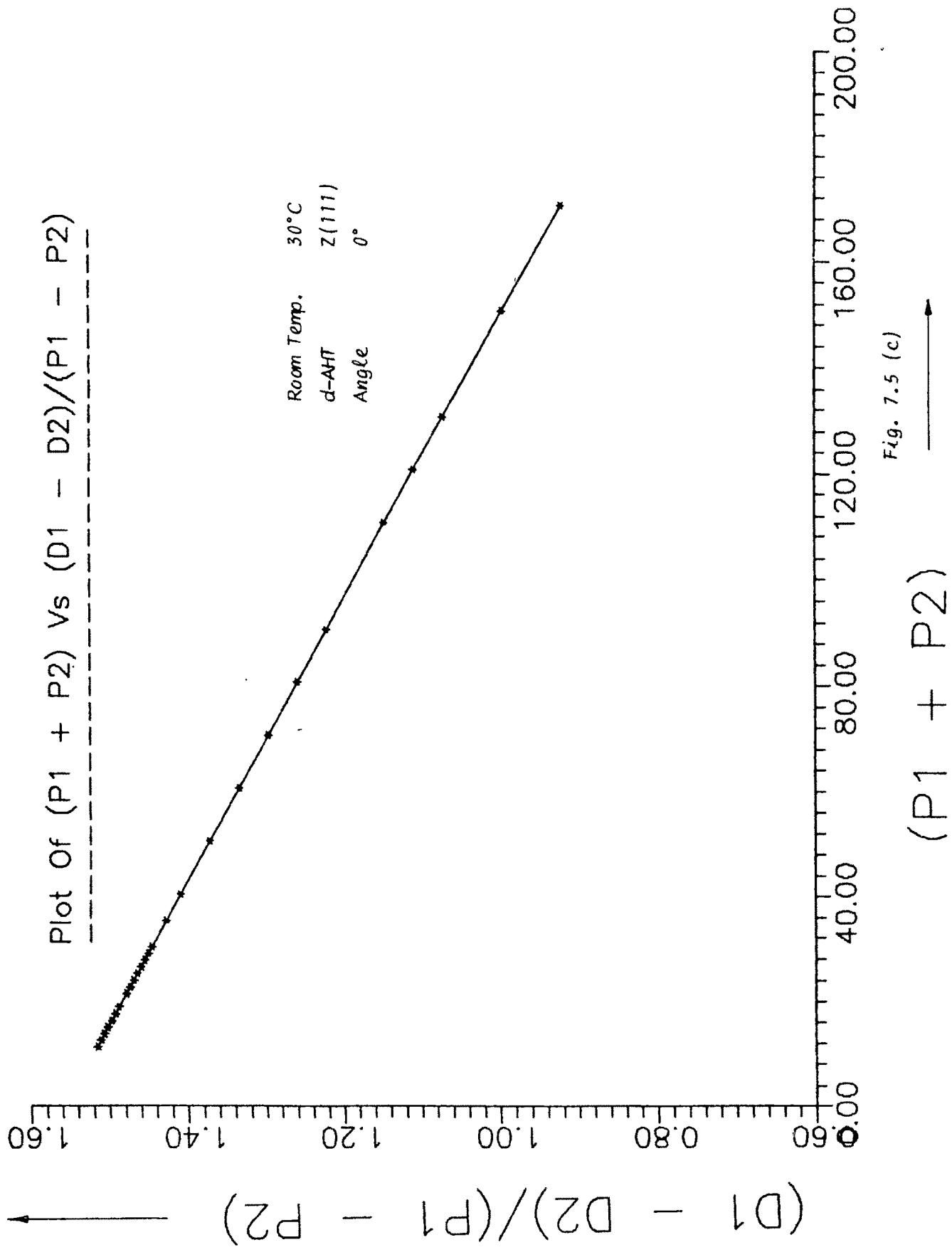


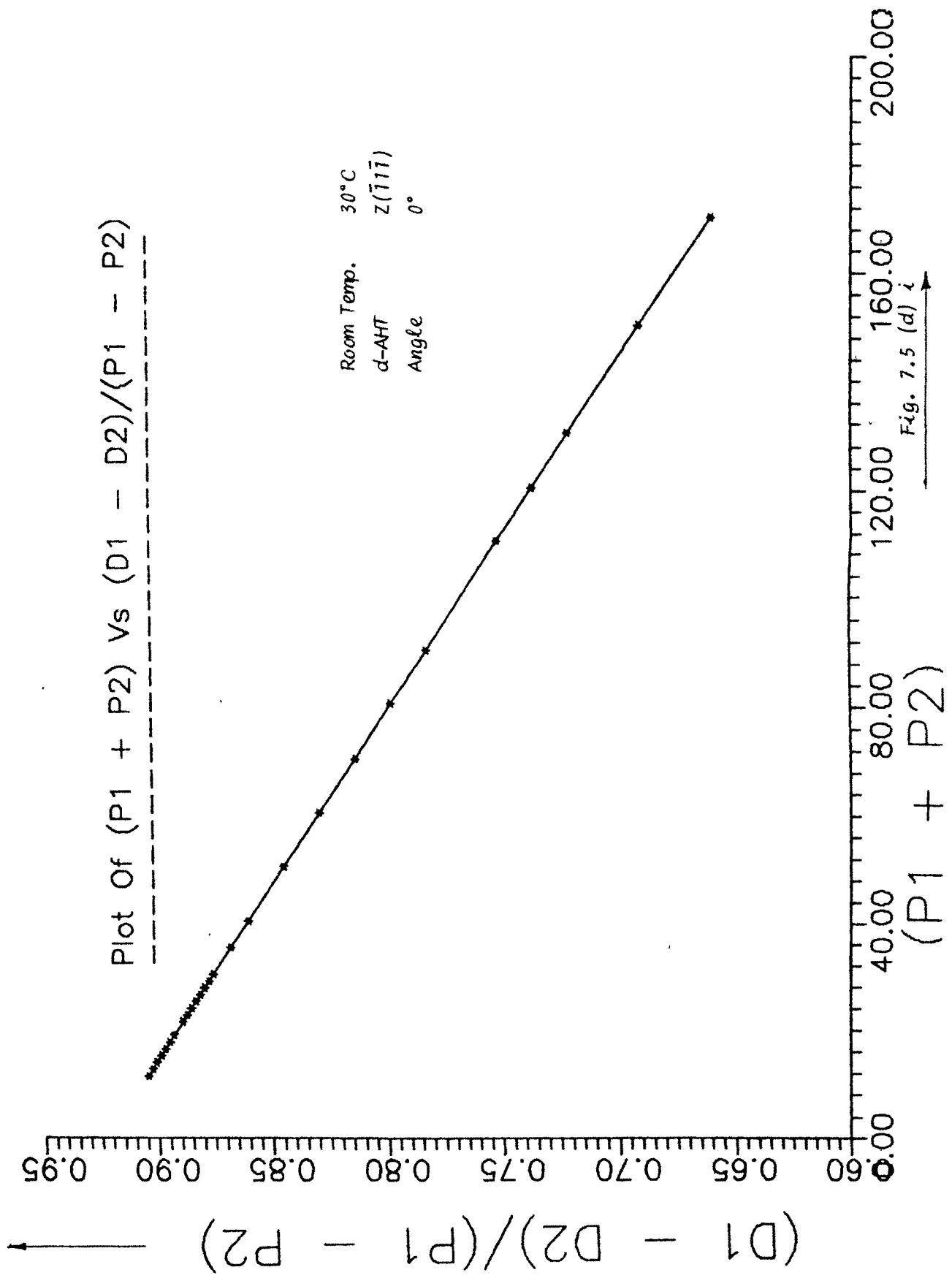


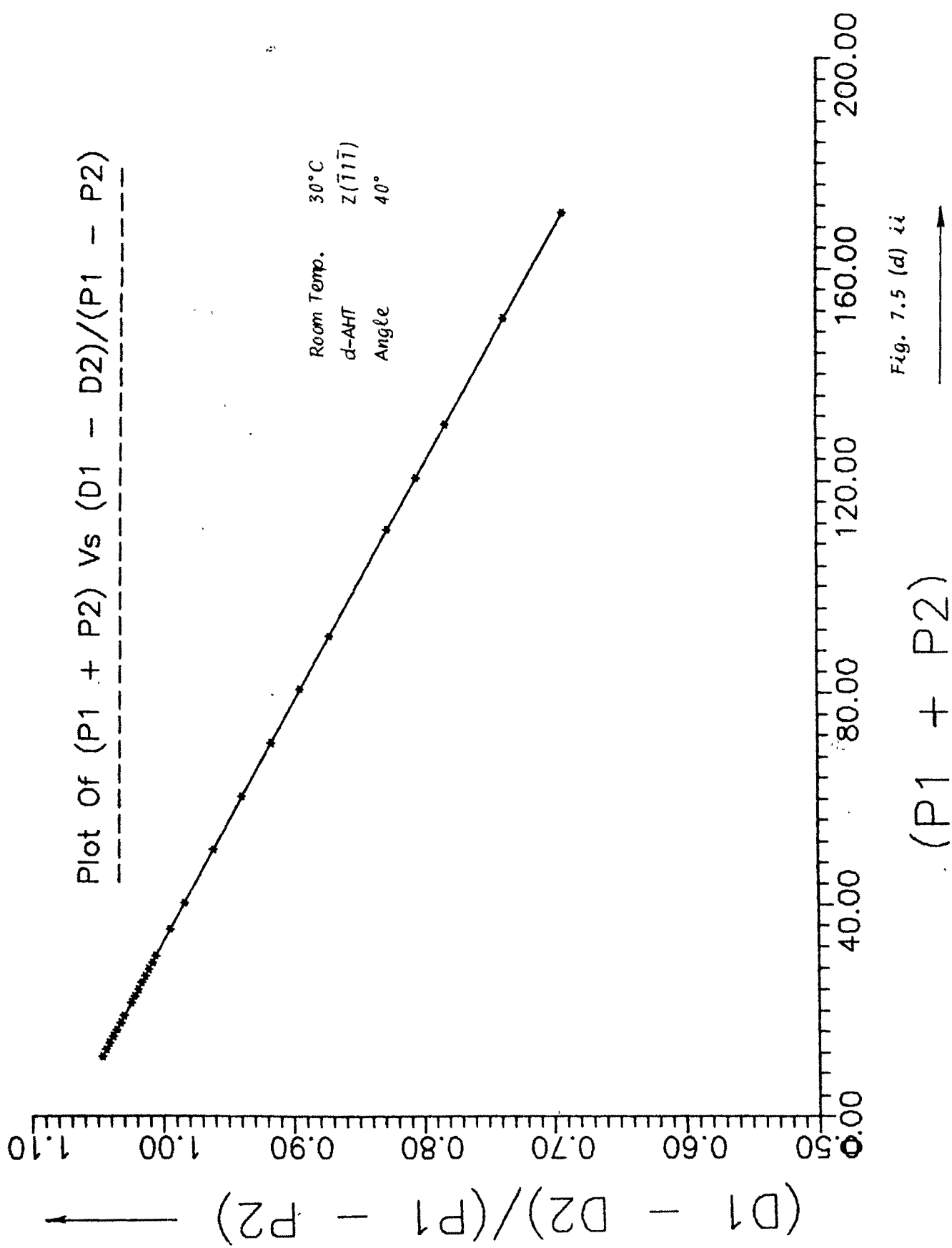




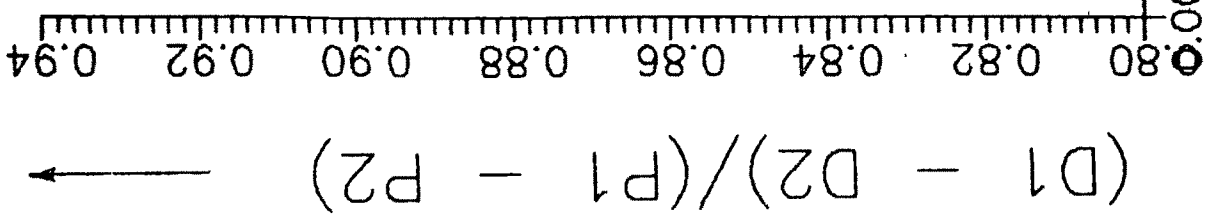








Plot Of $(P_1 + P_2)$ Vs $(D_1 - D_2)/(P_1 - P_2)$

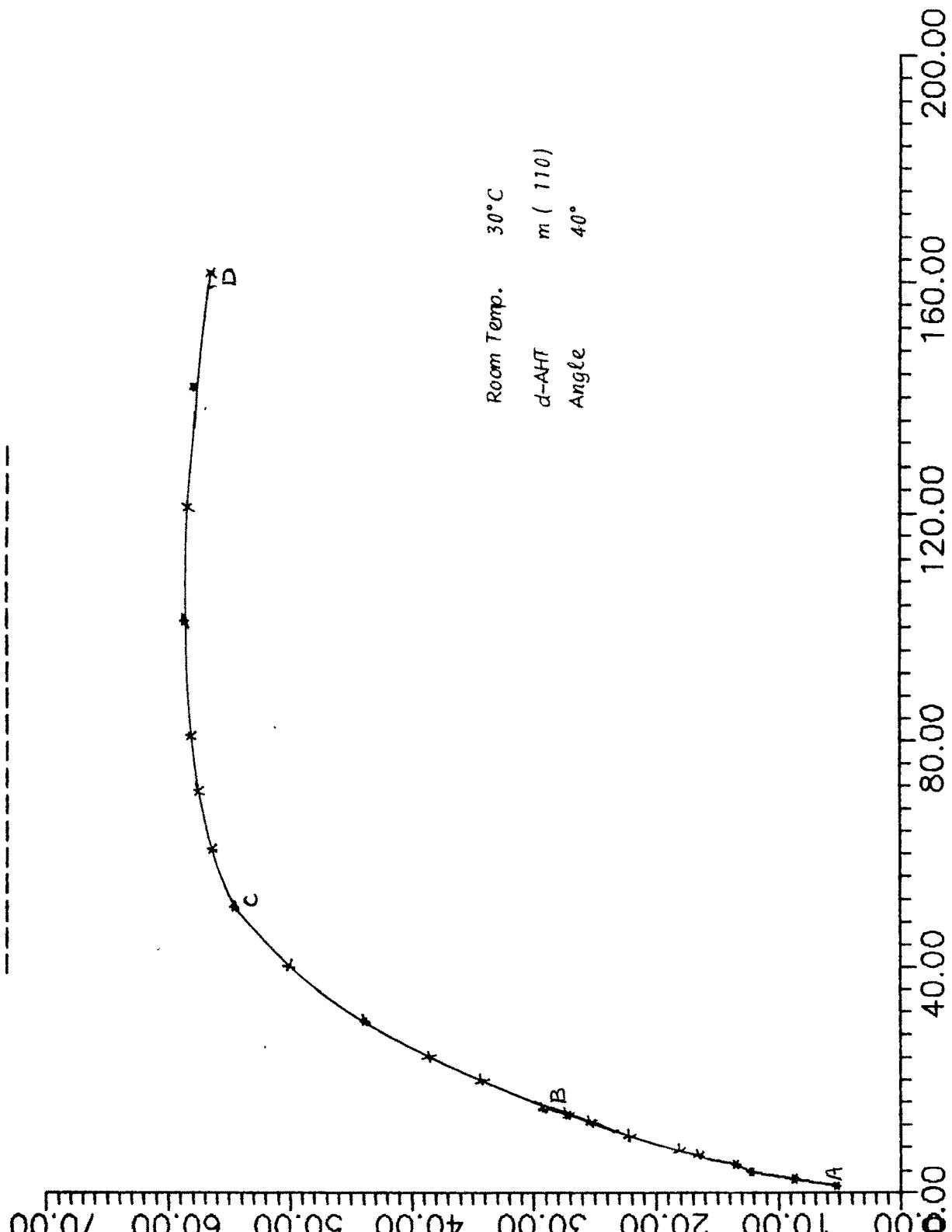


Room Temp. $30^{\circ}C$
 $d\text{-AHT}$
Angle 80°
 $Z(\bar{1}\bar{1}\bar{1})$

Fig. 7.5 (d) iii

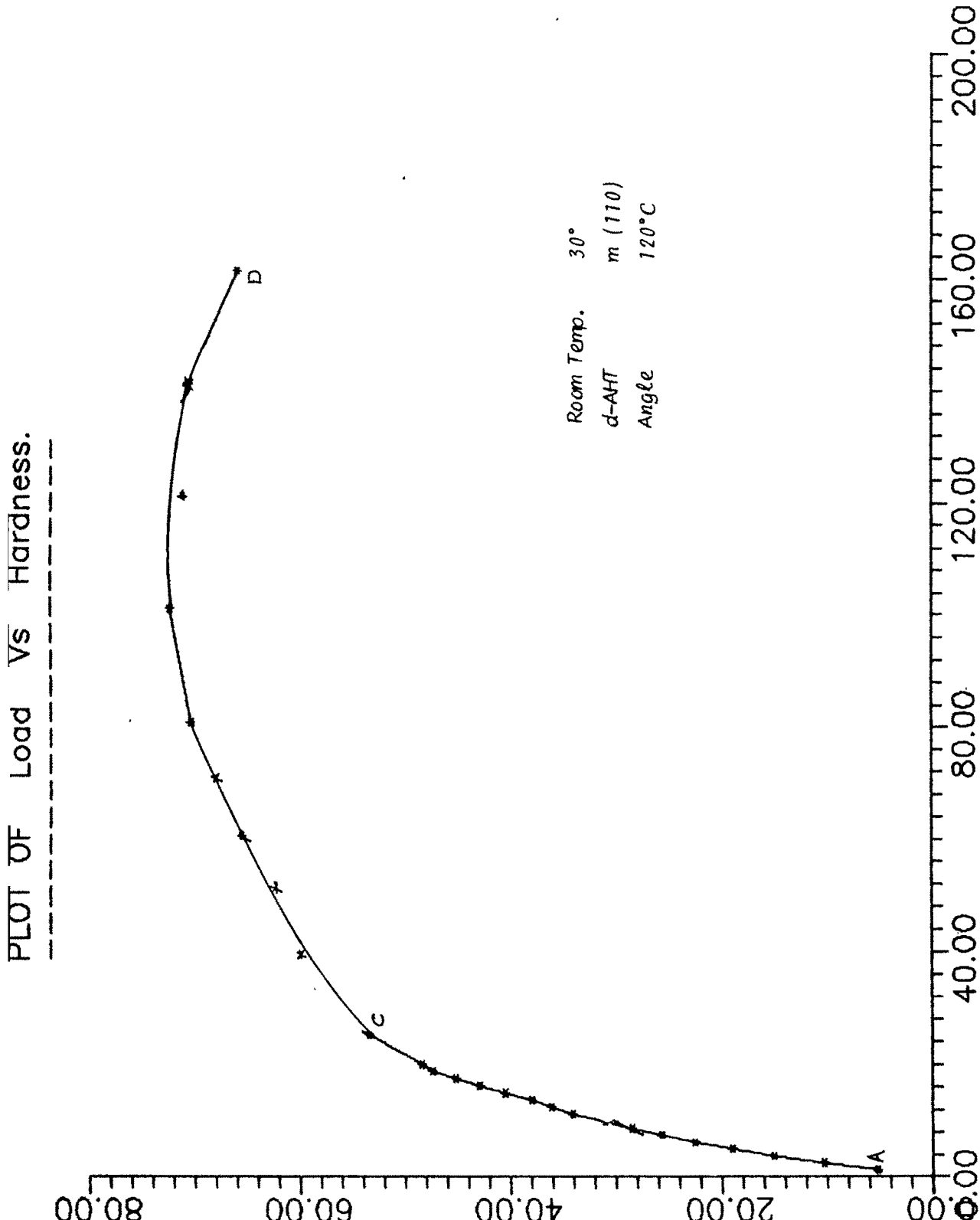
$(P_1 + P_2)$

PLOT OF Load Vs Hardness.



Hardness in kgms/m^2

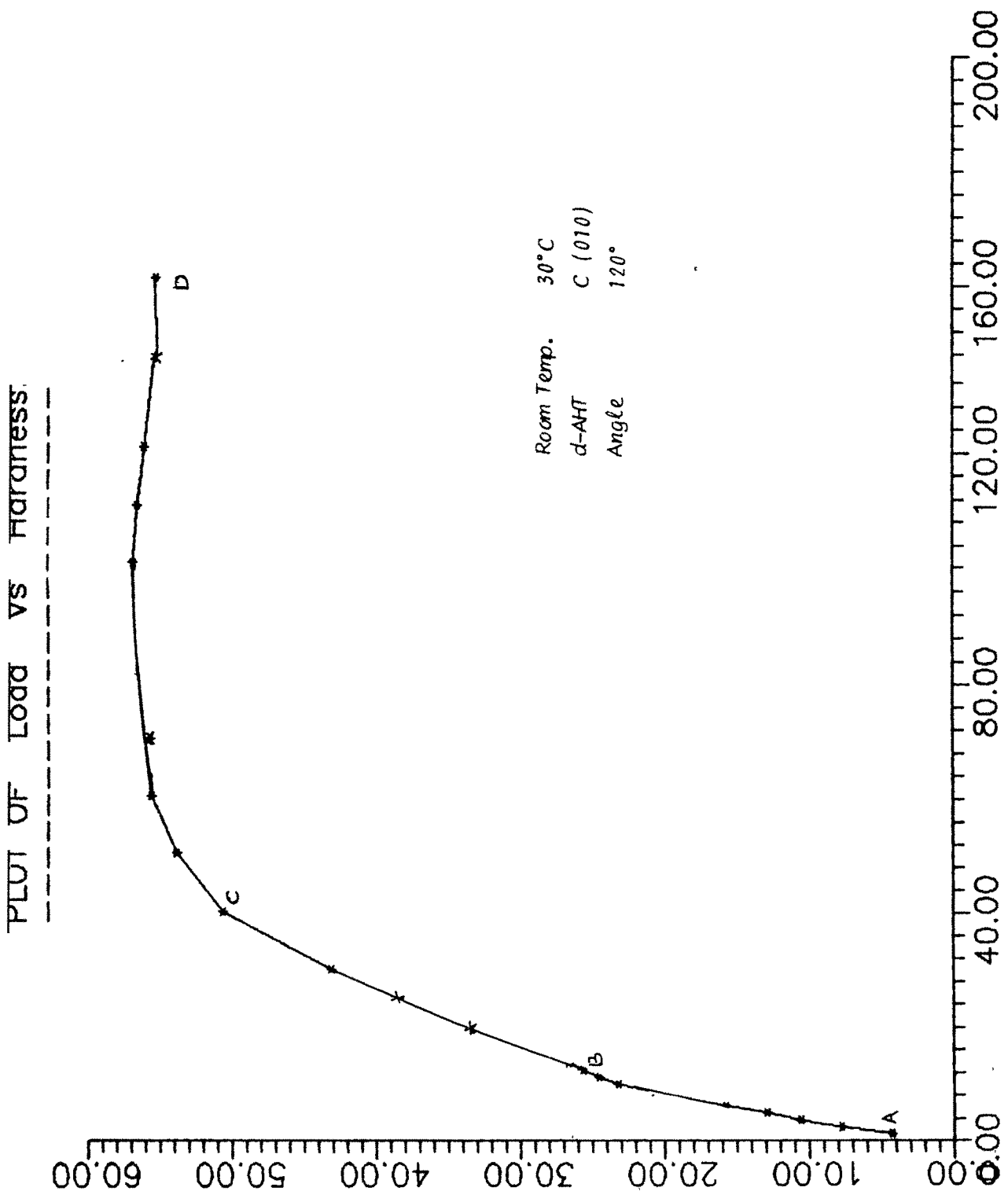
Fig. 7.6 (a) i



Hardness in kgms/m^2

Fig. 7.6 (a) ii

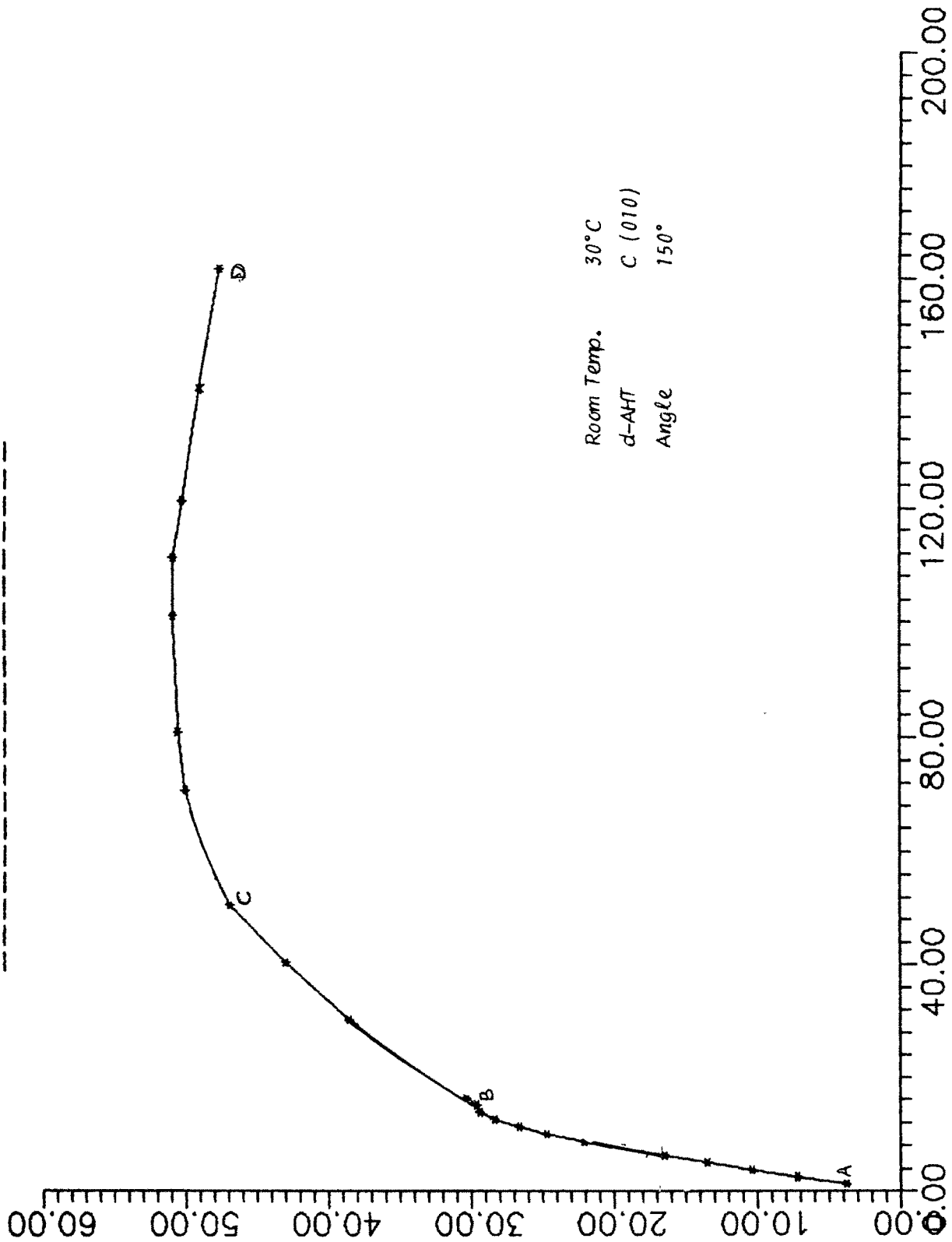
Load in Gms.



Hardness in kgms/m^2

Fig. 7.6 (b) i
Load in Gms.

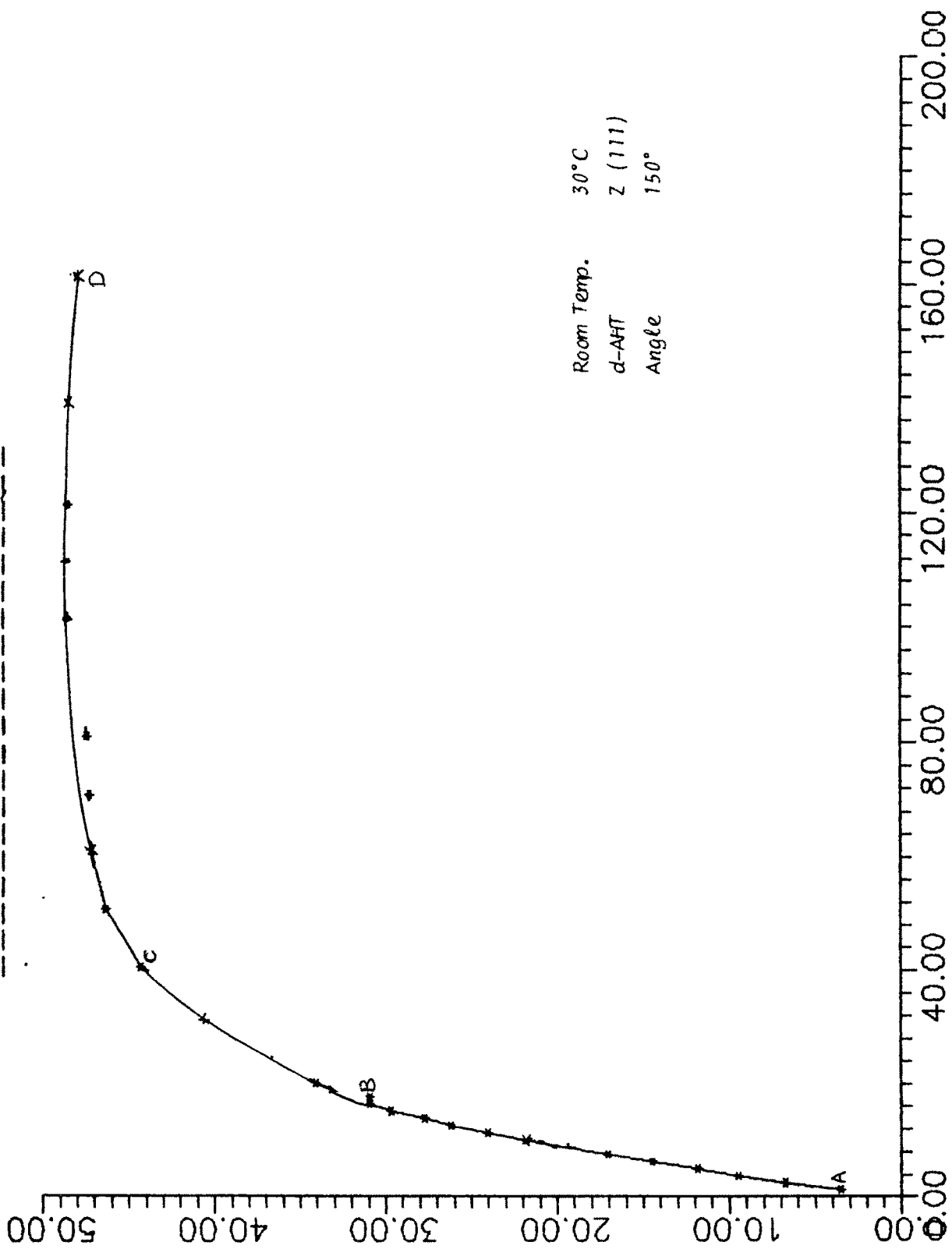
PLUT LOAD VS PLATEAU.



Hardness in kgms/m²

Fig. 7.6 (b) ii

PLOT OF Load Vs Hardness.

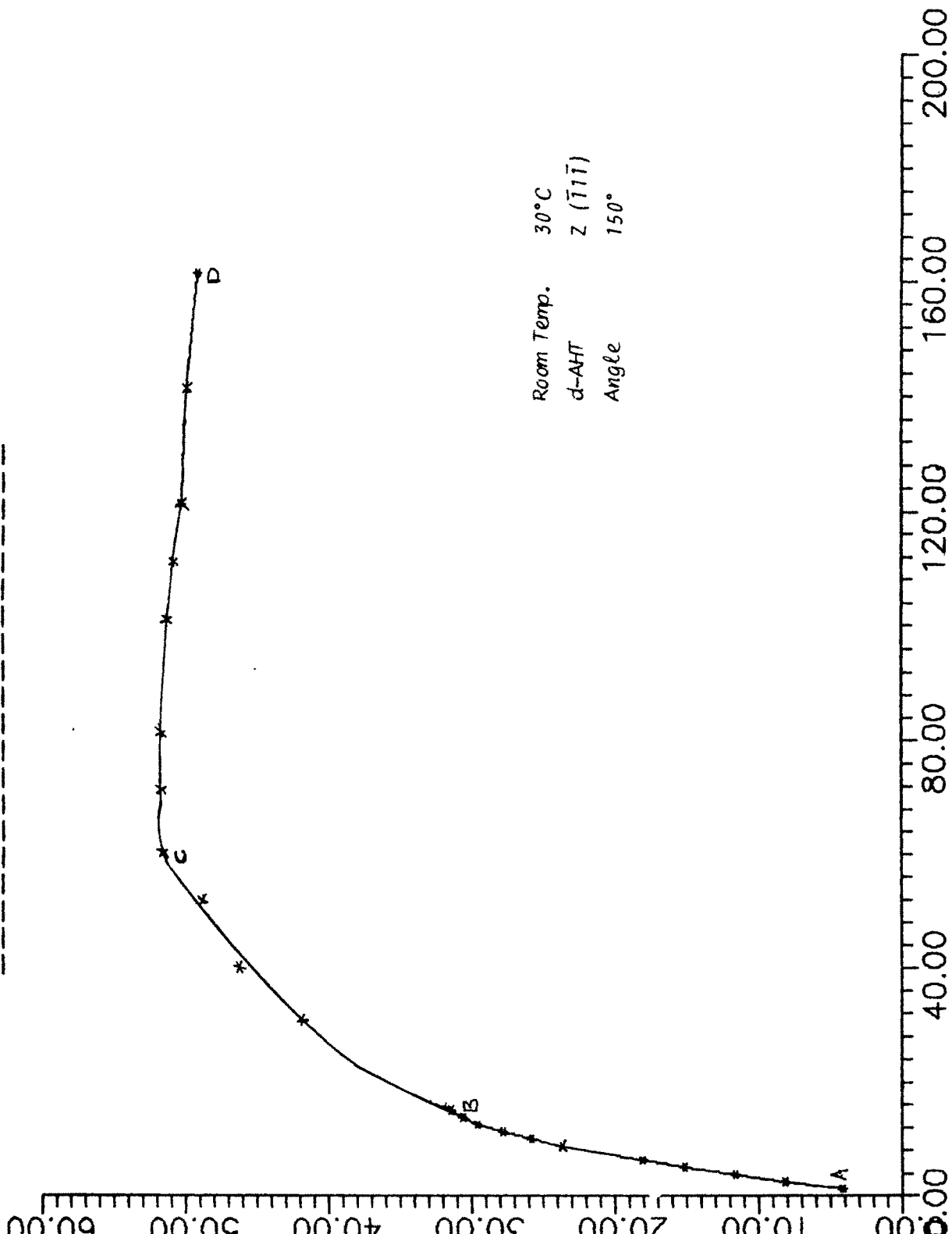


Hardness in kgms/mm^2

Fig. 7.6 (c)

Load in Gms.

PLOT OF Load Vs Hardness.

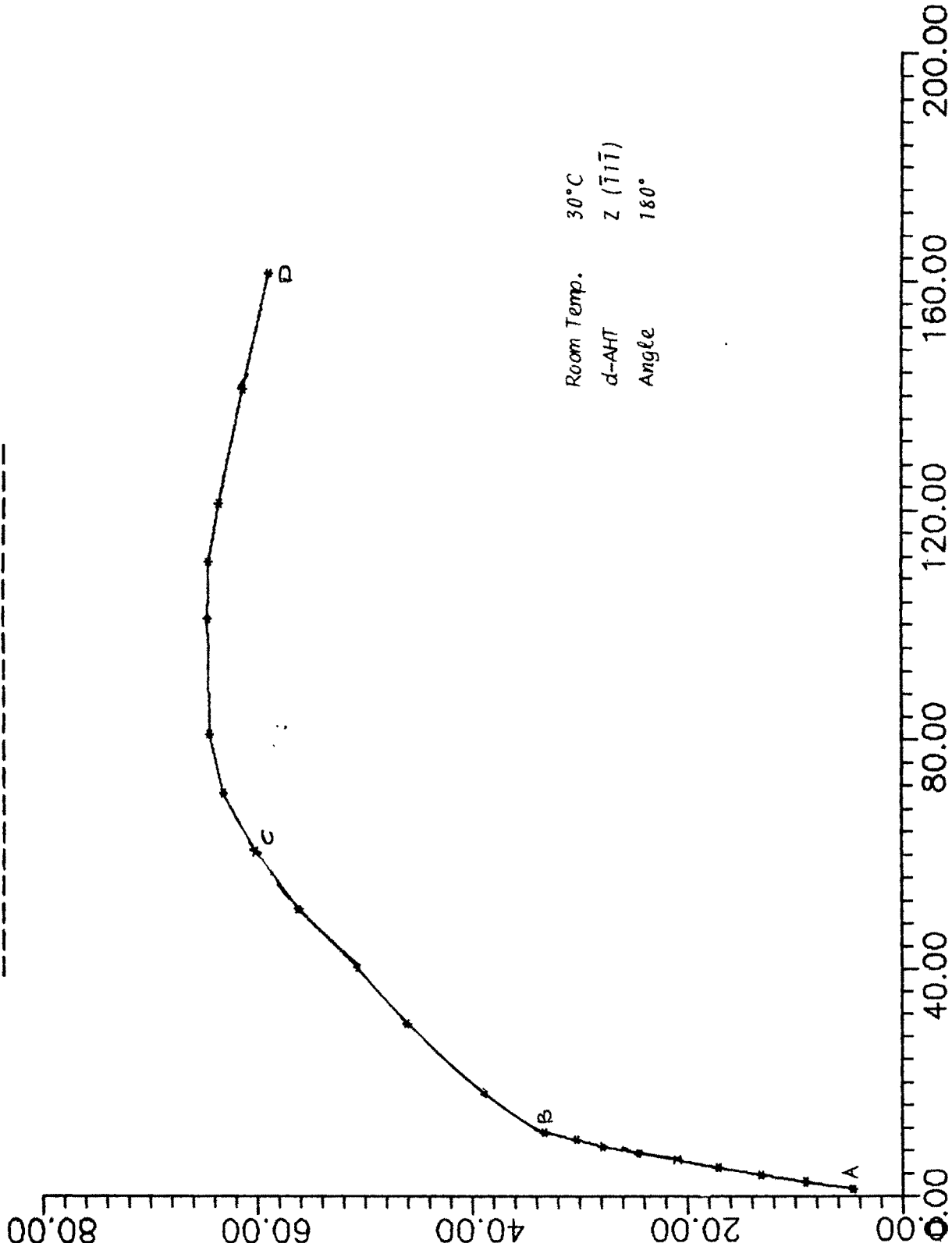


Hardness in kgms/m^2

Fig. 7.6 (d) i

Load in Gms.

FLUJ UR Load vs Hardness.

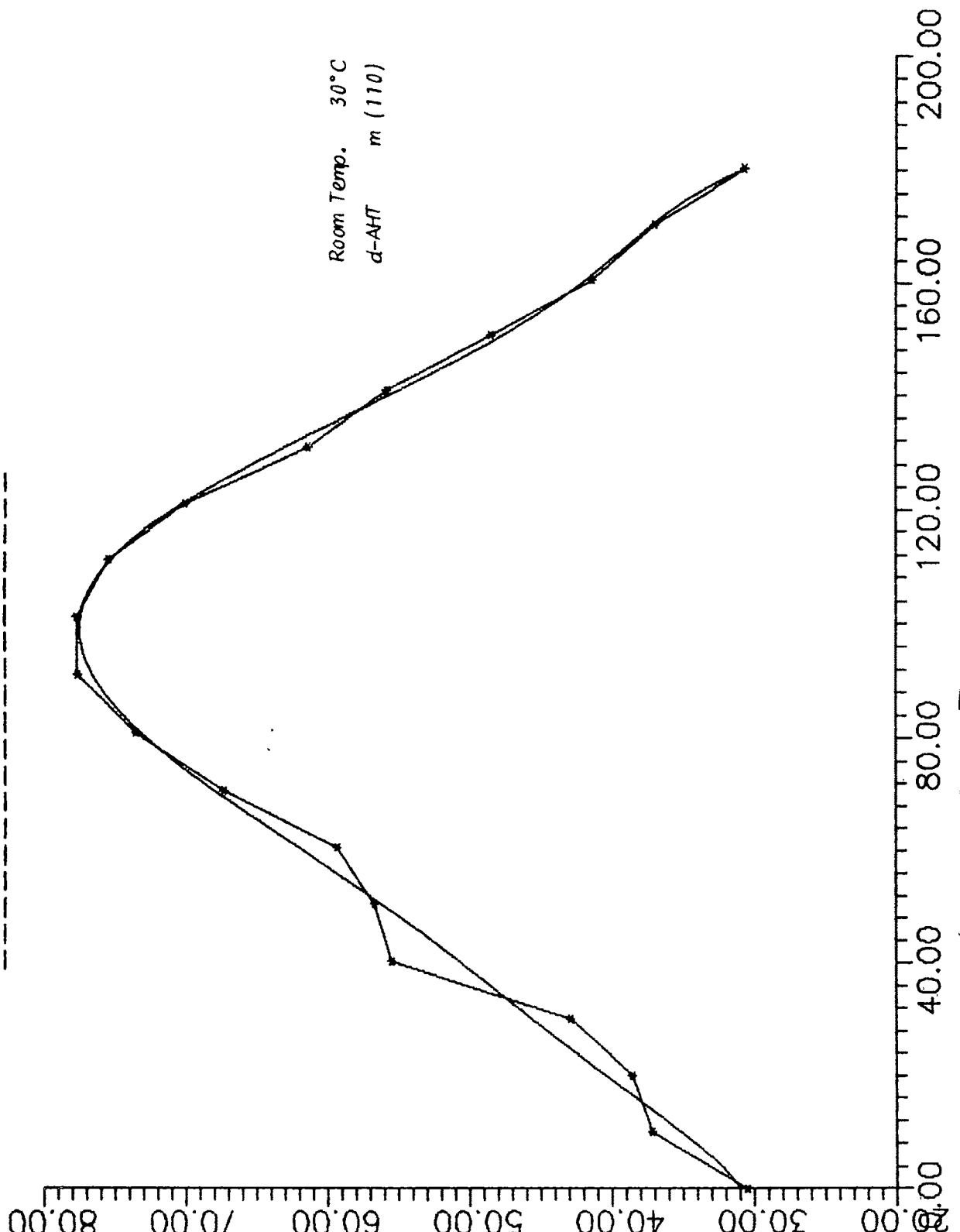


Hardness in kgms/m^2

Fig. 7.6 (d) ii

Load in Gms.

Plot of Angle vs Hardness.

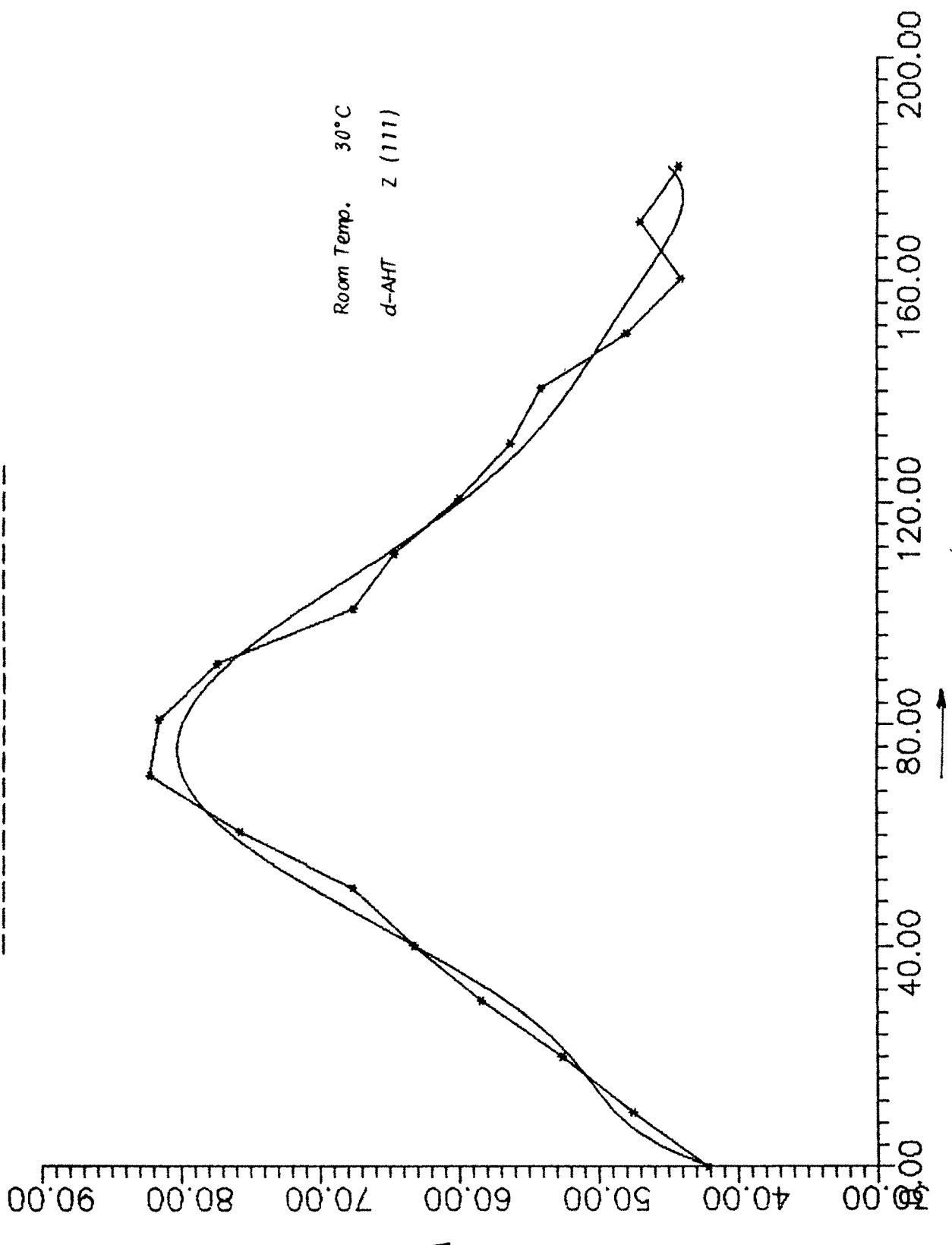


HARDNESS IN KGM/SQM

ANGLE IN DEGREES

Fig. 7.7 (a)

PLOT OF ANGLE VS Hardness.



HARDNESS IN KGMS/SQM

Fig. 7.7 (b)

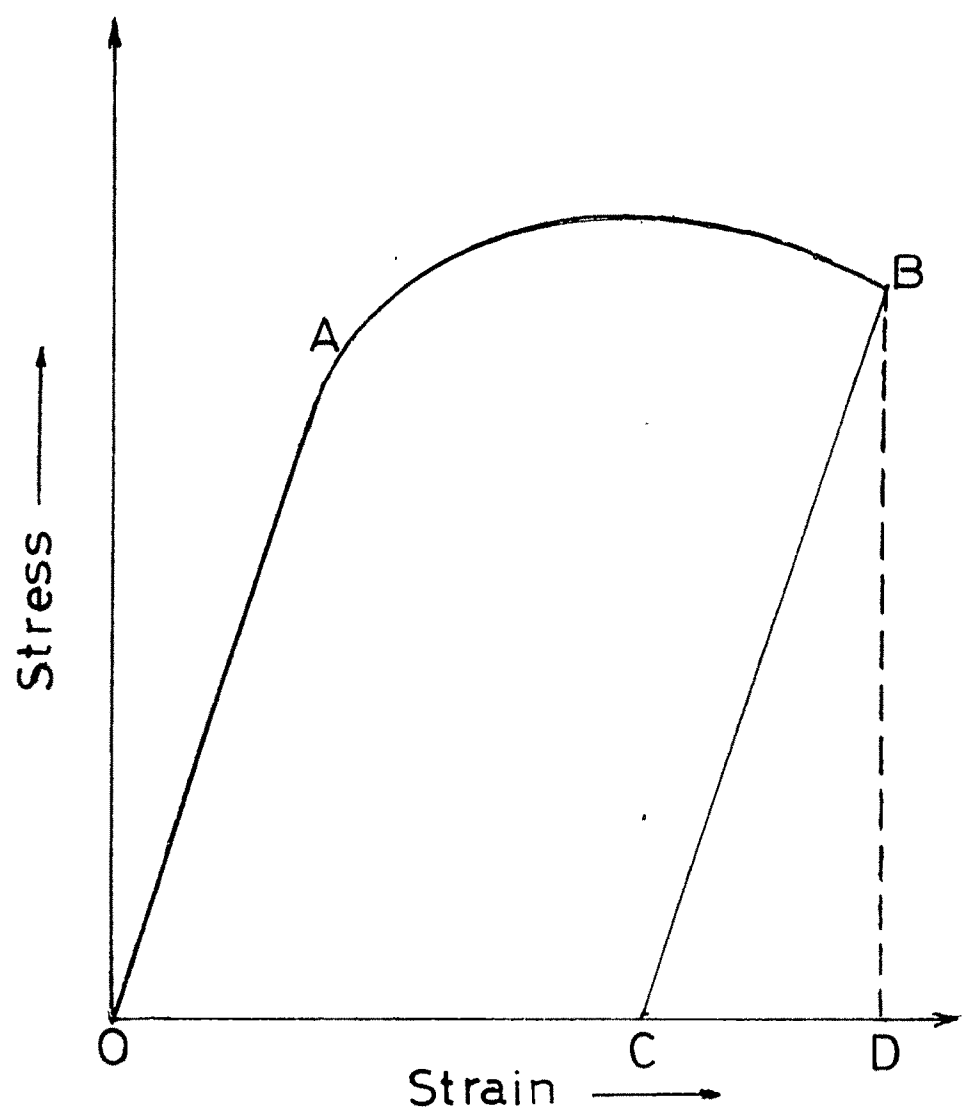


FIG.7.8

REFERENCES

01. Westbrook, J.H & Conrad, H
Quoted in "The Science of Hardness Testing & Its Research Applications", American Society for Metals, Metal Park, Ohio, 1973.
02. Joshi, D.R
Ph.D Thesis, M S Uni., Baroda, 1989.

LIST OF TABLES

- 7.1 (a,b,c,d) Table of logarithms of longer diagonal length of Knoop indentor mark corresponding to logarithms of load,slopes, n_1 and n_2 and intercepts a_1 and a_2 for various orientations of the Knoop indenter on d-AHT prism face,cleavage face and sphenoidal faces respectively at room temperature
- 7.2 (a,b,c,d) Table of Angle,A,slopes n_2 obs, n_3 mod, W_2 , b_2 and a_2 of the plots $\log d$ Vs $\log P$,for d-AHT prism face (m-110),cleavage face (c-010), sphenoidal faces (z-111) and (z-111) respectively at room temperature.
- 7.3 (a,b,c,d) Values of constants A,B,C derived from the quadratic equation for various orientations on d-AHT,prism,cleavage and sphenoidal faces,. respectively at room temperature.
- 7.4 (a to f) Percentage deviation of the observed diagonal length calculated from the equations :-
- i) $P = ad^n$
 - ii) $D = AP^2 + BP + C$
- for various faces and orientations of d-AHT at room temperature.

- 7.5 (a,b,c,d) Knoop hardness numbers corresponding to different loads for various orientations of Knoop indenter, on d-AHT prism, cleavage and sphenoidal faces respectively at room temperature.
- 7.6 Knoop hardness values obtained from plot of H Vs P (mean hardness, H) and from equations 7.33 & 7.32 respectively for different faces and various orientations of d-AHT, at room temperature.
- 7.7 Percentage deviation of calculated H by using equation 7.33 & 7.32 from the observed mean hardness, H , for different faces and various orientations of d-AHT, at room temperature.
- 7.8 Mean hardness number H , for various orientations on d-AHT, prism, cleavage and sphenoidal faces at room temperature.
- 7.9 Percentage deviation of Hardness calculated from the quadratic equation from the observed mean hardness value for d-AHT prism and cleavage face when the longer diagonal of Knoop indenter is along [001]
- 7.10 Anisotropic coefficients for different faces of d-AHT single crystals.
- 7.11 Hardness number H_K of different crystals for different orientations.
- 7.12 Hardness anisotropic coefficients for different crystals.

CAPTION TO FIGURES

- 7.1 Plot of log P Vs log d for d-AHT faces at room temperature for various orientations
a) m(110) face
b) c(010) face
c) z(111) face
d) z(111) face
- 7.2 Plot of d^2 Vs d^n for different d-AHT faces for various orientations at room temperature.
- 7.3 Plot of log d Vs log (P-W) for different d-AHT faces for various orientations at room temperature.
- 7.4 A graphical plot of load Vs diagonal length,d.
- 7.5 Plot of $(P_1 + P_2)$ Vs $(D_1 - D_2)/(P_1 - P_2)$ for different d-AHT faces for various orientations.
- 7.6 Plot of load Vs Hardness for different d-AHT faces for various orientations.
- 7.7 (a,b) Plot of Angle Vs Hardness for d-AHT prism and sphenoidal faces respectively.
- 7.8 Stress - strain diagram.